Western Graduate&PostdoctoralStudies

Western University
Scholarship@Western

Electronic Thesis and Dissertation Repository

7-27-2023 10:00 AM

Eosinophilic Asthma Response to Therapy: 129Xe Magnetic Resonance Imaging and Computed Tomography

Marrissa Joan McIntosh, *The University of Western Ontario*

Supervisor: Parraga, Grace, *The University of Western Ontario*

A thesis submitted in partial fulfillment of the requirements for the Doctor of Philosophy degree in Medical Biophysics

© Marrissa Joan McIntosh 2023

Follow this and additional works at: https://ir.lib.uwo.ca/etd

 Part of the Medical Biophysics Commons

Recommended Citation

McIntosh, Marrissa Joan, "Eosinophilic Asthma Response to Therapy: 129Xe Magnetic Resonance Imaging and Computed Tomography" (2023). *Electronic Thesis and Dissertation Repository*. 9400.
https://ir.lib.uwo.ca/etd/9400

This Dissertation/Thesis is brought to you for free and open access by Scholarship@Western. It has been accepted for inclusion in Electronic Thesis and Dissertation Repository by an authorized administrator of Scholarship@Western. For more information, please contact wlswadmin@uwo.ca.

Abstract

Novel biologic therapies, such as anti-interleukin-5 receptor α (anti-IL-5Rα) or benralizumab, have been developed to treat patients with severe eosinophilic asthma who experience frequent exacerbations, poor quality of life and increased risk of mortality. Whether this therapy results in disease modifying activity, specifically in the asthmatic airways and pulmonary vasculature, is still poorly understood. Pulmonary structure and function may be evaluated using computed tomography (CT) and hyperpolarized noble gas magnetic resonance imaging (MRI), respectively. Computed tomography has previously been utilized to measure airway dimensions, mucus occlusions and pulmonary blood volumes. In contrast, hyperpolarized gas MRI allows for the *in vivo* visualization and quantification of ventilation abnormalities, which are thought to reflect airway abnormalities such as airway inflammation and mucus plugging. Therefore, CT and MRI are poised to non-invasively evaluate the pulmonary structural and functional changes in eosinophilic asthma patients initiated on anti-IL-5Rα therapy. The overarching objective of this thesis was to use hyperpolarized ^{129}Xe MRI and chest CT to evaluate pulmonary function and structure following continuous anti-IL-5Rα therapy and to compare with pre-treatment measurements to better our understanding of the mechanisms responsible for improved asthma control and airflow obstruction. We first determined the upper limit of normal and minimal clinically important difference for ^{129}Xe MRI ventilation defect percent (VDP) and showed that the upper limit of normal varied with age and the minimal clinically important difference was 2%. Next, we measured ^{129}Xe MRI VDP after a single dose of anti-IL-5Rα and showed that VDP improvements were influenced by baseline CT mucus plugs. We evaluated a subset of these same participants after 2.5-years of continuous treatment and revealed that early ^{129}Xe MRI VDP improvements were sustained and that there was a near complete resolution of CT mucus plugs. Finally, we measured pulmonary blood volumes following 2.5-years of therapy and showed that there was a normalization and redistribution of blood from the larger to smaller vessels in eosinophilic asthma. Together, these results point towards mechanisms that may be responsible for improvements in airflow obstruction and asthma control and suggest that anti-IL-5Rα results in disease-modifying activity in patients with eosinophilic asthma.

Keywords

Asthma, Eosinophilic Asthma, Airways, Pulmonary Blood Vessels, Hyperpolarized Noble Gas MRI, Computed Tomography, Mucus Plugs, Anti-IL-5Rα, Ventilation Abnormalities

Summary for Lay Audience

Patients with eosinophilic asthma have difficulty breathing, which means they must be treated with very strong medications. Unfortunately, many of these patients still end up in the hospital because of their breathing trouble. New treatments, such as anti-IL-5Rα, have improved breathing problems in these patients, but the reasons for these changes are still not understood. This thesis used structural computed tomography (CT) and functional magnetic resonance imaging (MRI) to better understand how lung structure and function change after treatment with anti-IL-5Rα. First, we needed to know how much MRI ventilation needed to change before the patient would feel a difference, which we saw was 2%. Next, we measured MRI ventilation before and after one dose of treatment and saw that patients with many mucus plugs had more improvements in MRI ventilation. In the same groups of patients, we saw that the MRI ventilation changes after one treatment were still improved after 2.5 years, and that mucus plugs were gone. Finally, we measured volumes of blood in the lungs after 2.5 years of treatment. We saw that blood had moved from the larger blood vessels to the smaller blood vessels and that blood volumes in asthma patients after treatment were the same as blood volumes in healthy people. Together, these results tell us that airway function and structure, and blood vessel volumes improve after treatment with anti-IL-5Rα. These improvements may be causing improvements in breathing and this may help us understand which patients will get better using this medication.

Co-Authorship Statement

This thesis contains four manuscripts: three of these manuscripts have been published in scientific journals and one manuscript has been submitted for publication. As first author of two of these manuscripts and co-first author alongside Harkiran K Kooner of two of these manuscripts, I significantly contributed to all aspects of these studies as well as manuscript preparation and submission. Specifically, I made intellectual contributions to all study designs and was responsible for the organization and management of study visits, and I also acquired the majority of the pulmonary function test and imaging data. I was responsible for analyzing the hyperpolarized gas images to measure ventilation defects and the computed tomography images to generate blood volumes, performing statistical analysis and interpretation, and drafting, final approval and submission of the manuscripts. As Principal Investigator and Supervisor, Dr. Grace Parraga provided continuous guidance and was responsible for study and experimental design, data analysis and interpretation, drafting and final revisions and approval of the manuscripts. She is also the guarantor of study data integrity and responsible for Good Clinical Practice. The management of study visits and acquisition of pulmonary function test and imaging data were performed under the supervision of Danielle Knipping and Angela Wilson. MRI of research participants was performed by David Reese. Polarization of ^{129}Xe was performed by Dr. Alexander Matheson, Jonathan MacNeil, Maksym Sharma and Tamas Lindenmaier. For each manuscript within this thesis, all co-authors approved the final draft and the specific author contributions are listed below:

Chapter 2 is an original research article entitled "*^{129}Xe MRI Ventilation Defects in Asthma: What is the Upper Limit of Normal and Minimal Clinically Important Difference?"* and was published in the journal *Academic Radiology* in 2023 as a technical report. This manuscript was co-authored by Marrissa J McIntosh, Alexander Biancaniello, Harkiran K Kooner, Anurag Bhalla, Hana Serajeddini, Cory Yamashita, Grace Parraga and Rachel L Eddy. Alexander Biancaniello assisted with data analysis and interpretation. Harkiran K Kooner was responsible for data interpretation. Anurag Bhalla, Hana Serajeddini and Cory Yamashita assisted with clinical interpretation of the data. Rachel L Eddy assisted with data analysis, interpretation of the data and drafting the final manuscript.

Chapter 3 is an original research article entitled "*Asthma Control, Airway Mucus and ^{129}Xe MRI Ventilation after a Single Benralizumab Dose"* and was published in the journal *Chest* in 2022. This manuscript was co-authored by Marrissa J McIntosh, Harkiran K Kooner, Rachel L Eddy, Samira Jeimy, Christopher Licskai, Constance A Mackenzie, Sarah Svenningsen, Parameswaran Nair, Cory Yamashita and Grace Parraga. Marrissa J McIntosh and Harkiran K Kooner are co-first authors and equally contributed to this manuscript. Harkiran K Kooner was responsible for data analysis and interpretation and was responsible for the first draft of the manuscript. Rachel L Eddy assisted with data acquisition and interpretation. Samira Jeimy, Christopher Licskai, Constance A Mackenzie and Cory Yamashita were responsible for recruiting study participants, clinical input on the study design and interpretation of the data. Sarah Svenningsen and Parameswaran Nair contributed to the study design and were responsible for interpretation of the data.

Chapter 4 is an original research article entitled *"CT Mucus Score and ^{129}Xe MRI Ventilation Defects after 2.5-years Anti-IL-5Rα in Eosinophilic Asthma"* and was published in the journal *Chest* in 2023. This manuscript was co-authored by Marrissa J McIntosh, Harkiran K Kooner, Rachel L Eddy, Angela Wilson, Hana Serajeddini, Anurag Bhalla, Christopher Licskai, Constance A Mackenzie, Cory Yamashita and Grace Parraga. Marrissa J McIntosh and Harkiran K Kooner are co-first authors and equally contributed to this manuscript. Harkiran K Kooner was responsible for data acquisition, analysis and interpretation, and for preparing the first draft of the manuscript. Rachel L Eddy contributed to data acquisition and interpretation. Angela Wilson was responsible for coordination and completion of study participant visits. Hana Serajeddini and Anurag Bhalla assisted with interpretation of the data. Christopher Licskai, Constance A Mackenzie and Cory Yamashita were responsible for recruiting study participants, clinical input on the study design and interpretation of the data.

Chapter 5 is an original research article entitled *"Pulmonary Vascular Differences in Eosinophilic Asthma after 2.5-years Anti-IL-5Rα Treatment"* and was submitted to the *American Journal of Respiratory and Critical Care Medicine*. A shortened version of **Chapter 5** was resubmitted to the same journal as a research letter. This manuscript was co-authored by Marrissa J McIntosh, Alexander M Matheson, Harkiran K Kooner, Rachel L Eddy, Hana Serajeddini, Cory Yamashita and Grace Parraga. Alexander M Matheson was responsible for

the development of pulmonary vascular CT measurements and assisted with data interpretation and acquisition. Harkiran K Kooner assisted with data interpretation and acquisition. Rachel L Eddy contributed to data acquisition and interpretation. Hana Serajeddini assisted with data interpretation. Cory Yamashita was responsible for clinical input on the study design and clinical interpretation of the data.

Acknowledgments

First and foremost, I would like to thank my supervisor and mentor, Dr. Grace Parraga, for providing me with your unwavering support and guidance throughout my graduate studies. I am forever grateful for the countless opportunities you have given me, all the accomplishments I have achieved with your encouragement and insight, and for showing me that a true leader will always put those who they lead first. This was especially true during the COVID-19 pandemic where you refused to let any of your students fall behind. Thank you for always being patient with me as I navigated graduate school alongside motherhood. Your drive and passion for your research and the growth of your students has truly sparked my desire to continue on a career path in academia.

To my advisory committee, Dr. Corey Baron, Dr. Aaron Fenster, Dr. Sarah Mattonen and Dr. Cory Yamashita, thank you for your invaluable insight and support for my research and growth as a scientist. To Dr. Baron, thank you for always diligently critiquing my work and providing valuable insight about the limitations and improvements that could be made. To Dr. Fenster, thank you for always validating the importance of my work and providing valuable context about the technical aspects of my project, and also agreeing to write me scholarship recommendations which have resulted in two sources of funding. To Dr. Mattonen, thank you for always asking me the tough questions during my PhD reclassification and mid-level examinations, which have helped me prepare for my final thesis defense. A special thank you to Dr. Yamashita, who was instrumental in the study design and recruitment of participants whose data are used in this thesis. I also want to thank you for your valuable clinical insight especially as I prepared these manuscripts for publication.

To Kiran, my co-first author in two of these works, thank you for all of the work you have done to help me complete the projects within this thesis, including listening to my crazy ideas about mucus and vessels. Thank you for allowing me to mentor you in any way that I could, although I truly believe you are my research equal.

To Maks and Alex M, thank you for being with me for my entire graduate journey and for talking me off various research ledges. Thank you for your companionship, for helping me achieve my research goals, and co-authoring numerous abstracts and manuscripts with me. I could not have asked for a more enjoyable lab atmosphere than I had with the two of you.

To Rachel, thank you for being my mentor, my inspiration and my friend. Thank you for taking me under your wing during the final year of your PhD and for teaching me everything I needed to know to successfully pursue my research. Thank you for spending countless nights discussing asthma with me and for providing your valuable insight about my future career. I am so thankful for everything that you have done for me.

To Angela, thank you for being a surrogate mother to me. Thank you for always providing a shoulder to cry on, treats to snack on and the motivation to keep going. Thank you for always keeping me on track and for always setting a positive atmosphere during patient visits. To Paulina and Alexander B, thank you for allowing me to be one of your many mentors in the lab and I hope that you will keep in touch in your future endeavours. To Andrea, Jonathan, Tamas, Ivailo and Danielle, thank you for all of your contributions to my growth and development as a researcher and a person. To Sam and Ali, thank you for eagerly listening to my advice and for your desire to learn everything you can from me in the few short months that our time in the lab has overlapped.

Thank you to my friends and family, whom I could not have been able to complete this degree without you. Thank you to my mom, Jeanna, for always taking care of Ross when I couldn't; when I did not have care for him when I began my graduate studies and at the beginning of the COVID-19 pandemic, when I travelled to conferences, and when I needed to focus on my research and degree. Thank you for being my rock and for always being there for me. Thank you to my siblings, John, Matt, Josh, Kathryn, Daniel and Kelsey, for always being proud of me, and for always asking me for advice about school. Thank you to my Dad, who I know has been watching proudly over me for the last four years. To my son Ross Kevin, thank you for being a constant motivator to accomplish my goals and always giving me all of your love at the end of a hard day.

Finally, thank you to my sources of funding, the National Science and Engineering Research Council and the Canadian Respiratory Research Network, and travel funding from the Canadian Institute of Health Research.

Table of Contents

List of Tables

List of Figures

List of Appendices

List of Abbreviations

ACQ	Asthma Control Questionnaire
AQLQ	Asthma Quality of Life Questionnaire
ATS	American Thoracic Society
A_X	Reactance Area
BD	Bronchodilator
BMI	Body Mass Index
BV_5	Blood volume in vessels with cross-sectional-area < 5 mm^2
BV_{5-10}	Blood volume in vessels with cross-sectional-area 5-10 mm^2
BV_{10}	Blood volume in vessels with cross-sectional-area > 10 mm^2
COPD	Chronic Obstructive Pulmonary Disease
CEV	Cumulative Expiratory Volume
CT	Computed Tomography
DL_{CO}	Diffusing Capacity of the Lung for Carbon Monoxide
ERS	European Respiratory Society
ERV	Expiratory Reserve Volume
FeNO	Fraction of Exhaled Nitric Oxide
FEV_1	Forced Expiratory Volume in One Second
FOT	Forced Oscillation Technique
FOV	Field of View
FRC	Functional Residual Capacity
FVC	Forced Vital Capacity
GM-CSF	Granulocyte Macrophage-Colony Stimulating Factor
GINA	Global Initiative for Asthma
HU	Hounsfield Unit
IC	Inspiratory Capacity
ICS	Inhaled Corticosteroid
IgE	Immunoglobulin E
IL-5	Interleukin 5
IRV	Inspiratory Reserve Volume
LA	Lumen Area
LABA	Long-acting Beta-agonist
LAMA	Long-acting Muscarinic Antagonist
LCI	Lung Clearance Index
LTRA	Leukotriene Receptor Antagonist
MBW	Multibreath Washout
MCID	Minimal Clinically Important Difference
MRI	Magnetic Resonance Imaging
NO	Nitric Oxide
OCS	Oral Corticosteroids
PC_{20}	Provocative Concentration Required to Decrease FEV_1 by 20%
PEF	Peak Expiratory Flow
PET	Positron Emission Tomography
R_5	Resistance at 5 Hz
R_{5-19}	Resistance at 5 Hz minus Resistance at 19 Hz

R_{19}	Resistance at 19 Hz
RA_{950}	Relative Area of the Lung <-950 HU
RV	Residual Volume
SABA	Short-acting Beta-agonist
Sacin	Phase III Slope Analysis of Acinar Airways
Scond	Phase III Slope Analysis of Conducting Airways
SD	Standard Deviation
SGRQ	St. George's Respiratory Questionnaire
SPECT	Single Photon Emission Computed Tomography
TAC	Total Airway Count
TBV	Total Blood Volume
TE	Echo Time
Th2	T helper 2
TLC	Total Lung Capacity
TR	Repetition Time
TSLP	Thymic Stromal Lymphopoetin
ULN	Upper Limit Normal
UTE	Ultra-short Echo Time
VC	Vital Capacity
VD	Deadspace
VDP	Ventilation Defect Percent
VDV	Ventilation Defect Volume
VT	Tidal Volume
WA%	Wall Area Percent
WT	Wall thickness
X_5	Reactance at 5 Hz

Chapter 1

1 INTRODUCTION

Eosinophilic asthma is a chronic pulmonary disease characterized by eosinophilic airway infiltration. Novel biologic therapies have been shown to improve disease control and airflow limitations however the mechanisms responsible for these changes are poorly understood. In this thesis, pulmonary structural and functional changes following the initiation of the biologic therapy anti-IL-5Rα (benralizumab) are evaluated using computed tomography (CT) and hyperpolarized ^{129}Xe magnetic resonance imaging (MRI) to better understand the influence of anti-IL-5Rα on eosinophilic airways and pulmonary blood vessels.

1.1 Motivation and Rationale

Asthma is one of the most common chronic diseases, which globally affects more than 300 million people.[10] Approximately 5% of patients with asthma have severe disease and half of these patients have the eosinophilic subtype.[5] Asthma prevalence, particularly in developed Western Countries such as Canada, has been rising over the past several decades (**Figure 1-1**),[7] with more than 2.8 million adolescents and adults affected.[11] The rate of mortality and hospitalizations related to asthma in Canada, however, have been decreasing over time and marked changes in these rates appear to coincide with the advent of new asthma therapies (**Figure 1-2**).[7,8] According to the Global Initiative for Asthma (GINA) guidelines, the goal of asthma therapy is to control asthma symptoms,[5] but despite the therapeutic advances made over the last 50 years, a large proportion of asthma patients remain uncontrolled,[12] with the estimated 20-year economic burden of poorly controlled asthma to cost $213 billion.[13]

"Asthma remission" describes the symptom-free state that some patients with asthma may enter, regardless of the resolution of their underlying asthma pathology.[14,15] While the specific mechanisms responsible for remission are not well understood,[16] disease-modifying therapies[17] may help achieve this goal.[18] Disease remission has been achieved in other inflammatory

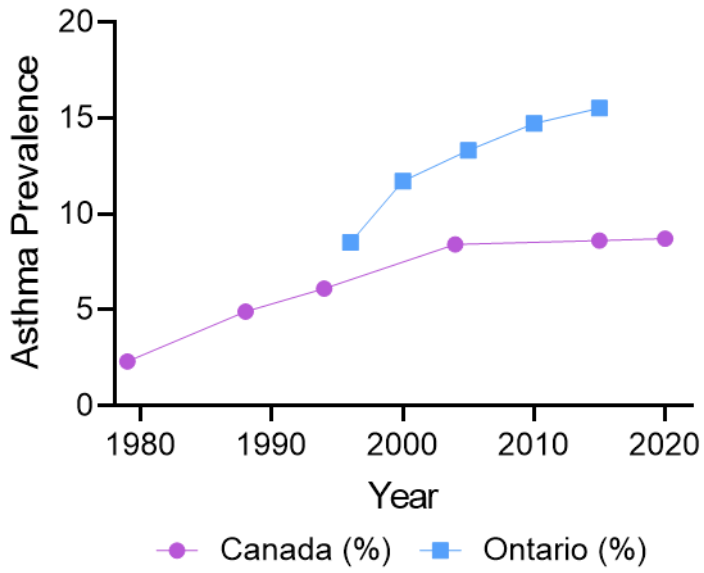

Figure 1-1. Asthma Prevalence in Canada and Ontario from 1979-2020
Data from Cockcroft, Can J Respir Crit Care Sleep Med (2022).[7]

conditions, such as rheumatoid arthritis, through the use of monoclonal antibodies.[19,20] Severe eosinophilic asthma patients experience high rates of mortality[21-23] and exacerbations[23-25] and poor disease control.[14,15] The advent of successful monoclonal antibody therapy, such as anti-interleukin-5 receptor α (anti-IL-5Rα) or benralizumab,[26,27] may help some of these patients achieve disease remission. Anti-IL-5Rα therapy results in significant reductions in exacerbations and improvements in airflow obstruction.[20,21] The mechanisms responsible for these changes and whether anti-IL-5Rα results in disease-modifying activity is still not well understood. This is, in part, due to a lack of sensitive, specific and non-invasive evaluations of the eosinophilic asthma pathophysiology. The spirometry measurement of the forced expiratory volume in 1 second (FEV_1) is a global measurement of airflow limitation and is the primary tool used to evaluate airway hyperresponsiveness and airflow variability, as well as treatment response in patients with asthma. However, spirometry can only inform on the

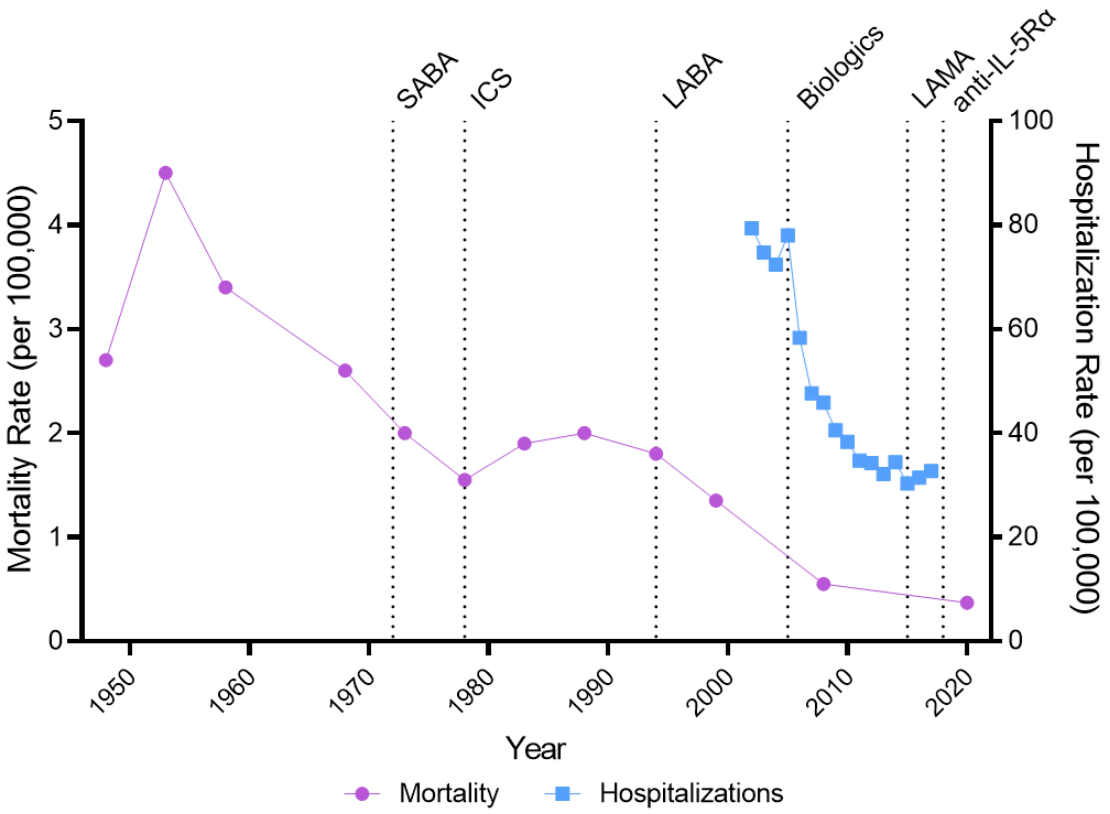

Figure 1-2. Annual Rate of Mortality and Hospitalizations in Canada
Asthma mortality and hospitalization rates in Canada. Dotted lines indicate the initial date of marketing of modern asthma therapies in Canada.
Mortality and asthma therapy marketing data from Cockcroft, Can J Respir Crit Care Sleep Med (2022).[7] Hospitalization data from Lee et al, Ann Allergy Asthma Immunol (2022).[8]
Abbreviations: SABA=short acting beta agonist; ICS=inhaled corticosteroids; LABA=long acting beta agonist; LAMA=long acting muscarinic antagonist; anti-IL-5Rα=anti interleukin 5 receptor α.

severity of the airflow obstruction and does not provide information about the source of the obstruction or the pathological mechanisms responsible for airflow limitation improvement after therapy. The fraction of exhaled nitric oxide (FeNO) measures nitric oxide in exhaled breath and is considered to be a biomarker of eosinophilic airway inflammation.[137,138] The production of nitric oxide in the lung is driven by IL-13.[28] While biologic therapy that targets the IL-4/IL-13 pathway results in significant reductions in FeNO levels post-treatment,[29] pivotal clinical trials investigating anti-IL-5Rα demonstrated that FeNO was insensitive to airway inflammation changes following anti-IL-5Rα initiation.[26,27] Thus, neither spirometry nor FeNO can provide clues about whether anti-IL-5Rα results in disease-modifying effects in

eosinophilic asthma. Therefore, there is an urgent need to develop measurements that can inform on severe eosinophilic asthma pathophysiology and the pulmonary structural and functional responses associated with anti-IL-5Rα driven eosinophil depletion in patients with severe eosinophilic asthma.

Pulmonary functional magnetic resonance imaging (MRI) using hyperpolarized noble gas was first introduced nearly three decades ago,[30] and since then has been used as a tool to visualize the *in vivo* ventilation distribution of patients with asthma. Ventilation defects in asthma have been shown to be distinctly wedge shaped,[31-36] spatially persistent over the short- and long-term,[34,36,37] and associated with poor asthma control[38] and exacerbations[38,39] as well as airway inflammation,[40,41] sputum eosinophilia[40] and luminal occlusions.[42,43] Moreover, previous investigations have shown that ventilation defects respond to asthma therapy.[33,44-49] Despite the evidence to support the clinical use of hyperpolarized gas MRI to monitor asthma progression and treatment response, its use in both clinical and research settings has been limited. In fact, the Food and Drug Administration only approved the clinical use of ^{129}Xe MRI in December of 2022 and the first clinical scan in North America was completed in 2023 at the Cincinnati Children's Hospital Medical Center.[50] In contrast, pulmonary structural imaging using computed tomography (CT), which provides a three-dimensional image of the lung, airways and vasculature, has been indicated for the evaluation of severe asthma for more than a decade,[51,52] and has been used in large asthma cohort trials such as the Severe Asthma Research Program to quantify pulmonary airway dimensions,[53,54] mucus plugging[55,56] and blood volumes,[57] which were associated with eosinophilia. Thus, pulmonary imaging is poised to evaluate the short- and long-term influence of eosinophilic depletion via biologic therapy on pulmonary structure and function. Therefore, the overarching objective of this thesis is to exploit sensitive MRI and CT measurements of airway function, and airway and vascular

structure following the initiation of anti-IL-5Rα in patients with poorly controlled eosinophilic asthma. Using this information, we may be able to discern whether anti-IL-5Rα results in disease-modifying effects and thus may be used to help achieve asthma remission in some patients.

In this chapter, the relevant background information required to motivate the original research presented in **Chapters 2-5** is provided. A general overview of the structure and function of the lung is described (**1.2**) followed by a description of asthma pathophysiology (**1.3**). The clinical tools used to evaluate pulmonary function are provided next (**1.4**). Asthma treatments are discussed (**1.5**), after which a description of pulmonary imaging evaluations and their context in asthma is given (**1.6**). Finally, the hypotheses and objectives of this thesis are provided (**1.7**).

1.2 Respiratory Structure and Function

The respiratory system is comprised of the upper and lower respiratory tracts. The upper tract contains the nose and nostrils, nasal cavity, mouth, the pharynx or throat and the larynx or voice box, while the lower tract consists of the lungs and airway tree. The lungs are contained within the thoracic cavity and consist of lobes, airways, alveoli and blood vessels, with the primary function of the lung being to exchange inhaled oxygen with carbon dioxide. To achieve this, the lungs work together with the abdominal wall and diaphragmatic muscles, to take in atmospheric air (inspiration). The external intercostal muscles move the rib cage upward while the diaphragm moves downward to increase the surface area of the thorax. This, in turn, causes the pressure in the airways to be decreased compared with atmospheric air. A pressure-gradient is created and atmospheric air is pulled into the respiratory system through the nose or mouth, through the pharynx, past the larynx and through the trachea, bronchi and bronchioles, into the alveoli where the exchange of oxygen and carbon dioxide in the blood

(gas-exchange) occurs. Following gas-exchange, the rectis abdominis, internal and external oblique muscles and the transversus abdominis contract, thus increasing the intra-abdominal pressure, pushing the diaphragm upwards and forcing air out of the lung (expiration).

1.2.1 Airways: Conducting and Respiratory Zones

The lung consists of 23 generations of airways which are divided into the conducting and respiratory zones, shown in **Figure 1-3**. The primary function of the conducting zone is to serve as a conduit for inhaled air as it moves towards the alveoli and to humidify this air. Since the airways in the conducting zone do not participate in gas exchange, these airways are termed the anatomic dead space (VD) and contain approximately 150 mL of air. The conducting zone of the airways begins with the trachea, which then bifurcates into the two main bronchi. Airway diameter gradually decreases with each airway bifurcation. The right main bronchi then branches into three lobar bronchi (right upper, right middle and right lower) while the left main bronchi branches into only two lobar bronchi (left upper and left lower). Each of these airway branches forms one of the five pulmonary lobes of the same name, which are separated by lobar fissures; airway branches do not cross between lobes. The lobar bronchi then branch into a total of 19 segmental bronchi, depicted and labelled in **Figure 1-4**. The segmental bronchi then branch into the bronchioles, which continue to branch for approximately 12 more generations. The bronchioles lead into the terminal bronchioles, concluding the conducting zone. Airways in the conducting zone consist of thick walls of mucosa, smooth muscle and cartilage, and these walls are lined with cilia to capture and remove dust or other particles from the lung. While the trachea and main bronchi are lined with cartilage only, the walls of the subsequent airway generations are also lined with smooth muscle up to and including generation 11. From generation 12 onward, the airways are lined with smooth muscle only.

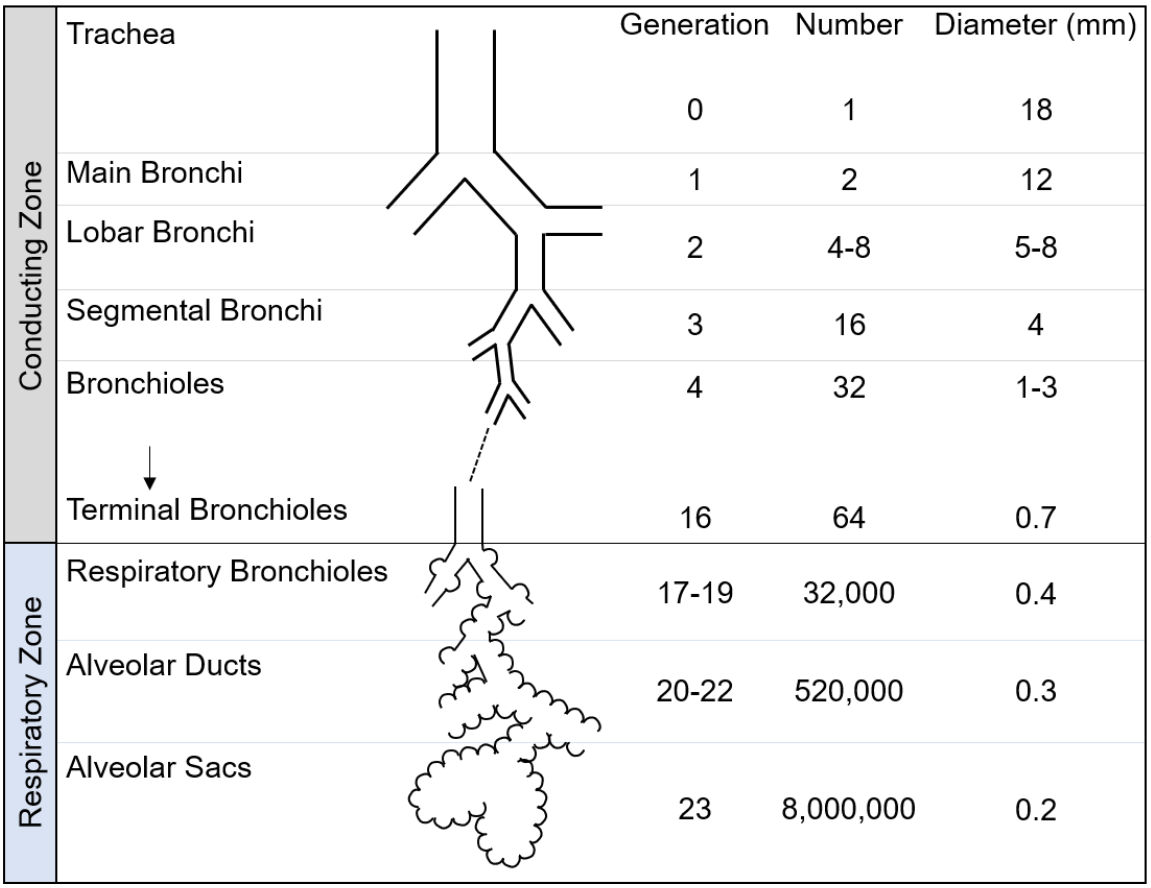

Figure 1-3. Schematic of Airway Tree Conducting and Respiratory Zone
The human airway tree consists of the conducting zone and respiratory zone, with corresponding generation, number and diameter shown. Adapted from Nunn's Applied Respiratory Physiology, 8th edition.[6]

Due to the lack of structural support from cartilage, these airways are embedded in the lung parenchyma.

While the function of the conducting zone is the transport and humidification of inhaled air, and the subsequent expiration of air, the function of the respiratory zone is to facilitate gas exchange. The respiratory zone consists of the respiratory bronchioles, alveolar ducts and alveolar sacs. Alveoli begin to bud on the walls of the respiratory bronchioles and become

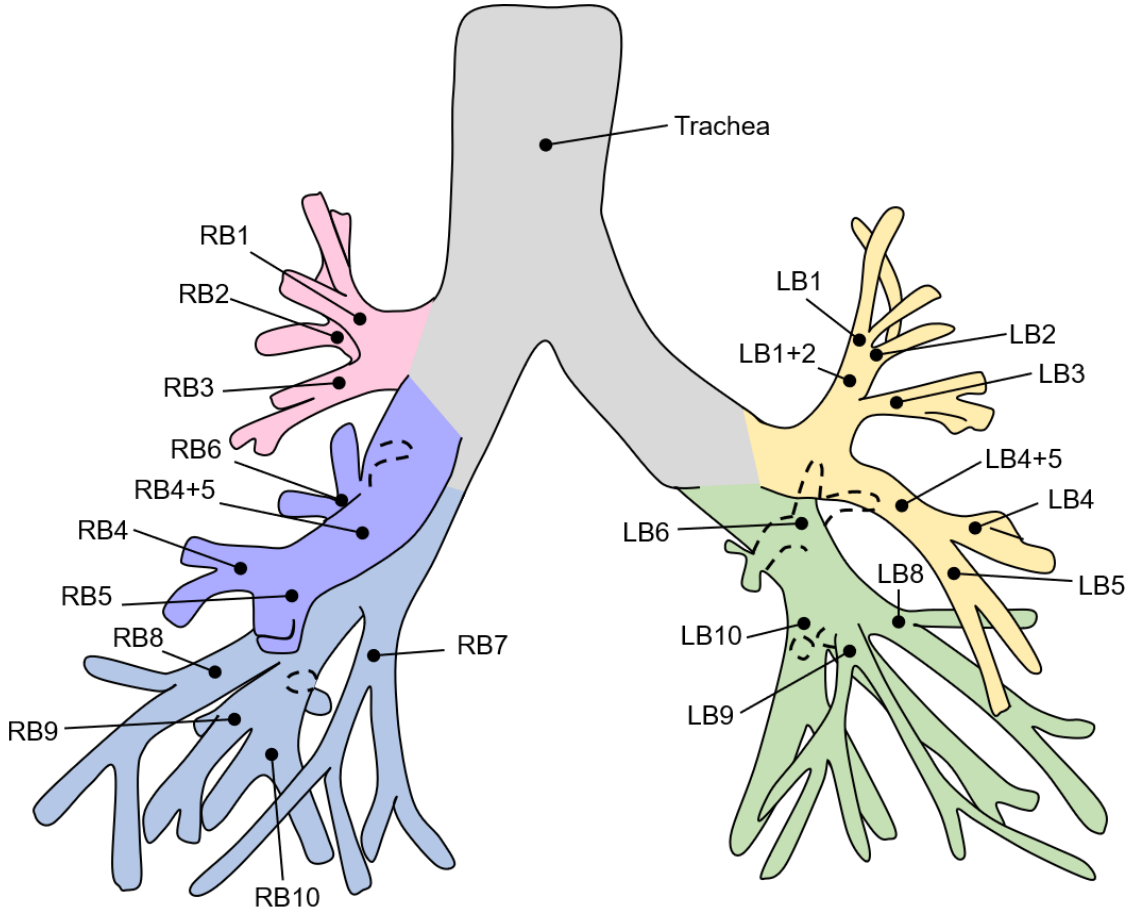

Figure 1-4. Labelled Airway Tree Diagram
Airways branch from the trachea into the two main bronchi and then into the five pulmonary lobes, with airway branches color-coded by lobe as follows: pink=right upper lobe, purple=right middle lobe, blue=right lower lobe, yellow=left upper lobe, green=left lower lobe. The entire airway tree branches for 23 generations, terminating in the alveoli. Adapted from Sheel, et al. J Appl Physiol (2009).[4]

more numerous as the airway generation increases. The alveolar ducts do not contain any airway walls and their passage-like structure is formed by the openings of the alveoli surrounding them. Finally, the alveolar sacs complete the respiratory zone and the airway tree, and consists of a group of approximately 17 alveoli. The structure and function of the alveoli will be described in more detail in **Section 1.2.2**. The respiratory zone contains millions of airways and alveoli, and thus holds approximately 2.5 to 3.0 L of air at rest.

1.2.2 Alveoli: Site of Gas Exchange

The alveoli are microscopic sacs surrounded by a net of capillaries and whose primary function is to facilitate the exchange of oxygen and carbon dioxide. There are approximately 400 million alveoli in the healthy adult lung, which varies in each individual based on their height and lung volume. The alveoli are also lined with surfactant, which reduces the surface tension of the alveoli, subsequently preventing the air sacs from sticking together and collapsing during breathing. The barrier between the alveolar epithelium and capillary epithelium is termed the blood-gas interface. This interface is very thin (~0.3 μm) and the total surface area of the alveoli is between 50 to 100 m^2. According to Fick's Law of Diffusion, the rate of gas transfer is proportional to the area of the tissue and is inversely proportional to the thickness of the tissue, thus the lung is well suited for efficient gas-exchange.

1.2.3 Vasculature

The pulmonary vasculature stems from the pulmonary artery in the heart and consist of arteries, arterioles, capillaries, veins and venules. The pulmonary arteries and arterioles run parallel to the airways up to the terminal bronchioles, after which they form a net of capillaries that surround the alveoli. Much like the systemic vasculature, blood travels from the arteries to the arterioles and then into the capillaries, whose diameter is approximately the width of a single red blood cell (7 μm), so that this blood may participate in gas exchange. The now oxygenated blood drains from the capillaries into the pulmonary venules, then veins, and back to the heart so that it may be pumped to the rest of the body. The pulmonary arteries may constrict in response to alveolar hypoxia, which in turn causes the terminal bronchioles to dilate.[58]

The lungs also contain the bronchial vasculature. While the purpose of the pulmonary vasculature is to oxygenate blood, the purpose of the bronchial vasculature is to supply the conducting airways with blood which provides heat, oxygen and nutrients so that the

conducting airways may properly function. These vessels run adjacent to the airways up to the terminal bronchioles.

1.2.4 Ventilation

Ventilation is the process by which inspired air is carried through the conducting zone and to the respiratory zone so that this air may participate in gas exchange. The amount of air that leaves the lung on expiration per unit time (typically minutes) is defined as the total ventilation, which is described mathematically in **Equation 1-1**:

Equation 1-1

$$\text{Total ventilation}\left[{}^{\text{L}}/_{\text{min}}\right] = \text{Breathing frequency}\left[{}^{\text{breathes}}/_{\text{min}}\right] \cdot \text{VT}\left[{}^{\text{L}}/_{\text{breath}}\right]$$

where VT is the tidal volume. In a healthy adult at rest, VT is approximately 500 mL and, assuming a breathing frequency of 14 breaths/minute, the total ventilation would be 7 L/min. While the volume of air entering the lungs may be 500 mL, approximately 150 mL does not reach the alveoli during a single breath. This volume remains within the anatomic dead space (VD) and its purpose is to prevent the airways from collapsing during breathing. The volume of air that reaches the alveoli and participates in gas exchange is defined as the alveolar ventilation, described in **Equation 1-2**:

Equation 1-2

$$\text{Alveolar ventilation}\left[{}^{\text{L}}/_{\text{min}}\right] = \text{Breathing frequency}\left[{}^{\text{breaths}}/_{\text{min}}\right] \cdot (\text{VT} - \text{VD})\left[{}^{\text{L}}/_{\text{breath}}\right]$$

Using the previous example, the alveolar ventilation would be equal to 4.9 L/min. While 7 L of air may enter the lung each minute, only 4.9 L will reach the alveoli and participate in gas exchange.

1.3 Pathophysiology of Asthma

1.3.1 Definition and Diagnosis of Asthma

According to GINA guidelines,[5] asthma is defined by variable airflow limitation and respiratory symptoms. These limitations and symptoms may be caused by airway hyperresponsiveness and/or airway inflammation, and both are typically associated with the disease. A patient presenting with multiple respiratory symptoms that are typical of asthma (i.e. wheeze, shortness of breath, cough, chest tightness) may be referred to pulmonary function testing to confirm variable airflow limitation. Variable expiratory airflow limitation is evaluated using spirometry, which will be explained in further detail in **Section 1.4.1**, and can be defined by a reduced forced expiratory volume in 1 second (FEV_1) in combination with an abnormally low FEV_1 to forced vital capacity (FVC) ratio, excessive variability in twice-daily peak expiratory flow (PEF) over the course of two weeks, variation in FEV_1 or PEF between visits or a significant increase in these measurements following 4 weeks of anti-inflammatory treatment, or by one or more positive responsiveness or challenge tests.

Bronchodilator (BD) responsiveness (previously termed "reversibility"), is defined as an increase in FEV_1 greater than 200 mL and 12% from baseline, measured at least 10 minutes after the administration of 200-400 µg of salbutamol (albuterol). In contrast, exercise and bronchial challenge tests are defined as a decrease in FEV_1. Spirometry is obtained prior to and following exercise on a treadmill or exercise bike, with a positive test being defined as a decrease in FEV_1 of >200 mL or 10% from baseline. During a bronchial challenge test, patients will inhale either methacholine, histamine, hypertonic saline or mannitol; methacholine is most commonly used due to its limited number of side effects.[59] A decrease from baseline in FEV_1 of ≥20% after methacholine, or ≥15% after hypertonic saline or mannitol is a positive test; the dosage of methacholine required to decrease an individuals FEV_1 by 20% is termed PC_{20}. It is

important to note that BD responsiveness,[60-62] and variable airflow limitation following exercise[63] and bronchial provocation[64-66] challenges have been reported in a number of respiratory diseases other than asthma, so while a negative test can help exclude a diagnosis of asthma, a positive test does not necessarily confirm asthma.

1.3.2 Asthma Airway Remodelling

Early histological investigations in patients with fatal asthma revealed airway wall thickening, cellular infiltration of the airway and partial or complete luminal occlusion by mucus plugs,[67] which is now recognized as airway remodelling. Airway remodelling is a characteristic feature of asthma[68] and is broadly defined as any change in composition, distribution, thickness, mass or volume and/or number of structural components observed in the airway wall.[69-71] As shown in **Figure 1-5**,[3] asthma airways, as compared to those of a healthy individual, have narrowed and obstructed lumens. The major components of airway remodelling are surface epithelial metaplasia with increased epithelial thickness, goblet cell hyperplasia and increased mucus secretion, subepithelial fibrosis, increased thickness of smooth muscle, and angiogenesis.[72-74] The consequences of these processes may manifest as mucus hypersecretion and bronchial constriction or narrowing,[74] and may lead to an irreversible loss of lung function.[72] In asthma, airway smooth muscle is responsible for rapid bronchoconstriction, which describes the contraction of the airway wall and subsequent reduction in luminal diameter, in response to various stimuli or irritants; this is termed airway hyperresponsiveness. In addition, the airway smooth muscle in patients with asthma resists relaxation which may result in the frequent use of bronchodilators (beta-2 agonists). Airway remodelling[75] and the frequent use of beta-2 agonists may contribute to a loss of BD reversibility in some patients with asthma.[76]

Chronic airway inflammation in asthma may also contribute to airway remodelling. Airway inflammation is an immune-related response to irritants, and thus many types of immune cells

may be responsible for inflammation, including eosinophils; eosinophilic asthma and airway inflammation will be described in further detail in **Section 1.3.4**. Briefly, eosinophils infiltrate airway walls, causing wall thickening and mediating the formation of mucus plugs,[77] both of which contribute to airflow obstruction and airway remodelling.

1.3.3 Pulmonary Vascular Remodelling

Although asthma is primarily thought to be an airways disease, previous histological[9,78] and radiological[57] investigations have discovered evidence of pulmonary vascular remodelling,[79] which is described as an increased number of vessels, increased size of vessels in the airway walls, increased vascular permeability, angiogenesis and increased vascular leakage and oedema.[80] Some of these features are shown in **Figure 1-5**. Patients with asthma have an increased vessel density as compared to healthy controls and patients with chronic obstructive pulmonary disease (COPD)[81] and these vascular changes are associated with remodelling of the airway,[81-85] increased blood flow,[86] asthma severity[87,88] and airflow obstruction.[81] It has been postulated that these changes may contribute to increased eosinophil trafficking to the airways.[80,89,90] Moreover, eosinophils in the airway may promote vascular endothelial growth factor,[91] which may play a role in pulmonary vascular remodelling.[80]

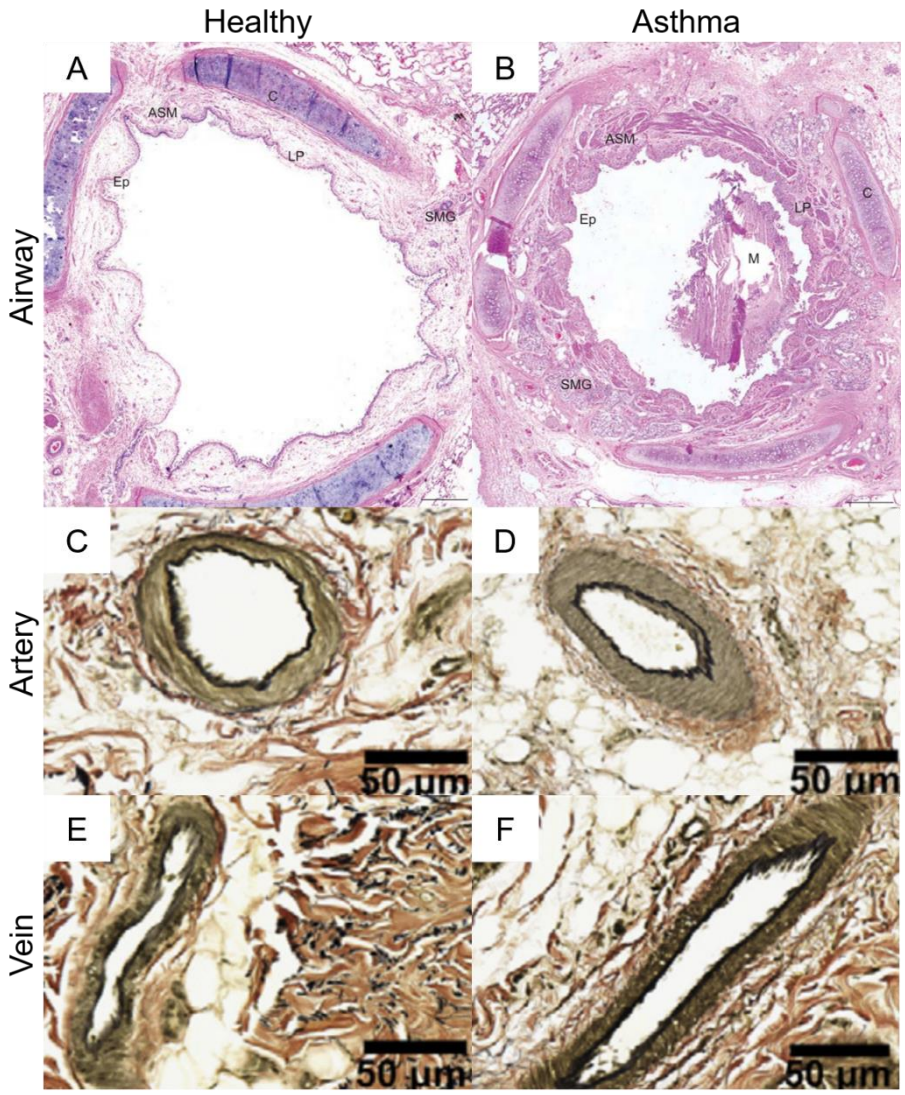

Figure 1-5. Airway and Vessel Remodelling
Airway of a healthy patient (A) has thin walls and patent lumen, compared to the airway of an asthma patient (B), with thick walls, narrow and obstructed lumen by mucus plug. Healthy arteries (C) and veins (E) have thinner vessel walls compared to asthma arteries (D) and veins (F).
Airway images reprinted from Araujo, et al. Eur Respir J (2008)[3] and vascular images reprinted from Mostaço-Guidolin, et al. Am J Respir Cell Mol Bio (2021),[9] with permission (Appendix A).

1.3.4 Eosinophilic Asthma Subtype

Asthma is a heterogenous disease that may be subdivided into several endotypes and phenotypes. T helper 2 (Th2) high is one such endotype and is characterized by abnormally high airway and systemic eosinophilia, thickened basement membrane and corticosteroid responsiveness.[92,93] The important role that eosinophils play in the pathology of asthma has

been acknowledged for more than a century,[94] and abnormal eosinophil levels in the peripheral blood and bronchoalveolar lavage fluid in patients with asthma was first observed in 1990 by Bousquet and colleagues.[95] Since then, it has been shown that increased airway eosinophilia is associated with asthma severity[96,97] and airflow obstruction,[97] and is predictive of asthma control loss.[98,99] Eosinophilia in the airways may be responsible for many characteristic features of asthma, including mucus hypersecretion[100] and airway hyperresponsiveness,[91] inflammation[101] and remodelling.[91] In addition, it has been suggested that eosinophil peroxidase may mediate mucus plug formation.[55]

The pathway from eosinophil differentiation to infiltration of the airways is complex and outside the scope of this thesis. Briefly, eosinophil differentiation is regulated by transcription factors. Eosinophil maturation occurs in the bone marrow which is mediated by IL-5, IL-3 and granulocyte macrophage-colony stimulating factor (GM-CSF). The migration of the eosinophil from the bone marrow to the airways is triggered by eosinophil chemoattractants such as eotaxins, although it has been suggested that the initial migration of peripheral eosinophils is caused by prostoglandin-D2,[102] which is released from activated mast cells.[103] Eosinophilic infiltration of the airways is mediated by IL-5, IL-13 and eotaxins, and eosinophils are then activated by IL-5, eotaxins and chemokine ligand 5, along with immunoglobulin E (IgE) and thymic stromal lymphopoietin (TSLP). Finally, eosinophil degranulation may occur via conventional exocytosis, cytolysis or piecemeal degranulation. Eosinophil survival is promoted by IL-3, IL-5, GM-CSF, and eotaxins, as well as the activation of toll-like receptor 7. Eosinophilic airway inflammation is initiated by IL-5 and IL-13, while airway hyperresponsiveness and mucus hypersecretion may be driven by IL-13. The cytokine IL-4 is responsible for the expansion of Th2-type cells, along with their ability to secrete IL-5.

While the eosinophilic asthma subtype typically responds well to corticosteroids, systemic and airway eosinophils remain in some asthma patients despite high doses of this therapy.[104] This has prompted the development of several monoclonal antibody therapies that specifically target the cytokines essential for eosinophil development and survival, which will be discussed in detail in **Sections 1.5.2** and **1.5.3**.

1.4 Clinical Tools to Evaluate Asthma

1.4.1 Spirometry

Spirometry is the primary pulmonary function test used to diagnose and evaluate asthma. This test records the volume and flow of forcefully exhaled air, termed the forced vital capacity (FVC) maneuver, and is measured at the mouth. To perform this maneuver, patients are seated in an upright position with their feet on the floor. Using nose clips to restrict airflow through the nasal passages, the patient tightly seals their mouth around the mouthpiece. Following 3-4 tidal breaths, the patient is instructed to fully inhale to total lung capacity and then completely and forcefully exhale the air in their lungs. An example of the volume-time curve and measurements obtained by this maneuver are shown in **Figure 1-6**. FVC is a measure of the total volume that a patient can forcefully exhale from full inspiration, while the forced expiratory volume in 1 second (FEV_1) is the volume of air forcefully exhaled during the first second of the FVC maneuver. The peak expiratory flow (PEF) is another commonly used spirometry measurement for the monitoring of asthma, which is the maximum flow rate achieved during the FVC maneuver. While these measurements may be reported in raw form (i.e. L or L/s), they may also be standardised as the percent of the predicted ($\%_{pred}$) value for a healthy person, based on patient age, sex, height, weight and ethnicity. In asthma, these measurements are typically reduced.

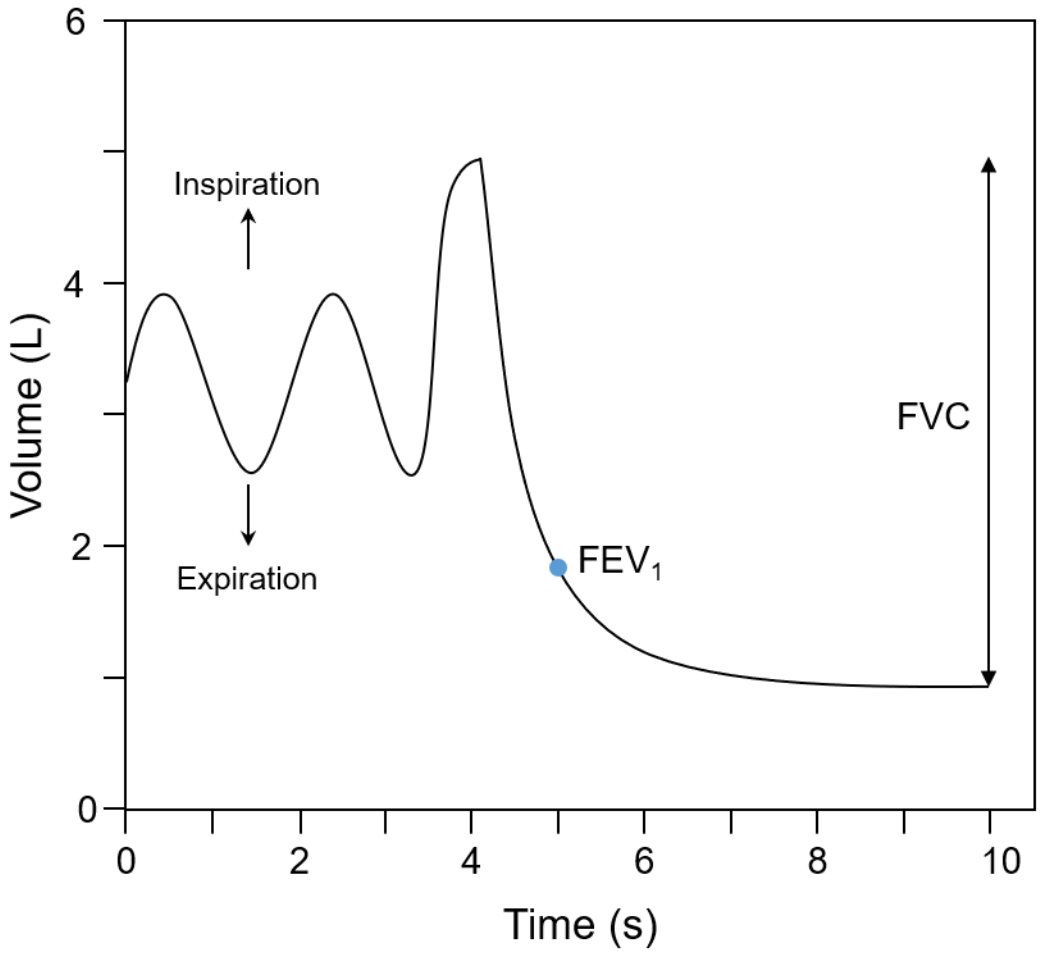

Figure 1-6. Typical Spirometry Volume-Time Curve
Spirometry device records forcefully exhaled breath to measure the forced expiratory volume in 1 second (FEV_1) and forced vital capacity (FVC).

1.4.2 Plethysmography

Plethysmography sensitively measures lung capacities and volumes using Boyle's Law. Boyle's Law states that, in a closed system such as the one during plethysmography, when the temperature of a given gas is constant, then the product of the pressure of that gas is inversely proportional to the volume. To perform these maneuvers, the patient is enclosed in a "body box" chamber, such that the volume is kept constant and the changes in pressure directly represent changes in the lung that occur during the breathing maneuvers. In the same position as spirometry, the patient firmly closes their mouth around the mouthpiece and uses nose clips.

Following 3-4 tidals breaths, the patient firmly places their hands on their cheeks to dampen pressure changes that might occur in the cheeks. Next, the patient performs a shallow panting maneuver while the shutter in the mouthpiece is open, followed by closed shutter panting. Finally, the shutter re-opens, the patient returns to tidal breathing and completes the test with a full inhalation and full exhalation at normal effort.

A typical volume-time curve and the measurements obtained from plethysmography is shown in **Figure 1-7**. Tidal volume (VT) is the amount of gas inhaled and exhaled during normal breathing. Functional residual capacity (FRC) is the volume of gas in the lung as the end of a normal exhalation while the residual volume (RV) is the volume of gas left in the lungs after a full exhalation. Total lung capacity (TLC) is the amount of gas in the lungs after a full inhalation. Inspiratory capacity (IC) is the volume of gas inhaled from the bottom of a tidal breath or FRC and the inspiratory reserve volume (IRV) is the difference in volume between TLC and the top of a tidal breath. Expiratory reserve volume (ERV) is the amount of air that can be exhaled from FRC. Finally, the vital capacity (VC) is the total volume of air that can be inhaled from residual volume, or the volume of air that can be exhaled from TLC. These measurements, again, may be expressed as a percent of a predicted ($\%_{pred}$) value for a healthy participant.

In asthma, air-trapping can cause RV, FRC and TLC to increase; the ratio of RV to TLC (RV/TLC) is typically used to measure air-trapping from plethysmography. Air-trapping in asthma may be caused by smooth muscle dysfunction, airway inflammation or mucus plugging.

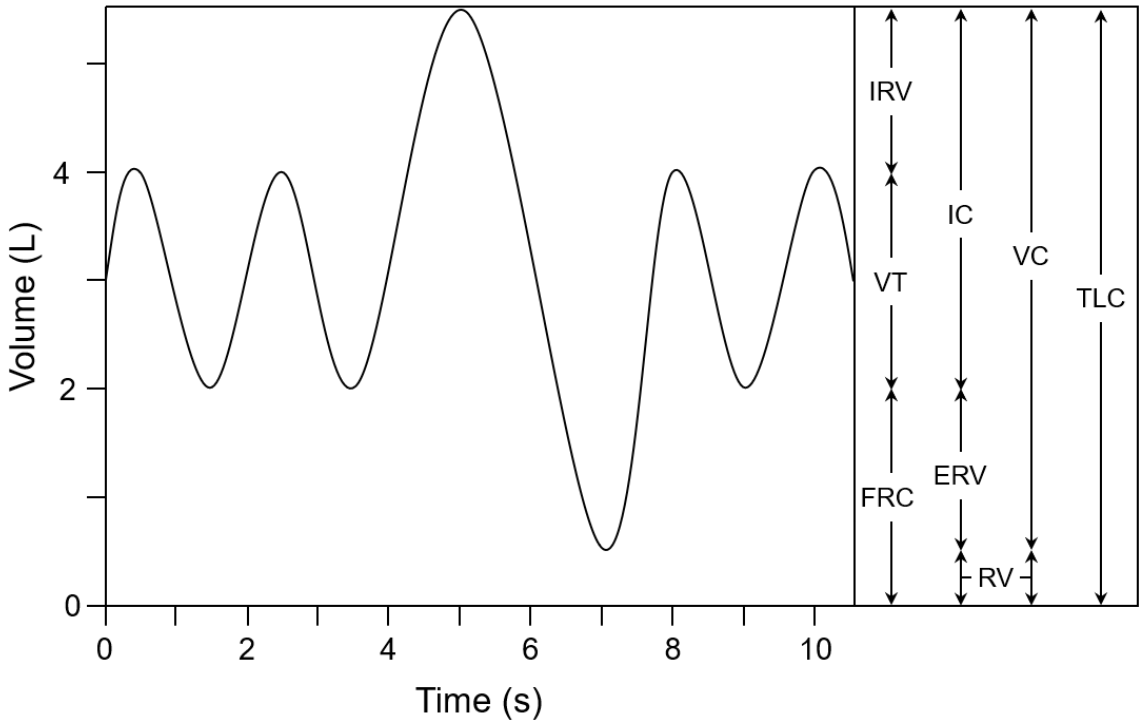

Figure 1-7. Plethysmography Volume-Time Curve
Plethysmograph records breathing maneuvers to measure lung volumes and capacities.
Abbreviations: FRC=functional residual capacity; VT=tidal volume; IRC=inspiratory reserve volume; RV=residual volume; ERV=expiratory reserve volume; IC=inspiratory capacity; VC=vital capacity; TLC=total lung capacity.

1.4.3 Diffusing Capacity of the Lung

The diffusing capacity of the lung for carbon monoxide (DL_{CO}) test indirectly measures the capacity of the lung for gas exchange across the alveolar capillary membrane. While oxygen can be limited by both diffusion and perfusion, carbon monoxide is only limited by diffusion, hence, here it is used to measure the diffusing capacity of the lung. The binding affinity of carbon monoxide for hemoglobin is approximately 210-times greater than that of oxygen. Moreover, the concentration of carbon monoxide in the gas mixture is extremely low. Thus, the pressure of carbon monoxide in the pulmonary capillaries during a DL_{CO} test is constant.

While the patient is seated in an upright position with nose clips secured, the test begins with four tidal breaths after which the patient must exhale to RV. After this, the patient rapidly breathes in the gas mixture to TLC and holds their breath for 8 seconds before exhaling

completely. The gas mixture used for this test contains 0.3% carbon monoxide, 21% oxygen, a balance of nitrogen and a tracer gas. Due to anatomic deadspace, the first 150 mL of exhaled breath is discarded, after which the partial pressure of carbon monoxide is measured and expressed in units of mL CO/min/kPa or as a percent predicted.

The diffusing capacity may be influenced by several factors, including the thickness and area of the alveolar membrane, the volume of blood in the capillaries and the concentration and binding properties of hemoglobin. In asthma, DL_{CO} is typically within normal limits but, in some cases, it may be elevated.[105-107] This elevation may be explained by an increase in pulmonary capillary volume.[108]

1.4.4 Additional Pulmonary Function Tests

1.4.4.1 Oscillometry

The forced oscillation technique (FOT) was first developed nearly 70 years ago.[109] This technique measures lung biomechanics, specifically respiratory system impedance, which may be further separated into real and imaginary components – resistance and reactance. In contrast to other pulmonary function tests, oscillometry requires minimal coaching and patient effort. In an upright position with nose clips on, the patient supports their cheeks to reduce the influence of upper airway shunt on impedance measurements. The oscillometry device superimposes a multi-frequency airwave onto the patients spontaneous tidal breathing. Notable measurements include the resistance at 5 Hz (R_5) and 19 Hz (R_{19}), which reflect the total airway and large airway resistance, respectively, the frequency dependence of resistance (R_{5-19}), reactance at 5 Hz (X_5) and the area between the reactance curve and the x-axis (A_X). In asthma, resistance and reactance are sensitive to airway narrowing[110,111] and the small airways,[112] and are associated with asthma symptoms, control and severity,[113-116] CT airway structure[117] and hyperpolarized noble gas MRI ventilation heterogeneity.[116,118] Furthermore, oscillometry

measurements respond to bronchodilation[119-122] and bronchoconstriction,[123] as well as inhaled corticosteroid (ICS) and long-acting bronchodilator therapy.[124-126]

1.4.4.2 Inert Gas Washout

Both single-breath[127] and multi-breath[128] washout (MBW) techniques have previously been employed to measure ventilation heterogeneity, although the multi-breath washout test is more commonly used. To perform multi-breath washout, the patient sits upright with nose clips on and breathes in 100% oxygen while the concentration of a tracer gas, typically nitrogen (N_2), is measured. Once the tracer gas reaches $1/40^{th}$ of its initial concentration, the test ends. The primary measurements obtained from multi-breath washout testing are the cumulative expiratory volume (CEV), FRC and the ratio of CEV to FRC, reported as the lung clearance index (LCI)[129] which is the number of breathes required to completely exchange the gas within the lung. Phase III slope analysis may also be performed to determine the ventilation heterogeneity in the acinar (Sacin) and conducting (Scond) airways.[129]

MBW measurements are greater in patients with asthma as compared to healthy controls.[130,131] Furthermore, despite normal spirometry, LCI has been shown to be abnormal in adults[132] and children with well-controlled asthma[133] which suggests it may be more sensitive to early disease changes. In addition, MBW indices have been shown to be predictive of airway hyperresponsiveness,[134] correlate with asthma control[135,136] and airflow obstruction,[137] and respond to inhaled corticosteroids[134,136,138] and bronchodilators.[130,139]

1.4.4.3 Fraction of Exhaled Nitric Oxide

Nitric oxide (NO) has been recognized as a biomarker of airway inflammation in asthma[140,141] and can be measured in exhaled breath using the fraction of exhaled nitric oxide (FeNO) test,[142] although FeNO is considered an indirect measurement of IL-13 airway inflammation.[142,143] NO is upregulated by inflammatory cells such as eosinophils,[144] plays a role in smooth muscle

relaxation, vasodilation and inflammatory mediator,[145] and may also act as a bronchodilator.[146] NO is significantly correlated with eosinophilia found in blood, sputum, bronchoalveolar lavage and biopsied lung specimens.[147-151] FeNO is elevated in patients with asthma,[152,153] and may be used to select patients that are likely to respond to corticosteroids.[142,154,155]

1.4.5 Validated Questionnaires

Patient-reported quality of life, symptoms and control related to respiratory illness or disease may be evaluated using a number of questionnaires including the Asthma Control Questionnaire (ACQ),[156] Asthma Quality of Life Questionnaire (AQLQ)[157] and the St. George's Respiratory Questionnaire (SGRQ).[158] These questionnaires are self-completed under the supervision of clinical staff or research personnel, and each has been adopted as a clinical trial endpoint.[47,159-162]

ACQ is a 7-item questionnaire that evaluates the adequacy of control over the previous week. The first five items evaluate asthma symptoms (awakening in the night by symptoms, symptoms immediately after waking, activity limitation, dyspnea and wheeze), while the final two evaluate the use of rescue medication and airflow limitation as measured by FEV_1. Each question is measured on a 7-point scale and may be reported as the ACQ-5 (asthma symptoms), ACQ-6 (asthma symptoms+rescue medication) or ACQ-7 (asthma symptoms+rescue medication+airflow limitation), with a higher score indicating worse control. The threshold for uncontrolled asthma has been determined to be an ACQ score ≥ 1.5[163] and the minimal clinically important difference (MCID) to be 0.5.[156]

AQLQ is a 32-item questionnaire that evaluates patient quality of life over the previous two weeks. These items may be subdivided into four domains – symptoms (11 questions), activity limitation (12 questions), emotional function (5 questions) and environmental exposure (4 questions). Some of the concerns addressed by AQLQ include how often the patient

experiences wheeze, shortness of breath, the need to clear their throat, or are woken in the night by their asthma. These questions are scored on a 7-point scale, with one corresponding to poor quality of life and seven corresponding to good quality of life, and the total AQLQ score is calculated as the mean of all 32 questions. While the upper limit of normal for AQLQ remains to be determined, the MCID has previously been calculated to be 0.5.[164]

The St. George's Respiratory Questionnaire is a 50-item questionnaire designed to evaluate quality of life in patients with chronic airflow limitation. Similar to AQLQ, these items may be subdivided into three domains – symptoms, impacts and activity. Questions include how often the patient experiences cough, whether their breathing makes it difficult to carry things upstairs, or whether they are embarrassed of their cough in public. The MCID for SGRQ is 4 points[165] and the upper limit normal is between 5 and 7 points.[166]

1.5 Treatment of Asthma

Asthma is typically treated with controller, reliever and add-on therapies. The Global Initiative for Asthma (GINA) recommends a stepwise approach to asthma management as shown in **Figure 1-8**. When a patients' asthma is considered poorly controlled then they are "stepped up" on treatment; conversely, when a patients' asthma is well controlled, their physician may decide to "step down" treatment. Controller treatments are taken daily and the goal of these therapies is to maintain symptom control. Reliever or "rescue" treatments are taken as needed when symptoms become worse or during an exacerbation or asthma flare-up. If a patient still reports symptoms despite being prescribed high dosages of controller treatments, they may be prescribed a variety of add-on therapies in an attempt to gain or regain control of asthma symptoms.

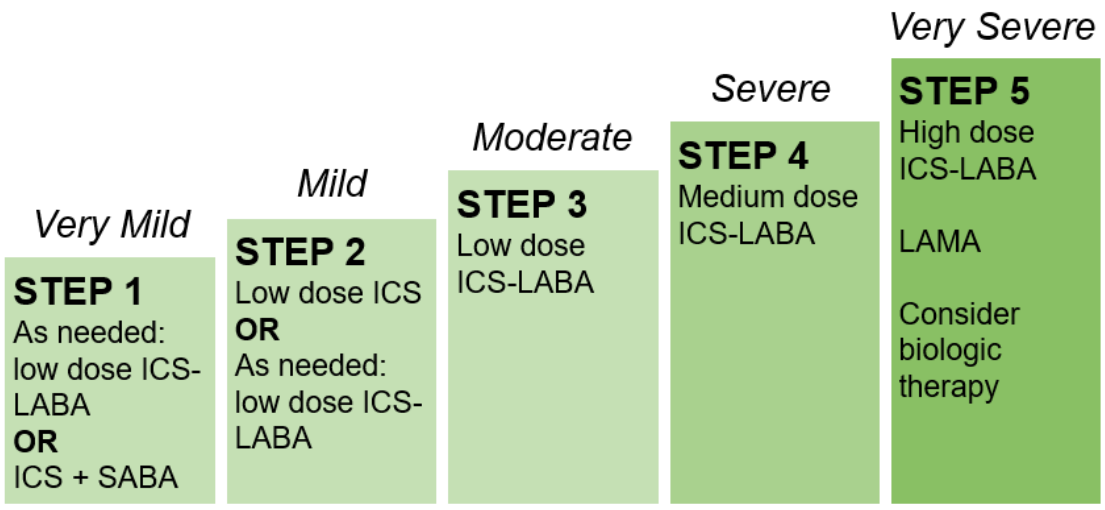

Figure 1-8. GINA Step-up Treatment Guidelines
Adapted from the Global Initiative for Asthma (GINA) Global Strategy for Asthma Management and Prevention 2022 report.[5]

It is important to note that there are several additional causes for poor symptom control in asthma, regardless of the dosage and type of medication being prescribed. These can include incorrect inhaler technique, poor adherence, persistent exposure at work or home to irritants, comorbidities or an incorrect diagnosis. Therefore, it is important to have objective measurements that are related to asthma control and can sensitively measure response to therapy.

1.5.1 Controller and Reliever Treatment

There are two main types of controller and reliever medications prescribed for patients with asthma – corticosteroids and beta-2 agonists. Corticosteroids are considered one of the most effective treatments for asthma and were first used to treat an acute asthma exacerbation nearly 70 years ago.[167] Inhaled corticosteroids directly reduce inflammation in the airway by blocking inflammatory pathways,[168] and its use as a controller medication reduces asthma symptoms, the risk of exacerbations and bronchial hyperresponsiveness[169] and also improves quality of life in patients with asthma. Corticosteroid therapy in asthma may be taken both orally (OCS)

and in an inhaled form (ICS), although only ICS is used as a controller; the negative side effects associated with OCS use has led it to become an add-on treatment only.[5]

Beta-2 agonists primarily target airway smooth muscle and may be prescribed as short-acting and long-acting beta-agonists (SABA and LABA, respectively). The 2022 GINA guidelines recommend that asthma patients are primarily prescribed combined inhaled corticosteroid (ICS) and long-acting beta2-agonist (LABA) therapy, while SABA may be recommended as a reliever therapy. The combination of ICS and LABA has been shown to improve symptom control and lung function in patients with asthma.[170,171]

1.5.2 Add-on Treatment

Leukotriene antagonists (LTRA) block the action of chemical messengers that play a role in the inflammatory response in the airways, reducing both bronchoconstriction and inflammation. Clinical trials have shown that LTRA improves airflow obstruction, exacerbation rates and disease control, although further studies have shown that the addition of LTRA to ICS therapy is comparable or worse than the combination of LABA and ICS.[172,173]

Long-acting muscarinic-antagonists (LAMA) also target the smooth muscle component of asthma by blocking the acetylcholine-mediated bronchoconstriction by binding to airway smooth muscle M_3 receptors.[174] LAMA may be taken in a separate puffer, but may also be combined with LABA, or ICS-LABA into a single puffer. In placebo-controlled trials, the addition of LAMA to ICS-LABA therapy resulted in fewer exacerbations and improved FEV_1, although no differences in quality of life were observed.[175]

Bronchial thermoplasty uses radiofrequency energy to heat the airway wall tissue and reduce the amount of airway smooth muscle,[176] and has been shown to improve asthma control and quality of life while also reducing exacerbations following treatment[160,177]; these promising results were demonstrated to persist for up to five years.[178] Although bronchial thermoplasty

has been shown to be safe and efficacious,[160,177] the invasive nature of the treatment may explain why this procedure is one of the last treatments prescribed to control asthma symptoms. More recently, monoclonal antibody biologic therapies targeting the eosinophilic component of asthma have been introduced and are described in **Table 1-1**. These include omalizumab, reslizumab, mepolizumab, dupilumab, tezepelumab and benralizumab.[179] For the purposes of this thesis, only benralizumab (anti-IL-5Rα) will be described in more detail.

Table 1-1. Biologic Therapies for Eosinophilic Asthma and Therapeutic Targets

Biologic Agent	Therapeutic Target
Benralizumab	IL-5Rα
Dupilumab	IL-4Rα
Mepolizumab	IL-5
Omalizumab	IgE
Reslizumab	IL-5
Tezepelumab	TSLP

1.5.3 Anti-IL-5Rα

As shown in **Figure 1-9**, the anti-IL-5Rα antibody binds to the FcγRIIIα receptor on the eosinophil, thus preventing the binding of IL-5 cytokine to the eosinophil. Next, anti-IL-5Rα signals to natural killer cells to induce eosinophil apoptosis.[1] This results in a near complete depletion of eosinophils in the bone marrow, blood and airways within 24 hours of administration.[180,181]

In the pivotal phase III clinical trials CALIMA and SIROCCO,[26,27] FEV_1 significantly improved after 1 year from baseline in patients treated with anti-IL-5Rα as compared to placebo. Furthermore, treated patients experienced improved asthma symptoms, control and quality of life, as well as a 27-40% reduction in exacerbation risk; anti-IL-5Rα had no significant effect on FeNO. The BORA[182] and MELTEMI[183] trials extended these initial clinical trials for one and four more years, respectively. These extensions demonstrated that

the improvements in exacerbation rate and airflow obstruction observed after 1 year were maintained.

Due to the high cost of biologic therapies, there is growing interest to identify characteristics that may help select patients that will respond to these therapies. In a small group of 24 patients with eosinophilic asthma, baseline eosinophil count greater than 100 cells/μL and FeNO greater than 40 ppb significantly predicted anti-IL-5Rα responders.[184] In contrast, patients with low levels of serum inflammatory markers were more likely to respond to anti-IL-5Rα after 4 months. A larger cohort study revealed that improvement in ACQ and decreased OCS after 3-months of anti-IL-5Rα therapy significantly discriminated responders from non-responders.[185] The lack of consensus about which measurements to use to predict anti-IL-5Rα responders may be due to a lack of consensus about how to define responders. Each study outlined here used a different test to define response, including a reduction in ACQ greater than the MCID, improvement in FEV_1 greater than 10% or a reduction in OCS use or exacerbation rate, respectively. Before a consensus can be reached about what constitutes anti-IL-5Rα response, we first must understand the mechanisms responsible for such improvements.

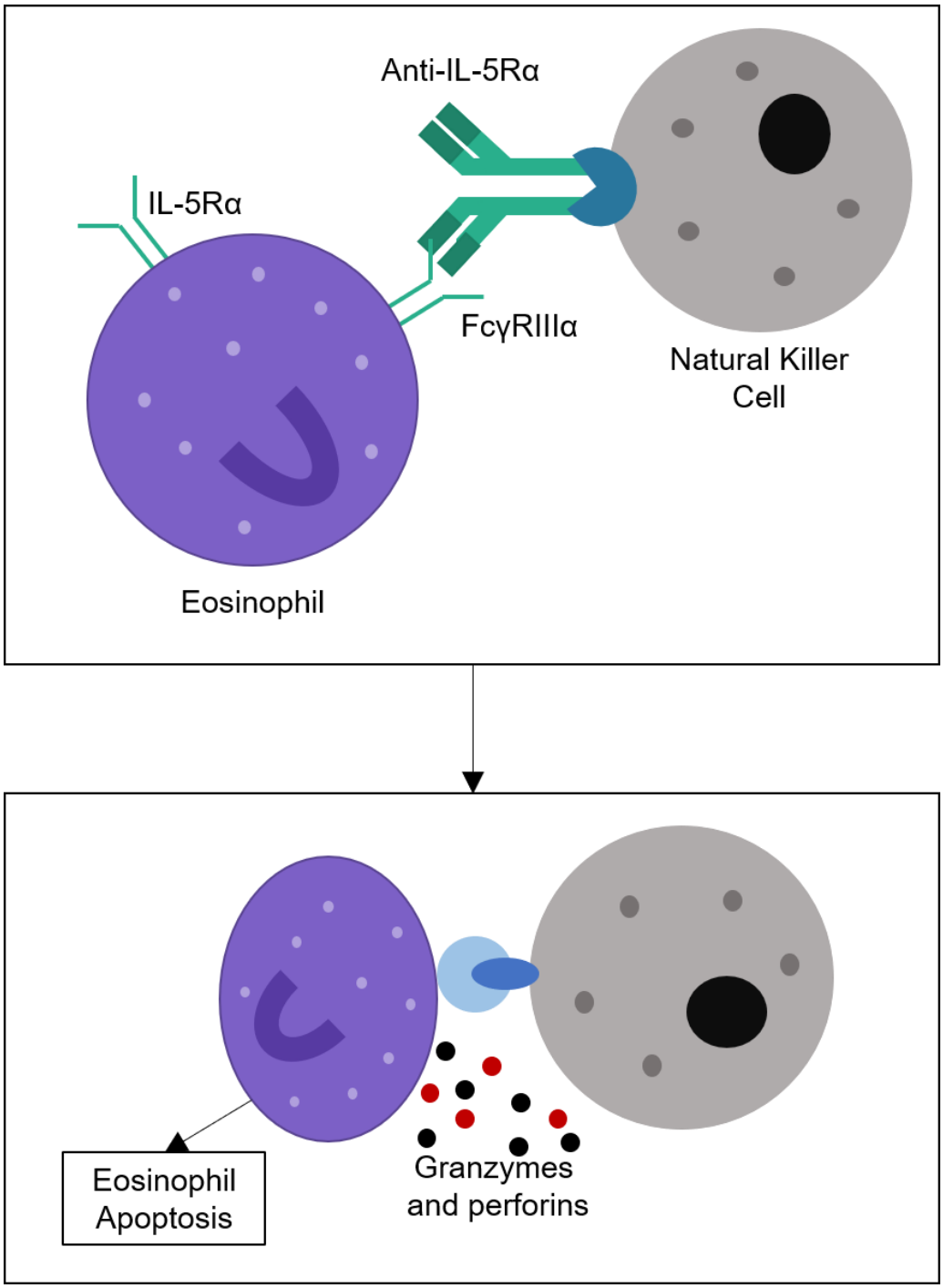

Figure 1-9. Anti-IL-5Rα Mechanism of Action
Anti-IL-5Rα binds to the FcγRIIIα receptor on eosinophils then signals to natural killer cells to induce eosinophil apoptosis.
Adapted from Pelaia, et al. BioMed Res Int (2018).[1]

1.6 Imaging Lung Structure and Function in Asthma

1.6.1 Planar X-ray

Chest radiography is one of the most common image modalities used to evaluate the lung, however, it is limited to a two-dimensional projection of lung structure. With the patient standing upright, the x-ray source is positioned at their back so that the beam enters from the posterior side and exits from the anterior side. The x-rays are absorbed to different degrees in different tissues, which is described as x-ray attenuation. High attenuating tissues absorb many x-rays and appear white on the resultant x-ray image, while low attenuating tissues appear black. Chest x-ray is not routinely acquired in patients with asthma and its primary role is to rule out other causes of respiratory symptoms such as the presence or absence of pneumonia, although hyperinflation, bronchial wall thickening and large volumes of mucus may also be detected using chest x-ray.[186-189]

1.6.2 X-ray Computed Tomography

Computed tomography (CT) imaging is made possible by the use of an x-ray source and detector array. These are situated opposite of each other and rotate around the patient to acquire multiple images at different angles. Chest x-ray is acquired while the patient is supine and under breathhold conditions, typically full inspiration or full expiration. CT images are reconstructed into a three-dimensional image using techniques such as filtered back projection or iterative reconstruction.[190]

Voxel values in a CT image represent the x-ray attenuation coefficient – that is the reduction in the intensity of the x-ray beam, by either absorption or deflection. This value is conventionally measured in Hounsfield units (HU),[191] with water having an x-ray attenuation coefficient of 0 HU, while air has HU of -1000 and the lung parenchyma has HU of approximately -800. The x-ray attenuation coefficient depends on several tissue and beam

properties such as the mass density and composition of the material, as well as the photon energy interacting with that material. The radiation dose associated with a conventional chest CT acquisition is between 7-8 mSV,[192] while low-dose and ultra low-dose protocols subject the patient to radiation doses close to 1.6 mSv[193,194] and 0.1-0.4 mSv,[195,196] respectively.

Qualitative pulmonary CT findings in asthma include airway wall thickening, dilation and narrowing, bronchiectasis, mucoid impaction and air-trapping, as well as vascular remodelling. Advances in image processing techniques and software, including VIDAvision and Insights (VIDA Diagnostics Inc., Coralville, IA, USA) allow for the quantification of airway and vessel morphology in addition to tissue densities, and these methods and their context in asthma are described in this chapter.

1.6.2.1 Airways

Airway morphology measurements are typically quantified using inspiratory CT. Semi-automated and automated algorithms recognize the cylindrical shape of the airway, as well as the inherent contrast between the vascularized airway wall and the air-filled lumen. Some investigations have shown that airways as small as 0.88 mm in diameter, or approximately the sixth generation, can be resolved using CT,[197-199] however, the smallest detectable CT airway will depend on the resolution of the image, according to Nyquist's Theorem.[200] CT airway measurements include wall thickness (WT, WT%) and wall area (WA, WA%), as well as lumen area (LA) and total airway count (TAC).

Computed tomography investigations in asthma have revealed thicker airway walls[53,201,202] and narrower airway lumens[201] as compared to patients with COPD and healthy controls. Airway walls are thicker in patients with more severe disease,[53,203-205] and is associated with airflow obstruction[53,202,206] and airway hyperresponsiveness.[53,207] Moreover, in asthma, increased sputum eosinophil counts were associated with thicker airway walls and narrower airway

lumens as measured using CT.[208] In both COPD[209] and asthma,[205] TAC was diminished across disease severity. Furthermore, in asthma, TAC was associated with airway wall thickness[205] and, in COPD, was related to the number of terminal bronchioles measured using micro-CT.[210] There are few investigations that have measured the effect of various asthma treatments on quantitative CT airway measurements in humans. Following bronchial thermoplasty, airway walls were thinner[211,212] and the airway lumen was dilated,[211] while ICS significantly reduced airway wall thickening in asthma patients.[213,214]

1.6.2.2 Mucus Occlusion

Luminal plugging is a key characteristic feature of asthma[215-218] and has been identified using CT.[42,55] While it has been thought that chronic cough and phlegm indicate airway luminal plugging,[215] recent studies in asthma[55] have observed that up to 40% of patients with CT evidence of luminal plugging failed to report these symptoms, demonstrating the importance of pulmonary imaging to evaluate asthma pathophysiology. CT luminal occlusions may be quantified as a "mucus score"[55] with a range of 0 to 20.

High CT identified luminal plugging is associated with decreased lung function and increased air trapping[42,55] and airway wall thickness,[219-221] worse health-related quality of life,[55] sputum eosinophilia[55] and FeNO.[42] Asthma patients with CT mucus plugs have an enhanced spirometric response to bronchodilator,[55] although post-BD spirometry in patients with CT mucus plugs is still worse than in patients without. This suggests that patients with high mucus scores may require additional treatment – potentially biologic therapies with mucoregulatory effects[222-225] – to improve airflow obstruction, disease symptoms and overall quality of life. CT luminal plugs have also been shown to be persistent over 5 years in patients with asthma and often occurred in the same airway segment,[55,56] which suggests that certain airways may

be more susceptible to luminal plugging, possibly by abnormal mucus hypersecretion, ciliary dysfunction, or airway narrowing or thickening.[219]

1.6.2.3 Parenchyma

Due to CT-resolution limits, the evaluation of small airways (< 2 mm) is difficult. Air-trapping, visualized as regions of low-attenuation on CT, is often thought of as an indirect measurement of small airway abnormalities. This metric is typically quantified using full-expiration CT images and is expressed as the percentage of low attenuation area (LAA) of voxels less than a given threshold, most commonly described as -856 HU.[226] CT air-trapping in asthma is associated with pulmonary function measures of central and peripheral airflow obstruction, airways resistance and air trapping,[227-229] is significantly greater than in healthy controls,[227-229] and is associated with markers of severe disease, including hospitalizations.[230] Moreover, clinical trials have revealed that CT air-trapping was significantly reduced in response to ICS[231] and LTRA[232] as well as bronchial thermoplasty.[212]

1.6.2.4 Vasculature

CT pulmonary vasculature may be quantified using automated algorithms[233] to generate blood volumes in the small (<5 mm^2 cross sectional area) to large (>10 mm^2 cross sectional area) vessels. Abnormal CT vascular measurements have been associated with disease severity and poor outcomes in patients with COPD,[58,234-239] though few investigations have explored CT pulmonary vascular remodelling in asthma. The Severe Asthma Research Program[57] revealed that patients with asthma had reduced small vessel volumes as compared to healthy controls, and this vascular remodelling was related to asthma control and severity, as well as eosinophilia.[57] Moreover, more severe vascular pruning was associated with an increased risk of exacerbations.

1.6.3 Nuclear Medicine

Nuclear medicine techniques utilize radioisotopes or radiolabelled tracers to image lung function, including ventilation, perfusion and ventilation-perfusion mismatch. These images are typically combined with anatomical images, such as planar x-ray or CT, to relate pulmonary function to pulmonary structure. Hybrid nuclear medicine imaging systems using either CT or MRI have become available for the simultaneous imaging of lung function and structure.[240-242]

1.6.3.1 Scintigraphy

Scintigraphy measures gamma radiation emitted from the radioisotopes to produce two-dimensional images. Patients in the supine position are given radioactive or radiolabelled isotopes via injection or through inhalation. Once in the body, these isotopes undergo collisions with atoms to produce gamma radiation that is subsequently detected by gamma cameras. High signal intensity or "hot spots" in these images indicate high levels of the radionuclide in that region. Common pulmonary evaluations using scintigraphy include ventilation and perfusion (V/Q). Radioisotopes are typically inhaled as a gas, aerosolized liquid or aerosolized solid particles, and include ^{99m}Technetium (Tc) diethylenetriaminepentaacetic acid, ^{99m}Tc-labelled solid graphite hydrophobic particles, ^{133}Xenon (Xe) or ^{81m}Krypton for ventilation imaging, and ^{99m}Tc-macro aggregated albumin for perfusion imaging. While scintigraphy is most commonly used to evaluate pulmonary embolisms, it was the first imaging modality to measure the ventilation distribution in patients with asthma more than 50 years ago, and has since revealed significant ventilation abnormalities in asthma.[243] Ventilation and perfusion response to bronchoprovocation in asthma,[244-246] as well as the regional deposition of asthma medications in the lung[247-249] have been assessed using scintigraphy.[244-246]

1.6.3.2 Single Photon Emission Computed Tomography

Similar to scintigraphy, single photon emission CT (SPECT) uses gamma cameras, however, this modality detects photons and is able to provide three-dimensional images. Photons emitted from the radiotracer interact with the tissue to cause scatter and attenuation, similar to computed tomography. The same radiotracers that are used in scintigraphy may also be used in SPECT, with multiple two-dimensional images being acquired and then reconstructed to form a three-dimensional image. The total dose to the patient from this scan varies based on the radiotracer used. For example, the approximate radiation dose to the patient from a combined V/Q scan using ^{99m}Tc as the radiotracer is 2-3 mSv.[250]

The first demonstration of the ventilation distribution in asthma imaged using SPECT was completed in 1986.[251] Technegas[252] was used for SPECT imaging in healthy participants[253,254] and patients with asthma[254,255] to measure airway closure, which was, in asthma, related to hyperresponsiveness and small airways disease.[255] SPECT ventilation abnormalities in some patients with asthma were responsive to asthma therapy,[256,257] and were more numerous and/or had a greater volume after methacholine challenge.[255,258] Furthermore, SPECT imaging has been used in a pilot study to visualize airway inflammation in patients with asthma,[259] and, more recently, SPECT imaging has been used to detect the distribution of ^{99m}Tc labelled eosinophils.[260]

1.6.3.3 Positron Emission Tomography

Position emission tomography (PET) also provides a three-dimensional image. Positron-emitting radiotracers may be used to measure pulmonary ventilation, perfusion and blood flow, as well as metabolic activity. The radiotracer will emit a positron once inside the body, which only travels a short distance before colliding with an electron and annihilating, thus producing two 511 keV photons that are emitted at 180°. These photons are detected by PET detectors

oriented around the patient. The spatial location of the source particle may be determined and a three-dimensional volumetric image may then be reconstructed.[261]

One of the most common molecules used for PET imaging is ^{18}F-fluorodeoxyglucose (^{18}F-FDG) which may be used to image inflammation.[262] While several studies have shown increased FDG uptake in inflammatory lung conditions,[263,264] asthma investigations have reported conflicting results. There was regionally increased FDG uptake in asthma patients as compared to healthy controls following allergen challenge in one study,[265] while another showed no difference between FDG uptake in asthma versus healthy volunteers;[264] however, ^{11}C-labelled PK11195, which binds to macrophages, was increased in patients with asthma in this study. Ventilation may also be evaluated using the PET radiotracer nitrogen-13 ($^{13}N_2$), which can be injected as a bolus or inhaled. When injected, $^{13}N_2$ perfuses into the lung and is subsequently washed out by ventilation. Signal intense regions may thus correspond to regions of gas trapping. Using this technique, perfusion to ventilation defect regions was reduced following bronchoconstriction in asthma.[266] In contrast, when used as an inhaled agent, signal intense regions correspond to well-ventilated regions of the lung.

1.6.4 Magnetic Resonance Imaging

Magnetic resonance imaging (MRI) is an ionizing-radiation-free image modality that uses an external magnetic field to align the spin of specific nuclei in the body. These nuclei return to their original spin following the application of radiofrequency (RF) waves and they subsequently emit RF energy. MR images are acquired during this release of energy. MRI is conventionally used to excite protons (^{1}H) and thus provides excellent soft tissue contrast. Structural and functional MR imaging techniques and applications are discussed in this section.

1.6.4.1 Conventional ^{1}H MRI

Due to the low ^{1}H density of lung tissue (~0.1 g/cm^{3}), the signal-to-noise ratio (SNR) within the lung is relatively low when using a conventional ^{1}H acquisition. Susceptibility artefacts due to the alveolar air-tissue interfaces and the extremely rapid signal dephasing and decay, alongside cardiac and respiratory motion, also make this acquisition technically challenging. Ultra-short echo time (UTE) MRI techniques have been developed to reduce the time between RF excitation and data acquisition such that lung tissue signal may be acquired before the signal decays. In asthma, UTE MRI has been used to evaluate structural properties of the lung. The mean UTE signal intensity in asthma patients was significantly lower than in healthy controls and was related to mean lung density measured using CT, hyperpolarized noble gas MRI ventilation abnormalities and pulmonary function test measurements.[267] In addition, in asthma, UTE-measured bronchial wall dimensions were comparable to those measured using CT.[268] Pulmonary edema following allergen challenge has also been measured using UTE in both animal models[269] and humans.[270]

Recent technical developments in the field have demonstrated the feasibility of 0.55 T MRI for pulmonary evaluations.[271] The elongated T2* (10 ms for 0.55 T versus 2 ms for 1.5 T) and improved field homogeneity[271] at this magnet strength addresses some of the limitations of conventional ^{1}H MRI described previously. Initial investigations[271-273] have demonstrated that 0.55 T MR images were comparable to CT and were able to detect pulmonary abnormalities including cysts, bronchial wall thickening, consolidation and nodules. These results are promising; however, additional work must be done to evaluate the robustness of this method, the reproducibility and repeatability of the images, and to compare quantitative airway, vessel and tissue measurements with those generated using quantitative CT.

1.6.4.2 Hyperpolarized Noble Gas MRI

Hyperpolarized gas MRI enables the visualization of airway function by using ^{3}He or ^{129}Xe as an inhaled contrast agent. The first hyperpolarized noble gas MR image was acquired in an excised rat lung using ^{129}Xe in 1994 by Albert and colleagues,[30] and the first human images were acquired shortly after using ^{3}He. [226,227] Using spin-exchange optical pumping, the spin density of the noble gas can be increased 100,000 times greater than thermal polarization. Circularly polarized light is aimed at a cell containing an alkali metal, typically rubidium, which polarizes the material. The noble gas collides with the polarized material, transferring angular momentum to the noble gas and increasing the nuclear-spin polarization. The acquisition of hyperpolarized gas images requires highly-trained personnel and specialized equipment to polarize the gas (polarizer) and acquire the images (radiofrequency coil), as well as an MRI scanner equipped with multi-nuclear capabilities.

Despite the first hyperpolarized images being acquired using ^{129}Xe,[30] the field quickly moved in favour of ^{3}He imaging[274,275] due to its larger nuclear magnetic moment and gyromagnetic ratio (32.434 MHz/T for ^{3}He versus 11.777 MHz/T for ^{129}Xe) and higher levels of polarization (30-40% for ^{3}He versus 8-25% for ^{129}Xe) as compared to ^{129}Xe. However, in recent years, depleting global quantities and increased cost of ^{3}He,[276] as well as improvements in ^{129}Xe polarization equipment[277,278] and the ability of ^{129}Xe to diffuse across the alveolar capillary membrane and bind to red blood cells,[279] has pushed the field towards ^{129}Xe as the contrast agent of choice.[280] In fact, owing in part to its excellent safety and tolerability in healthy volunteers and patients with lung disease,[281-283] hyperpolarized ^{129}Xe MRI is now approved for clinical use in the United Kingdom and the United States of America.

Ventilation

The acquisition of static ventilation MR images is the most common application of MRI using hyperpolarised noble gases. To obtain these images, patients are positioned supine in the MR scanner and may inhale up to 1.0 L of gas,[29,31] after which three-dimensional whole lung images may be acquired during a relatively short breath-hold of 10-12 seconds. The ventilation distribution in patients with normal, healthy lungs is homogenous throughout the lung; however, in patients with asthma, regions of low signal or signal void caused by partially or fully obstructed airways,[284] can be seen throughout the lung. This signal intensity variation is often described as ventilation heterogeneity or ventilation defects, as shown in **Figure 1-10**. Ventilation defects in patients with asthma may be caused by segmental or subsegmental airway obstructions, and, as such, are characteristically wedge- and pyramidal-shaped.[31-36] These abnormalities are clinically relevant because they are uniquely predictive of asthma control,[38] worsen with increasing asthma severity,[35] and correlate with clinical measures of airflow obstruction,[285] ventilation heterogeneity[38,49] and small airway abnormalities.[116,118] Furthermore, they have been shown to be reproducible temporally, spatially[34,36,37,286] and across multiple sites,[287] and are comparable to those visualized using scintigraphy[288] and SPECT.[289-291]

The initial quantification of MRI ventilation abnormalities was achieved using reader-based scoring systems,[33,35,292] in which ventilation defects were described categorically as mild, moderate or severe,[292] or simply counted.[33,35] There are inherent challenges associated with reader-based scoring systems, such as inter- and intra-reader variability. Thus, quantitative segmentations completed either manually[293] or semi-automatically[235,236 294,295] were developed to measure validated biomarkers including ventilated volume[293] and percentage ventilation volume,[292] or the ventilation defect volume[296] and ventilation defect percent (VDP),[297] with VDP being the most commonly reported measurement. VDP measurements may be quantified

using several methods, including linear binning,[298,299] signal intensity thresholding[295] or K-means clustering.[294] In this thesis, a semi-automated K-means clustering algorithm was used to quantify ventilation abnormalities.[104] Using this algorithm, ventilation images are separated into four distinct clusters, with the lowest signal intensity cluster being clustered again, resulting in a total of five clusters. The lowest signal intensity cluster is then used to estimate the volume of signal void or ventilation defects. This volume is normalized to the total thoracic cavity volume to calculate VDP.

Asthma investigations have uncovered evidence to suggest that hyperpolarized gas MRI ventilation defects are related to asthma pathophysiology. Following both methacholine challenge[31,36,300] and exercise testing,[31] the number and size of ventilation abnormalities increased. MRI abnormalities worsened to a greater degree after methacholine than spirometry[36,301] and were spatially persistent and/or recurrent.[36,37] Moreover, ventilation abnormalities in asthma decrease in number and size following bronchodilator[49,298,302,303] and bronchial thermoplasty treatments,[46-48] as shown in **Figure 1-10**. Ventilation abnormalities are quantitatively related to airway inflammation,[40,41] sputum eosinophilia[40] and FeNO,[300] and spatially correspond to mucus occluded airways.[42,304] As such, MRI ventilation has been shown to improve following anti-T2 therapy[44,45] (**Figure 1-10**). CT evidence of airway narrowing,[118] remodelling[205] and air-trapping[296] have also been shown to be associated with MRI ventilation heterogeneity. Together, these results suggest that airway hyperresponsiveness, inflammation, and remodelling as well as mucus occlusions contribute to the ventilation distribution visualized using hyperpolarized gas MRI.

Because of the important relationships between pathological features of eosinophilic asthma and ventilation defects, improvements following therapy and the temporal and spatial

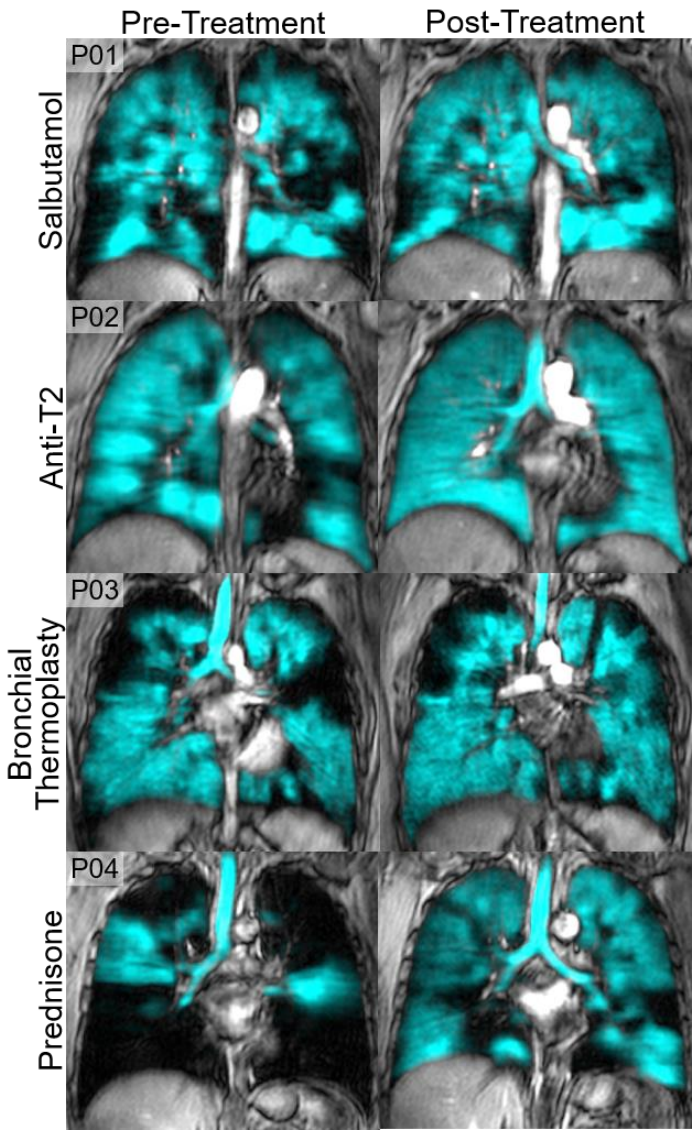

Figure 1-10. ^{129}Xe MRI Ventilation Pre and Post-Treatment in Asthma
^{129}Xe MRI ventilation (cyan) co-registered with ^{1}H (greyscale) before and after treatment. Adapted and reprinted from Kooner, et al. Respirology (2022),[2] with permission (Appendix A).

persistence of defects, hyperpolarized gas MRI may be an invaluable tool to evaluate response to anti-IL-5Rα therapy in eosinophilic asthma patients.

Diffusion Weighted

Diffusion-weighted MRI provides a tool to measure the alveolar microstructure by taking advantage of the random Brownian motion of the noble gas in the airspace. The restricted motion of the gas in the alveoli and terminal bronchioles is quantified as the "apparent"

diffusion coefficient (ADC).[305-307] Previous work has shown that the destruction of alveolar walls[281,282] or alveolar enlargement via air-trapping[308] results in increased diffusion and therefore greater ADC values. Furthermore, ADC values tend to increase with age.[309] These changes may be reflective of natural physiologic enlargement of the airways over time or senile emphysema. In patients with asthma but not in healthy controls, MRI ADC significantly increased following a methacholine challenge and these abnormalities were shown to resolve post-bronchodilator.[300]

Dissolved Phase

Hyperpolarized ^{129}Xe is able to diffuse across the alveoli, through the alveolar-capillary membrane, into the capillaries and then the red blood cells[310] due to its relatively high Ostwald solubility coefficient.[311] The ^{129}Xe uptake in each of these compartments may be imaged and quantified by taking advantage of the distinct resonance frequency shifts of ^{129}Xe.[266,267] Each "dissolved-phase" peak may be separated; the gas phase peak at 0 ppm, the alveolar-capillary membrane peak at approximately 198 ppm and the red blood cell peak at approximately 218 ppm.[312,313] Measurements acquired using this technique are typically expressed as the ratio between peaks, including the membrane to gas, red blood cell to gas, and red blood cell to membrane ratios,[314] which may reflect physiological characteristics including gas-blood barrier wall thickness,[315] surface-to-volume ratio,[316] gas transfer efficiency[265,267,275] or pulmonary perfusion. [317,318]

A limited number of studies to date have used dissolved phase imaging to investigate asthma. Patients with asthma have demonstrated both increased and decreased red blood cell to membrane ratio.[314] An elevated ratio may indicate angiogenesis or cardiovascular compensation while a decreased ratio may reflect tissue destruction or a decreased surface-to-volume ratio, perhaps caused by air-trapping.[314,319] In the same study, older asthma patients

reported diminished red blood cell to gas ratio while younger asthma patients did not.[319] However, recent studies[320,321] have revealed that dissolved phase ratios may be age dependent, and whether these previous asthma findings hold true following age-corrections[322] remains to be determined.

1.7 Thesis Hypotheses and Objectives

Eosinophilic asthma[102,323] and the mechanism of action of anti-IL-5Rα on systemic and airway eosinophil depletion[179,181] have been well characterized. However, the influence of such treatment on pulmonary structure and function in poorly-controlled eosinophilic asthma is not well understood. Specifically, whether anti-IL-5Rα results in disease-modifying effects[17] and whether it may play a role in asthma remission[16] are not yet known. Lung function changes following asthma therapy are evaluated using pulmonary function tests, such as spirometry and FeNO. Spirometry is a measurement of airflow obstruction, however, it can only inform on the severity of the airflow obstruction and cannot provide information about the source of the obstruction which, in asthma, may be the result of luminal occlusion or narrowing, or airway wall thickening, inflammation or smooth muscle dysfunction, or a combination of these. Therefore, spirometry cannot provide information about the pathophysiology responsible for airflow limitation improvements following therapy. In contrast, FeNO is considered to be a biomarker of eosinophilic inflammation.[137,138] In pivotal clinical trials, however, it was insensitive to airway inflammation changes following anti-IL-5Rα initiation.[26,27] This may be, in part, due to the fact that IL-13, and not IL-5, induces the production of nitric oxide in the lung.[28] Thus, neither spirometry nor FeNO can provide clues about whether anti-IL-5Rα results in disease-modifying effects in eosinophilic asthma. These limitations have prompted the development of sensitive and specific pulmonary imaging techniques, such as hyperpolarized

noble gas MRI and quantitative CT airway and vascular measurements, which may be used to evaluate regional functional and structural abnormalities which are spatially and quantitatively related to several characteristic features of eosinophilic asthma, including sputum eosinophilia, and airway luminal occlusions, narrowing and wall thickening, as well as disease severity and control.

Thus, the overarching objective of this thesis was to use hyperpolarized ^{129}Xe MRI and chest CT to evaluate pulmonary function and structure following continuous anti-IL-5Rα therapy and to compare with pre-treatment measurements to better our understanding of the mechanisms responsible for improved asthma control and airflow obstruction.

The overarching hypothesis is that airway function measured via ^{129}Xe MRI VDP and airway and vessel structure measured via chest CT would be significantly improved following anti-IL-5Rα treatment initiation, and that imaging biomarkers would significantly explain improved asthma control. The specific hypotheses and objectives for each chapter are described below.

We first wanted to determine the threshold for clinically relevant changes in and for abnormal ^{129}Xe MRI ventilation measurements, to better characterize asthma and its response to treatment in the context of ventilation MRI. Based on previous work which showed that ^{129}Xe MRI was more sensitive to ventilation abnormalities than ^{3}He MRI, we hypothesized that the upper limit of normal (ULN) and minimal clinically important difference (MCID) for ^{129}Xe VDP would differ from previously calculated values for ^{3}He MRI. In **Chapter 2**, the objective was to determine the ULN using a group of healthy participants across a range of ages, and to determine the MCID for ^{129}Xe MRI VDP in asthma patients across a range of disease severity.

We next wanted to explore whether ventilation defects in eosinophilic asthma would change after the initiation of anti-IL-5Rα (benralizumab) and how quantitative CT airway measurements may influence this potential response. The aim of **Chapter 3** was to quantify

early ^{129}Xe MRI ventilation defect changes after a first injection of benralizumab and then to examine whether baseline mucus impacted such changes. We hypothesized that ^{129}Xe MRI VDP would significantly improve 28-days after the first injection of benralizumab in patients with poorly-controlled eosinophilic asthma.

To further understand the longitudinal effect of anti-IL-5Rα on pulmonary structure and function, we evaluated the same participants after long-term, continuous therapy. In **Chapter 4**, we aimed to measure ^{129}Xe MRI ventilation defects and CT mucus score after 1- and 2.5-years of therapy and compare longitudinal measurements with those acquired pre-treatment. We hypothesized that early ventilation improvements would be maintained with long-term therapy and that baseline luminal occlusions would be resolved at 2.5-years.

Finally, based on previous work in severe asthma demonstrating significant associations between vascular remodelling and eosinophilia, we wondered whether CT pulmonary vessel measurements would change in response to anti-IL-5Rα-driven eosinophilic depletion. Accordingly, the objective of **Chapter 5** was to quantify pulmonary vascular volume in the small and large pulmonary vessels in patients with poorly-controlled, eosinophilic asthma prior to anti-IL-5Rα treatment initiation and following 2.5-years of therapy. We hypothesized that long-term anti-IL-5Rα biologic therapy would influence the finding of pulmonary vessel changes in severe asthma.

In **Chapter 6**, I provide an overview and summary of the important findings and conclusions of **Chapters 2-5**. Next, the general limitations of this work as well as specific limitations of each chapter are discussed. This thesis concludes with an outline of future investigations that will build on the foundations provided by this thesis.

1.8 References

1. Pelaia, C., *et al.* Benralizumab: From the Basic Mechanism of Action to the Potential Use in the Biological Therapy of Severe Eosinophilic Asthma. *Biomed Res Int* (2018).

2. Kooner, H.K., *et al.* Pulmonary functional MRI: Detecting the structure-function pathologies that drive asthma symptoms and quality of life. *Respirology* **27**, 114-133 (2022).

3. Araujo, B.B., *et al.* Extracellular matrix components and regulators in the airway smooth muscle in asthma. *Eur Respir J* **32**, 61-69 (2008).

4. Sheel, A.W., *et al.* Evidence for dysanapsis using computed tomographic imaging of the airways in older ex-smokers. *J Appl Physiol (1985)* **107**, 1622-1628 (2009).

5. Global Initiative for Asthma (GINA). Global Strategy for Asthma Management and Prevention. (2022).

6. Lumb, A. *Nunn's applied respiratory physiology*, (Elsevier, New York, 2017).

7. Cockcroft, D.W. History of asthma in Canada. *Can J Respir Crit Care Sleep Med* **6**, 375-382 (2022).

8. Lee, T.Y., *et al.* 16-year trends in asthma hospital admissions in Canada. *Ann Allergy Asthma Immunol* **129**, 475-480 e472 (2022).

9. Mostaco-Guidolin, L.B., Yang, C.X. & Hackett, T.L. Pulmonary Vascular Remodeling Is an Early Feature of Fatal and Nonfatal Asthma. *Am J Respir Cell Mol Biol* **65**, 114-118 (2021).

10. Asher, M.I., *et al.* Worldwide time trends in the prevalence of symptoms of asthma, allergic rhinoconjunctivitis, and eczema in childhood: ISAAC Phases One and Three repeat multicountry cross-sectional surveys. *Lancet* **368**, 733-743 (2006).

11. Canada, S. Canadian Community Health Survey (CCHS). (2020).

12. Sadatsafavi, M., McTaggart-Cowan, H., Chen, W. & FitzGerald, J.M. Quality of life and asthma symptom control: room for improvement in care and measurement. *Value Health* **18**, 1043-1049 (2015).

13. Zafari, Z., Sadatsafavi, M., Chen, W. & FitzGerald, J.M. The projected economic and health burden of sub-optimal asthma control in Canada. *Respir Med* **138**, 7-12 (2018).

14. Carpaij, O.A., *et al.* Childhood factors associated with complete and clinical asthma remission at 25 and 49 years. *Eur Respir J* **49**(2017).

15. Vonk, J.M., *et al.* Childhood factors associated with asthma remission after 30 year follow up. *Thorax* **59**, 925-929 (2004).

16. Thomas, D., McDonald, V.M., Pavord, I.D. & Gibson, P.G. Asthma remission: what is it and how can it be achieved? *Eur Respir J* **60**(2022).

17. Busse, W.W., Melen, E. & Menzies-Gow, A.N. Holy Grail: the journey towards disease modification in asthma. *Eur Respir Rev* **31**(2022).

18. Menzies-Gow, A., *et al.* An expert consensus framework for asthma remission as a treatment goal. *J Allergy Clin Immunol* **145**, 757-765 (2020).

19. Arnold, S., *et al.* Discontinuation of biologic DMARDs in a real-world population of patients with rheumatoid arthritis in remission: outcome and risk factors. *Rheumatology (Oxford)* **61**, 131-138 (2021).

20. Schlager, L., Loiskandl, M., Aletaha, D. & Radner, H. Predictors of successful discontinuation of biologic and targeted synthetic DMARDs in patients with rheumatoid arthritis in remission or low disease activity: a systematic literature review. *Rheumatology (Oxford)* **59**, 324-334 (2020).

21. Ulrik, C.S. & Frederiksen, J. Mortality and markers of risk of asthma death among 1,075 outpatients with asthma. *Chest* **108**, 10-15 (1995).

22. Hospers, J.J., Schouten, J.P., Weiss, S.T., Postma, D.S. & Rijcken, B. Eosinophilia is associated with increased all-cause mortality after a follow-up of 30 years in a general population sample. *Epidemiology* **11**, 261-268 (2000).

23. Tupper, O.D. & Ulrik, C.S. Long-term predictors of severe exacerbations and mortality in a cohort of well-characterised adults with asthma. *Respir Res* **22**, 269 (2021).

24. Tran, T.N., Khatry, D.B., Ke, X., Ward, C.K. & Gossage, D. High blood eosinophil count is associated with more frequent asthma attacks in asthma patients. *Ann Allergy Asthma Immunol* **113**, 19-24 (2014).

25. Zeiger, R.S., *et al.* High blood eosinophil count is a risk factor for future asthma exacerbations in adult persistent asthma. *J Allergy Clin Immunol Pract* **2**, 741-750 (2014).

26. Bleecker, E.R., *et al.* Efficacy and safety of benralizumab for patients with severe asthma uncontrolled with high-dosage inhaled corticosteroids and long-acting beta2-agonists (SIROCCO): a randomised, multicentre, placebo-controlled phase 3 trial. *Lancet* **388**, 2115-2127 (2016).

27. FitzGerald, J.M., *et al.* Benralizumab, an anti-interleukin-5 receptor alpha monoclonal antibody, as add-on treatment for patients with severe, uncontrolled, eosinophilic asthma (CALIMA): a randomised, double-blind, placebo-controlled phase 3 trial. *Lancet* **388**, 2128-2141 (2016).

28. Ricciardolo, F.L.M. & Silkoff, P.E. Perspectives on exhaled nitric oxide. *J Breath Res* **11**, 047104 (2017).

29. Pelaia, C., *et al.* Biological Therapy of Severe Asthma with Dupilumab, a Dual Receptor Antagonist of Interleukins 4 and 13. *Vaccines (Basel)* **10**(2022).

30. Albert, M.S., *et al.* Biological magnetic resonance imaging using laser-polarized 129Xe. *Nature* **370**, 199-201 (1994).

31. Samee, S., *et al.* Imaging the lungs in asthmatic patients by using hyperpolarized helium-3 magnetic resonance: assessment of response to methacholine and exercise challenge. *J Allergy Clin Immunol* **111**, 1205-1211 (2003).

32. Altes, T.A., *et al.* Clinical correlates of lung ventilation defects in asthmatic children. *J Allergy Clin Immunol* **137**, 789-796 e787 (2016).

33. Altes, T.A., *et al.* Hyperpolarized 3He MR lung ventilation imaging in asthmatics: preliminary findings. *J Magn Reson Imaging* **13**, 378-384 (2001).

34. de Lange, E.E., *et al.* Changes in regional airflow obstruction over time in the lungs of patients with asthma: evaluation with 3He MR imaging. *Radiology* **250**, 567-575 (2009).

35. de Lange, E.E., *et al.* Evaluation of asthma with hyperpolarized helium-3 MRI: correlation with clinical severity and spirometry. *Chest* **130**, 1055-1062 (2006).

36. de Lange, E.E., *et al.* The variability of regional airflow obstruction within the lungs of patients with asthma: assessment with hyperpolarized helium-3 magnetic resonance imaging. *J Allergy Clin Immunol* **119**, 1072-1078 (2007).

37. Eddy, R.L., Svenningsen, S., Licskai, C., McCormack, D.G. & Parraga, G. Hyperpolarized Helium 3 MRI in Mild-to-Moderate Asthma: Prediction of Postbronchodilator Reversibility. *Radiology* **293**, 212-220 (2019).

38. Svenningsen, S., Nair, P., Guo, F., McCormack, D.G. & Parraga, G. Is ventilation heterogeneity related to asthma control? *Eur Respir J* **48**, 370-379 (2016).

39. Mummy, D.G., *et al.* Ventilation defects on hyperpolarized helium-3 MRI in asthma are predictive of 2-year exacerbation frequency. *J Allergy Clin Immunol* **146**, 831-839 e836 (2020).

40. Svenningsen, S., *et al.* Sputum Eosinophilia and Magnetic Resonance Imaging Ventilation Heterogeneity in Severe Asthma. *Am J Respir Crit Care Med* **197**, 876-884 (2018).

41. Svenningsen, S., *et al.* What are ventilation defects in asthma? *Thorax* **69**, 63-71 (2014).

42. Svenningsen, S., *et al.* CT and Functional MRI to Evaluate Airway Mucus in Severe Asthma. *Chest* **155**, 1178-1189 (2019).

43. Mummy, D.G., *et al.* Mucus Plugs in Asthma at CT Associated with Regional Ventilation Defects at Helium 3 MRI. *Radiology*, 204616 (2021).

44. Svenningsen, S., Eddy, R.L., Kjarsgaard, M., Parraga, G. & Nair, P. Effects of Anti-T2 Biologic Treatment on Lung Ventilation Evaluated by MRI in Adults With Prednisone-Dependent Asthma. *Chest* **158**, 1350-1360 (2020).

45. Svenningsen, S., Haider, E.A., Eddy, R.L., Parraga, G. & Nair, P. Normalisation of MRI ventilation heterogeneity in severe asthma by dupilumab. *Thorax* **74**, 1087-1088 (2019).

46. Svenningsen, S., *et al.* Bronchial thermoplasty guided by hyperpolarised gas magnetic resonance imaging in adults with severe asthma: a 1-year pilot randomised trial. *ERJ Open Res* **7**(2021).

47. Hall, C.S., *et al.* Single-Session Bronchial Thermoplasty Guided by (129)Xe Magnetic Resonance Imaging. A Pilot Randomized Controlled Clinical Trial. *Am J Respir Crit Care Med* **202**, 524-534 (2020).

48. Thomen, R.P., *et al.* Regional ventilation changes in severe asthma after bronchial thermoplasty with (3)He MR imaging and CT. *Radiology* **274**, 250-259 (2015).

49. Safavi, S., *et al.* Evaluating post-bronchodilator response in well-controlled paediatric severe asthma using hyperpolarised 129Xe-MRI: A pilot study. *Respir Med* **180**, 106368 (2021).

50. Cincinnati Children's Images First Clinical Patient in North America Using Novel Xenon Gas. (2023).

51. Bateman, E.D., *et al.* Global strategy for asthma management and prevention: GINA executive summary. *Eur Respir J* **31**, 143-178 (2008).

52. Network, B.T.S.S.I.G. British guideline on the management of asthma a national clinical guideline. *Thorax* **63**, 64 (2008).

53. Aysola, R.S., *et al.* Airway remodeling measured by multidetector CT is increased in severe asthma and correlates with pathology. *Chest* **134**, 1183-1191 (2008).

54. Krings, J.G., *et al.* Quantitative CT metrics are associated with longitudinal lung function decline and future asthma exacerbations: Results from SARP-3. *J Allergy Clin Immunol* **148**, 752-762 (2021).

55. Dunican, E.M., *et al.* Mucus plugs in patients with asthma linked to eosinophilia and airflow obstruction. *J Clin Invest* **128**, 997-1009 (2018).

56. Tang, M., *et al.* Mucus Plugs Persist in Asthma, and Changes in Mucus Plugs Associate with Changes in Airflow over Time. *Am J Respir Crit Care Med* **205**, 1036-1045 (2022).

57. Ash, S.Y., *et al.* Pruning of the Pulmonary Vasculature in Asthma. The Severe Asthma Research Program (SARP) Cohort. *Am J Respir Crit Care Med* **198**, 39-50 (2018).

58. Chaouat, A., Naeije, R. & Weitzenblum, E. Pulmonary hypertension in COPD. *Eur Respir J* **32**, 1371-1385 (2008).

59. Davis, B.E., Blais, C.M. & Cockcroft, D.W. Methacholine challenge testing: comparative pharmacology. *J Asthma Allergy* **11**, 89-99 (2018).

60. Bleecker, E.R., Emmett, A., Crater, G., Knobil, K. & Kalberg, C. Lung function and symptom improvement with fluticasone propionate/salmeterol and ipratropium bromide/albuterol in COPD: response by beta-agonist reversibility. *Pulm Pharmacol Ther* **21**, 682-688 (2008).

61. Levine, H., *et al.* Reversible airway obstruction in cystic fibrosis: Common, but not associated with characteristics of asthma. *J Cyst Fibros* **15**, 652-659 (2016).

62. Tashkin, D.P., *et al.* Bronchodilator responsiveness in patients with COPD. *Eur Respir J* **31**, 742-750 (2008).

63. Joshi, S., *et al.* Exercise-induced bronchoconstriction in school-aged children who had chronic lung disease in infancy. *J Pediatr* **162**, 813-818 e811 (2013).

64. Ramsdale, E.H., Morris, M.M., Roberts, R.S. & Hargreave, F.E. Bronchial responsiveness to methacholine in chronic bronchitis: relationship to airflow obstruction and cold air responsiveness. *Thorax* **39**, 912-918 (1984).

65. Ramsdale, E.H., Morris, M.M., Roberts, R.S. & Hargreave, F.E. Asymptomatic bronchial hyperresponsiveness in rhinitis. *J Allergy Clin Immunol* **75**, 573-577 (1985).

66. van Haren, E.H., *et al.* The effects of the inhaled corticosteroid budesonide on lung function and bronchial hyperresponsiveness in adult patients with cystic fibrosis. *Respir Med* **89**, 209-214 (1995).

67. Huber, H.L. & Koessler, K.K. The pathology of bronchial asthma. *Arch Intern Med* **30**, 689-760 (1922).

68. Bousquet, J., *et al.* Asthma: a disease remodeling the airways. *Allergy* **47**, 3-11 (1992).

69. Bai, T.R. Evidence for airway remodeling in chronic asthma. *Curr Opin Allergy Clin Immunol* **10**, 82-86 (2010).

70. Bergeron, C., Al-Ramli, W. & Hamid, Q. Remodeling in asthma. *Proc Am Thorac Soc* **6**, 301-305 (2009).

71. Hirota, N. & Martin, J.G. Mechanisms of airway remodeling. *Chest* **144**, 1026-1032 (2013).

72. Tang, M.L., Wilson, J.W., Stewart, A.G. & Royce, S.G. Airway remodelling in asthma: current understanding and implications for future therapies. *Pharmacol Ther* **112**, 474-488 (2006).

73. Hsieh, A., Assadinia, N. & Hackett, T.L. Airway remodeling heterogeneity in asthma and its relationship to disease outcomes. *Front Physiol* **14**, 1113100 (2023).

74. Fahy, J.V., Corry, D.B. & Boushey, H.A. Airway inflammation and remodeling in asthma. *Curr Opin Pulm Med* **6**, 15-20 (2000).

75. Wilson, J.W., Li, X. & Pain, M.C. The lack of distensibility of asthmatic airways. *Am Rev Respir Dis* **148**, 806-809 (1993).

76. Haney, S. & Hancox, R.J. Recovery from bronchoconstriction and bronchodilator tolerance. *Clin Rev Allergy Immunol* **31**, 181-196 (2006).

77. George, L. & Brightling, C.E. Eosinophilic airway inflammation: role in asthma and chronic obstructive pulmonary disease. *Ther Adv Chronic Dis* **7**, 34-51 (2016).

78. Saetta, M., Di Stefano, A., Rosina, C., Thiene, G. & Fabbri, L.M. Quantitative structural analysis of peripheral airways and arteries in sudden fatal asthma. *Am Rev Respir Dis* **143**, 138-143 (1991).

79. Postma, D.S. & Timens, W. Remodeling in asthma and chronic obstructive pulmonary disease. *Proc Am Thorac Soc* **3**, 434-439 (2006).

80. Harkness, L.M., Kanabar, V., Sharma, H.S., Westergren-Thorsson, G. & Larsson-Callerfelt, A.K. Pulmonary vascular changes in asthma and COPD. *Pulm Pharmacol Ther* **29**, 144-155 (2014).

81. Hashimoto, M., Tanaka, H. & Abe, S. Quantitative analysis of bronchial wall vascularity in the medium and small airways of patients with asthma and COPD. *Chest* **127**, 965-972 (2005).

82. Dunnill, M.S. The pathology of asthma, with special reference to changes in the bronchial mucosa. *J Clin Pathol* **13**, 27-33 (1960).

83. Kuwano, K., *et al.* Small airways dimensions in asthma and in chronic obstructive pulmonary disease. *Am Rev Respir Dis* **148**, 1220-1225 (1993).

84. Li, X. & Wilson, J.W. Increased vascularity of the bronchial mucosa in mild asthma. *Am J Respir Crit Care Med* **156**, 229-233 (1997).

85. McDonald, D.M. Angiogenesis and remodeling of airway vasculature in chronic inflammation. *Am J Respir Crit Care Med* **164**, S39-45 (2001).

86. Kumar, S.D., Emery, M.J., Atkins, N.D., Danta, I. & Wanner, A. Airway mucosal blood flow in bronchial asthma. *Am J Respir Crit Care Med* **158**, 153-156 (1998).

87. Vrugt, B., *et al.* Bronchial angiogenesis in severe glucocorticoid-dependent asthma. *Eur Respir J* **15**, 1014-1021 (2000).

88. Salvato, G. Quantitative and morphological analysis of the vascular bed in bronchial biopsy specimens from asthmatic and non-asthmatic subjects. *Thorax* **56**, 902-906 (2001).

89. Detoraki, A., *et al.* Angiogenesis and lymphangiogenesis in bronchial asthma. *Allergy* **65**, 946-958 (2010).

90. Zanini, A., Chetta, A., Imperatori, A.S., Spanevello, A. & Olivieri, D. The role of the bronchial microvasculature in the airway remodelling in asthma and COPD. *Respir Res* **11**, 132 (2010).

91. Doherty, T. & Broide, D. Cytokines and growth factors in airway remodeling in asthma. *Curr Opin Immunol* **19**, 676-680 (2007).

92. Berry, M., *et al.* Pathological features and inhaled corticosteroid response of eosinophilic and non-eosinophilic asthma. *Thorax* **62**, 1043-1049 (2007).

93. Fahy, J.V. Eosinophilic and neutrophilic inflammation in asthma: insights from clinical studies. *Proc Am Thorac Soc* **6**, 256-259 (2009).

94. Ellis, A. The pathological anatomy of bronchial asthma. *Am J Med Sci* **186**, 407 (1908).

95. Bousquet, J., *et al.* Eosinophilic inflammation in asthma. *N Engl J Med* **323**, 1033-1039 (1990).

96. Louis, R., *et al.* The relationship between airways inflammation and asthma severity. *Am J Respir Crit Care Med* **161**, 9-16 (2000).

97. Woodruff, P.G., *et al.* Relationship between airway inflammation, hyperresponsiveness, and obstruction in asthma. *J Allergy Clin Immunol* **108**, 753-758 (2001).

98. Deykin, A., *et al.* Sputum eosinophil counts predict asthma control after discontinuation of inhaled corticosteroids. *J Allergy Clin Immunol* **115**, 720-727 (2005).

99. Jatakanon, A., Lim, S. & Barnes, P.J. Changes in sputum eosinophils predict loss of asthma control. *Am J Respir Crit Care Med* **161**, 64-72 (2000).

100. Grunig, G., *et al.* Requirement for IL-13 independently of IL-4 in experimental asthma. *Science* **282**, 2261-2263 (1998).

101. Barrett, N.A. & Austen, K.F. Innate cells and T helper 2 cell immunity in airway inflammation. *Immunity* **31**, 425-437 (2009).

102. McBrien, C.N. & Menzies-Gow, A. The Biology of Eosinophils and Their Role in Asthma. *Front Med (Lausanne)* **4**, 93 (2017).

103. Lewis, R.A., *et al.* Prostaglandin D2 generation after activation of rat and human mast cells with anti-IgE. *J Immunol* **129**, 1627-1631 (1982).

104. Meijer, R.J., *et al.* Accuracy of eosinophils and eosinophil cationic protein to predict steroid improvement in asthma. *Clin Exp Allergy* **32**, 1096-1103 (2002).

105. Saydain, G., Beck, K.C., Decker, P.A., Cowl, C.T. & Scanlon, P.D. Clinical significance of elevated diffusing capacity. *Chest* **125**, 446-452 (2004).

106. Collard, P., Njinou, B., Nejadnik, B., Keyeux, A. & Frans, A. Single breath diffusing capacity for carbon monoxide in stable asthma. *Chest* **105**, 1426-1429 (1994).

107. Weitzman, R.H. & Wilson, A.F. Diffusing capacity and over-all ventilation:perfusion in asthma. *Am J Med* **57**, 767-774 (1974).

108. Keens, T.G., *et al.* Evaluation of the single-breath diffusing capacity in asthma and cystic fibrosis. *Chest* **76**, 41-44 (1979).

109. Dubois, A.B., Botelho, S.Y., Bedell, G.N., Marshall, R. & Comroe, J.H., Jr. A rapid plethysmographic method for measuring thoracic gas volume: a comparison with a nitrogen washout method for measuring functional residual capacity in normal subjects. *J Clin Invest* **35**, 322-326 (1956).

110. Kaczka, D.W., Lutchen, K.R. & Hantos, Z. Emergent behavior of regional heterogeneity in the lung and its effects on respiratory impedance. *J Appl Physiol (1985)* **110**, 1473-1481 (2011).

111. Lutchen, K.R. & Gillis, H. Relationship between heterogeneous changes in airway morphometry and lung resistance and elastance. *J Appl Physiol (1985)* **83**, 1192-1201 (1997).

112. Tgavalekos, N.T., Venegas, J.G., Suki, B. & Lutchen, K.R. Relation between structure, function, and imaging in a three-dimensional model of the lung. *Ann Biomed Eng* **31**, 363-373 (2003).

113. Heijkenskjold Rentzhog, C., *et al.* Overall and peripheral lung function assessment by spirometry and forced oscillation technique in relation to asthma diagnosis and control. *Clin Exp Allergy* **47**, 1546-1554 (2017).

114. Takeda, T., *et al.* Relationship between small airway function and health status, dyspnea and disease control in asthma. *Respiration* **80**, 120-126 (2010).

115. van der Wiel, E., ten Hacken, N.H., Postma, D.S. & van den Berge, M. Small-airways dysfunction associates with respiratory symptoms and clinical features of asthma: a systematic review. *J Allergy Clin Immunol* **131**, 646-657 (2013).

116. Young, H.M., Guo, F., Eddy, R.L., Maksym, G. & Parraga, G. Oscillometry and pulmonary MRI measurements of ventilation heterogeneity in obstructive lung disease: relationship to quality of life and disease control. *J Appl Physiol (1985)* **125**, 73-85 (2018).

117. Karayama, M., *et al.* Respiratory impedance is correlated with airway narrowing in asthma using three-dimensional computed tomography. *Clin Exp Allergy* **48**, 278-287 (2018).

118. Eddy, R.L., Westcott, A., Maksym, G.N., Parraga, G. & Dandurand, R.J. Oscillometry and pulmonary magnetic resonance imaging in asthma and COPD. *Physiol Rep* **7**, e13955 (2019).

119. Delacourt, C., *et al.* Use of the forced oscillation technique to assess airway obstruction and reversibility in children. *Am J Respir Crit Care Med* **161**, 730-736 (2000).

120. Kaczka, D.W., Ingenito, E.P., Israel, E. & Lutchen, K.R. Airway and lung tissue mechanics in asthma. Effects of albuterol. *Am J Respir Crit Care Med* **159**, 169-178 (1999).

121. Van Noord, J.A., Smeets, J., Clement, J., Van de Woestijne, K.P. & Demedts, M. Assessment of reversibility of airflow obstruction. *Am J Respir Crit Care Med* **150**, 551-554 (1994).

122. Zerah, F., Lorino, A.M., Lorino, H., Harf, A. & Macquin-Mavier, I. Forced oscillation technique vs spirometry to assess bronchodilatation in patients with asthma and COPD. *Chest* **108**, 41-47 (1995).

123. Duiverman, E.J., Neijens, H.J., Van der Snee-van Smaalen, M. & Kerrebijn, K.F. Comparison of forced oscillometry and forced expirations for measuring dose-related responses to inhaled methacholine in asthmatic children. *Bull Eur Physiopathol Respir* **22**, 433-436 (1986).

124. Akamatsu, T., *et al.* Forced oscillation technique as a predictor of FEV1 improvement in asthma. *Respir Physiol Neurobiol* **236**, 78-83 (2017).

125. Ohbayashi, H., Kudo, S. & Ariga, M. Evaluation of Rapid Onset of Action of ICS/LABA Combination Therapies on Respiratory Function in Asthma Patients: A Single-Center, Open-Label, Randomized, Crossover Trial. *Pulm Ther* **4**, 159-169 (2018).

126. Sugawara, H., Saito, A., Yokoyama, S., Tsunematsu, K. & Takahashi, H. Comparison of therapeutic effects of inhaled corticosteroids on three subtypes of cough variant asthma as classified by the impulse oscillometry system. *Respir Res* **20**, 41 (2019).

127. Fowler, W.S. Lung function studies; uneven pulmonary ventilation in normal subjects and in patients with pulmonary disease. *J Appl Physiol* **2**, 283-299 (1949).

128. Robertson, J.S., Siri, W.E. & Jones, H.B. Lung ventilation patterns determined by analysis of nitrogen elimination rates; use of mass spectrometer as a continuous gas analyzer. *J Clin Invest* **29**, 577-590 (1950).

129. Robinson, P.D., *et al.* Consensus statement for inert gas washout measurement using multiple- and single- breath tests. *Eur Respir J* **41**, 507-522 (2013).

130. Gustafsson, P.M. Peripheral airway involvement in CF and asthma compared by inert gas washout. *Pediatr Pulmonol* **42**, 168-176 (2007).

131. Zwitserloot, A., Fuchs, S.I., Muller, C., Bisdorf, K. & Gappa, M. Clinical application of inert gas Multiple Breath Washout in children and adolescents with asthma. *Respir Med* **108**, 1254-1259 (2014).

132. Bourdin, A., *et al.* Nitrogen washout slope in poorly controlled asthma. *Allergy* **61**, 85-89 (2006).

133. Macleod, K.A., *et al.* Ventilation heterogeneity in children with well controlled asthma with normal spirometry indicates residual airways disease. *Thorax* **64**, 33-37 (2009).

134. Downie, S.R., *et al.* Ventilation heterogeneity is a major determinant of airway hyperresponsiveness in asthma, independent of airway inflammation. *Thorax* **62**, 684-689 (2007).

135. Farah, C.S., *et al.* The role of the small airways in the clinical expression of asthma in adults. *J Allergy Clin Immunol* **129**, 381-387, 387 e381 (2012).

136. Farah, C.S., *et al.* Ventilation heterogeneity predicts asthma control in adults following inhaled corticosteroid dose titration. *J Allergy Clin Immunol* **130**, 61-68 (2012).

137. Thompson, B.R., *et al.* Peripheral lung function in patients with stable and unstable asthma. *J Allergy Clin Immunol* **131**, 1322-1328 (2013).

138. Verbanck, S., Schuermans, D., Paiva, M. & Vincken, W. The functional benefit of anti-inflammatory aerosols in the lung periphery. *J Allergy Clin Immunol* **118**, 340-346 (2006).

139. Verbanck, S., Schuermans, D., Paiva, M. & Vincken, W. Nonreversible conductive airway ventilation heterogeneity in mild asthma. *J Appl Physiol (1985)* **94**, 1380-1386 (2003).

140. Barnes, P.J. & Kharitonov, S.A. Exhaled nitric oxide: a new lung function test. *Thorax* **51**, 233-237 (1996).

141. Smith, A.D., Cowan, J.O., Brassett, K.P., Herbison, G.P. & Taylor, D.R. Use of exhaled nitric oxide measurements to guide treatment in chronic asthma. *N Engl J Med* **352**, 2163-2173 (2005).

142. Dweik, R.A., *et al.* An official ATS clinical practice guideline: interpretation of exhaled nitric oxide levels (FENO) for clinical applications. *Am J Respir Crit Care Med* **184**, 602-615 (2011).

143. Lane, C., *et al.* Epithelial inducible nitric oxide synthase activity is the major determinant of nitric oxide concentration in exhaled breath. *Thorax* **59**, 757-760 (2004).

144. Ricciardolo, F.L. Multiple roles of nitric oxide in the airways. *Thorax* **58**, 175-182 (2003).

145. Ricciardolo, F.L., Sterk, P.J., Gaston, B. & Folkerts, G. Nitric oxide in health and disease of the respiratory system. *Physiol Rev* **84**, 731-765 (2004).

146. Kacmarek, R.M., *et al.* Inhaled nitric oxide. A bronchodilator in mild asthmatics with methacholine-induced bronchospasm. *Am J Respir Crit Care Med* **153**, 128-135 (1996).

147. Berlyne, G.S., Parameswaran, K., Kamada, D., Efthimiadis, A. & Hargreave, F.E. A comparison of exhaled nitric oxide and induced sputum as markers of airway inflammation. *J Allergy Clin Immunol* **106**, 638-644 (2000).

148. Jatakanon, A., Lim, S., Kharitonov, S.A., Chung, K.F. & Barnes, P.J. Correlation between exhaled nitric oxide, sputum eosinophils, and methacholine responsiveness in patients with mild asthma. *Thorax* **53**, 91-95 (1998).

149. Lim, S., *et al.* Relationship between exhaled nitric oxide and mucosal eosinophilic inflammation in mild to moderately severe asthma. *Thorax* **55**, 184-188 (2000).

150. Payne, D.N., *et al.* Relationship between exhaled nitric oxide and mucosal eosinophilic inflammation in children with difficult asthma, after treatment with oral prednisolone. *Am J Respir Crit Care Med* **164**, 1376-1381 (2001).

151. Warke, T.J., *et al.* Exhaled nitric oxide correlates with airway eosinophils in childhood asthma. *Thorax* **57**, 383-387 (2002).

152. Alving, K., Weitzberg, E. & Lundberg, J.M. Increased amount of nitric oxide in exhaled air of asthmatics. *Eur Respir J* **6**, 1368-1370 (1993).

153. Kharitonov, S.A., *et al.* Increased nitric oxide in exhaled air of asthmatic patients. *Lancet* **343**, 133-135 (1994).

154. Smith, A.D., *et al.* Exhaled nitric oxide: a predictor of steroid response. *Am J Respir Crit Care Med* **172**, 453-459 (2005).

155. Saleh, D., Ernst, P., Lim, S., Barnes, P.J. & Giaid, A. Increased formation of the potent oxidant peroxynitrite in the airways of asthmatic patients is associated with induction of nitric oxide synthase: effect of inhaled glucocorticoid. *FASEB J* **12**, 929-937 (1998).

156. Juniper, E.F., O'Byrne, P.M., Guyatt, G.H., Ferrie, P.J. & King, D.R. Development and validation of a questionnaire to measure asthma control. *Eur Respir J* **14**, 902-907 (1999).

157. Juniper, E.F., Buist, A.S., Cox, F.M., Ferrie, P.J. & King, D.R. Validation of a standardized version of the Asthma Quality of Life Questionnaire. *Chest* **115**, 1265-1270 (1999).

158. Jones, P.W., Quirk, F.H., Baveystock, C.M. & Littlejohns, P. A self-complete measure of health status for chronic airflow limitation. The St. George's Respiratory Questionnaire. *Am Rev Respir Dis* **145**, 1321-1327 (1992).

159. Castro, M., *et al.* Reslizumab for poorly controlled, eosinophilic asthma: a randomized, placebo-controlled study. *Am J Respir Crit Care Med* **184**, 1125-1132 (2011).

160. Castro, M., *et al.* Effectiveness and safety of bronchial thermoplasty in the treatment of severe asthma: a multicenter, randomized, double-blind, sham-controlled clinical trial. *Am J Respir Crit Care Med* **181**, 116-124 (2010).

161. Cox, G., *et al.* Asthma control during the year after bronchial thermoplasty. *N Engl J Med* **356**, 1327-1337 (2007).

162. Chavannes, N.H., *et al.* Integrated disease management improves one-year quality of life in primary care COPD patients: a controlled clinical trial. *Prim Care Respir J* **18**, 171-176 (2009).

163. Juniper, E.F., Bousquet, J., Abetz, L., Bateman, E.D. & GOAL Committee. Identifying 'well-controlled' and 'not well-controlled' asthma using the Asthma Control Questionnaire. *Respir Med* **100**, 616-621 (2006).

164. Juniper, E.F., Guyatt, G.H., Willan, A. & Griffith, L.E. Determining a minimal important change in a disease-specific Quality of Life Questionnaire. *J Clin Epidemiol* **47**, 81-87 (1994).

165. Jones, P.W. St. George's Respiratory Questionnaire: MCID. *Copd* **2**, 75-79 (2005).

166. Ferrer, M., *et al.* Interpretation of quality of life scores from the St George's Respiratory Questionnaire. *Eur Respir J* **19**, 405-413 (2002).

167. Christie, R., *et al.* CONTROLLED trial of effects of cortisone acetate in chronic asthma; report to the Medical Research Council by the subcommittee on clini-cal trials in asthma. *Lancet* **271**, 798-803 (1956).

168. Barnes, P.J. Anti-inflammatory actions of glucocorticoids: molecular mechanisms. *Clin Sci (Lond)* **94**, 557-572 (1998).

169. Barnes, P.J. Effect of corticosteroids on airway hyperresponsiveness. *Am Rev Respir Dis* **141**, S70-76 (1990).

170. Ducharme, F.M., Ni Chroinin, M., Greenstone, I. & Lasserson, T.J. Addition of long-acting beta2-agonists to inhaled corticosteroids versus same dose inhaled corticosteroids for chronic asthma in adults and children. *Cochrane Database Syst Rev*, CD005535 (2010).

171. O'Byrne, P.M., Naya, I.P., Kallen, A., Postma, D.S. & Barnes, P.J. Increasing doses of inhaled corticosteroids compared to adding long-acting inhaled beta2-agonists in achieving asthma control. *Chest* **134**, 1192-1199 (2008).

172. Deykin, A., *et al.* Combination therapy with a long-acting beta-agonist and a leukotriene antagonist in moderate asthma. *Am J Respir Crit Care Med* **175**, 228-234 (2007).

173. Price, D., *et al.* Leukotriene antagonists as first-line or add-on asthma-controller therapy. *N Engl J Med* **364**, 1695-1707 (2011).

174. Gosens, R., Zaagsma, J., Meurs, H. & Halayko, A.J. Muscarinic receptor signaling in the pathophysiology of asthma and COPD. *Respir Res* **7**, 73 (2006).

175. Kew, K.M. & Dahri, K. Long-acting muscarinic antagonists (LAMA) added to combination long-acting beta2-agonists and inhaled corticosteroids (LABA/ICS) versus LABA/ICS for adults with asthma. *Cochrane Database Syst Rev* **2016**, CD011721 (2016).

176. Cox, P.G., Miller, J., Mitzner, W. & Leff, A.R. Radiofrequency ablation of airway smooth muscle for sustained treatment of asthma: preliminary investigations. *Eur Respir J* **24**, 659-663 (2004).

177. Pavord, I.D., *et al.* Safety and efficacy of bronchial thermoplasty in symptomatic, severe asthma. *Am J Respir Crit Care Med* **176**, 1185-1191 (2007).

178. Wechsler, M.E., *et al.* Bronchial thermoplasty: Long-term safety and effectiveness in patients with severe persistent asthma. *J Allergy Clin Immunol* **132**, 1295-1302 (2013).

179. Brusselle, G.G. & Koppelman, G.H. Biologic Therapies for Severe Asthma. *N Engl J Med* **386**, 157-171 (2022).

180. Busse, W.W., *et al.* Safety profile, pharmacokinetics, and biologic activity of MEDI-563, an anti-IL-5 receptor alpha antibody, in a phase I study of subjects with mild asthma. *J Allergy Clin Immunol* **125**, 1237-1244 e1232 (2010).

181. Laviolette, M., *et al.* Effects of benralizumab on airway eosinophils in asthmatic patients with sputum eosinophilia. *J Allergy Clin Immunol* **132**, 1086-1096 (2013).

182. FitzGerald, J.M., *et al.* Two-Year Integrated Efficacy And Safety Analysis Of Benralizumab In Severe Asthma. *J Asthma Allergy* **12**, 401-413 (2019).

183. Korn, S., *et al.* Integrated Safety and Efficacy Among Patients Receiving Benralizumab for Up to 5 Years. *J Allergy Clin Immunol Pract* **9**, 4381-4392 e4384 (2021).

184. Watanabe, H., *et al.* Blood eosinophil count and FeNO to predict benralizumab effectiveness in real-life severe asthma patients. *J Asthma* **59**, 1796-1804 (2022).

185. Kroes, J.A., *et al.* Clinical response to benralizumab can be predicted by combining clinical outcomes at 3 months with baseline characteristics. *ERJ Open Res* **9**(2023).

186. Gillam, G.L., McNicol, K.N. & Williams, H.E. Chest deformity, residual airways obstruction and hyperinflation, and growth in children with asthma. II. Significance of chronic chest deformity. *Arch Dis Child* **45**, 789-799 (1970).

187. Rebuck, A.S. Radiological aspects of severe asthma. *Australas Radiol* **14**, 264-268 (1970).

188. Paganin, F., *et al.* Chest radiography and high resolution computed tomography of the lungs in asthma. *Am Rev Respir Dis* **146**, 1084-1087 (1992).

189. Petheram, I.S., Kerr, I.H. & Collins, J.V. Value of chest radiographs in severe acute asthma. *Clin Radiol* **32**, 281-282 (1981).

190. Goldman, L.W. Principles of CT and CT technology. *J Nucl Med Technol* **35**, 115-128; quiz 129-130 (2007).

191. Hounsfield, G.N. Computerized transverse axial scanning (tomography). 1. Description of system. *Br J Radiol* **46**, 1016-1022 (1973).

192. Mettler, F.A., Jr., Huda, W., Yoshizumi, T.T. & Mahesh, M. Effective doses in radiology and diagnostic nuclear medicine: a catalog. *Radiology* **248**, 254-263 (2008).

193. Bourbeau, J., *et al.* Canadian Cohort Obstructive Lung Disease (CanCOLD): Fulfilling the need for longitudinal observational studies in COPD. *Copd* **11**, 125-132 (2014).

194. Regan, E.A., *et al.* Genetic epidemiology of COPD (COPDGene) study design. *Copd* **7**, 32-43 (2010).

195. Kim, Y., *et al.* Ultra-Low-Dose CT of the Thorax Using Iterative Reconstruction: Evaluation of Image Quality and Radiation Dose Reduction. *AJR Am J Roentgenol* **204**, 1197-1202 (2015).

196. Huber, A., *et al.* Performance of ultralow-dose CT with iterative reconstruction in lung cancer screening: limiting radiation exposure to the equivalent of conventional chest X-ray imaging. *Eur Radiol* **26**, 3643-3652 (2016).

197. Amirav, I., Kramer, S.S., Grunstein, M.M. & Hoffman, E.A. Assessment of methacholine-induced airway constriction by ultrafast high-resolution computed tomography. *J Appl Physiol (1985)* **75**, 2239-2250 (1993).

198. Forkert, L., Watanabe, H., Sutherland, K., Vincent, S. & Fisher, J.T. Quantitative videobronchoscopy: a new technique to assess airway caliber. *Am J Respir Crit Care Med* **154**, 1794-1803 (1996).

199. Seneterre, E., Paganin, F., Bruel, J.M., Michel, F.B. & Bousquet, J. Measurement of the internal size of bronchi using high resolution computed tomography (HRCT). *Eur Respir J* **7**, 596-600 (1994).

200. Shannon, C.E. Communication in the presence of noise. *Proceedings of the IRE* **37**, 10-21 (1949).

201. Oguma, T., *et al.* Longitudinal shape irregularity of airway lumen assessed by CT in patients with bronchial asthma and COPD. *Thorax* **70**, 719-724 (2015).

202. Niimi, A., *et al.* Airway wall thickness in asthma assessed by computed tomography. Relation to clinical indices. *Am J Respir Crit Care Med* **162**, 1518-1523 (2000).

203. Awadh, N., Muller, N.L., Park, C.S., Abboud, R.T. & FitzGerald, J.M. Airway wall thickness in patients with near fatal asthma and control groups: assessment with high resolution computed tomographic scanning. *Thorax* **53**, 248-253 (1998).

204. Little, S.A., *et al.* High resolution computed tomographic assessment of airway wall thickness in chronic asthma: reproducibility and relationship with lung function and severity. *Thorax* **57**, 247-253 (2002).

205. Eddy, R.L., *et al.* Is Computed Tomography Airway Count Related to Asthma Severity and Airway Structure and Function? *Am J Respir Crit Care Med* **201**, 923-933 (2020).

206. Kasahara, K., Shiba, K., Ozawa, T., Okuda, K. & Adachi, M. Correlation between the bronchial subepithelial layer and whole airway wall thickness in patients with asthma. *Thorax* **57**, 242-246 (2002).

207. Berair, R., *et al.* Associations in asthma between quantitative computed tomography and bronchial biopsy-derived airway remodelling. *Eur Respir J* **49**(2017).

208. Inoue, H., *et al.* CT-assessed large airway involvement and lung function decline in eosinophilic asthma: The association between induced sputum eosinophil differential counts and airway remodeling. *J Asthma* **53**, 914-921 (2016).

209. Kirby, M., *et al.* Total Airway Count on Computed Tomography and the Risk of Chronic Obstructive Pulmonary Disease Progression. Findings from a Population-based Study. *Am J Respir Crit Care Med* **197**, 56-65 (2018).

210. Kirby, M., *et al.* Computed Tomography Total Airway Count Is Associated with the Number of Micro-Computed Tomography Terminal Bronchioles. *Am J Respir Crit Care Med* **201**, 613-615 (2020).

211. Ishii, S., Iikura, M., Hojo, M. & Sugiyama, H. Use of 3D-CT airway analysis software to assess a patient with severe persistent bronchial asthma treated with bronchial thermoplasty. *Allergol Int* **66**, 501-503 (2017).

212. Konietzke, P., *et al.* Quantitative CT detects changes in airway dimensions and air-trapping after bronchial thermoplasty for severe asthma. *Eur J Radiol* **107**, 33-38 (2018).

213. Niimi, A., *et al.* Effect of short-term treatment with inhaled corticosteroid on airway wall thickening in asthma. *Am J Med* **116**, 725-731 (2004).

214. Lee, Y.M., *et al.* High-resolution CT findings in patients with near-fatal asthma: comparison of patients with mild-to-severe asthma and normal control subjects and changes in airway abnormalities following steroid treatment. *Chest* **126**, 1840-1848 (2004).

215. Burgel, P.R. & Martin, C. Mucus hypersecretion in COPD: should we only rely on symptoms? *Eur Respir Rev* **19**, 94-96 (2010).

216. Gibson, R.L., Burns, J.L. & Ramsey, B.W. Pathophysiology and management of pulmonary infections in cystic fibrosis. *Am J Respir Crit Care Med* **168**, 918-951 (2003).

217. Hays, S.R. & Fahy, J.V. The role of mucus in fatal asthma. *Am J Med* **115**, 68-69 (2003).

218. Hogg, J.C. The pathology of asthma. *APMIS* **105**, 735-745 (1997).

219. Tran, C., *et al.* Luminal mucus plugs are spatially associated with airway wall thickening in severe COPD and asthma: A single-centered, retrospective, observational study. *Respir Med* **202**, 106982 (2022).

220. Yoshida, Y., *et al.* Changes in airway diameter and mucus plugs in patients with asthma exacerbation. *PloS one* **15**, e0229238 (2020).

221. Okumura, K., *et al.* Mucus plugs and bronchial wall thickening on three-dimensional computed tomography in patients with unexplained chronic cough whose sputum yielded filamentous Basidiomycetes. *Eur Radiol* **30**, 3268-3276 (2020).

222. Brightling, C.E., *et al.* Efficacy and safety of tralokinumab in patients with severe uncontrolled asthma: a randomised, double-blind, placebo-controlled, phase 2b trial. *Lancet Respir Med* **3**, 692-701 (2015).

223. Hanania, N.A., *et al.* Efficacy and safety of lebrikizumab in patients with uncontrolled asthma (LAVOLTA I and LAVOLTA II): replicate, phase 3, randomised, double-blind, placebo-controlled trials. *Lancet Respir Med* **4**, 781-796 (2016).

224. Rabe, K.F., *et al.* Efficacy and Safety of Dupilumab in Glucocorticoid-Dependent Severe Asthma. *N Engl J Med* **378**, 2475-2485 (2018).

225. Wenzel, S., *et al.* Dupilumab efficacy and safety in adults with uncontrolled persistent asthma despite use of medium-to-high-dose inhaled corticosteroids plus a long-acting

beta2 agonist: a randomised double-blind placebo-controlled pivotal phase 2b dose-ranging trial. *Lancet* **388**, 31-44 (2016).

226. Jain, N., *et al.* Quantitative computed tomography detects peripheral airway disease in asthmatic children. *Pediatr Pulmonol* **40**, 211-218 (2005).

227. Newman, K.B., Lynch, D.A., Newman, L.S., Ellegood, D. & Newell, J.D., Jr. Quantitative computed tomography detects air trapping due to asthma. *Chest* **106**, 105-109 (1994).

228. Laurent, F., Latrabe, V., Raherison, C., Marthan, R. & Tunon-de-Lara, J.M. Functional significance of air trapping detected in moderate asthma. *Eur Radiol* **10**, 1404-1410 (2000).

229. Gono, H., Fujimoto, K., Kawakami, S. & Kubo, K. Evaluation of airway wall thickness and air trapping by HRCT in asymptomatic asthma. *Eur Respir J* **22**, 965-971 (2003).

230. Busacker, A., *et al.* A multivariate analysis of risk factors for the air-trapping asthmatic phenotype as measured by quantitative CT analysis. *Chest* **135**, 48-56 (2009).

231. Tunon-de-Lara, J.M., *et al.* Air trapping in mild and moderate asthma: effect of inhaled corticosteroids. *J Allergy Clin Immunol* **119**, 583-590 (2007).

232. Zeidler, M.R., *et al.* Montelukast improves regional air-trapping due to small airways obstruction in asthma. *Eur Respir J* **27**, 307-315 (2006).

233. Estepar, R.S., *et al.* Computational Vascular Morphometry for the Assessment of Pulmonary Vascular Disease Based on Scale-Space Particles. *Proc IEEE Int Symp Biomed Imaging*, 1479-1482 (2012).

234. Estepar, R.S., *et al.* Computed tomographic measures of pulmonary vascular morphology in smokers and their clinical implications. *Am J Respir Crit Care Med* **188**, 231-239 (2013).

235. Hale, K.A., Niewoehner, D.E. & Cosio, M.G. Morphologic changes in the muscular pulmonary arteries: relationship to cigarette smoking, airway disease, and emphysema. *Am Rev Respir Dis* **122**, 273-278 (1980).

236. Magee, F., Wright, J.L., Wiggs, B.R., Pare, P.D. & Hogg, J.C. Pulmonary vascular structure and function in chronic obstructive pulmonary disease. *Thorax* **43**, 183-189 (1988).

237. Minai, O.A., Chaouat, A. & Adnot, S. Pulmonary hypertension in COPD: epidemiology, significance, and management: pulmonary vascular disease: the global perspective. *Chest* **137**, 39S-51S (2010).

238. Rahaghi, F.N., *et al.* Arterial and Venous Pulmonary Vascular Morphology and Their Relationship to Findings in Cardiac Magnetic Resonance Imaging in Smokers. *J Comput Assist Tomogr* **40**, 948-952 (2016).

239. Wright, J.L., *et al.* The structure and function of the pulmonary vasculature in mild chronic obstructive pulmonary disease. The effect of oxygen and exercise. *Am Rev Respir Dis* **128**, 702-707 (1983).

240. Bybel, B., *et al.* SPECT/CT imaging: clinical utility of an emerging technology. *Radiographics* **28**, 1097-1113 (2008).

241. Kapoor, V., McCook, B.M. & Torok, F.S. An introduction to PET-CT imaging. *Radiographics* **24**, 523-543 (2004).

242. Quick, H.H. Integrated PET/MR. *J Magn Reson Imaging* **39**, 243-258 (2014).

243. Fujita, J., *et al.* Tc-99m Technegas scintigraphy to evaluate the lung ventilation in patients with oral corticosteroid-dependent bronchial asthma. *Ann Nucl Med* **13**, 247-251 (1999).

244. Novey, H., Wilson, A., SURPRENANT, E. & Bennett, L. Significance of early ventilation-perfusion defects in asthma. in *Journal of Allergy*, Vol. 43 179 (MOSBY-ELSEVIER 360 PARK AVENUE SOUTH, NEW YORK, NY 10010-1710 USA, 1969).

245. Wilson, A.F., *et al.* The significance of regional pulmonary function changes in bronchial asthma. *Am J Med* **48**, 416-423 (1970).

246. Parameswaran, K., Knight, A.C., Keaney, N.P., Williams, E.D. & Taylor, I.K. Ventilation and perfusion lung scintigraphy of allergen-induced airway responses in atopic asthmatic subjects. *Can Respir J* **14**, 285-291 (2007).

247. Newman, S., Salmon, A., Nave, R. & Drollmann, A. High lung deposition of 99mTc-labeled ciclesonide administered via HFA-MDI to patients with asthma. *Respir Med* **100**, 375-384 (2006).

248. Newman, S.P., Rivero, X., Luria, X., Hooper, G. & Pitcairn, G.R. A scintigraphic study to evaluate the deposition patterns of a novel anti-asthma drug inhaled from the Cyclohaler dry powder inhaler. *Adv Drug Deliv Rev* **26**, 59-67 (1997).

249. Hirst, P.H., Bacon, R.E., Pitcairn, G.R., Silvasti, M. & Newman, S.P. A comparison of the lung deposition of budesonide from Easyhaler, Turbuhaler and pMDI plus spacer in asthmatic patients. *Respir Med* **95**, 720-727 (2001).

250. Farrow, C. & King, G. SPECT Ventilation Imaging in Asthma. *Semin Nucl Med* **49**, 11-15 (2019).

251. Orphanidou, D., Hughes, J.M., Myers, M.J., Al-Suhali, A.R. & Henderson, B. Tomography of regional ventilation and perfusion using krypton 81m in normal subjects and asthmatic patients. *Thorax* **41**, 542-551 (1986).

252. Burch, W.M., Sullivan, P.J. & McLaren, C.J. Technegas--a new ventilation agent for lung scanning. *Nucl Med Commun* **7**, 865-871 (1986).

253. King, G.G., Eberl, S., Salome, C.M., Meikle, S.R. & Woolcock, A.J. Airway closure measured by a technegas bolus and SPECT. *Am J Respir Crit Care Med* **155**, 682-688 (1997).

254. King, G.G., Eberl, S., Salome, C.M., Young, I.H. & Woolcock, A.J. Differences in airway closure between normal and asthmatic subjects measured with single-photon emission computed tomography and technegas. *Am J Respir Crit Care Med* **158**, 1900-1906 (1998).

255. Farrow, C.E., *et al.* Airway closure on imaging relates to airway hyperresponsiveness and peripheral airway disease in asthma. *J Appl Physiol (1985)* **113**, 958-966 (2012).

256. McDonald, V.M., *et al.* Imaging for precision medicine: can V-P SPECT measure mepolizumab response in asthma? *Respirol Case Rep* **9**, e00717 (2021).

257. Rutting, S., *et al.* Effect of combination inhaled therapy on ventilation distribution measured by SPECT/CT imaging in uncontrolled asthma. *J Appl Physiol (1985)* **131**, 621-629 (2021).

258. Farrow, C.E., *et al.* Peripheral ventilation heterogeneity determines the extent of bronchoconstriction in asthma. *J Appl Physiol (1985)* **123**, 1188-1194 (2017).

259. George-Grandon, D.M. Imaging Inflammation in Asthma with Tc-99m HMPAO/SPECT. *J Allergy Clin Immunol* **125**, AB6 (2010).

260. Farahi, N., *et al.* In vivo imaging reveals increased eosinophil uptake in the lungs of obese asthmatic patients. *J Allergy Clin Immunol* **142**, 1659-1662 e1658 (2018).

261. Musch, G. & Venegas, J.G. Positron emission tomography imaging of regional pulmonary perfusion and ventilation. *Proc Am Thorac Soc* **2**, 522-527, 508-529 (2005).

262. Iking, J., *et al.* Imaging Inflammation with Positron Emission Tomography. *Biomedicines* **9**(2021).

263. Chen, D.L., *et al.* Quantifying pulmonary inflammation in cystic fibrosis with positron emission tomography. *Am J Respir Crit Care Med* **173**, 1363-1369 (2006).

264. Jones, H.A., Marino, P.S., Shakur, B.H. & Morrell, N.W. In vivo assessment of lung inflammatory cell activity in patients with COPD and asthma. *Eur Respir J* **21**, 567-573 (2003).

265. Taylor, I.K., *et al.* Imaging allergen-invoked airway inflammation in atopic asthma with [18F]-fluorodeoxyglucose and positron emission tomography. *Lancet* **347**, 937-940 (1996).

266. Harris, R.S., *et al.* Regional pulmonary perfusion, inflation, and ventilation defects in bronchoconstricted patients with asthma. *Am J Respir Crit Care Med* **174**, 245-253 (2006).

267. Sheikh, K., *et al.* Ultrashort echo time MRI biomarkers of asthma. *J Magn Reson Imaging* **45**, 1204-1215 (2017).

268. Benlala, I., *et al.* Evaluation of bronchial wall thickness in asthma using magnetic resonance imaging. *Eur Respir J* **59**(2022).

269. Ble, F.X., *et al.* Allergen-induced lung inflammation in actively sensitized mice assessed with MR imaging. *Radiology* **248**, 834-843 (2008).

270. Vogel-Claussen, J., *et al.* Quantification of pulmonary inflammation after segmental allergen challenge using turbo-inversion recovery-magnitude magnetic resonance imaging. *Am J Respir Crit Care Med* **189**, 650-657 (2014).

271. Campbell-Washburn, A.E., *et al.* Opportunities in Interventional and Diagnostic Imaging by Using High-Performance Low-Field-Strength MRI. *Radiology* **293**, 384-393 (2019).

272. Campbell-Washburn, A.E., *et al.* T2-weighted Lung Imaging Using a 0.55-T MRI System. *Radiol Cardiothorac Imaging* **3**, e200611 (2021).

273. Heiss, R., *et al.* High-performance low field MRI enables visualization of persistent pulmonary damage after COVID-19. *Magn Reson Imaging* **76**, 49-51 (2021).

274. Bachert, P., *et al.* Nuclear magnetic resonance imaging of airways in humans with use of hyperpolarized 3He. *Magn Reson Med* **36**, 192-196 (1996).

275. MacFall, J.R., *et al.* Human lung air spaces: potential for MR imaging with hyperpolarized He-3. *Radiology* **200**, 553-558 (1996).

276. Shea, D. & Morgan, D. The helium-3 shortage: supply, demand, and options for Congress. (Library of Congress, Congressional Research Service, 2010).

277. Hersman, F.W., *et al.* Large production system for hyperpolarized 129Xe for human lung imaging studies. *Acad Radiol* **15**, 683-692 (2008).

278. Nikolaou, P., *et al.* Near-unity nuclear polarization with an open-source 129Xe hyperpolarizer for NMR and MRI. *Proc Natl Acad Sci U S A* **110**, 14150-14155 (2013).

279. Cleveland, Z.I., *et al.* Hyperpolarized Xe MR imaging of alveolar gas uptake in humans. *PloS one* **5**, e12192 (2010).

280. Cho, A. Physics. Helium-3 shortage could put freeze on low-temperature research. *Science* **326**, 778-779 (2009).

281. Lutey, B.A., *et al.* Hyperpolarized 3He MR imaging: physiologic monitoring observations and safety considerations in 100 consecutive subjects. *Radiology* **248**, 655-661 (2008).

282. Shukla, Y., *et al.* Hyperpolarized 129Xe magnetic resonance imaging: tolerability in healthy volunteers and subjects with pulmonary disease. *Acad Radiol* **19**, 941-951 (2012).

283. Driehuys, B., *et al.* Chronic obstructive pulmonary disease: safety and tolerability of hyperpolarized 129Xe MR imaging in healthy volunteers and patients. *Radiology* **262**, 279-289 (2012).

284. Kauczor, H.U., *et al.* Normal and abnormal pulmonary ventilation: visualization at hyperpolarized He-3 MR imaging. *Radiology* **201**, 564-568 (1996).

285. Ebner, L., *et al.* Hyperpolarized 129Xenon Magnetic Resonance Imaging to Quantify Regional Ventilation Differences in Mild to Moderate Asthma: A Prospective Comparison Between Semiautomated Ventilation Defect Percentage Calculation and Pulmonary Function Tests. *Invest Radiol* **52**, 120-127 (2017).

286. Eddy, R.L., *et al.* Nonidentical Twins With Asthma: Spatially Matched CT Airway and MRI Ventilation Abnormalities. *Chest* **156**, e111-e116 (2019).

287. Svenningsen, S., *et al.* Reproducibility of Hyperpolarized (129)Xe MRI Ventilation Defect Percent in Severe Asthma to Evaluate Clinical Trial Feasibility. *Acad Radiol* **28**, 817-826 (2021).

288. Altes, T.A., *et al.* Ventilation imaging of the lung: comparison of hyperpolarized helium-3 MR imaging with Xe-133 scintigraphy. *Acad Radiol* **11**, 729-734 (2004).

289. Doganay, O., *et al.* Time-series hyperpolarized xenon-129 MRI of lobar lung ventilation of COPD in comparison to V/Q-SPECT/CT and CT. *Eur Radiol* **29**, 4058-4067 (2019).

290. Stavngaard, T., *et al.* Hyperpolarized 3He MRI and 81mKr SPECT in chronic obstructive pulmonary disease. *Eur J Nucl Med Mol Imaging* **32**, 448-457 (2005).

291. Radadia, N., *et al.* Comparison of ventilation defects quantified by Technegas SPECT and hyperpolarized 129Xe MRI. *Front Physiol* **14**, 615 (2023).

292. Donnelly, L.F., *et al.* Cystic fibrosis: combined hyperpolarized 3He-enhanced and conventional proton MR imaging in the lung--preliminary observations. *Radiology* **212**, 885-889 (1999).

293. Woodhouse, N., *et al.* Combined helium-3/proton magnetic resonance imaging measurement of ventilated lung volumes in smokers compared to never-smokers. *J Magn Reson Imaging* **21**, 365-369 (2005).

294. Kirby, M., *et al.* Hyperpolarized 3He magnetic resonance functional imaging semiautomated segmentation. *Acad Radiol* **19**, 141-152 (2012).

295. Couch, M.J., *et al.* A two-center analysis of hyperpolarized (129)Xe lung MRI in stable pediatric cystic fibrosis: Potential as a biomarker for multi-site trials. *J Cyst Fibros* **18**, 728-733 (2019).

296. Fain, S.B., *et al.* Evaluation of structure-function relationships in asthma using multidetector CT and hyperpolarized He-3 MRI. *Acad Radiol* **15**, 753-762 (2008).

297. Kirby, M., Wheatley, A., McCormack, D.G. & Parraga, G. Development and application of methods to quantify spatial and temporal hyperpolarized 3He MRI ventilation dynamics: preliminary results in chronic obstructive pulmonary disease. in *Medical Imaging 2010: Biomedical Applications in Molecular, Structural, and Functional Imaging*, Vol. 7626 762605 (International Society for Optics and Photonics, 2010).

298. He, M., Driehuys, B., Que, L.G. & Huang, Y.T. Using Hyperpolarized (129)Xe MRI to Quantify the Pulmonary Ventilation Distribution. *Acad Radiol* **23**, 1521-1531 (2016).

299. He, M., *et al.* Extending semiautomatic ventilation defect analysis for hyperpolarized (129)Xe ventilation MRI. *Acad Radiol* **21**, 1530-1541 (2014).

300. Costella, S., *et al.* Regional pulmonary response to a methacholine challenge using hyperpolarized (3)He magnetic resonance imaging. *Respirology* **17**, 1237-1246 (2012).

301. Kruger, S.J., *et al.* Hyperpolarized Helium-3 MRI of exercise-induced bronchoconstriction during challenge and therapy. *J Magn Reson Imaging* **39**, 1230-1237 (2014).

302. Svenningsen, S., *et al.* Hyperpolarized ^{3}He and ^{129}Xe MRI: Difference in Asthma Before Bronchodilation. *Journal of Magnetic Resonance Imaging* **38**, 9 (2013).

303. Marshall, H., *et al.* Peripheral and proximal lung ventilation in asthma: Short-term variation and response to bronchodilator inhalation. *J Allergy Clin Immunol* **147**, 2154-2161 e2156 (2021).

304. Mummy, D.D.E., Lampkins T, Zha W, Evans M, Schiebler M, Nagle SK, Sorkness RL, Jarjour NN, Fahy JV, Fain SB. Ventilation defects in asthma on hyperpolarized gas MRI are associated with airway mucus plugs on CT. *Am J Respir Crit Care Med* **197**, 2017-2018 (2018).

305. Saam, B.T., *et al.* MR imaging of diffusion of (3)He gas in healthy and diseased lungs. *Magn Reson Med* **44**, 174-179 (2000).

306. Yablonskiy, D.A., *et al.* Quantitative in vivo assessment of lung microstructure at the alveolar level with hyperpolarized 3He diffusion MRI. *Proc Natl Acad Sci U S A* **99**, 3111-3116 (2002).

307. Salerno, M., *et al.* Emphysema: hyperpolarized helium 3 diffusion MR imaging of the lungs compared with spirometric indexes--initial experience. *Radiology* **222**, 252-260 (2002).

308. Wang, C., *et al.* Assessment of the lung microstructure in patients with asthma using hyperpolarized 3He diffusion MRI at two time scales: comparison with healthy subjects and patients with COPD. *J Magn Reson Imaging* **28**, 80-88 (2008).

309. Altes, T.A., Mata, J., de Lange, E.E., Brookeman, J.R. & Mugler, J.P., 3rd. Assessment of lung development using hyperpolarized helium-3 diffusion MR imaging. *J Magn Reson Imaging* **24**, 1277-1283 (2006).

310. Kaushik, S.S., *et al.* Measuring diffusion limitation with a perfusion-limited gas--hyperpolarized 129Xe gas-transfer spectroscopy in patients with idiopathic pulmonary fibrosis. *J Appl Physiol* **117**, 577-585 (2014).

311. Weathersby, P.K. & Homer, L.D. Solubility of inert gases in biological fluids and tissues: a review. *Undersea Biomed Res* **7**, 277-296 (1980).

312. Mugler, J.P., 3rd, *et al.* MR imaging and spectroscopy using hyperpolarized 129Xe gas: preliminary human results. *Magn Reson Med* **37**, 809-815 (1997).

313. Wagshul, M.E., *et al.* In vivo MR imaging and spectroscopy using hyperpolarized 129Xe. *Magn Reson Med* **36**, 183-191 (1996).

314. Qing, K., *et al.* Regional mapping of gas uptake by blood and tissue in the human lung using hyperpolarized xenon-129 MRI. *J Magn Reson Imaging* **39**, 346-359 (2014).

315. Driehuys, B., *et al.* Imaging alveolar-capillary gas transfer using hyperpolarized 129Xe MRI. *Proceedings of the National Academy of Sciences of the United States of America* **103**, 18278-18283 (2006).

316. Butler, J.P., *et al.* Measuring surface-area-to-volume ratios in soft porous materials using laser-polarized xenon interphase exchange nuclear magnetic resonance. *J Phys Condens Matter* **14**, L297-304 (2002).

317. Mansson, S., Wolber, J., Driehuys, B., Wollmer, P. & Golman, K. Characterization of diffusing capacity and perfusion of the rat lung in a lipopolysaccaride disease model using hyperpolarized 129Xe. *Magn Reson Med* **50**, 1170-1179 (2003).

318. Cleveland, Z.I., *et al.* In vivo MR imaging of pulmonary perfusion and gas exchange in rats via continuous extracorporeal infusion of hyperpolarized 129Xe. *PloS one* **7**, e31306 (2012).

319. Qing, K., *et al.* Assessment of lung function in asthma and COPD using hyperpolarized 129Xe chemical shift saturation recovery spectroscopy and dissolved-phase MRI. *NMR Biomed* **27**, 1490-1501 (2014).

320. Wang, J.M., *et al.* Using hyperpolarized (129)Xe MRI to quantify regional gas transfer in idiopathic pulmonary fibrosis. *Thorax* **73**, 21-28 (2018).

321. Willmering, M.M., *et al.* Pediatric (129) Xe Gas-Transfer MRI-Feasibility and Applicability. *J Magn Reson Imaging* **56**, 1207-1219 (2022).

322. Plummer, J.W., *et al.* Childhood to adulthood: Accounting for age dependence in healthy-reference distributions in (129) Xe gas-exchange MRI. *Magn Reson Med* (2022).

323. Greenfeder, S., Umland, S.P., Cuss, F.M., Chapman, R.W. & Egan, R.W. Th2 cytokines and asthma. The role of interleukin-5 in allergic eosinophilic disease. *Respir Res* **2**, 71-79 (2001).

Chapter 2

2 ^{129}XE MRI VENTILATION DEFECTS IN ASTHMA: WHAT IS THE UPPER LIMIT OF NORMAL AND MINIMAL CLINICALLY IMPORTANT DIFFERENCE?

To better interpret ^{129}Xe MRI VDP in a clinical context, we estimated the minimal clinically important difference across a range of asthma severities using anchor-based and distribution-based approaches, and the upper limit of normal across a range of ages in healthy participants.

The contents of this chapter were previously published in the journal Academic Radiology: MJ McIntosh, A Biancaniello, HK Kooner, H Serajeddini, C Yamashita, G Parraga and RL Eddy. ^{129}Xe MRI Ventilation Defects in Asthma: What is the Upper Limit of Normal and Minimal Clinically Important Difference? Acad Radiol. 2023. *This article is available under the terms of the Creative Commons License BY-NC-ND 4.0.*

2.1 Introduction

Over the past two decades, pulmonary functional MRI using inhaled hyperpolarized ^{3}He or ^{129}Xe gas has provided a way to quantify ventilation heterogeneity as ventilation defect percent (VDP).[1] In asthma, MRI VDP was shown to be related to patient-reported symptoms and quality-of-life,[2,3] as well as sputum eosinophilia[4] and airway mucus-occlusions.[5,6] MRI VDP is sensitive to treatment response in patients with asthma,[7-9] and a number of small randomized treatment studies have also been performed using VDP.[10,11] However, in order to better understand treatment response in individual patients and the clinical meaning of VDP response beyond statistical significance, it has been important to estimate the minimal clinically important difference (MCID)[12] and upper limit of normal (ULN) for MRI VDP.

The MCID for hyperpolarized ^{3}HeMRI VDP was previously calculated using both anchor-(4%) and distribution-based (2%) approaches in patients with asthma.[13] In addition, the ULN for hyperpolarized ^{3}HeMRI VDP was estimated in healthy, elderly never-smokers.[14] The relationship of hyperpolarized MRI measurements with age was also previously demonstrated for ^{3}HeMRI apparent diffusion coefficients[15] and ^{129}XeMRI gas-exchange measurements.[16] Previous studies have shown that the number and volume of ventilation defects[17,18] increase

with age, and thus, the ULN of 3He VDP based on older participants may not reflect the same value in younger participants.

The limited global supply and increased cost of ^{3}He gas[19] have driven the research and clinical translation of hyperpolarized ^{129}Xe gas as the mainstay for pulmonary functional MRI. In head-to-head research comparisons in asthma[7] and chronic obstructive pulmonary disease,[20] ^{129}XeMRI VDP was significantly greater than ^{3}He VDP in the same participants, perhaps because of the substantial difference in density and viscosity,[7,21] as well as diffusivity,[22] which restricts ^{129}Xe gas flow through occluded, remodeled or inflamed airways.

We hypothesized, based on previous work, that the ULN and MCID would differ for ^{129}Xe VDP as compared to ^{3}He. Hence, we aimed to determine the ULN based on healthy participants across a range of ages and to determine the MCID for ^{129}XeMRI VDP in patients with asthma across a range of disease severity.

2.2 Methods

2.2.1 Study Participants and Design

Healthy participants and participants with a clinical diagnosis of asthma,[23,24] aged 18-80 years provided written informed consent to one of four approved protocols (www.ClinicalTrials.gov; healthy participants: NCT02484885, asthma: NCT02351141/NCT02263794/NCT03733535). All datasets were retrospectively evaluated. Data from this study are available at https://apilab.ca or directly from the corresponding author.

2.2.2 Spirometry and Asthma Questionnaires

Participants completed spirometry and ^{129}XeMRI within ~30 minutes. Asthma participants also completed the asthma control questionnaire (ACQ-7).[25] Spirometry[26] was performed to measure the forced expiratory volume in 1-second (FEV_1) and forced vital capacity (FVC)

according to American Thoracic Society guidelines using a whole-body plethysmograph (MedGraphics, Saint Paul, USA). For all participants, pre-bronchodilator measurements were evaluated. ACQ-7[25] was self-administered under the supervision of qualified study personnel.

2.2.3 Image Acquisition

Anatomic proton (^{1}H) and ^{129}Xe static ventilation MRI were acquired using a 3.0T scanner (Discovery MR750; GE Healthcare, Milwaukee, USA) with broadband capability as previously described [7] using coronal fast-spoiled gradient-recalled-echo sequences. Supine participants were coached to inhale a 1.0L bag (Tedlar; Jensen Inert Products, Coral Springs, USA) (400mL ^{129}Xe+600mL ^{4}He for ^{129}XeMRI and 1.0L N_2 for ^{1}H MRI) from functional residual capacity with acquisition under breath-hold conditions. ^{129}Xe gas was polarized to 30-40% (Polarean; Xenispin 9820, Durham, USA).

2.2.4 Image Analysis

Quantitative MRI analysis was performed using a pipeline which included semi-automated k-means segmentation algorithm after co-registration of the ^{1}H MRI thoracic cavity volume[27] using Matlab 2019a (Mathworks, Natick, USA), which classifies ^{129}Xe voxels into five signal intensity clusters (signal void+noise or ventilation defect volume (VDV) and four signal intensity clusters ranging from low to high). The clustered ^{129}Xe image was co-registered to the thoracic cavity mask segmented from ^{1}H MRI, and VDP was generated by normalizing the volume of signal void regions within the ^{1}H thoracic cavity mask (or VDV) to the thoracic cavity mask volume. Data were randomized and quantified by one of three trained observers (AB, four-months experience; MJM, three-years experience; RLE, seven-years experience).

2.2.5 Estimation of MCID and ULN

The MCID was measured based on pre-bronchodilator VDP measurements using anchor- and distribution-based approaches.[12] ACQ-7 was used to calculate the anchor-based MCID while the distribution-based (or data-driven) MCID was defined by VDP measurement precision as the standard error of measurement (SEM) or smallest detectable difference (SDD).[12,27] To evaluate the SDD for ^{129}Xe VDP, images from a subset of 10 asthma participants were quantified by two observers (AB, MJM). Participants were hand-selected to represent the full range of VDP in this cohort, and five repeated segmentation rounds were performed in randomized order, separated by at least 24-hours to minimize memory bias (10-datasets×5-rounds×2-observers), as previously described.[27] The SDD was calculated according to[28]:

$$SDD \geq z_{\propto}\sqrt{2}SEM$$

where z_{α}=1.96, corresponding to significance level α=0.05. *SEM* was the standard error of measurement from intraobserver variability, calculated using as:

$$SEM = \sqrt{\widehat{\sigma_e}^2}$$

where $\widehat{\sigma_e}^2$ was the intraobserver repeated measures variance. The ULN was calculated based on healthy controls as previously described[14]:

$$ULN = 95\%\ confidence\ interval = \bar{x} + 1.96 \cdot \frac{\sigma}{\sqrt{n}}$$

where, for healthy participants, $\bar{x}$ was the mean VDP, σ the standard deviation of VDP and n the sample size.

2.2.6 Statistical Analysis

SPSS Statistics 25.0 (IBM, Armonk, USA) was used for all statistical analyses. Data were tested for normality using Shapiro-Wilk tests and nonparametric tests were performed when data were not normally distributed. Differences between healthy and asthma participants were

evaluated using independent samples t-tests or Mann-Whitney U-tests. Univariate relationships were measured using Pearson (r) or Spearman (ρ) correlation coefficients. The Holm-Bonferroni correction was used for multiple comparisons. Results were considered statistically significant when the probability of making a type I error was <5% ($p<0.05$).

2.3 Results

2.3.1 Demographics and Study Design

A CONSORT diagram in **Figure 2-1** shows that 176 participants were enrolled (asthma n=130, healthy n=47). Sixty-seven participants (asthma n=58, healthy n=9) did not complete ^{129}XeMRI static ventilation imaging, five (asthma n=4, healthy n=1) had images acquired axially using a different MRI sequence, four (asthma n=1, healthy n=3) had images with low signal-noise ratio and two asthma participants had images with artifacts, and thus, were not evaluable. Seven (asthma n=4, healthy n=3) were excluded for tobacco, cannabis and/or vape use and nine (asthma n=6, healthy n=3) were excluded for lung disease or illness. Hence, we evaluated 55 participants with asthma (52±13-years, 34 female), including two GINA2, 10 GINA3, 17 GINA4 and 26 GINA5 participants, and 27 healthy participants (41±20-years, 15 female).

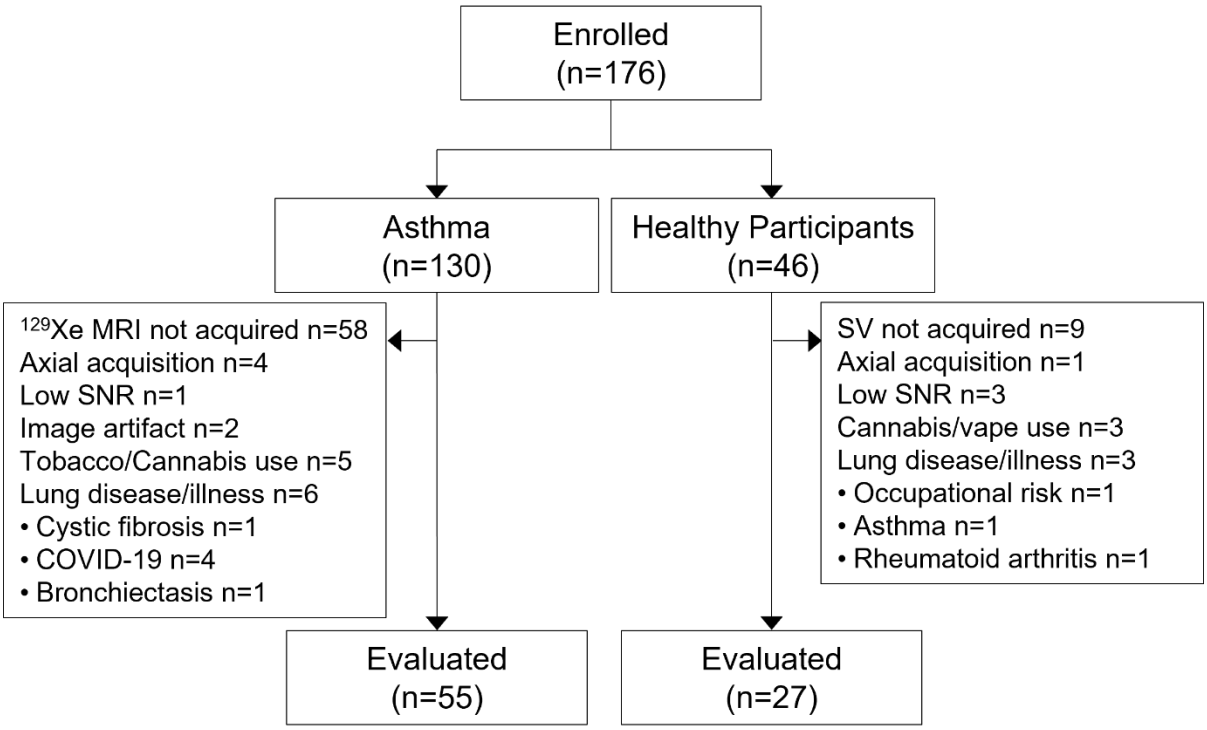

Figure 2-1. CONSORT diagram

SNR=signal-noise ratio; SV=static ventilation

Table 2-1 provides a summary of demographics characteristics, pulmonary function and MRI measurements for all participants, while **Table 2-2** provides a by-participant listing. Participants with asthma were significantly different than healthy participants for age (p=.04), body mass index (p<.001), FEV_1 (p<.001), FVC (p<.001), FEV_1/FVC (p<.001), VDV (p<.001) and VDP (p<.001). The proportion of females was not different between groups.

2.3.2 Upper Limit of Normal for ^{129}Xe MRI VDP

We used the 95% confidence interval to calculate the ULN in healthy participants as previously described.[14] **Figure 2-2** shows the relationship for age with VDP in healthy and asthma participants. VDP was significantly related to age for healthy participants (ρ=.56, p=.003), with a linear regression equation of VDP=.04·Age-.01, but not for asthma (ρ=.14, p=.3). Due to the significant age-VDP relationship in healthy participants, we calculated the ULN by age tertile as 1.3% for 18-39-years, 2.5% for 40-59-years and 3.8% for 60-years or older. The increase in ULN VDP with increasing age for three representative healthy participants is shown qualitatively in **Figure 2-3** with co-registered ^{1}H-^{129}Xe static ventilation images.

Table 2-1. Demographic characteristics, pulmonary function and MRI measurements

Parameter	All participants (n=82)	Healthy Controls (n=27)	Asthma (n=55)	Sig. p
Age years	48 ± 16	41 ± 20	52 ± 13	**.04**
Female n (%)	49 (60)	15 (56)	34 (62)	.6
BMI* kg/m^2	28 ± 6	25 ± 4	30 ± 6	**<.001**
ACQ	2.5 ± 1.4	-	2.5 ± 1.4	-
Pulmonary function				
FEV_1* $\%_{pred}$	77 ± 27	102 ± 12	67 ± 24	**<.001**
FVC* $\%_{pred}$	87 ± 20	105 ± 11	80 ± 19	**<.001**
FEV_1/FVC*	68 ± 16	78 ± 9	64 ± 17	**<.001**
^{129}Xe MRI				
VDV mL	474 ± 644	62 ± 46	676 ± 703	**<.001**
VDP %	9.7 ± 12.0	1.6 ± 1.2	13.7 ± 12.9	**<.001**

Data are reported as mean ± standard deviation, unless indicated otherwise.

BMI=body mass index; ACQ=asthma control questionnaire; FEV_1=forced expiratory volume in 1-second; $\%_{pred}$=percent of predicted; FVC=forced vital capacity; VDV=ventilation defect volume; VDP=ventilation defect percent; p=Holm-Bonferroni corrected independent samples t-test significance value for differences between healthy controls and participants with asthma.
Pulmonary function and MRI measurements are pre-bronchodilator.

BMI*: Healthy Controls n=25
FEV_1*: Healthy Controls n=20, Asthma n=54
FVC*, FEV_1/FVC*: Healthy Controls n=20, Asthma n=53

Table 2-2. By-participant listing of demographic, pulmonary function and imaging measurements

Participant	Age years	Sex	GINA	FEV_1 $\%_{pred}$	FVC $\%_{pred}$	FEV_1/FVC %	ACQ-7	VDP %
Healthy								
H01	19	F	-	116	114	90	-	0.9
H02	19	M	-	106	117	76	-	2.0
H03	20	M	-	99	98	83	-	0.9
H04	22	F	-	-	-	-	-	1.0
H05	23	F	-	-	-	-	-	0.8
H06	24	F	-	98	94	85	-	1.6
H07	24	F	-	-	-	-	-	0.0
H08	24	F	-	99	99	96	-	0.6
H09	24*	M	-	-	-	-	-	0.1
H10	26	F	-	92	87	91	-	0.8
H11	27*	F	-	-	-	-	-	0.6
H12	28	M	-	112	115	79	-	1.5
H13	30	M	-	103	104	81	-	0.7
H14	34	F	-	-	-	-	-	0.9
H15	37	M	-	93	109	68	-	2.4
H16	46	M	-	89	95	74	-	3.2
H17	46	F	-	-	-	-	-	0.8
H18	49	M	-	110	114	75	-	1.5
H19	51	M	-	120	112	83	-	2.0
H20	59	F	-	101	103	76	-	0.9
H21	62	F	-	129	134	74	-	1.5
H22	64	M	-	79	106	55	-	1.8
H23	67	M	-	95	101	72	-	4.2
H24	68	F	-	105	101	79	-	4.1
H25	69	M	-	101	99	75	-	4.1
H26	79	F	-	96	95	74	-	2.9
H27	79	F	-	93	99	70	-	1.3
Mean ± SD	41 ± 20	-	-	102 ± 12	105 ± 11	78 ± 9		1.6 ± 1.2
Asthma								
A01	56	M	4	37	80	35	3.14	47.9
A02	44	F	4	95	103	74	1.00	2.8
A03	42	M	4	69	82	67	1.43	7.4
A04	48	F	5	78	88	69	2.29	4.5
A05	41	M	2	107	108	79	1.71	3.6
A06	35	F	3	77	97	66	1.14	1.0
A07	38	M	4	44	106	33	1.00	12.6
A08	46	M	5	50	75	52	1.86	17.2
A09	59	M	5	113	103	79	0.14	9.2
A10	66	F	3	90	85	81	1.71	2.4
A11	54	M	5	105	102	79	3.14	7.9
A12	72	F	3	116	102	85	2.00	4.0
A13	52	F	2	87	90	76	0.86	2.1
A14	47	M	5	15	27	0	4.71	16
A15	69	M	3	99	89	81	0.43	2.2
A16	39	F	5	44	44	82	1.86	5.6
A17	45	M	5	34	61	44	2.71	23.2
A18	55	F	5	77	85	71	1.43	2.4
A19	31	F	5	33	68	42	2.00	13.7

A20	47	F	5	99	99	80	2.29	0.6
A21	21	F	5	103	103	88	2.71	0.6
A22	45	F	5	103	106	78	1.57	0.4
A23	40	F	5	67	84	65	2.29	22.9
A24	49	F	5	-	-	-	3.43	4.9
A25	32	F	4	67	67	84	3.14	3.7
A26	55	M	4	36	62	44	4.71	33.0
A27	53	M	5	47	57	63	5.43	7.9
A28	43	F	5	60	70	70	3.71	1.7
A29	39	M	5	66	86	61	3.86	9.5
A30	59	M	5	51	84	46	2.86	44.5
A31	65	F	4	42	69	47	3.14	21.9
A32	72	F	4	65	78	63	1.14	10.7
A33	59	M	4	88	98	68	0.57	4.2
A34	70	M	3	56	65	63	1.00	15.2
A35	59	F	5	50	73	53	2.00	22.7
A36	62	M	4	47	-	-	4.43	15.8
A37	74	F	5	59	69	66	0.86	7.9
A38	20	F	4	43	93	41	3.71	53.3
A39	55	F	4	27	37	57	4.86	25.0
A40	71	F	5	47	63	57	1.43	18.1
A41	49	F	3	91	90	81	1.43	2.5
A42	56	F	4	90	84	83	0.86	0.7
A43	60	F	5	64	69	72	1.86	13.1
A44	62	M	5	70	89	59	3.29	26.3
A45	29	F	4	76	102	64	5.14	1.8
A46	65	M	4	57	67	63	0.86	31.2
A47	60	F	3	69	75	71	2.00	11.1
A48	64	M	5	77	87	66	3.43	3.4
A49	70	F	3	61	59	78	2.71	5.9
A50	56	F	4	49	64	59	2.71	27.0
A51	64	F	3	82	75	84	2.43	11.6
A52	43	M	4	92	108	68	3.57	13.7
A53	44	F	5	72	89	65	3.86	30.5
A54	35	F	5	46	91	42	5.29	32.8
A55	65	F	3	37	55	51	3.71	30.7
Mean ± SD	52±13	-	-	67±24	80±19	64±17	2.5±1.4	13.7±12.9

GINA=Global Initiative for Asthma disease severity grade; FEV_1=forced expiratory volume in 1 second; $\%_{pred}$=percent of predicted value; FVC=forced vital capacity; ACQ-7=asthma control questionnaire; VDP=ventilation defect percent; *estimated age; F=female; M=male; SD=standard deviation. Dotted lines represent age tertiles in healthy participants.

Pulmonary function and MRI measurements are pre-bronchodilator.

VDP values were generated from a single measurement by one of three observers.

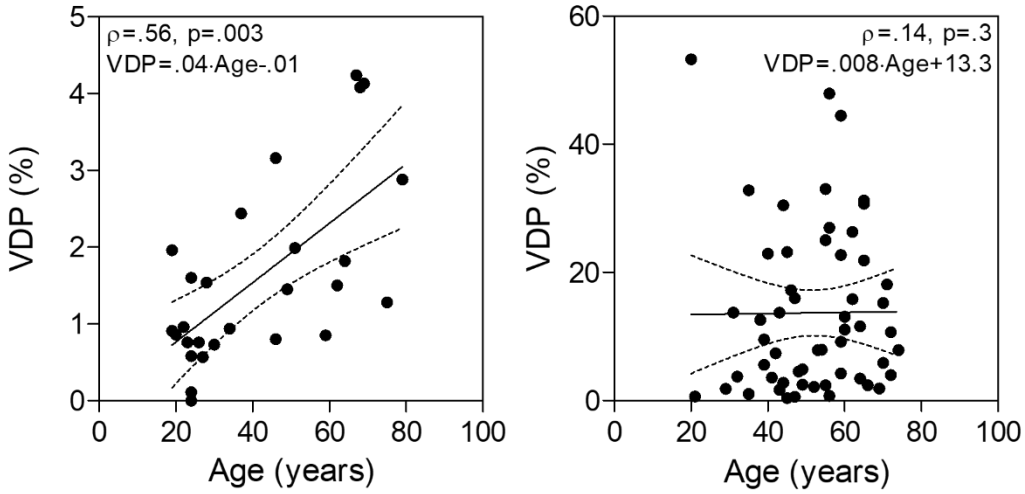

Figure 2-2. Relationship for participant age and ^{129}Xe VDP
Left panel: ^{129}Xe MRI VDP was significantly related to age in healthy participants (ρ=.37, p=.003), with a linear regression equation of VDP=.04·Age-.01. The 95% CI [lower limit of normal, upper limit of normal] for VDP in healthy controls and by age tertile was: all [1.1%, 2.0%], 18-39 years [0.6%, 1.3%], 40-59 years [0.8%, 2.5%], 60-80 years [1.9%, 3.8%].
Right panel: ^{129}Xe MRI VDP was not related to age in participants with asthma (ρ=.14, p=.3).

VDP=ventilation defect percent; ρ=Spearman correlation coefficient

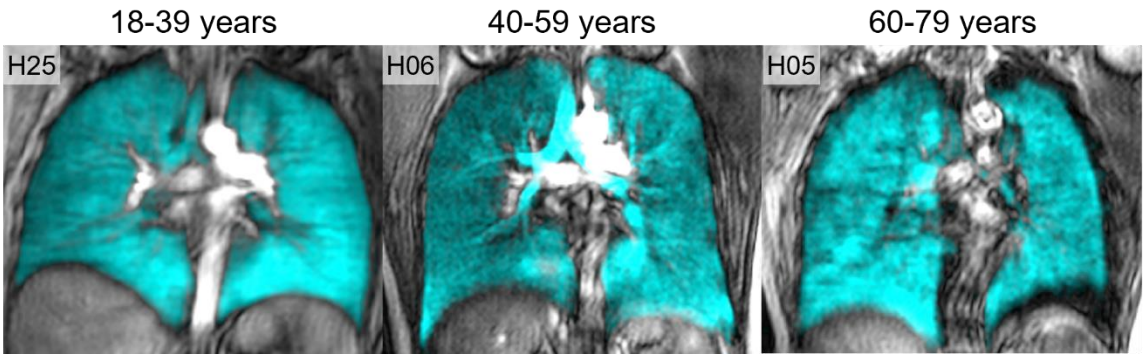

Figure 2-3. ^{129}Xe MRI in healthy participants
Representative healthy participants illustrating center coronal slice ^{129}Xe MRI for: HV25: 23yo female, VDP=0.8%; H06: 51yo male, VDP=2.0%; H05: 68yo female, VDP=4.1%.

2.3.3 MCID for ^{129}Xe MRI VDP

In participants with asthma, mean pre-bronchodilator VDP was 13.7±12.9% and mean ACQ score was 2.5±1.4. ACQ-7 and ^{129}Xe VDP were significantly but moderately correlated (**Figure 2-4**; r=.37, p=.006) with a linear regression equation (R^2=.14, p=.006) of VDP=3.5·ACQ+4.9. Using this equation and the same anchor-based approach as previously described,[13] a difference of the ACQ score MCID of 0.5 units[25] resulted in a VDP difference (ΔVDP=3.5(0.5)) and ultimately, VDP MCID of 1.75% (2% to nearest whole-number). **Figure 2-4** also shows the previous ^{3}He results for comparison, where the anchor-based MCID was 4%.[13]

For the distribution-based approach, SEM was 0.4% and 0.3% and subsequent SDD was 2.5% and 2.0% for the two observers, respectively. Therefore, the mean SDD and distribution-based MCID was 2.25% (2% to nearest whole-number), in line with the updated ^{129}Xe anchor-based MCID.

Figure 2-5 shows co-registered ^{1}H-^{129}Xe static ventilation images in three representative participants with asthma to illustrate the ULN to evaluate cross-sectional VDP, as well as the MCID to evaluate bronchodilator response. While all participants had VDP greater than the ULN (>2%), only A14 showed a VDP response to bronchodilator greater than the MCID (≥2%).

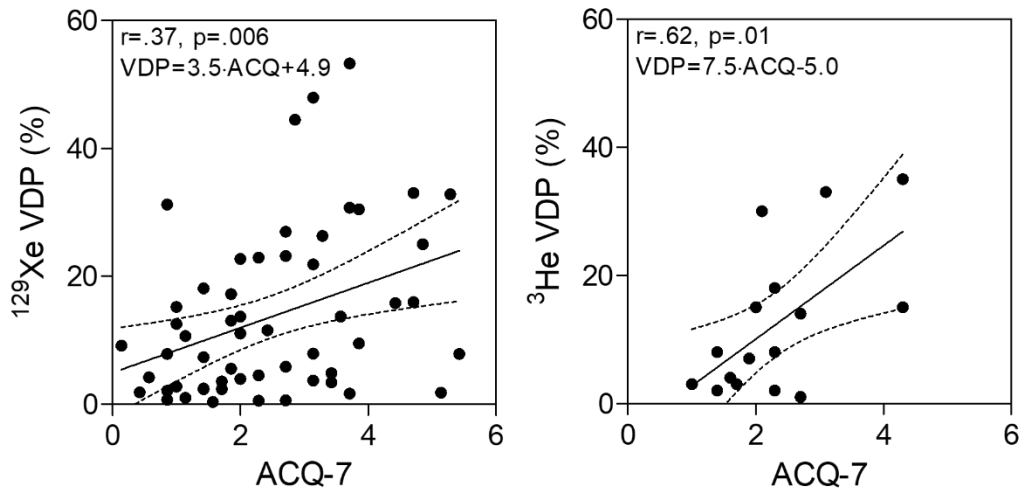

Figure 2-4. ^{129}Xe MRI VDP minimal clinically important difference based on asthma control
Left panel: Asthma control questionnaire (ACQ) score was significantly correlated with ^{129}Xe MRI ventilation defect percent (VDP; r=.37, p=.006) in 55 participants with asthma, with a linear regression equation of VDP=3.5·ACQ+4.9.
Right panel: ACQ-7 was correlated with ^{3}He MRI VDP (r=.62, p=.01), with a linear regression equation of VDP=7.5·ACQ-5.0, as previously published in different participants with severe, poorly controlled asthma (reference 13).

VDP=ventilation defect percent; ACQ=asthma control questionnaire; r=Pearson correlation coefficient

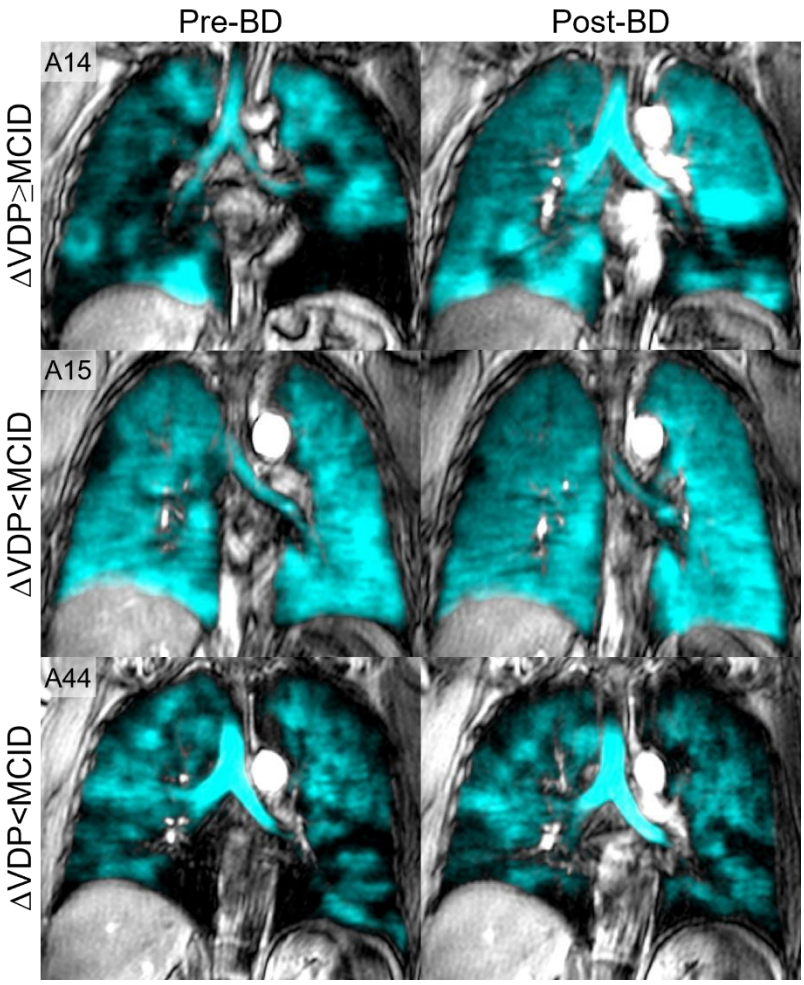

Figure 2-5. ^{129}Xe MRI in participants with asthma

Three representative participants with asthma showing coronal center slice ^{129}Xe MRI co-registered with anatomic ^{1}H MRI VDP. All participants had VDP greater than the upper limit of normal (ULN), and therefore 'abnormal' VDP, pre- and post-bronchodilator (BD).

In participant A14 there was a post-BD change in ^{129}Xe MRI VDP (ΔVDP> minimal clinically important difference [MCID] of 2%), however neither A15 nor A44 showed a clinically relevant change (ΔVDP<MCID of 2%). A14: 47yo male, GINA5, ACQ=4.7, pre-BD VDP=16%, post-BD VDP=3%, ΔVDP=-13%; A15: 69yo male, GINA3, ACQ=0.4, pre-BD VDP=2.2%, post-BD VDP=2.2%, ΔVDP=0%; A44: 62yo male, GINA5, ACQ=3.3, pre-BD VDP=26%, post-BD VDP=26%, ΔVDP=0%.

BD=bronchodilator

2.4 Discussion

In a diverse group of patients with asthma and in healthy participants, we observed: 1) a significant relationship for VDP with age in healthy but not asthma participants, 2) the ULN for ^{129}XeMRI VDP of 2.0% for all healthy participants, and 1.3% for ages 18-39-years, 2.5% for 40-59-years and 3.8% for 60-years or older, 3) anchor-based and distribution-based MCID for ^{129}XeMRI VDP of 2% in participants with asthma, and, 4) a significant relationship for ACQ with ^{129}XeMRI VDP in participants with asthma.

Age-dependent relationships in healthy participants have been demonstrated for ^{3}He apparent diffusion coefficients,[15] ^{3}He ventilation defects[17,18] and ^{129}XeMRI gas exchange measurements.[16] Here we demonstrated ^{129}XeMRI VDP age-dependence in healthy participants, which was not observed in asthma. Another study showed significantly greater VDP in older patients with asthma compared with younger patients,[29] however was dominated by mild-moderate patients. Our study was dominated by patients with severe asthma, which could explain the differences.

We calculated the ULN for all healthy participants and by age tertile to better understand ventilation defect abnormalities in the context of aging as 2.0%, which overall is less than previous reports for ^{3}He (4.3%).[14] The ULN for ^{3}He was previously determined in a group of 51 healthy, elderly never-smokers with mean age 71±6-years (minimum-maximum=61-84-years), which, while older than the total sample evaluated here (41±20-years, minimum-maximum=19-79-years), was similar in age to the oldest age tertile in our sample (70±7-years) with an ULN of 3.8%. Therefore, the ^{3}He and ^{129}Xe VDP ULN were similar when considering age-matched cohorts (4.3% and 3.8%, respectively). Ebner et al[30] previously estimated a much greater VDP threshold of 12.4±6.1% to differentiate healthy participants from patients, using a visual reader score. Although relationships with age were not evaluated there, the differences

could be explained by the fact that regions of low ^{129}Xe signal intensity may be classified as ventilation defects by a reader, but semi-automatically quantified as "hypo-intense ventilation" and not "ventilation defect" using current algorithms.[27,31] The age-dependence of ^{129}Xe VDP and the lower ULN estimates for younger tertiles demonstrated here (1.3% for 18-39 years, 2.5% for 40-59 years) highlight the importance to account for patient age when interpreting ^{129}XeMRI VDP.

We also reported anchor- and distribution-based MCID for ^{129}Xe VDP in asthma to be 1.75% and 2.25%, respectively. Both values were lower than the previously described ^{3}He anchor-based estimate of 4%.[13] In head-to-head comparisons, ^{129}XeMRI VDP is also larger (worse) than ^{3}He MRI VDP, when these values are measured in the same patients with obstructive lung disease.[7,20] ^{129}XeMRI VDP is more sensitive to airway narrowing, inflammation and luminal occlusion in patients, perhaps because of its physical properties. In patients with asthma in particular, the more diffusive ^{3}He can be observed to leak into regions of the lung through narrowed airways that ^{129}Xe does not.[7] We wondered if these findings would also result in different ULN and MCID for ^{129}XeMRI VDP as compared to ^{3}HeMRI. Based on the increased sensitivity of ^{129}Xe VDP (worse than ^{3}He VDP, for the same airway inflammation or narrowing), one might expect the ULN of ^{129}Xe VDP and the MCID in asthma to differ compared to ^{3}He. We also evaluated a larger group of participants across mild, moderate and severe asthma compared with previous ^{3}He VDP MCID results in only severe, poorly controlled asthma,[2,13] which may drive the different ACQ-VDP relationship.

Here we focused on cross-sectional VDP segmentation reproducibility, however normal physiologic and other technical reproducibility are also important to be considered in the context of MCID. In this regard, same-day repeated ^{129}XeMRI measurements in asthma patients showed robust VDP reproducibility with limits of agreement ±1.52%[29] which is

consistent with VDP segmentation reproducibility estimated here. We considered both anchor- and distribution-based approaches because clinically relevant changes in any measurement are inherently tied to the precision with which those measurements are made. The smallest detectable difference for ^{3}He and ^{129}Xe were the same (2%),[27] which was not surprising because both were determined using the same semi-automated segmentation method.[27] Although the anchor- and distribution-based methods are only two of nine reported methods to calculate MCID,[12] both estimated an equivalent ^{129}Xe VDP MCID. Alternative MCID methods[12] are based on perception of change as reported by the patient or treating physician, data for which we did not acquire directly acquire and could not evaluate. However, the validated ACQ[25] is based on self-reports about the prior seven days and hence this does reflect at least cross-sectional self-reported perceptions.

We also observed the significant, but moderate, relationship between ^{129}Xe VDP and patient-reported asthma control. Previous work revealed the relationship between ^{3}He VDP and ACQ in 18 patients with severe, poorly controlled asthma.[2] We confirm and extend these findings in a larger patient group across a greater range of asthma severity[23,24] for ^{129}XeMRI VDP. These results support the validity of ACQ as an anchor for estimating VDP MCID and support the notion that MRI ventilation abnormalities influence symptoms and control in asthma.[2,3]

This study has a number of limitations including the focus on a single chronic airways disease, dominated by patients with severe asthma. It will be important to consider the ^{129}Xe VDP MCID in the context of other airway and parenchyma diseases. Because we considered a range of VDP in the distribution-based approach to account for disease-severity effects, the MCID of 2% could be translatable to other lung conditions including in children. Although the anchor- and distribution-based approaches resulted in the same MCID, the ACQ specifically measures

asthma control,[25] so MCID for other conditions should be prospectively evaluated in the future using validated anchors.

Our study also focused on a semi-automated algorithm (segmentation+registration) to measure VDP employing k-means clustering of ^{129}Xe signal intensity.[27] Other methods include mean-anchored thresholding,[32] linear binning,[31] or fuzzy c-means,[33] which may generate different VDP values per participant and likely have different precision. Certainly, automated methods[34] have the potential to further improve precision. We did not perform bias-field correction of the ^{129}Xe signal intensity because the field artefacts at our center are rather infrequent because of the use of rigid coils. This could have a greater impact on VDP measurement using other coils, and some software packages include such a correction.[31,35] Moreover, we used 1.0L inhaled doses for all participants rather than participant-specific volumes,[36] and this could further contribute to differences in measured VDP.[37] Recommendations for standardized ^{129}XeMRI methods[36] will likely focus next on standardizing VDP measurement algorithms and this may help determine generalizable MCID and ULN values.

2.4.1 Conclusion

We demonstrated the age-dependence of ^{129}Xe MRI VDP and estimated the ULN and MCID across a range of asthma severity. With the emerging use of ^{129}Xe MRI VDP as a clinical and clinical trial endpoint,[38] the MCID for asthma and ULN for healthy participants by age, provide a way to interpret ^{129}Xe MRI VDP measurements.

2.5 References

1. Fain, S.B., *et al.* Functional lung imaging using hyperpolarized gas MRI. *J Magn Reson Imaging* **25**, 910-923 (2007).

2. Svenningsen, S., Nair, P., Guo, F., McCormack, D.G. & Parraga, G. Is ventilation heterogeneity related to asthma control? *Eur Respir J* **48**, 370-379 (2016).

3. Mummy, D.G., *et al.* Ventilation defect percent in helium-3 magnetic resonance imaging as a biomarker of severe outcomes in asthma. *J Allergy Clin Immunol* **141**, 1140-1141.e1144 (2018).

4. Svenningsen, S., *et al.* Sputum Eosinophilia and Magnetic Resonance Imaging Ventilation Heterogeneity in Severe Asthma. *Am J Respir Crit Care Med* **197**, 876-884 (2018).

5. Svenningsen, S., *et al.* CT and Functional MRI to Evaluate Airway Mucus in Severe Asthma. *Chest* **155**, 1178-1189 (2019).

6. Mummy, D.G., *et al.* Mucus Plugs in Asthma at CT Associated with Regional Ventilation Defects at (3)He MRI. *Radiology* **303**, 184-190 (2022).

7. Svenningsen, S., *et al.* Hyperpolarized (3) He and (129) Xe MRI: differences in asthma before bronchodilation. *J Magn Reson Imaging* **38**, 1521-1530 (2013).

8. Thomen, R.P., *et al.* Regional ventilation changes in severe asthma after bronchial thermoplasty with (3)He MR imaging and CT. *Radiology* **274**, 250-259 (2015).

9. McIntosh, M.J., *et al.* Asthma Control, Airway Mucus, and (129)Xe MRI Ventilation After a Single Benralizumab Dose. *Chest* **162**, 520-533 (2022).

10. Hall, C.S., *et al.* Single-Session Bronchial Thermoplasty Guided by (129)Xe Magnetic Resonance Imaging. A Pilot Randomized Controlled Clinical Trial. *Am J Respir Crit Care Med* **202**, 524-534 (2020).

11. Svenningsen, S., *et al.* Bronchial thermoplasty guided by hyperpolarised gas magnetic resonance imaging in adults with severe asthma: a 1-year pilot randomised trial. *ERJ Open Res* **7**(2021).

12. Wells, G., *et al.* Minimal clinically important differences: review of methods. *J Rheumatol* **28**, 406-412 (2001).

13. Eddy, R.L., Svenningsen, S., McCormack, D.G. & Parraga, G. What is the minimal clinically important difference for helium-3 magnetic resonance imaging ventilation defects? *Eur Respir J* **51**(2018).

14. Pike, D., Kirby, M., Guo, F., McCormack, D.G. & Parraga, G. Ventilation heterogeneity in ex-smokers without airflow limitation. *Acad Radiol* **22**, 1068-1078 (2015).

15. Fain, S.B., *et al.* Detection of age-dependent changes in healthy adult lungs with diffusion-weighted 3He MRI. *Acad Radiol* **12**, 1385-1393 (2005).

16. Plummer, J.W., *et al.* Childhood to adulthood: Accounting for age dependence in healthy-reference distributions in (129) Xe gas-exchange MRI. *Magn Reson Med* (2022).

17. Choudhri, A.F., Altes, T.A., Stay, R.M., Mugler, J.P. & de Lange, E.E. The occurrence of ventilation defects in the lungs of healthy subjects as demonstrated by hyperpolarized helium-3 MR imaging. in *RSNA SSA21-05* (2007).

18. Parraga, G., Mathew, L., Etemad-Rezai, R., McCormack, D.G. & Santyr, G.E. Hyperpolarized 3He magnetic resonance imaging of ventilation defects in healthy elderly volunteers: initial findings at 3.0 Tesla. *Acad Radiol* **15**, 776-785 (2008).

19. Cho, A. Physics. Helium-3 shortage could put freeze on low-temperature research. *Science* **326**, 778-779 (2009).

20. Kirby, M., *et al.* Hyperpolarized 3He and 129Xe MR imaging in healthy volunteers and patients with chronic obstructive pulmonary disease. *Radiology* **265**, 600-610 (2012).

21. Kirby, M., *et al.* Pulmonary ventilation visualized using hyperpolarized helium-3 and xenon-129 magnetic resonance imaging: differences in COPD and relationship to emphysema. *J Appl Physiol (1985)* **114**, 707-715 (2013).

22. Chen, X.J., *et al.* Spatially resolved measurements of hyperpolarized gas properties in the lung in vivo. Part I: diffusion coefficient. *Magn Reson Med* **42**, 721-728 (1999).

23. Global Initiative for Asthma (GINA). Global Strategy for Asthma Management and Prevention. 23, 61, 63 (2022).

24. Global Initiative for Asthma (GINA). Pocket Guide for Asthma Management and Prevention. 10, 22, 30 (2022).

25. Juniper, E.F., Svensson, K., Mork, A.C. & Stahl, E. Measurement properties and interpretation of three shortened versions of the asthma control questionnaire. *Respir Med* **99**, 553-558 (2005).

26. Miller, M.R., *et al.* Standardisation of spirometry. *Eur Respir J* **26**, 319-338 (2005).

27. Kirby, M., *et al.* Hyperpolarized 3He magnetic resonance functional imaging semiautomated segmentation. *Academic radiology* **19**, 141-152 (2012).

28. Eliasziw, M., Young, S.L., Woodbury, M.G. & Fryday-Field, K. Statistical methodology for the concurrent assessment of interrater and intrarater reliability: using goniometric measurements as an example. *Phys Ther* **74**, 777-788 (1994).

29. Ebner, L., *et al.* Hyperpolarized 129Xenon Magnetic Resonance Imaging to Quantify Regional Ventilation Differences in Mild to Moderate Asthma: A Prospective Comparison Between Semiautomated Ventilation Defect Percentage Calculation and Pulmonary Function Tests. *Invest Radiol* **52**, 120-127 (2017).

30. Ebner, L., *et al.* Multireader Determination of Clinically Significant Obstruction Using Hyperpolarized (129)Xe-Ventilation MRI. *AJR Am J Roentgenol* **212**, 758-765 (2019).

31. He, M., *et al.* Extending semiautomatic ventilation defect analysis for hyperpolarized (129)Xe ventilation MRI. *Acad Radiol* **21**, 1530-1541 (2014).

32. Thomen, R.P., *et al.* Hyperpolarized (129)Xe for investigation of mild cystic fibrosis lung disease in pediatric patients. *J Cyst Fibros* **16**, 275-282 (2017).

33. Hughes, P.J.C., *et al.* Spatial fuzzy c-means thresholding for semiautomated calculation of percentage lung ventilated volume from hyperpolarized gas and (1) H MRI. *J Magn Reson Imaging* **47**, 640-646 (2018).

34. Astley, J.R., *et al.* Large-scale investigation of deep learning approaches for ventilated lung segmentation using multi-nuclear hyperpolarized gas MRI. *Sci Rep* **12**, 10566 (2022).

35. Lu, J., *et al.* Bias field correction in hyperpolarized (129) Xe ventilation MRI using templates derived by RF-depolarization mapping. *Magn Reson Med* **88**, 802-816 (2022).

36. Niedbalski, P.J., *et al.* Protocols for multi-site trials using hyperpolarized (129) Xe MRI for imaging of ventilation, alveolar-airspace size, and gas exchange: A position paper from the (129) Xe MRI clinical trials consortium. *Magn Reson Med* **86**, 2966-2986 (2021).

37. Hughes, P.J.C., *et al.* Assessment of the influence of lung inflation state on the quantitative parameters derived from hyperpolarized gas lung ventilation MRI in healthy volunteers. *J Appl Physiol (1985)* **126**, 183-192 (2019).

38. Driehuys, B. Crossing the Chasm(s): Demonstrating the Clinical Value of Hyperpolarized Gas MRI. *Acad Radiol* **24**, 1-3 (2017).

Chapter 3

3 ASTHMA CONTROL, AIRWAY MUCUS AND ^{129}XE MRI VENTILATION AFTER A SINGLE BENRALIZUMAB DOSE

To better understand the mechanistic links between rapid eosinophil depletion via anti-IL-5Rα (benralizumab) and airway function, we evaluated the response of ^{129}Xe MRI ventilation abnormalities following 28-days of treatment and investigated the influence of baseline CT mucus plugs on this response.

The contents of this chapter were previously published in the journal Chest: MJ McIntosh, HK Kooner, RL Eddy, S Jeimy, C Licskai, CA Mackenzie, S Svenningsen, P Nair, C Yamashita and G Parraga. Asthma Control, Airway Mucus and ^{129}Xe MRI Ventilation after a Single Benralizumab Dose. Chest. 2022; 162(3): 520-533. This article is available under the terms of the Creative Commons License BY-NC-ND 4.0.

3.1 Introduction

In patients with severe asthma, unpredictable episodes of breathlessness, frequent exacerbations and reduced quality-of-life are common, despite high-dose inhaled and oral corticosteroids.[1] Severe eosinophilic asthma, a subtype of severe asthma, is characterized by eosinophilic infiltration of the airways with airway inflammation[2] and lumen obstruction or narrowing.[3] Anti-interleukin-5 (IL-5) biologic treatments are directed at the eosinophilic component of airway inflammation by eliminating blood and airway eosinophils.[4] Anti-IL-5Rα (benralizumab) binds to the IL-5 receptor on eosinophils and to natural killer cell receptors, which induces eosinophil apoptosis,[4] resulting in depleted blood eosinophils within 2 hours of treatment[5] and downstream improvements in asthma control and quality-of-life.[6-8] Whilst the mechanism of action of anti-IL-5 therapy on eosinophil depletion has been characterized,[5,9] the influence on small and large airway structure and function, including airway occlusion, is not well-understood. Airway luminal occlusions, which typically consist of mucin,[10] plasma proteins[11] and inflammatory cells,[12,13] may be non-invasively quantified using x-ray computed tomography (CT).[14] In asthma, mucus plugs are associated with eosinophilia[3] and are believed to partially result from eosinophil-driven oxidation.

Asthma investigations that harness the unique capabilities of hyperpolarized ^{3}He and ^{129}Xe magnetic resonance imaging (MRI)[15-17] have shown that ventilation defects[17,18] are related to airway inflammation[18,19] and remodeling,[20] and are spatially related to lobar[21] and segmental[22] mucus occlusions. Moreover, MRI ventilation defect percent (VDP)[23] is uniquely predictive of asthma control,[24] related to airway inflammation and sputum eosinophilia,[19] and sensitively responds to asthma interventions including bronchodilator,[17] bronchial thermoplasty[15] and anti-type 2 therapy.[16]

To develop mechanistic insight, we aimed to quantify ^{129}Xe MRI ventilation defect changes after a first injection of benralizumab and then examined if baseline mucus occlusions influenced potential response. We hypothesized that ^{129}Xe MRI VDP would significantly improve post-benralizumab.

3.2 Materials and Methods

3.2.1 Study Participants and Design

Participants 18-80 years of age with poorly controlled asthma according to the Global Initiative for Asthma (GINA)[25] and no exacerbation history within four weeks of enrolment provided written-informed consent to an ethics board (HSREB # 113224) and Health-Canada approved protocol (www.clinicaltrials.gov NCT03733535). Inclusion criteria consisted of: blood eosinophil count ≥300 cells/μL, forced expiratory volume in one second (FEV_1) post-bronchodilator (BD) reversibility[26] and poorly controlled asthma, measured using the asthma control questionnaire score (ACQ-6) ≥1.5 at screening.[27] The protocol was amended to include participants with no response to oral corticosteroids and enrolment blood eosinophil count

<300 cells/μL but with clinically significant[25] sputum (>2%) or blood eosinophilia (>150 cells/μL) in the past 12 months.

Figure 3-1A provides the study design. During Visit 1, inclusion criteria were recorded. On Visit 2 (Day-0), pre- and post-BD spirometry, oscillometry and ^{129}Xe MRI, thoracic CT and fraction of exhaled nitric oxide (FeNO) measurement were completed in addition to ACQ-6,[28] Asthma Quality-of-Life (AQLQ)[29] and St. George's Respiratory (SGRQ)[30] questionnaires. Visit 2 concluded with a 30 mg subcutaneous injection of benralizumab. Visit 3 (Day-14) provided participants a choice to perform repeat post-BD spirometry and ^{129}Xe MRI or participate in a tele-visit to discuss adverse events, healthcare-utilization and symptom changes. Within 28±5 days of Visit 2, all participants returned to the laboratory for Visit 4 (Day-28) consisting of pre- and post-BD spirometry, oscillometry and ^{129}Xe MRI, FeNO, ACQ-6, AQLQ, SGRQ and eosinophil count.

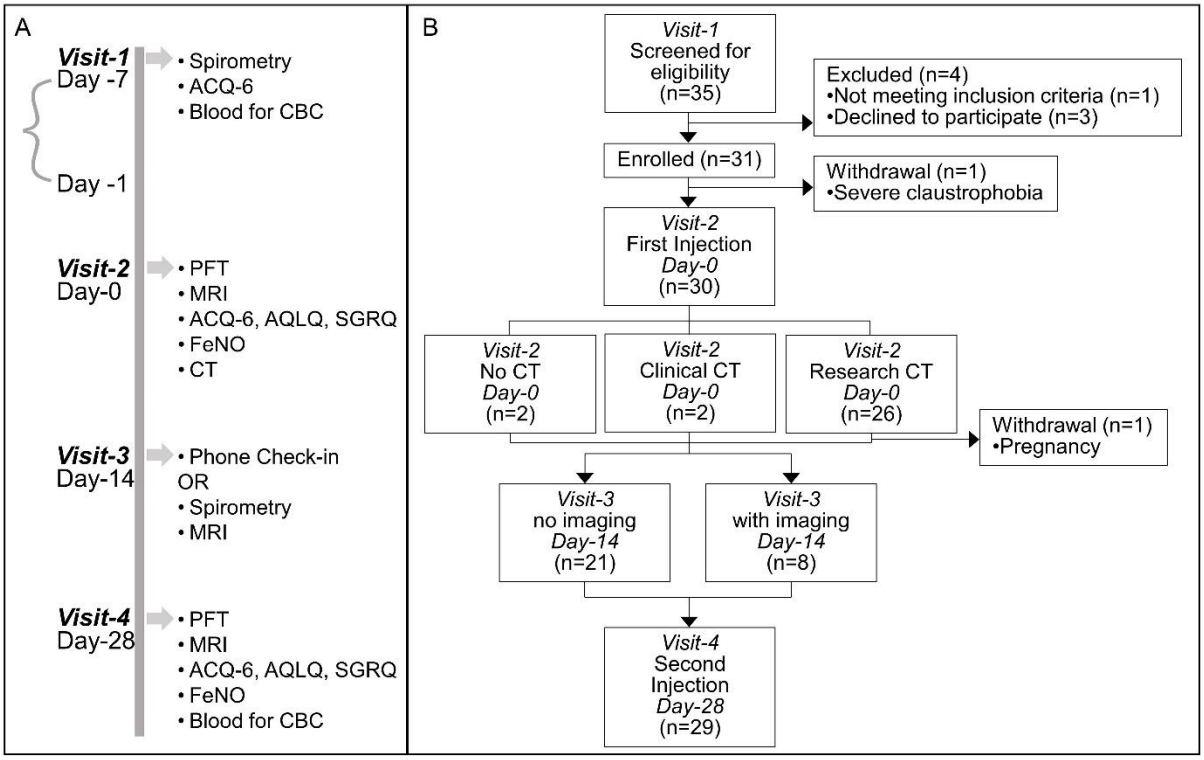

Figure 3-1. Study Design and Consort Diagram
A) Study design with Visit-1 as screening visit, Visit-2 on Day-0, Visit-3 on Day-14 and Visit-4 on Day-28.

B) Consort Diagram. Of the 35 participants screened for eligibility, one did not meet inclusion criteria, three declined to participate, one participant could not perform MRI due to severe claustrophobia and one participant tested positive for pregnancy after the first dose. Of 29 participants evaluated, eight participants completed optional Day-14 imaging and 21 did not. Twenty-seven participants consented to CT imaging and two participants did not.

ACQ=Asthma Control Questionnaire; PFT=Pulmonary Function Test; MRI=Magnetic Resonance Imaging; CT=Computed Tomography; AQLQ=Asthma Quality-of-Life Questionnaire; SGRQ=St. George's Respiratory Questionnaire; FeNO=Fraction of exhaled nitric oxide

3.2.2 Pulmonary Function Tests and Questionnaires

Participants performed spirometry[31] according to American Thoracic Society guidelines using a whole-body plethysmograph (MedGraphics Corporation, Saint Paul, MN, USA). FeNO[32] was measured according to guidelines using the NIOX VERO® system (Circassia Pharmaceuticals Inc, Morrisville, NC, USA). Oscillometry[33] was performed according to European Respiratory Society guidelines using a tremoFlo C-100 Airwave Oscillometry System (Thorasys, Montreal, QC, Canada) to measure resistance (R) and reactance between 5 and 37 Hz. Post-BD measurements were performed 15 minutes after inhalation of 4×100 µg Novo-Salbutamol Hydrofluoroalkane (Teva Novopharm, Toronto, Canada) using an AeroChamber (Trudell Medical International, London, Canada). Participants withheld asthma medications before each face-to-face study visit according to American Thoracic Society guidelines.[31] ACQ-6, AQLQ and SGRQ were self-administered under supervision.

3.2.3 Thoracic Imaging and Analysis

Anatomic ^{1}H and ^{129}Xe static ventilation MRI were acquired at 3.0 Tesla (Discovery MR750; GE Healthcare, Milwaukee, USA), as described.[17] Anatomic ^{1}H MRI was acquired using a fast-spoiled gradient-recalled-echo sequence (partial-echo acquisition; total acquisition time, 8 seconds; repetition-time msec/echo time msec, 4.7/1.2; flip-angle, 30°; field-of-view, 40×40cm^2; bandwidth, 24.4 kHz; 128×80 matrix, zero-filled to 128×128; partial-echo percent, 62.5%; 15-17×15mm slices). ^{129}Xe MRI was acquired using a three-dimensional fast-spoiled gradient-recalled echo sequence (total acquisition time, 14 s; repetition-time msec/echo time msec, 6.7/1.5; variable flip-angle; field-of-view, 40×40cm^2; bandwidth, 15.63 kHz; 128×128 matrix; 14×15mm slices). Supine participants were coached to inhale a 1.0L bag (Tedlar; Jensen Inert Products, Coral Springs, FL, USA) (400mL ^{129}Xe + 600mL ^{4}He for ^{129}Xe MRI and 1.0L N_2 for ^{1}H MRI) from the bottom of a tidal breath (functional residual capacity) with

acquisition under breath-hold conditions. ^{129}Xe gas was polarized to 30-40% (Polarean; Xenispin 9820, Durham, NC, USA).[34]

Quantitative MRI analysis was performed as previously described[35] using Matlab 2019a (Mathworks, Natick, MA, USA), which classifies voxels into five signal intensity clusters (signal void or ventilation defect volume and four signal intensity clusters ranging from low to high). VDP was generated by normalizing ventilation defect volume to the ^{1}H MRI thoracic cavity volume, as previously described.[23]

Within 30 minutes of MRI, CT was acquired post-BD after inhalation of 1.0L N_2 from functional residual capacity using a 64-slice LightSpeed VCT system (General Electric Healthcare, Milwaukee, WI, USA; parameters: 64×0.625 collimation, 120 peak kilovoltage, 100 mA, tube rotation time=500ms, pitch=1.25, standard reconstruction kernel, slice thickness=1.25mm, field-of-view=40cm^2), as previously described.[36]

CT images were analyzed using VIDAvision software (VIDA Diagnostics Inc., Coralville, IA, USA) to generate total airway count.[37] Anatomically equivalent segmental, subsegmental and sub-subsegmental airways for all airway paths (third to fifth generation) were also used to generate wall area percent[37] and lumen area.[38] As previously described,[3] mucus plugs were identified as airway regions with complete occlusion that were more radio-dense than the lumen. We scored mucus plugs by adapting a method previously developed by Dunican.[3,21] Two blinded observers in consensus scored the total number of mucus occlusions in the 20 segments to yield a whole lung mucus score for each participant. The mucus score frequency distribution was used to generate a dichotomization threshold based on the mean, similar to previous work.[20]

3.2.4 Endpoints and Statistical Analysis

The primary endpoint was the change in ^{129}Xe MRI VDP after a single dose of benralizumab on Day-28. Secondary endpoints included the change in blood eosinophils, FEV_1, ACQ-6, AQLQ, SGRQ and FeNO on Day-28. The change in FEV_1 and VDP on Day-14 and the relationship between Day-0 VDP with changes in asthma control were exploratory endpoints as was the relationship of mucus score with changes in asthma control.

SPSS (SPSS Statistics 25.0; IBM, Armonk, NJ, USA) was used for all statistical analyses. Data were tested for normality using Shapiro-Wilk tests and nonparametric tests were performed when data was not normally distributed. Differences between participant groups were evaluated using independent samples t-tests or Mann-Whitney U tests. Differences in pulmonary function tests, VDP, inflammation measurements and quality-of-life questionnaires were evaluated using repeated measures analysis of variance. Univariate relationships were measured using Pearson (r) or Spearman correlation (ρ) coefficients. Variables with Pearson or Spearman correlation significance p value$\leq$0.20[39] were used to generate multivariable models, using the stepwise approach, to predict the change in VDP and ACQ-6 on Day-28. Variables were tested for collinearity and models rejected when variance inflation factor$\geq$5.[40] Regression coefficients for the variables in the multivariable models were expressed as the standardized β. The Holm-Bonferroni correction was used for multiple comparisons. Results were considered statistically significant when the probability of making a type I error was less than 5% ($p<0.05$).

3.3 RESULTS

3.3.1 Participant Demographics

A CONSORT diagram provided in **Figure 3-1B** shows that from April 2019 to October 2019, 31 participants were enrolled and two participants withdrew. One of these participants withdrew due to extreme claustrophobia and did not receive treatment, while another participant completed Visit 2 but had a positive pregnancy test five days after Visit 2 (test was negative at screening) and was withdrawn. No adverse events were reported in this participant. Twenty-nine participants were evaluated (20 female, 9 male; mean age 59±12yr). Two participants declined CT imaging hence CT mucus occlusions were evaluated in 27 participants (18 female, 9 male; mean age 60±12yr).

Parameter mean ± SD (mean/MEDIAN: min-max)	All Participants (n=29)	Mucus Score < 5 (n=18)	Mucus Score ≥ 5 (n=9)	p
Age years	59 ± 12	62 ± 8	55 ± 17	-
Female n/%	16/69	11 (61)	5 (55)	-
BMI kg/m^2	29 ± 5	30 ± 6	27 ± 3	-
Pack-years	(7/0: 0-45)	(7/0: 0-45)	(8/0: 0-30)	-
Duration of Asthma	25 ± 22 (25; 1-64)	28 ± 22 (27; 1-63)	16 ± 16 (12; 1-64)	-
Pulmonary function				
Pre-BD FEV_1 mL	1800 ± 700	1900 ± 700	1600 ± 800	.6
Pre-BD $FEV_{1\%pred}$	62 ± 18	67 ± 17	54 ± 21	-
Post-BD FEV_1 mL	2100 ± 800	2300 ± 700	1900 ± 900	1.0
Post-BD $FEV_{1\%pred}$	74 ± 17	80 ± 14	64 ± 21	-
Pre-BD FEV_1/FVC	0.63 ± 0.13	0.66 ± 0.10	0.57 ± 0.13	-
Post-BD FEV_1/FVC	0.68 ± 0.11	0.70 ± 0.09	0.63 ± 0.14	-
Inflammatory markers				
Eos cells/μL	630 ± 380	520 ± 270	920 ± 420	**.04**
FeNO ppb	48 ± 35[†] (33; 7-141)	51 ± 37 (35; 7-141)	45 ± 34[‡] (30; 12-98)	1.0
Asthma QoL and control				
ACQ-6	2.3 ± 1.5	1.8 ± 1.3	3.1 ± 1.4	.2
AQLQ	4.3 ± 1.4	4.8 ± 1.4	3.9 ± 1.2	-
SGRQ	50 ± 21	45 ± 21	58 ± 17	-
CT imaging[†]				

TAC	140 ± 50	130 ± 23	160 ± 80	.9
Mucus Score	5 ± 9	1 ± 2	13 ± 11	-
Airway WA%	70 ± 2	70 ± 2	69 ± 2	-
Airway LA mm^2	8.02 ± 2.58	7.69 ± 2.67	8.67 ± 2.41	-
Airway WT mm	1.19 ± 0.13	1.19 ± 0.11	1.20 ± 0.18	-
Airway WT%	19 ± 1	19 ± 1	18 ± 1	-
MRI				
Pre-BD VDP	17 ± 10	13 ± 7	25 ± 11	**.008**
Post-BD VDP	12 ± 10	8 ± 7	21 ± 13	**.02**

Table 3-1 provides a summary of baseline characteristics for all participants and shows that ACQ-6,[27] blood eosinophils,[25] FeNO,[32] total airway count,[41] wall area percent,[41] mucus score,[3] pre- and post-BD FEV_1[26] and VDP[42] were abnormal. Six participants (P06, P11, P12, P24, P25, P29) reported >10-pack-years smoking history (mean/median [min-max]: 7/0 [0-45]). Mean asthma duration was 26±22 years.

As shown in **Table 3-3**, all participants had been prescribed inhaled corticosteroids (mean dose 910±570 µg/day), while 97%, 3%, 6% and 17% of participants were also prescribed long-acting β-agonists, long-acting muscarinic antagonists, leukotriene receptor antagonists and oral corticosteroids, respectively. In addition, a single participant (P10) received 80 mg methylprednisolone injection every 10 days, five received oral prednisone (5-15 mg/day) and two had previously received Xolair 300 mg.

Table 3-1. Baseline Demographic Characteristics

Parameter mean ± SD (mean/MEDIAN: min-max)	All Participants (n=29)	Mucus Score < 5 (n=18)	Mucus Score ≥ 5 (n=9)	p
Age years	59 ± 12	62 ± 8	55 ± 17	-
Female n/%	16/69	11 (61)	5 (55)	-
BMI kg/m^2	29 ± 5	30 ± 6	27 ± 3	-
Pack-years	(7/0: 0-45)	(7/0: 0-45)	(8/0: 0-30)	-
Duration of Asthma	25 ± 22 (25; 1-64)	28 ± 22 (27; 1-63)	16 ± 16 (12; 1-64)	-
Pulmonary function				
Pre-BD FEV_1 mL	1800 ± 700	1900 ± 700	1600 ± 800	.6
Pre-BD $FEV_{1\%pred}$	62 ± 18	67 ± 17	54 ± 21	-
Post-BD FEV_1 mL	2100 ± 800	2300 ± 700	1900 ± 900	1.0
Post-BD $FEV_{1\%pred}$	74 ± 17	80 ± 14	64 ± 21	-
Pre-BD FEV_1/FVC	0.63 ± 0.13	0.66 ± 0.10	0.57 ± 0.13	-
Post-BD FEV_1/FVC	0.68 ± 0.11	0.70 ± 0.09	0.63 ± 0.14	-
Inflammatory markers				
Eos cells/μL	630 ± 380	520 ± 270	920 ± 420	**.04**
FeNO ppb	48 ± 35† (33; 7-141)	51 ± 37 (35; 7-141)	45 ± 34‡ (30; 12-98)	1.0
Asthma QoL and control				
ACQ-6	2.3 ± 1.5	1.8 ± 1.3	3.1 ± 1.4	.2
AQLQ	4.3 ± 1.4	4.8 ± 1.4	3.9 ± 1.2	-
SGRQ	50 ± 21	45 ± 21	58 ± 17	-
CT imaging†				
TAC	140 ± 50	130 ± 23	160 ± 80	.9
Mucus Score	5 ± 9	1 ± 2	13 ± 11	-
Airway WA%	70 ± 2	70 ± 2	69 ± 2	-
Airway LA mm^2	8.02 ± 2.58	7.69 ± 2.67	8.67 ± 2.41	-
Airway WT mm	1.19 ± 0.13	1.19 ± 0.11	1.20 ± 0.18	-
Airway WT%	19 ± 1	19 ± 1	18 ± 1	-
MRI				
Pre-BD VDP	17 ± 10	13 ± 7	25 ± 11	**.008**
Post-BD VDP	12 ± 10	8 ± 7	21 ± 13	**.02**

BMI=body mass index; BD=bronchodilator; FEV_1=forced expiratory volume in 1 second; $\%_{pred}$=percent of predicted value; FVC=forced vital capacity; Eos=blood eosinophil count; FeNO=fraction of exhaled nitric oxide; ppb=parts per billion; QoL=quality-of-life; ACQ=Asthma Control Questionnaire; AQLQ=Asthma Quality-of-Life Questionnaire; SGRQ=St. George's Respiratory Questionnaire; CT=computed tomography; TAC=total airway count; WA=wall area; LA=lumen area; WT=wall thickness; VDP=ventilation defect percent; †n=27; ‡n=8

3.3.2 CT Mucus Plugs

Mucus plugs were scored in 27 participants and 18/27 (67%) participants showed CT evidence of at least one mucus plug, similar to previous findings.[3] Participants were dichotomized into two subgroups: 1) <5 mucus plugs (n=18; 11 females, 7 males; mean age 62±8yr), or, 2) ≥5 plugs (n=9; 5 females, 4 males; mean age 55±17yr) based on the mean of the mucus plug frequency distribution, as previously described.[20] **Table 3-1** shows that these two subgroups were significantly different for baseline eosinophil count (p=.04), pre-BD VDP (p=.008) and post-BD VDP (p=.02) but not ACQ-6.

3.3.3 Primary Endpoint: Change in MRI VDP on Day-28

Figure 3-2 shows representative ^{129}Xe ventilation MRI (cyan) co-registered with anatomical ^{1}H MRI (grey-scale) on Day-0 (pre- and post-BD) and Day-28 (post-BD) for two participants with mucus score<5 (P01 and P03) and two participants with mucus score≥5 (P09 and P29). For participants P01 and P03, each with only one mucus-plug, there were qualitatively similar ventilation defects on Day-0 and Day-28 (P01: ΔVDP=+1.8%; P03: ΔVDP=+1.5%). Participant P09 had six mucus-plugs in total and four mucus-plugs in the left-lower-lobe (LLL), for which there was decreased VDP on Day-28 (LLL ΔVDP=-9.2%). Participant P29 had 39 mucus-plugs in total and 23 mucus-plugs in the left-lung (LL) for which there was decreased VDP on Day-28 (LL ΔVDP=-9.3%).

As shown in **Figure 3-3**, mean ^{129}Xe MRI VDP was significantly improved (p=.001) on Day-28 in all participants. **Figure 3-6** and **Table 3-5** provide a summary of Day-14 responses.

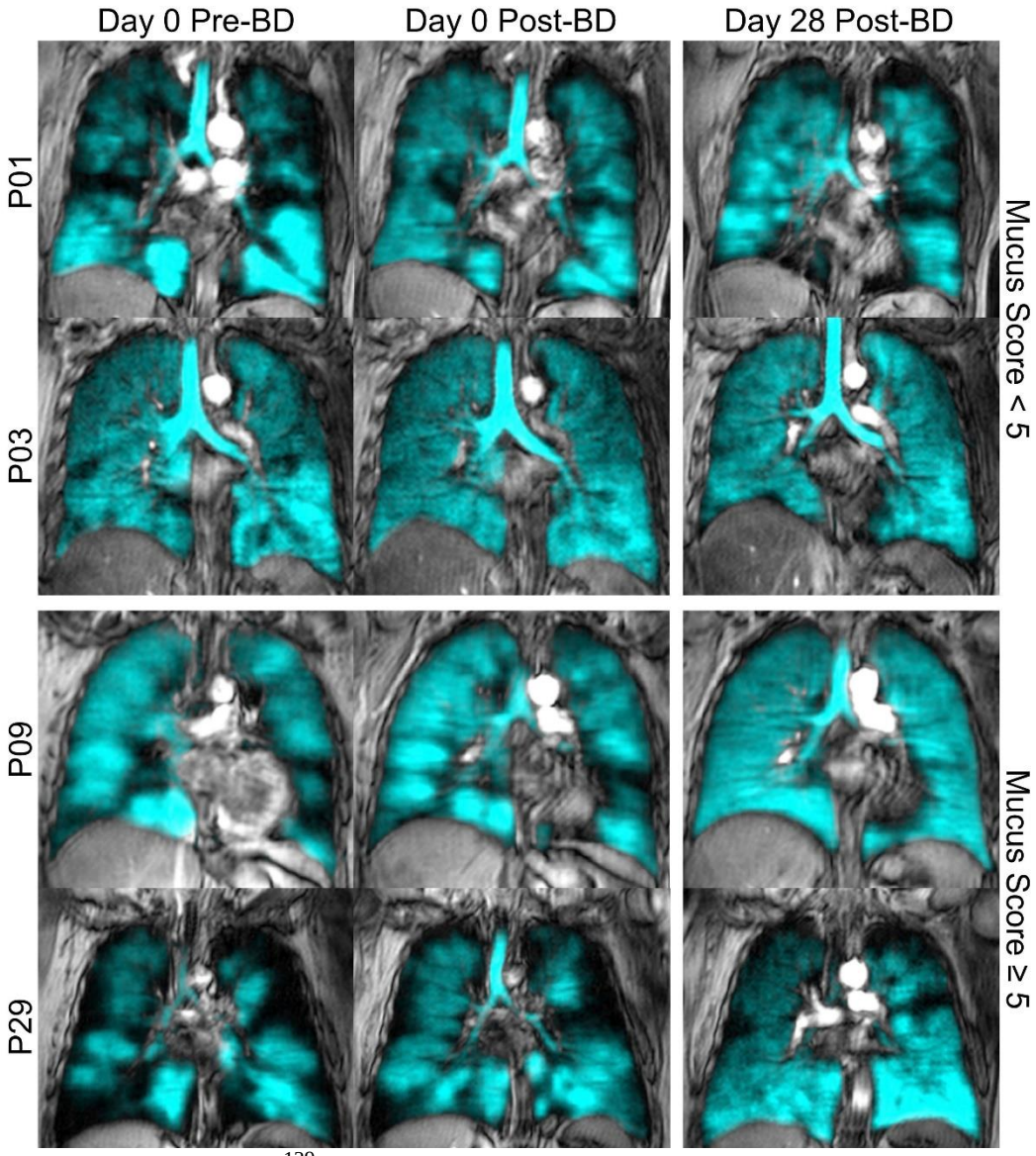

Figure 3-2. Representative ^{129}Xe MRI on Day-0 and Day-28
Centre coronal ^{129}Xe MRI slice (cyan) co-registered with ^{1}H MRI thoracic cavity (greyscale) on Day 0 (pre- and post-BD) and Day 28 (post-BD).

P01 was a 65-year-old female with mucus score=1 and Day-0 eosinophil count=100 cells/μL, FEV_1 pre/post-BD=42%/53%, ACQ-6 score=2.7, VDP pre/post-BD=18%/6%; Day-28 eosinophil count=0 cells/μL, FEV_1 post-BD=43%, ACQ-6 score=3.5, VDP post-BD=8%.

P03 was a 59-year-old male with mucus score=1 and Day-0 eosinophil count=600 cells/μL, FEV_1 pre/post-BD=88%/91%, ACQ-6 score=0.3, VDP pre/post-BD=6%/3%; Day-28 eosinophil count=0 cells/μL, FEV_1 post-BD=91%, ACQ-6 score=0.2, VDP post-BD=4%.

P09 was a 55-year-old female with mucus score=6 and Day-0 eosinophil count=1000 cells/μL, FEV_1 pre/post-BD=27%/39%, ACQ-6 score=4.7, VDP pre/post-BD=20%/7%; Day-28 eosinophil count=0 cells/μL, FEV_1 post-BD=84%, ACQ-6 score=1.3, VDP post-BD=0%.

P29 was a 65-year-old female with mucus score=39 and Day-0 eosinophil count=1700 cells/μL, FEV_1 pre/post-BD=37%/50%, ACQ-6 score=3.3, VDP pre/post-BD=38%/18%; Day-28 eosinophil count=0 cells/μL, FEV_1 post-BD=87%, ACQ-6 score=0, VDP post-BD=8%.

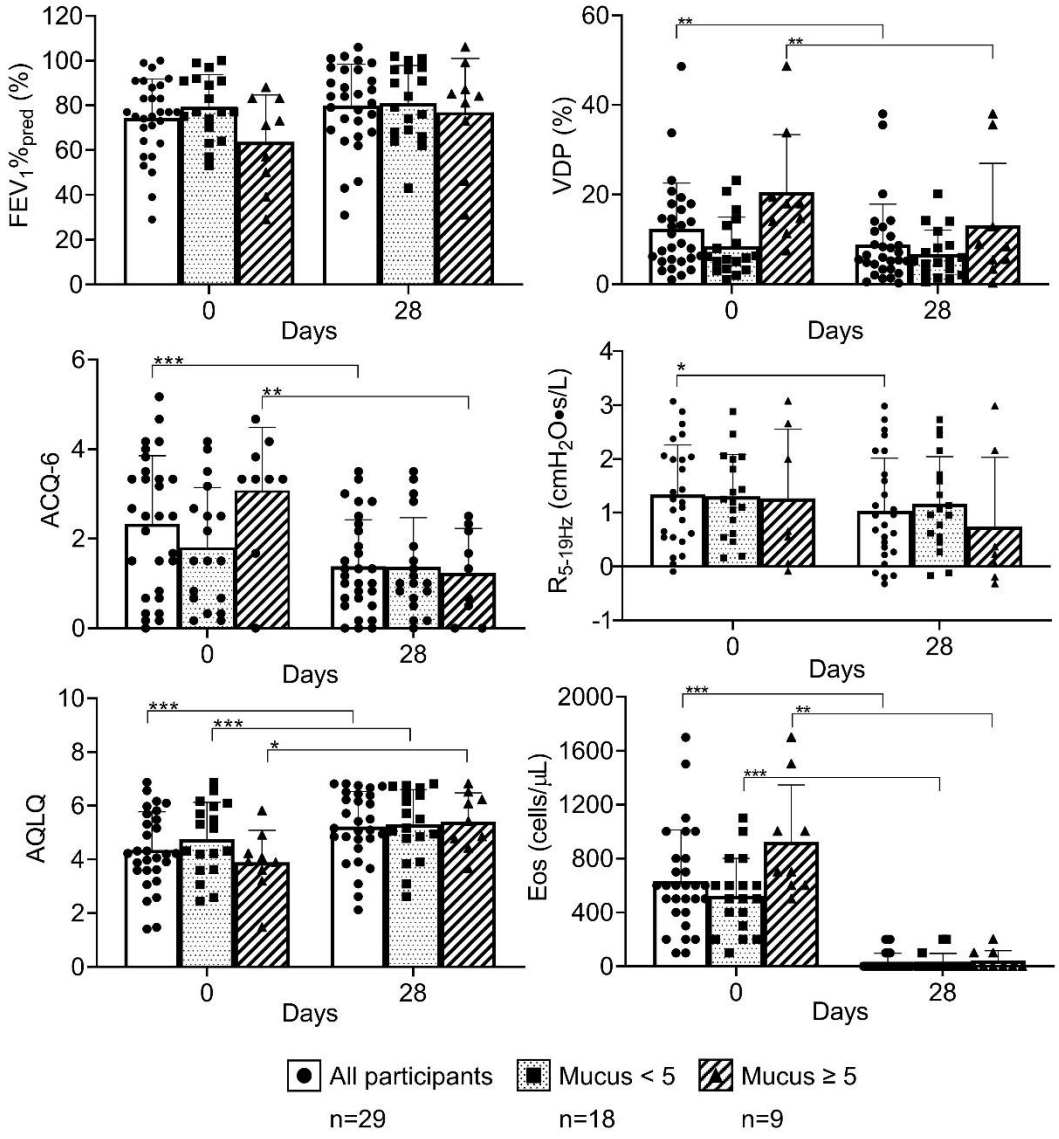

Figure 3-3. Biomarkers on Day-0 and Day-28 for all participants and mucus subgroups
Top left: $FEV_1\%_{pred}$ not significantly different for all participants ($p^{\dagger}$=.02, p=.06), mucus<5 ($p^{\dagger}$=.3, p=.3) or mucus≥5 ($p^{\dagger}$=.06, p=.1) subgroups on Day-28.
Top right: VDP significantly different for all participants ($p^{\dagger}$=.0002, p=.001) and mucus≥5 subgroup ($p^{\dagger}$=.002, p=.006) on Day 28 but not mucus<5 subgroup ($p^{\dagger}$=.03, p=.07).
Middle left: ACQ-6 score significantly different for all participants ($p^{\dagger}=6.0\times10^{-5}$, p=.0005) and mucus ≥ 5 subgroup ($p^{\dagger}$=.001, p=.006) on Day-28 but not mucus<5 subgroup ($p^{\dagger}$=.02, p=.09).
Middle right: $R_{5\text{-}19Hz}$ significantly different for all participants ($p^{\dagger}$=.02, p=.04) Day-28 but not mucus<5 ($p^{\dagger}$=.2, p=.5) or mucus≥5 subgroups ($p^{\dagger}$=.1, p=.2).
Bottom left: AQLQ score significantly different for all participants ($p^{\dagger}=9.0\times10^{-6}$, $p=9.0\times10^{-5}$), mucus<5 ($p^{\dagger}$=.0001, p=.0006) and mucus≥5 subgroup ($p^{\dagger}$=.005, p=.02) on Day-28.
Bottom right: Eosinophil count significantly different for all participants ($p^{\dagger}=2.0\times10^{-9}$, $p=2.0\times10^{-8}$), mucus<5 ($p^{\dagger}=6.0\times10^{-8}$, $p=4.0\times10^{-7}$) and mucus≥5 subgroup ($p^{\dagger}$=.0005, p=.003) on Day-28.

*FEV_1=forced expiratory volume in 1 second; $\%_{pred}$=percent of predicted value; VDP=ventilation defect percent; ACQ=asthma control questionnaire; $R_{5\text{-}19Hz}$=peripheral airway resistance; AQLQ=asthma quality-of-life questionnaire; Eos=eosinophil count; Box=mean; Whiskers=standard deviation; ***=p≤0.001; **=p≤0.01; *=p<0.05; $p^{\dagger}$=uncorrected values; p=Holm-Bonferroni corrected values*

3.3.4 Secondary Endpoints

Figure 3-3 also summarizes Day-0 and Day-28 FEV_1, ACQ-6, AQLQ scores as well as $R_{5\text{-}19Hz}$ and eosinophil count for all participants and both mucus score subgroups. In all participants, ACQ-6 (p=.0005), AQLQ (p<.0001), eosinophil count (p<.0001) and peripheral airways resistance ($R_{5\text{-}19Hz}$, p=.04) were significantly improved on Day-28 whereas FEV_1 (p=.06) was not. In the mucus≥5 subgroup, ACQ-6 (p=.006) and VDP (p=.006) significantly improved on Day-28 post-benralizumab, but this was not the case in the mucus<5 subgroup (ACQ-6 p=.09; VDP p=.07). **Figure 3-7** provides VDP and oscillometry results related to baseline FeNO subgroups. **Table 3-5** provides a by-participant list of spirometry, imaging and inflammatory markers at baseline and 14- and 28-days post-benralizumab which shows that 23/29 participants had complete eosinophil depletion on Day-28. **Table 3-6** provides a by-participant list of pre- and post-BD oscillometry measurements on Day-0 and Day-28. **Table 3-7** provides a by-participant list of Day-0 and Day-28 ACQ, AQLQ and SGRQ values. The mean change in pulmonary function, imaging and quality-of-life measurements on Day-28 with Holm-Bonferroni corrected p values are provided in **Table 3-8**.

Table 3-9 shows the weak to moderate relationships (with uncorrected p-values) for ΔACQ-6 with Day-0 mucus score (r=-.57, p=.002) and pre-BD VDP (r=-.46, p=.02) and for ΔAQLQ with Day-0 mucus score (ρ=.40, p=.04) and CT wall area percent (r=-0.50, p=.008). Baseline eosinophil count was also related to ΔACQ-6 (r=-.43, p=.02) and Δpost-BD VDP (ρ=-.58, p=.002). Baseline FEV_1 was not related to the change in AQLQ (pre-BD, p=.2; post-BD, p=.2) or ACQ (pre-BD, p=.4; post-BD, p=.4) 28-days post-benralizumab. Post-BD forced vital capacity, but not post-BD FEV_1, was related to the change in both post-BD VDP and FEV_1.

Figure 3-4 shows the details for the association of ΔACQ-6 on Day-28 with Day-0 VDP (A: r=-0.47, p=.03) and mucus score (B: r=-0.57, p=.002) as well as for the change in eosinophil

count with Day-0 VDP (C: ρ=-0.37, p=.049) and mucus score (D: ρ=-0.44, p=.045). Baseline mucus score significantly related to the change in VDP (E: r=-0.56, p=.01) and SGRQ (F: r=-0.51, p=.03) 28-days post-benralizumab.

We generated multivariable models to explain ΔACQ-6 on Day-28 and these are shown in **Table 3-2**. In three significant models, mucus score and VDP were significant variables for ΔACQ-6 on Day-28 whilst FEV_1, the ratio of FEV_1 to forced vital capacity, FeNO, and baseline eosinophils were not. We also generated a significant multivariable model (data not shown) to explain Δpost-BD VDP on Day-28 (R^2=0.666, p<.001) and this included Day-0 mucus (β=-0.650, p<.001), FeNO (β=-0.488, p=.005) and post-BD VDP reversibility (β=-0.464, p=.006). Hence greater mucus score and FeNO values alongside diminished post-bronchodilator reversibility explained improved post-BD VDP post-benralizumab.

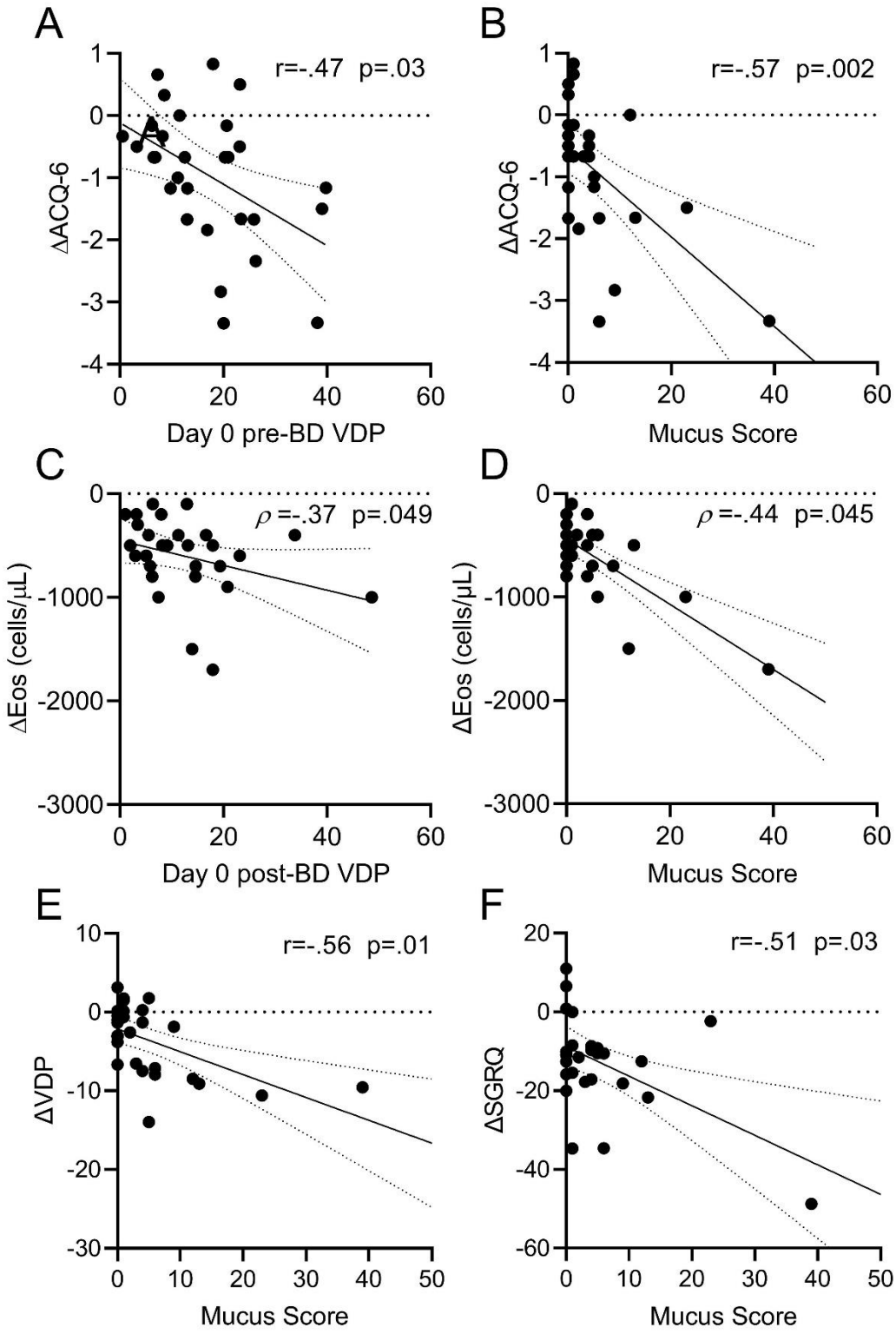

Figure 3-4. Relationships for VDP and mucus scores with eosinophils, ACQ-6 and SGRQ changes post-benralizumab

A) Linear correlation for Day-0 pre-BD VDP and change in ACQ-6 (r=-.47, p=.03) on Day-28

B) Linear correlation for Day-0 CT mucus score and change in ACQ-6 (r=-.57, p=.002) on Day-28
C) Linear correlation for Day-0 post-BD VDP and change in Eosinophil count (ρ=-.37; p=.049) on Day-28.
D) Linear correlation for Day-0 CT mucus score and change in Eosinophil count (ρ=-.44, p=.04) on Day-28.
E) Linear correlation for Day-0 CT mucus score and change in VDP (r=-.56; p=.01) on Day-28.
F) Linear correlation for Day-0 CT mucus score and change in SGRQ (r=-.51; p=.03) on Day-28.

BD=bronchodilator; VDP=ventilation defect percent; ACQ=asthma control questionnaire; Eos=blood eosinophil count; SGRQ=St. George's respiratory questionnaire

r=Pearson correlation; ρ=Spearman correlation; p=Holm-Bonferroni corrected p-value

Table 3-2. Multivariable Linear Regression Models

Parameter	R^2	ANOVA p	Unstandardized B	Standardized β	*p**	Excluded variables	Standardized β	*p**
ΔACQ-6								
Model 1	0.503	<.001						
Mucus Score			-0.010 ± 0.020	-0.709	**<.001**	Eos	-0.070	.8
						WA%	-0.199	.5
						VDP	-0.460	**.02**
						VDP†	0.275	.08
Model 2	0.537	<.001						
VDP			-0.052 ± 0.009	-0.733	**<.001**	Eos	-0.361	.2
						WA%	-0.039	.9
						VDP†	0.188	.3
						Mucus Score	-0.371	.06
Model 3	0.600	<.001						
Mucus Score			-0.052 ± 0.026	-0.371	0.06	Eos	-0.361	.2
VDP			-0.032 ± 0.013	-0.460	**0.02**	WA%	-0.039	.9
						VDP†	0.188	.3

R^2=goodness-of-fit; ANOVA=analysis of variance; B=unstandardized regression coefficient ± standard error; β=standardized regression coefficient; Δ=change at 28 days; ACQ=asthma control questionnaire; Eos=blood eosinophil count; WA%=wall area percent; VDP=ventilation defect percent; †bronchodilator reversibility; p*=coefficient significance.

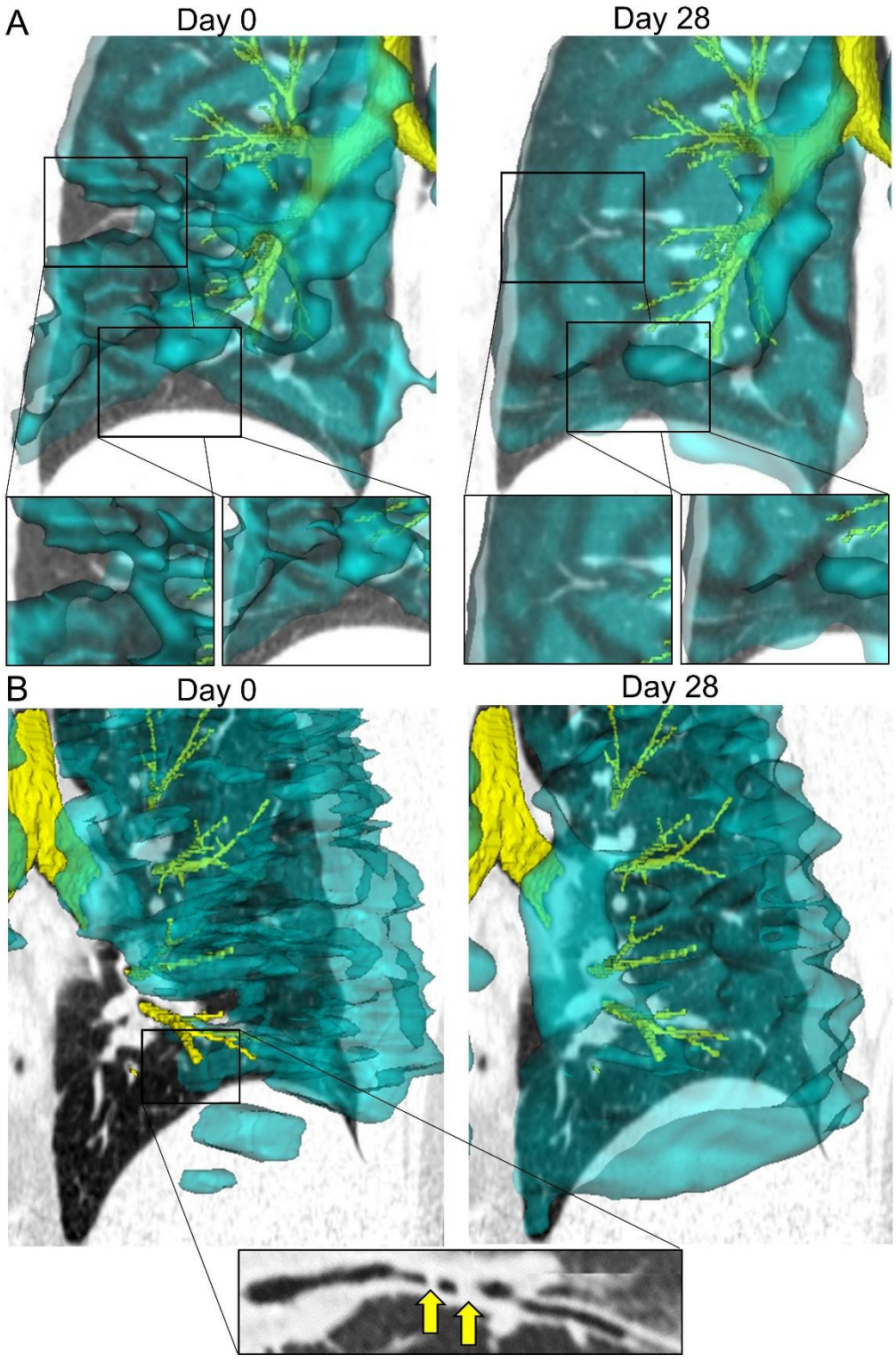

Figure 3-5. Relationship of ^{129}Xe MRI Ventilation Defects and Mucus Plugs
A) Day-0 (left) and Day-28 (right) ^{129}Xe ventilation co-registered with CT airway tree. Participant P26 is a 43-year-old female with Day-0/28 FEV_1=83%/102%, Day-0/28 ACQ-6=4.2/2.5 and Day-0/28 VDP=11%/3%. Left panel inset (Day-0) shows RB6 sub-subsegments (CT wall area%=67%, airway truncated) and RB8 (CT wall area%=72%, airway narrowed)

leading to two ventilation defects. Right panel insets (Day-28), show both ventilation defects resolved (ΔVDP on Day-28= -8%) post-benralizumab.

B) Day-0 (left) and Day-28 (right) posterior view of ^{129}Xe ventilation co-registered with CT airway tree. Participant P16 is a 62-year-old male with mucus score=13 and Day-0/28 FEV_1=88%/99%, Day-0/28 ACQ-6=4.3/1.7 and Day-0/28 VDP=18%/9%. Yellow arrows in left panel inset point to CT evidence of mucus plugs blocking RB10 subsegment leading to substantial ventilation defect. Right panel shows normalization of ventilation defect in the same region on Day-28, post-benralizumab.

3.4 Discussion

A hallmark of the mechanism of action of benralizumab is the depletion of blood[4] and sputum eosinophils[43] which in turn alters airway eosinophilic inflammation, thereby improving disease control and quality-of-life. To our knowledge, this study is the first to explore 28-day responses to a single dose of benralizumab in patients with moderate, GINA-4 asthma (24/29 not on maintenance prednisone) using non-invasive imaging measurements of airway function and airway mucus. Previous investigations focused on a mixture of different biologics[16,44] in prednisone-dependent asthma. In contrast, while the participants evaluated here were certainly poorly controlled, most had not been assessed to determine asthma severity and only five were receiving maintenance prednisone. Except for two participants, none of these participants had previously received any prior biologic therapy.

On Day-28 post-benralizumab we observed: 1) significantly improved mean VDP, eosinophil count, ACQ-6 and AQLQ scores, 2) significantly improved peripheral ($R_{5\text{-}19Hz}$) airways resistance (but not central airways resistance or reactance) in all participants, 3) significantly improved mean ACQ-6 and VDP in the ≥5 mucus-plugs subgroup, but not the <5 mucus-plugs subgroup, and, 4) pre-therapy VDP and mucus score values were significant variables in a model for ACQ-6 improvements post-benralizumab.

As expected, eosinophil count, ACQ-6 and AQLQ scores were significantly improved post-benralizumab. On Day-28, mean VDP was significantly improved for all participants. While mean VDP improved, it was still abnormal (≥4.3%)[42] for 21/29 participants on Day-28, suggesting that while airway eosinophilia was likely improved, airway inflammation was not completely abrogated and/or airway luminal obstructions remained. Evidence to support the latter stems from previous work that showed that up to one third of patients with asthma have persistent airway mucus occlusions despite normal sputum eosinophil counts.[21]

We also observed that peripheral airways resistance ($R_{5\text{-}19Hz}$) was significantly improved post-benralizumab in all participants. For context, previous work also showed that oscillometry detected airway functional improvements in benralizumab-treated patients before or in the absence of spirometry improvements.[45] Taken together, these findings suggest that the mechanism of action of benralizumab may involve the peripheral airways, even in patients with substantial mucus plugging. Importantly, baseline VDP and not $R_{5\text{-}19Hz}$ predicted response to treatment, suggesting that VDP might be a more sensitive measure of "peripheral airway lumenization" than $R_{5\text{-}19Hz}$, where "lumenization" refers to the opening of the peripheral airways to the extent that inhaled gas can move into the corresponding lung segments.

Both ACQ-6 and VDP significantly improved in participants in the ≥5 mucus-plugs subgroup, but not the <5 mucus-plugs subgroup, suggesting that mucus plugs may have cleared or became disrupted after treatment initiation, and this may have influenced ventilation improvements. It is important to note that we are assuming that eosinophils and mucus plugs are being depleted in the airways because of ventilation defect improvements downstream from mucus plugs, but we have not confirmed this. It also appeared that VDP and ACQ-6 responses were dominated by the ≥5 mucus-plugs subgroup. Importantly, the two mucus subgroups were significantly different for baseline eosinophil count and VDP, which suggests a direct mechanistic relationship between airway eosinophilia, mucus occlusions[3] and VDP.[21]

There was a significant association between mucus score before therapy and the change in VDP and ACQ-6, 28-days after therapy initiated. The change in VDP on Day-28 was also significantly and positively related to baseline eosinophil count (but not FeNO). The notion that airway eosinophil depletion may result in improved VDP via a reduction in mucus occlusions agrees with previous results that showed the relationship between eosinophils and mucus plugs[3] and studies that showed the association between ventilation defects with

eosinophils[19] and mucus plugs.[21,22] In multivariable models, VDP and mucus score both explained ΔACQ-6 score on Day-28 which suggests that patients with worse ventilation heterogeneity and more mucus occlusions may expect greater ACQ-6 improvements post-benralizumab. Improved mean VDP could be explained by greater baseline FeNO and mucus score, as well as diminished bronchodilator reversibility, which suggests that the benralizumab effect on airway function is mechanistically linked to eosinophilic inflammation and mucus plug changes or destabilization, and not smooth muscle dysfunction.

We also observed a relationship between forced vital capacity and the change in VDP, which was consistent with previous work,[46,47] which showed that forced vital capacity may serve as a surrogate for air trapping in severe, unstable asthma.

We acknowledge several study limitations, including the small sample size which was mainly older and female, and the open-label nature of this study. We recognize the small sample size, in particular, of the ≥5 mucus-plugs subgroup and the presence of a few participants with a relatively large mucus score. CT images acquired here were at functional residual capacity +1L, which differs from previous work.[3] In the current study, however, the mean functional residual capacity +1L volume is 0.8 of mean total lung capacity, which would have minimal impact on the visualization of airway mucus in this study. It appears that mucus plug score and ACQ-6 response to benralizumab may be related, so it is worth pointing out that 18/27 (67%) of the participants evaluated showed CT evidence of airway mucous, which is similar to reports from the Severe Asthma Research program cohort (65/96 or 68%).[3] We also recognize that the lack of follow-up CT and airway lumen sputum sampling also limits our ability to more deeply understand the role of airway mucus, eosinophils and ventilation defects in these patients.

3.5 Interpretation

We hypothesized that improved airway function could be directly measured following a first benralizumab dose and that the presence of airway mucus could influence this potential response. Twenty-eight days after a single dose, we observed significantly improved ^{129}Xe MRI ventilation defects and asthma control. In addition, this is the first study to reveal that, in poorly controlled asthma, MRI ventilation defects and CT mucus score measured prior to therapy explained significantly improved asthma control after a single benralizumab dose.

3.6 References

1. Chung, K.F., *et al.* International ERS/ATS guidelines on definition, evaluation and treatment of severe asthma. *Eur Respir J* **43**, 343-373 (2014).

2. Bousquet, J., *et al.* Eosinophilic inflammation in asthma. *N Engl J Med* **323**, 1033-1039 (1990).

3. Dunican, E.M., *et al.* Mucus plugs in patients with asthma linked to eosinophilia and airflow obstruction. *J Clin Invest* **128**, 997-1009 (2018).

4. Kolbeck, R., *et al.* MEDI-563, a humanized anti-IL-5 receptor alpha mAb with enhanced antibody-dependent cell-mediated cytotoxicity function. *J Allergy Clin Immunol* **125**, 1344-1353 e1342 (2010).

5. Moran, A.M., *et al.* Blood Eosinophil Depletion with Mepolizumab, Benralizumab, and Prednisolone in Eosinophilic Asthma. *Am J Respir Crit Care Med* **202**, 1314-1316 (2020).

6. Bleecker, E.R., *et al.* Efficacy and safety of benralizumab for patients with severe asthma uncontrolled with high-dosage inhaled corticosteroids and long-acting beta2-agonists (SIROCCO): a randomised, multicentre, placebo-controlled phase 3 trial. *Lancet* **388**, 2115-2127 (2016).

7. FitzGerald, J.M., *et al.* Benralizumab, an anti-interleukin-5 receptor alpha monoclonal antibody, as add-on treatment for patients with severe, uncontrolled, eosinophilic asthma (CALIMA): a randomised, double-blind, placebo-controlled phase 3 trial. *Lancet* **388**, 2128-2141 (2016).

8. Nair, P., *et al.* Oral Glucocorticoid-Sparing Effect of Benralizumab in Severe Asthma. *N Engl J Med* **376**, 2448-2458 (2017).

9. Chanez, P., McDonald, M., Garin, M. & Murphy, K. Early decreases in blood eosinophil levels with reslizumab. *J Allergy Clin Immunol* **143**, 1653-1655 (2019).

10. Sheehan, J.K., Richardson, P.S., Fung, D.C., Howard, M. & Thornton, D.J. Analysis of respiratory mucus glycoproteins in asthma: a detailed study from a patient who died in status asthmaticus. *Am J Respir Cell Mol Biol* **13**, 748-756 (1995).

11. Huber, H.L. & Koessler, K.K. The pathology of bronchial asthma. *Arch Intern Med* **30**, 689-760 (1922).

12. Fahy, J.V., Kim, K.W., Liu, J. & Boushey, H.A. Prominent neutrophilic inflammation in sputum from subjects with asthma exacerbation. *J Allergy Clin Immunol* **95**, 843-852 (1995).

13. Hogg, J.C. The pathology of asthma. *Clin Chest Med* **5**, 567-571 (1984).

14. Bhalla, M., *et al.* Cystic fibrosis: scoring system with thin-section CT. *Radiology* **179**, 783-788 (1991).

15. Hall, C.S., *et al.* Single-Session Bronchial Thermoplasty Guided by (129)Xe Magnetic Resonance Imaging. A Pilot Randomized Controlled Clinical Trial. *Am J Respir Crit Care Med* **202**, 524-534 (2020).

16. Svenningsen, S., Eddy, R.L., Kjarsgaard, M., Parraga, G. & Nair, P. Effects of Anti-T2 Biologic Treatment on Lung Ventilation Evaluated by MRI in Adults With Prednisone-Dependent Asthma. *Chest* **158**, 1350-1360 (2020).

17. Svenningsen, S., *et al.* Hyperpolarized (3) He and (129) Xe MRI: differences in asthma before bronchodilation. *J Magn Reson Imaging* **38**, 1521-1530 (2013).

18. Svenningsen, S., *et al.* What are ventilation defects in asthma? *Thorax* **69**, 63-71 (2014).

19. Svenningsen, S., *et al.* Sputum Eosinophilia and Magnetic Resonance Imaging Ventilation Heterogeneity in Severe Asthma. *Am J Respir Crit Care Med* **197**, 876-884 (2018).

20. Eddy, R.L., *et al.* Is Computed Tomography Airway Count Related to Asthma Severity and Airway Structure and Function? *Am J Respir Crit Care Med* **201**, 923-933 (2020).

21. Svenningsen, S., *et al.* CT and Functional MRI to Evaluate Airway Mucus in Severe Asthma. *Chest* **155**, 1178-1189 (2019).

22. Mummy, D.G., *et al.* Mucus Plugs in Asthma at CT Associated with Regional Ventilation Defects at Helium 3 MRI. *Radiology*, 204616 (2021).

23. Kirby, M., Wheatley, A., McCormack, D.G. & Parraga, G. Development and application of methods to quantify spatial and temporal hyperpolarized He-3 MRI ventilation dynamics: Preliminary results in chronic obstructive pulmonary disease. *Proc Spie* **7626**, 762605 (2010).

24. Svenningsen, S., Nair, P., Guo, F., McCormack, D.G. & Parraga, G. Is ventilation heterogeneity related to asthma control? *Eur Respir J* **48**, 370-379 (2016).

25. Global Initiative for Asthma (GINA). Global Strategy for Asthma Management and Prevention. (2020).

26. Pellegrino, R., *et al.* Interpretative strategies for lung function tests. *Eur Respir J* **26**, 948-968 (2005).

27. Juniper, E.F., Bousquet, J., Abetz, L., Bateman, E.D. & GOAL Committee. Identifying 'well-controlled' and 'not well-controlled' asthma using the Asthma Control Questionnaire. *Respir Med* **100**, 616-621 (2006).

28. Juniper, E.F., O'Byrne, P.M., Guyatt, G.H., Ferrie, P.J. & King, D.R. Development and validation of a questionnaire to measure asthma control. *Eur Respir J* **14**, 902-907 (1999).

29. Juniper, E.F., Buist, A.S., Cox, F.M., Ferrie, P.J. & King, D.R. Validation of a standardized version of the Asthma Quality of Life Questionnaire. *Chest* **115**, 1265-1270 (1999).

30. Jones, P.W., Quirk, F.H., Baveystock, C.M. & Littlejohns, P. A self-complete measure of health status for chronic airflow limitation. The St. George's Respiratory Questionnaire. *Am Rev Respir Dis* **145**, 1321-1327 (1992).

31. Miller, M.R., *et al.* Standardisation of spirometry. *Eur Respir J* **26**, 319-338 (2005).

32. American Thoracic Society & European Respiratory Society. ATS/ERS recommendations for standardized procedures for the online and offline measurement of exhaled lower respiratory nitric oxide and nasal nitric oxide, 2005. *Am J Respir Crit Care Med* **171**, 912-930 (2005).

33. King, G.G., *et al.* Technical standards for respiratory oscillometry. *Eur Respir J* **55**(2020).

34. Walker, T.G. & Happer, W. Spin-exchange optical pumping of noble-gas nuclei. *Rev Mod Phys* **69**, 629-642 (1997).

35. Kirby, M., *et al.* Hyperpolarized 3He magnetic resonance functional imaging semiautomated segmentation. *Acad Radiol* **19**, 141-152 (2012).

36. Kirby, M., *et al.* Longitudinal Computed Tomography and Magnetic Resonance Imaging of COPD: Thoracic Imaging Network of Canada (TINCan) Study Objectives. *Chronic Obstr Pulm Dis* **1**, 200-211 (2014).

37. Kirby, M., *et al.* Total Airway Count on Computed Tomography and the Risk of Chronic Obstructive Pulmonary Disease Progression. Findings from a Population-based Study. *Am J Respir Crit Care Med* **197**, 56-65 (2018).

38. Smith, B.M., *et al.* Comparison of spatially matched airways reveals thinner airway walls in COPD. The Multi-Ethnic Study of Atherosclerosis (MESA) COPD Study and the Subpopulations and Intermediate Outcomes in COPD Study (SPIROMICS). *Thorax* **69**, 987-996 (2014).

39. Sun, G.W., Shook, T.L. & Kay, G.L. Inappropriate use of bivariable analysis to screen risk factors for use in multivariable analysis. *J Clin Epidemiol* **49**, 907-916 (1996).

40. Vatcheva, K.P., Lee, M., McCormick, J.B. & Rahbar, M.H. Multicollinearity in Regression Analyses Conducted in Epidemiologic Studies. *Epidemiology (Sunnyvale)* **6**(2016).

41. Zach, J.A., *et al.* Quantitative computed tomography of the lungs and airways in healthy nonsmoking adults. *Investigative radiology* **47**, 596-602 (2012).

42. Pike, D., Kirby, M., Guo, F., McCormack, D.G. & Parraga, G. Ventilation heterogeneity in ex-smokers without airflow limitation. *Acad Radiol* **22**, 1068-1078 (2015).

43. Laviolette, M., *et al.* Effects of benralizumab on airway eosinophils in asthmatic patients with sputum eosinophilia. *J Allergy Clin Immunol* **132**, 1086-1096 (2013).

44. Svenningsen, S., Haider, E.A., Eddy, R.L., Parraga, G. & Nair, P. Normalisation of MRI ventilation heterogeneity in severe asthma by dupilumab. *Thorax* **74**, 1087-1088 (2019).

45. Shirai, T., *et al.* Oscillometry improves earlier than spirometry after benralizumab initiation in severe asthma. *Allergy* **75**, 2678-2680 (2020).

46. Sorkness, R.L., *et al.* Lung function in adults with stable but severe asthma: air trapping and incomplete reversal of obstruction with bronchodilation. *J Appl Physiol (1985)* **104**, 394-403 (2008).

47. Sorkness, R.L., *et al.* Obstruction phenotype as a predictor of asthma severity and instability in children. *J Allergy Clin Immunol* **142**, 1090-1099 e1094 (2018).

3.7 Supplement

3.7.1 Results:

Table 3-4 shows there was no significant difference among baseline characteristics for participants who completed a Day-14 face-to-face visit (n=8; 5 females, 3 males; mean age 60±9yr) or phone call (n=21; 15 females, 6 males; mean age 60±13yr).

On Day-14 and as shown in **Figure 3-6**, there was no clinically relevant improvement in FEV_1>MCID[1] in any participant (0/8) and no significant change in mean FEV_1 on Day-14. There was a VDP improvement >MCID [2] in 4/8 participants (P02, P15, P19, P24) on Day-14. Also shown in **Figure 3-6**, on Day-28 there were clinically relevant improvements in 15/29 participants for mean pre-BD VDP (Day-0=17±10%; Day-28=13±11%; Δ=-4.5±2.8%, p=.03) and mean post-BD VDP (Day-0=12±10%; Day-28=9±9%; Δ=-3.5±2.5%, p=.001). Participants with no MRI improvement on Day-14 had significantly worse SGRQ (62±11, p=.027) and lower eosinophil count (425±300 cells/μL, p=.048) at baseline than those with MRI improvements (SGRQ: 35±15; Blood eosinophils: 1000±355 cells/μL).

In all participants, eosinophil counts (Day-0=630±380 cells/μL; Day-28=30±70 cells/μL, p<.001), and SGRQ (Day-0=50±21; Day-28=37±19, p<.001) were significantly improved on Day-28 whereas FeNO (n=27; Day-0=48±35 ppb; Day-28=57±53 ppb, p=.2) was not.

In an exploratory analysis, participants were classified into three subgroups by baseline FeNO (<25 ppb, n=8; 25-50 ppb, n=9; >50 ppb, n=10).[3] Whilst there were no significant differences between the subgroups at baseline, **Figure 3-7** shows there was a VDP improvement >MCID[2] for the 25-50 ppb and >50 ppb FeNO subgroups, but not the <25 ppb FeNO subgroup. Reactance (X_5) (p=.002) and reactance area (A_X) (p=.007) both significantly improved on Day-28 in the >50 ppb FeNO subgroup.

We acknowledge the limitation of the small sample size of eight participants who completed an optional visit at Day-14.

3.7.2 References:

1. Santanello, N.C., Zhang, J., Seidenberg, B., Reiss, T.F. & Barber, B.L. What are minimal important changes for asthma measures in a clinical trial? *Eur Respir J* **14**, 23-27 (1999).

2. Eddy, R.L., Svenningsen, S., McCormack, D.G. & Parraga, G. What is the minimal clinically important difference for helium-3 magnetic resonance imaging ventilation defects? *Eur Respir J* **51**(2018).

3. Dweik, R.A., *et al.* An official ATS clinical practice guideline: interpretation of exhaled nitric oxide levels (FENO) for clinical applications. *Am J Respir Crit Care Med* **184**, 602-615 (2011).

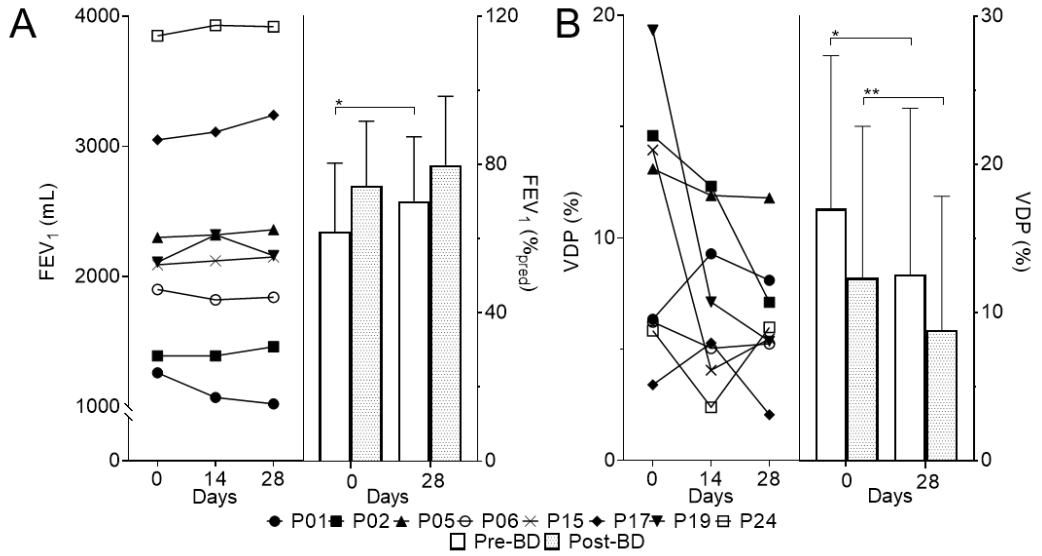

Figure 3-6. Spirometry and MRI on Day-0, -14 and -28

A)

Left panel shows post-BD FEV_1 for eight participants with 14-day imaging on Day-0, 14 and 28. There was no statistically significant change in mean FEV_1 on Day-14 (Day-0=2240±850mL or 76±15%, Day-14=2250±910mL or 76±17%, p=.9/1.0) or Day-28 (2270±930mL or 77±19%, p=1.0/1.0). On Day-28, change in FEV_1 > MCID for P01 (-240 mL).

Right panel shows FEV_1 box and whisker plot for all 29 participants on Day-0 and Day-28. Pre-BD FEV_1 was significantly different on Day-28 (Day-0=1770±740mL/62±18%, Day-28=2000±750mL/70±17%, p=.01/.02). Post-BD FEV_1 was not significantly different on Day-28 (Day-0=2120±780mL/74±17%, Day-28=2280±830mL/80±9%, p=.06/.06).

B)

Left panel shows post-BD MRI VDP for eight participants with 14-day imaging on Day-0, 14 and 28. There was no statistically significant change in mean VDP on Day-14 (Day-0=10±6%, Day-14, 7±4%, p=.5) or Day-28 (Day-28, 6±3%, p=.5). There were VDP changes > MCID on Day-14 for P02 (-2%), P15 (-10%), P19 (-12%) and P24 (-3%) and on Day-28 for P02 (-7%), P15 (-8%) and P19 (-14%).

Right panel shows box and whisker plot for VDP for all 29 participants on Day-0 and Day-28. Pre-and post-BD VDP was significantly different on Day-28 (Pre-BD Day-0=17±10%, Day-28=13±11%, p=.03; Post-BD VDP Day-0=12±10%, Day-28=9±9%, p=.001).

*Box=mean; Whiskers=standard deviation; White bars=pre-BD; grey bars=post-BD; ***=p≤0.001; **=p≤0.01; *=p<0.05; p=Holm-Bonferroni corrected values*

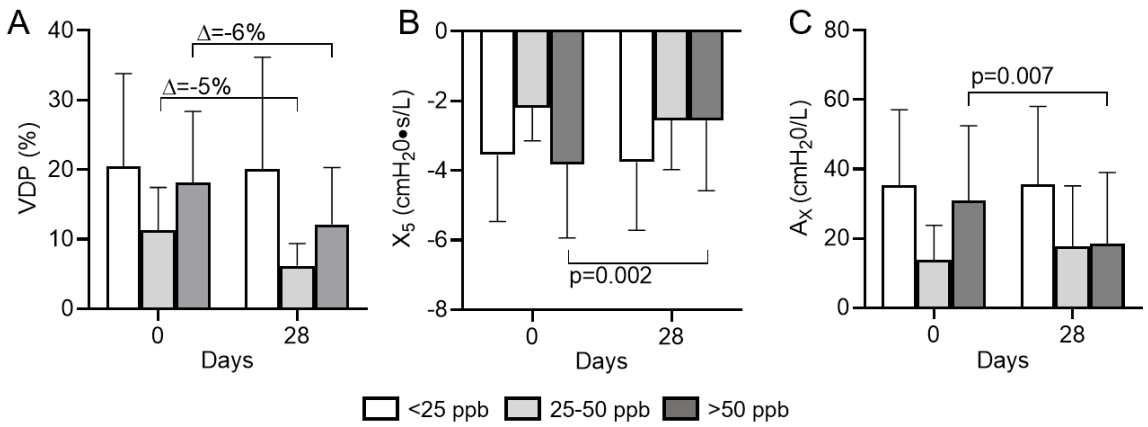

Figure 3-7. Ventilation and oscillometry at Day-28 by FeNO subgroups

VDP (A) in 25-50 ppb and >50 ppb subgroups showed clinically significant improvements and the reactance at 5Hz (B) and reactance area (C) in the >50 ppb subgroup showed statistically significant improvements at Day-28.

Table 3-3. Asthma Medications

Participant	ICS/LABA	OCS/LAMA/LTRA/Other
P01	Zenhale: 2 puffs TID 200/5 Spiriva: 2 puffs QD	
P02	Breo Ellipta: 1 puff QD 200/25	montelukast: 20 mg QD
P03	Symbicort: 2 puffs BID 200/6 Spiriva: 2 puffs QD	
P04	Symbicort: 1 puff BID	
P05	Symbicort: 2 puffs BID Pulmicort: 2 puffs BID 400	Prednisone: 5 mg TID Singulair: 10 mg QD
P06	Symbicort: 2 puffs BID 200/6 Spiriva: 2 puffs QD	Singulair: 10 mg QD
P07	Symbicort: 2 puffs BID 200/6	Prednisone: 5 mg QD Umeclidinium: 1 puff QD
P08	Advair: 2 puffs BID 250/25 Spiriva: 2 puffs QAM	
P09	Symbicort: 2 puffs BID 200/6 Spiriva: 1 puff QD	
P10	Symbicort: 2 puffs BID 200/6 Pulmicort: 2 puffs BID 400	methylprednisolone 80mg/mL Q10days
P11	Advair: 1 puff BID 500 Spiriva: 2 puffs QD	
P12	Symbicort: 2 puffs TID 200/6	
P13	Zenhale: 2 puffs TID 200/5 Breo Ellipta: 1 puff QD 200/25	
P14	Breo Ellipta: 1 puff QD 200/25 4 times/week	Prednisone: 10 mg QD *Xolair: 300 mg BIW
P15	Symbicort: 2 puffs BID 200/6 Arnuity Ellipta: 200 µg QD	
P16	Symbicort: 2 puffs QID 200/6 Spiriva: 2 puffs QD	Prednisone: 10 mg QD Singulair: 10 mg QD
P17	Zenhale: 2 puffs TID 200/5	
P18	Symbicort: 2 puffs BID 200/6 Tudorza: 1 puff BID at 400µg	
P19	Symbicort: 2 puffs BID 200/6	Singulair: 30 mg QD
P20	Alvesco: 2 puffs BID at 200µg	*Xolair: 300 mg BIW
P21	Spiriva: 1 puff QD at 18 µg Zenhale: 2 puffs QD 200/5	
P22	Symbicort: 2 puffs TID 200/6 Arnuity Ellipta: 1 puff QD Theophylline: 300 mg QD	
P23	Symbicort: 2 puffs BID 200/6	
P24	Zenhale: 2 puffs BID 200/5 Spiriva: 2 puffs QD	
P25	Zenhale: 2 puffs BID 200/5	
P26	Symbicort: 2 puffs BID 200/6 Spiriva: 2 puffs QID	Singulair: 10 mg QD
P27	Symbicort: 2 puffs BID 200/6 Spiriva: 2 puffs QID	
P28	Spiriva: 1 puff QD	Prednisone: 15 mg QD
P29	Symbicort: 2 puffs BID 200/6	

ICS=inhaled corticosteroid; LABA=long-acting beta-agonist; OCS=oral corticosteroid; LAMA=long-acting muscarinic antagonist; LTRA=leukotriene receptor antagonist; TID=three times a day; QD=once a day; BID=twice a day; QAM=every morning; Q=every;

QID=four times a day; BIW=twice a week *Xolair washout ≥8 weeks **Error! Reference s ource not found.**

Table 3-4. Baseline Demographic Characteristics

Parameter mean ± SD (mean/MEDIAN: min-max)	Participants 14-day Imaging (n=8)	Participants no 14-day Imaging (n=21)	p*
Age years	60 ± 9	60 ± 14	-
Female n (%)	5 (63)	15 (71)	-
BMI kg/m^2	29 ± 8	29 ± 4	-
Pack-years	(9/0:0-45)	(6/0: 0-30)	-
Duration of Asthma	33 ± 20	23 ± 22	-
Pulmonary function			
Pre-BD FEV_1 mL	1900 ± 800	1700 ± 700	1.0
Pre-BD $FEV_{1\%pred}$	65 ± 17	61 ± 19	-
Post-BD FEV_1 mL	2200 ± 900	2100 ± 800	1.0
Post-BD $FEV_{1\%pred}$	76 ± 15	74 ± 19	-
Pre-BD FEV_1/FVC	0.63 ± 0.09	0.62 ± 0.14	-
Post-BD FEV_1/FVC	0.69 ± 0.09	0.67 ± 0.12	-
Inflammatory markers			
Eos cells/μL	710 ± 430	600 ± 360	1.0
FeNO ppb	57 ± 41	45 ± 33‡	.7
Asthma QoL and control			
ACQ-6	2.1 ± 1.5	2.4 ± 1.6	1.0
AQLQ	4.2 ± 1.4	4.4 ± 1.5	-
SGRQ	48 ± 19	51 ± 22	-
CT imaging			
TAC	146 ± 43	137 ± 54‡	.7
Mucus Score	3 ± 4	6 ± 10‡	-
Airway WA%	70 ± 2	70 ± 2‡	-
Airway LA mm^2	8.24 ± 1.66	7.92 ± 2.92‡	-
Airway WT mm	1.24 ± 0.09	1.17 ± 0.14‡	-
Airway WT%	19 ± 1	18 ± 1‡	-
MRI			
Pre-BD VDP	15 ± 4	18 ± 12	1.0
Post-BD VDP	10 ± 6	13 ± 12	1.0

BMI=body mass index; BD=bronchodilator; FEV_1=forced expiratory volume in 1 second; $\%_{pred}$=percent of predicted value; FVC=forced vital capacity; Eos=blood eosinophil count; FeNO=fraction of exhaled nitric oxide; ppb=parts per billion; QoL=quality-of-life; ACQ=Asthma Control Questionnaire; AQLQ=Asthma Quality-of-Life Questionnaire; SGRQ=St. George's Respiratory Questionnaire; CT=computed tomography; TAC=total airway count; WA=wall area; LA=lumen area; WT=wall thickness; VDP=ventilation defect percent; *=Holm-Bonferroni corrected values showing significance between Day-14 imaging and no imaging groups ‡n=19

Table 3-5. Pre- and post-bronchodilator Spirometry, Imaging and Inflammatory Markers

	Pre-BD FEV_1 (mL)			Post-BD FEV_1 (mL)				Pre-BD VDP (%)			Post-BD VDP (%)				Eosinophil Count (cells/μL)			FeNO (ppb)			Mucus Score	TAC
	Day 0	Day 28	Δ**	Day 0	Day 14	Δ*	Day 28	Δ**	Day 0	Day 28	Δ**	Day 0	Day 14	Δ*	Day 28	Δ**	Day 0	Day 28	Δ**	Day 0	Day 28	Δ**	Day 0	Day 0
P01	1010	880	-130	1260	1070	-190	1020	-240	1010	880	-130	1260	1070	-190	1020	-240	1010	880	-130	1260	1070	-190	1020	-240
P02	1430	1410	-20	1390	1970	580	1460	70	1430	1410	-20	1390	1970	580	1460	70	1430	1410	-20	1390	1970	580	1460	70
P03	3120	2780	-340	3260			3230	-30	3120	2780	-340	3260			3230	-30	3120	2780	-340	3260			3230	-30
P04	1500	2050	550	2030			2420	390	1500	2050	550	2030			2420	390	1500	2050	550	2030			2420	390
P05	1490	2020	530	2300	2320	20	2360	60	1490	2020	530	2300	2320	20	2360	60	1490	2020	530	2300	2320	20	2360	60
P06	1270	1650	380	1900	1820	-80	1840	-60	1270	1650	380	1900	1820	-80	1840	-60	1270	1650	380	1900	1820	-80	1840	-60
P07	1180	1240	60	1540			1490	-50	1180	1240	60	1540			1490	-50	1180	1240	60	1540			1490	-50
P08	1420	1320	-100	1890			1520	-370	1420	1320	-100	1890			1520	-370	1420	1320	-100	1890			1520	-370
P09	680	1910	1230	990			2130	1140	680	1910	1230	990			2130	1140	680	1910	1230	990			2130	1140
P10	1010	900	-110	1370			1380	10	1010	900	-110	1370			1380	10	1010	900	-110	1370			1380	10
P11	740	830	90	820			860	40	740	830	90	820			860	40	740	830	90	820			860	40
P12	2540	2680	140	2740			2800	60	2540	2680	140	2740			2800	60	2540	2680	140	2740			2800	60
P13	2090	1910	-180	2250			2230	-20	2090	1910	-180	2250			2230	-20	2090	1910	-180	2250			2230	-20
P14	1700	1650	-50	1950			1810	-140	1700	1650	-50	1950			1810	-140	1700	1650	-50	1950			1810	-140
P15	1960	2010	50	2090	2120	30	2150	60	1960	2010	50	2090	2120	30	2150	60	1960	2010	50	2090	2120	30	2150	60
P16	3000	3730	730	3770			4240	470	3000	3730	730	3770			4240	470	3000	3730	730	3770			4240	470
P17	2590	2850	260	3050	3030	-20	3240	190	2590	2850	260	3050	3030	-20	3240	190	2590	2850	260	3050	3030	-20	3240	190
P18	1950	2320	370	2620			2860	240	1950	2320	370	2620			2860	240	1950	2320	370	2620			2860	240
P19	2030	2040	10	2110	2320	210	2160	50	2030	2040	10	2110	2320	210	2160	50	2030	2040	10	2110	2320	210	2160	50
P20	2740	3450	710	3170			3560	390	2740	3450	710	3170			3560	390	2740	3450	710	3170			3560	390
P21	1260	1440	180	1550			1790	240	1260	1440	180	1550			1790	240	1260	1440	180	1550			1790	240
P22	1420	1740	320	1640			1800	160	1420	1740	320	1640			1800	160	1420	1740	320	1640			1800	160
P23	2210	2360	150	2430			2580	150	2210	2360	150	2430			2580	150	2210	2360	150	2430			2580	150
P24	3570	3300	-270	3850	3930	80	3920	70	3570	3300	-270	3850	3930	80	3920	70	3570	3300	-270	3850	3930	80	3920	70
P25	1710	1890	180	2080			1910	-170	1710	1890	180	2080			1910	-170	1710	1890	180	2080			1910	-170
P26	2220	2860	640	2570			3290	720	2220	2860	640	2570			3290	720	2220	2860	640	2570			3290	720
P27	1390	1480	90	1550			1730	180	1390	1480	90	1550			1730	180	1390	1480	90	1550			1730	180
P28	1290	1580	290	2170			2190	20	1290	1580	290	2170			2190	20	1290	1580	290	2170			2190	20
P29	900	1900	1000	1240			2140	900	900	1900	1000	1240			2140	900	900	1900	1000	1240			2140	900
Mean	1770	2010	230	2120	2320	70	2280	160	1770	2010	230	2120	2320	70	2280	160	1770	2010	230	2120	2320	70	2280	160
±SD	±740	±750	±370	±780	±850	±230	±830	±320	±740	±750	±370	±780	±850	±230	±830	±320	±740	±750	±370	±780	±850	±230	±830	±320

BD=bronchodilator; FEV_1=forced expiratory volume in 1 second; VDP=ventilation defect percent; FeNO=fractional exhaled nitric oxide; ppb=parts per billion; TAC=total airway count; SD=standard deviation; *change on Day-14; **change on Day-28; †n=27

Table 3-6. Pre- and post-bronchodilator Oscillometry

	Pre-BD R_{5Hz} (cmH_2O•s/L)			Post-BD R_{5Hz} cmH_2O•s/L)			Pre-BD R_{5-19Hz} (cmH_2O•s/L)			Post-BD R_{5-19Hz} (cmH_2O•s/L)			Pre-BD X_{5Hz} (cmH_2O•s/L)			Post-BD X_{5Hz} (cmH_2O•s/L)			Pre-BD A_X (cmH_2O/L)			Post-BD A_X (cmH_2O/L)		
	Day 0	Day 28	Δ**	Day 0	Day 28	Δ**	Day 0	Day 28	Δ**	Day 0	Day 28	Δ**	Day 0	Day 28	Δ**	Day 0	Day 28	Δ**	Day 0	Day 28	Δ**	Day 0	Day 28	Δ**
P01	5.63	6.42	0.79	6.21	6.18	-0.03	2.84	2.35	-0.49	2.88	2.73	-0.15	-6.37	-6.91	-0.54	-4.46	-6.18	-1.72	57.02	68.17	11.15	41.95	53.24	11.29
P02	2.76	2.69	-0.07	2.67	3.06	0.39	0.48	0.40	-0.08	0.46	0.55	0.09	-1.72	-1.61	0.11	-2.00	-1.82	0.18	7.78	6.29	-1.49	9.50	7.65	-1.85
P03	3.80	4.42	0.62	3.54	3.51	-0.03	1.15	1.34	0.19	1.05	0.96	-0.09	-3.55	-5.69	-2.14	-2.54	-3.74	-1.20	28.25	49.47	21.22	18.46	26.62	8.16
P04	8.05	5.00	-3.05	3.89	3.54	-0.35	3.85	1.34	-2.51	1.25	0.77	-0.48	-5.90	-3.44	2.46	-3.19	-2.35	0.84	59.37	26.57	-32.80	18.83	12.20	-6.63
P05	7.57	4.20	-3.37	4.39	3.37	-1.02	4.25	1.15	-3.10	1.10	0.95	-0.15	-6.39	-1.76	4.63	-2.08	-1.44	0.64	61.99	10.97	-51.02	14.46	7.46	-7.00
P06	5.56	7.64	2.08	6.10	4.84	-1.26	2.36	3.60	1.24	2.46	1.71	-0.75	-6.64	-6.31	0.33	-5.25	-3.49	1.76	60.52	58.38	-2.14	44.45	29.51	-14.94
P07	6.05	6.53	0.48	4.95	5.54	0.59	2.95	2.85	-0.10	2.06	2.15	0.09	-8.33	-8.87	-0.54	-7.38	-6.88	0.50	80.37	79.12	-1.25	65.28	58.95	-6.33
P08	9.91	9.03	-0.88	7.69	8.68	0.99	4.46	3.34	-1.12	3.07	2.98	-0.09	-8.81	-5.20	3.61	-4.22	-4.51	-0.29	102.85	72.35	-30.50	52.12	66.47	14.35
P09	13.63	-	-	13.68	-	-	5.96	-	-	3.97	-	-	-9.08	-	-	-6.03	-	-	183.44	-	-	102.68	-	-
P10	6.89	6.97	0.08	5.64	6.13	0.49	3.35	3.06	-0.29	1.99	2.54	0.55	-8.42	-9.37	-0.95	-6.37	-5.10	1.27	87.24	95.64	8.40	56.24	48.17	-8.07
P11	6.03	5.52	-0.51	6.43	5.01	-1.42	2.86	2.68	-0.18	2.65	2.15	-0.50	-6.35	-6.50	-0.15	-7.17	-6.46	0.71	61.46	59.44	-2.02	72.49	55.90	-16.59
P12	6.00	5.98	-0.02	3.83	3.51	-0.32	1.04	1.53	0.49	0.54	0.45	-0.09	-2.56	-2.52	0.04	-1.57	-1.23	0.34	19.66	27.17	7.51	7.31	7.72	0.41
P13	4.88	6.65	1.77	3.79	3.98	0.19	1.78	3.52	1.74	1.19	-0.17	-1.36	-3.00	-5.63	-2.63	-1.86	-2.43	-0.57	28.67	56.13	27.46	14.87	19.22	4.35
P14	8.36	7.04	-1.32	5.70	6.29	0.59	3.55	2.89	-0.66	2.04	2.44	0.40	-7.14	-8.45	-1.31	-3.75	-5.42	-1.67	89.49	90.17	0.68	33.89	57.47	23.58
P15	2.97	2.89	-0.08	2.58	3.19	0.61	-0.01	-0.11	-0.10	0.05	0.22	0.17	-1.60	-1.46	0.14	-1.44	-1.66	-0.22	6.09	5.67	-0.42	5.55	6.91	1.36
P16	-	4.15	-	4.19	5.08	0.89	-	1.05	-	0.65	-0.20	-0.85	-	-2.48	-	-1.78	-1.04	0.74	-	17.36	-	8.02	3.35	-4.67
P17	3.55	3.29	-0.26	3.25	3.06	-0.19	1.55	1.30	-0.25	1.43	1.06	-0.37	-4.08	-2.85	1.23	-2.21	-2.78	-0.57	29.17	21.10	-8.07	13.88	16.52	2.64
P18	5.61	6.59	0.98	3.55	3.49	-0.06	2.94	3.45	0.51	1.38	1.13	-0.25	-7.88	-6.52	1.36	-4.70	-2.57	2.13	81.05	77.34	-3.71	40.61	19.83	-20.78
P19	4.93	-	-	5.32	-	-	0.67	-	-	0.59	-	-	-1.50	-	-	-1.50	-	-	6.82	-	-	7.08	-	-
P20	4.51	5.71	1.20	3.14	3.74	0.60	0.89	1.78	0.89	0.16	0.62	0.46	-1.42	-2.57	-1.15	-0.86	-1.44	-0.58	12.07	26.59	14.52	3.37	6.90	3.53
P21	-	9.93	-	-	7.01	-	-	2.57	-	-	1.92	-	-	-6.75	-	-	-3.17	-	-	89.47	-	-	31.06	-
P22	6.14	5.40	-0.74	5.26	4.95	-0.31	2.89	1.93	-0.96	1.81	1.59	-0.22	-3.96	-2.85	1.11	-2.99	-2.51	0.48	48.87	31.29	-17.58	32.06	28.85	-3.21
P23	7.35	4.23	-3.12	5.47	4.31	-1.16	2.66	0.09	-2.57	0.62	-0.12	-0.74	-5.26	-1.29	3.97	-3.42	-1.34	2.08	69.02	5.02	-64.00	27.92	4.75	-23.17
P24	3.47	3.82	0.35	2.34	2.61	0.27	0.62	0.76	0.14	0.19	0.27	0.08	-1.73	-2.10	-0.37	-1.48	-1.66	-0.18	13.53	19.52	5.99	6.12	7.11	0.99
P25	5.22	4.87	-0.36	4.33	4.80	0.46	1.61	1.10	-0.50	0.86	1.33	0.47	-2.59	-2.11	0.49	-2.04	-2.59	-0.55	25.33	16.91	-8.43	13.22	15.02	1.79
P26	5.66	5.28	-0.38	3.78	2.73	-1.05	1.29	0.45	-0.84	-0.09	-0.32	-0.23	-2.31	-1.40	0.91	-1.58	-0.87	0.71	21.89	8.92	-12.97	5.97	2.15	-3.82
P27	6.12	5.63	-0.49	3.84	3.56	-0.28	1.66	1.97	0.31	0.54	0.36	-0.18	-2.98	-2.89	0.09	-2.12	-1.62	0.50	43.12	38.26	-4.86	20.53	10.45	-10.08
P28	13.18	8.26	-4.92	7.05	4.91	-2.14	6.40	2.17	-4.23	2.37	0.68	-1.69	-8.79	-2.83	5.96	-3.34	-1.45	1.89	129.72	47.47	-82.25	37.36	7.75	-29.61
P29	7.98	6.45	-1.53	6.85	4.96	-1.89	2.05	1.37	-0.68	1.99	0.04	-1.94	-4.20	-2.31	1.89	-4.22	-1.27	2.95	52.61	20.67	-31.94	39.70	3.80	-35.90
Mean	6.13±	5.62±	-0.51±	1.48±	1.39±	-0.21±	2.38±	1.85±	-0.53±	1.33±	1.03±	-0.30±	-4.88±	-4.14±	0.74±	-3.23±	-2.84±	0.39±	51.09±	40.74±	-10.34±	27.08±	22.46±	-4.62±
±SD	2.30	1.61	0.56	0.29	0.27	0.40	1.46	1.11	0.37	0.92	0.98	0.26	2.51	2.55	0.72	1.80	1.82	0.50	32.31	28.23	8.58	19.87	20.71	5.63

Note: Participants with missing measurements on Day-0 or Day-28 were not used to calculate mean or standard deviation. BD=bronchodilator; R=resistance; X=reactance; A_X=area under reactance curve; SD=standard deviation; **change on Day-28

Table 3-7. Asthma Quality-of-Life and Control

	ACQ-6			AQLQ			SGRQ		
Participant	Day 0	Day 28	Δ**	Day 0	Day 28	Δ**	Day 0	Day 28	Δ**
P01	2.67	3.5	0.83	2.4	2.6	0.2	72	72	0
P02	0.67	0	-0.67	6.1	6.8	0.7	20	10	-10
P03	0.33	0.17	-0.16	6.0	6.7	0.8	39	5	-35
P04	0.33	0.17	-0.16	6.6	6.4	-0.1	9	20	11
P05	1.5	1	-0.5	5.2	5.2	0.0	64	47	-17
P06	4.17	3	-1.17	2.6	3.9	1.3	65	53	-13
P07	0.17	0.83	0.66	5.5	5.7	0.2	24	16	-9
P08	3.33	2.17	-1.16	4.1	4.4	0.4	43	32	-10
P09	4.67	1.33	-3.34	1.5	4.8	3.4	81	46	-35
P10	0.67	1	0.33	5.7	6.4	0.7	44	24	-20
P11	3.83	2.33	-1.5	3.6	3.7	0.1	67	65	-2
P12	1.5	1	-0.5	5.3	6.2	0.9	32	39	7
P13	0.83	0.5	-0.33	6.2	6.7	0.5	27	28	1
P14	1.5	1.17	-0.33	4.3	4.9	0.6	35	26	-9
P15	0	0	0	5.8	6.8	1.0	25	12	-13
P16	3.33	1.67	-1.66	4.2	5.4	1.2	65	44	-22
P17	2.5	0.83	-1.67	4.3	5.5	1.2	46	30	-16
P18	0.17	0.67	0.5	6.9	6.8	-0.1	14	4	-10
P19	1.67	0.67	-1	3.9	6.1	2.2	44	35	-9
P20	3.5	2.83	-0.67	3.1	3.1	0.0	79	69	-11
P21	2.5	1.33	-1.17	4.0	5.1	1.1	50	43	-7
P22	2.17	1.5	-0.67	4.2	4.8	0.6	59	41	-18
P23	2.5	1.83	-0.67	4.2	4.8	0.6	65	50	-15
P24	4	3.33	-0.67	3.6	3.8	0.3	51	52	1
P25	3.17	1.33	-1.84	3.6	5.1	1.4	59	47	-12
P26	4.17	2.5	-1.67	3.9	4.8	0.9	70	60	-11
P27	3.33	0.5	-2.83	4.9	6.2	1.3	59	41	-18
P28	5.17	2.83	-2.34	1.4	2.1	0.7	85	62	-23
P29	3.33	0	-3.33	3.2	6.5	3.3	65	17	-49
Mean±SD	2.33±1.52	1.38±1.04	-0.95±0.34	4.3±1.4	5.2±1.3	0.9±0.4	50±21	37±19	-13±5

ACQ=Asthma Control Questionnaire; AQLQ=Asthma Quality-of-Life Questionnaire; SGRQ=St George's Respiratory Questionnaire; SD=standard deviation

Table 3-8. Mean Change Post-Benralizumab on Day-28

Parameter mean±SD	Day-0	Day 28	Δ	$p^{\dagger}$	p
All participants (n=29)					
Pre-BD FEV_1 ml	1770±740	2010±750	230±200	**0.002**	**0.012**
Post-BD FEV_1 ml	2120±780	2280±830	160±210	**0.015**	0.06
Eosinophils cells/µL	630±380	30±70	-600±70	**1.69×10^{-9}**	**2.0×10^{-8}**
FeNO (n=27) ppb	48±35	57±53	9±12	0.223	0.223
ACQ score	2.33±1.52	1.38±1.04	-0.95±0.34	**5.5×10^{-5}**	**0.0005**
AQLQ score	4.3±1.4	5.2±1.3	0.9±0.4	**9.0×10^{-6}**	**9.0×10^{-5}**
SGRQ score	50±21	37±19	-13±5	**5.0×10^{-6}**	**5.5×10^{-5}**
Pre-BD VDP %	17.0±10.3	12.6±11.2	-4.5±2.8	**0.0058**	**0.03**
Post-BD VDP %	12.3±10.2	8.8±9.0	-3.5±2.5	**0.00016**	**0.001**
$R_{5\text{-}19Hz}$ (n=26) cmH_2O•s/L	1.33±0.92	1.03±0.98	-0.30±0.26	**0.022**	**0.043**
Mucus<5 (n=18)					
Eosinophils cells/µL	520±280	30±70	-490±70	**6.35×10^{-8}**	**3.81×10^{-7}**
Post-BD FEV_1 $\%_{pred}$	79±14	81±17	2±5	0.28	0.28
ACQ score	1.8±1.3	1.4±1.1	-0.4±0.4	**0.022**	0.09
AQLQ score	4.8±1.4	5.3±1.3	0.5±0.4	**0.00013**	**0.0006**
Post-BD VDP %	8±7	7±5	-1.7±2.0	**0.025**	0.07
$R_{5\text{-}19Hz}$ cmH_2O•s/L	1.3±0.8	1.2±0.9	-0.1±0.3	0.24	0.49
Mucus≥5 (n=9)					
Eosinophils cells/µL	920±420	40±70	-880±140	**0.0005**	**0.003**
Post-BD FEV_1 $\%_{pred}$	64±21	77±24	13±11	0.06	0.12
ACQ score	3.1±1.4	1.2±1.0	-1.8±0.6	**0.001**	**0.006**
AQLQ score	3.9±1.2	5.4±1.1	1.5±0.5	**0.005**	**0.02**
Post-BD VDP %	21±13	13±14	-7.4±6.3	**0.0015**	**0.006**
$R_{5\text{-}19Hz}$ (n=7) cmH_2O•s/L	1.3±1.3	0.7±1.3	-0.5±0.7	0.1	0.19

BD=bronchodilator; FEV_1=forced expiratory volume in 1 second; FeNO=fraction of exhaled nitric oxide; ppb=parts per billion; ACQ=asthma control questionnaire; AQLQ=asthma quality-of-life questionnaire; SGRQ=St. George's Respiratory Questionnaire; VDP=ventilation defect percent; $R_{5\text{-}19Hz}$=peripheral airway resistance; $\%_{pred}$=percent of predicted value; $p^{\dagger}$=uncorrected significance value; p=Holm-Bonferroni corrected significance value

Table 3-9. Relationships between benralizumab response and Day-0 measurements

	Δpost-BD VDP		Δpre-BD FEV_1		Δpost-BD FEV_1		ΔAQLQ		ΔACQ-6	
	r/ρ	p	r/ρ	r/ρ	r/ρ	p	r/ρ	p	r/ρ	p
BMI	.29	.1	.02	.9	-.03	.9	-.07	.7	.11	.6
Pulmonary Function										
Pre-BD FEV_1	.09	.7	**-.44**	**.02**	-.28	.2	-.23	.2	.16	.4
Post-BD FEV_1	.15	.5	-.16	.4	-.12	.6	-.26	.2	.15	.4
Pre-BD FVC	.23	.3	**-.54**	**.004**	-.51	.008	-.35	.08	.20	.3
Post-BD FVC	**.41**	**.04**	**-.40**	**.05**	**-.46**	**.02**	**-.43**	**.03**	.24	.2
Pre-BD FEV_1/FVC	.14	.5	-.20	.3	-.04	.8	-.004	1.0	.22	.3
Post-BD FEV_1/FVC	.09	.7	-.05	.8	.07	.7	.10	.6	.15	.5
Inflammatory Markers										
Eos	**-.58**	**.002**	.20	.3	.32	.1	.34	.08	**-.43**	**.02**
FeNO	-.04	.9	.25	.2	.24	.2	-.02	.9	.07	.7
Asthma quality-of-life and control										
ACQ-6	-.22	.3	.36	.06	.25	.2	.32	.1	**-.71**	**<.001**
AQLQ	.24	.2	**-.43**	**.02**	-.30	.1	**-.48**	**.01**	**.53**	**.004**
SGRQ	-.28	.2	**.44**	**.02**	.33	.09	.35	.07	**-.54**	**.003**
CT Imaging										
TAC	-.48	.01	.02	.9	.14	.5	-.07	.7	-.02	.93
Mucus Score	-.56	.003	.18	.4	.22	.3	**.40**	**.04**	**-.57**	**.002**
WA%	.30	.1	-.27	.2	-.35	.07	**-.50**	**.008**	.31	.1
LA	**-.38**	**.05**	.09	.6	.18	.4	.29	.1	-.20	.3
WT	-.26	.2	-.16	.4	-.15	.5	-.12	.6	-.03	.9
WT%	.14	.5	-.12	.6	-.12	.6	-.31	.1	.17	.4
MRI										
Pre-BD VDP	-.28	.2	**.42**	**.03**	.33	.1	-.02	.9	**-.46**	**.02**
Post-BD VDP	-.47	.01	.24	.2	.17	.4	.09	.7	-.24	.2
VDP reversibility	-.30	.1	-.35	.07	-.27	.2	-.11	.6	.33	.09

Note: Δpre-BD VDP significantly related to Day-0 VDP reversibility (r=.80, p<.001) and ΔSGRQ significantly related to Day-0 SGRQ (r=-.40, p=.04), but no other Day-0 measurements.

BMI=body mass index; BD=bronchodilator; FEV_1=forced expiratory volume in 1 second; FVC=forced vital capacity; Eos=blood eosinophil count; FeNO=fraction of exhaled nitric oxide; ACQ=Asthma Control Questionnaire; AQLQ=Asthma Quality-of-Life Questionnaire; SGRQ=St. George's Respiratory Questionnaire; CT=computed tomography; TAC=total airway count; WA=wall area; LA=lumen area; WT=wall thickness; MRI=magnetic resonance imaging; VDP=ventilation defect percent; Δ=change on Day-28; r=Pearson correlation coefficient; ρ=Spearman correlation coefficient; p=significance value.

Chapter 4

4 CT MUCUS SCORE AND ^{129}XE MRI VENTILATION DEFECTS AFTER 2.5-YEARS ANTI-IL-5RA IN EOSINOPHILIC ASTHMA

To better understand the long-term effect of anti-IL-5Rα on airway structure and function, we evaluated a subset of the same participants described in Chapter 3 after 1- and 2.5-years of continuous therapy. We compared longitudinal CT airway and MRI ventilation measurements and compared these with pre-treatment measurements.

The contents of this chapter were previously published in the journal Chest: MJ McIntosh, HK Kooner, RL Eddy, A Wilson, H Serajeddini, A Bhalla, C Licskai, CA Mackenzie, C Yamashita and G Parraga. CT Mucus Score and ^{129}Xe MRI Ventilation Defects after 2.5-years Anti-IL-5Rα in Eosinophilic Asthma. Chest. 2023. *This article is available under the terms of the Creative Commons License BY-NC-ND 4.0.*

4.1 Introduction

In poorly controlled eosinophilic asthma patients, CT airway mucus-occlusions and ^{129}Xe magnetic resonance imaging (MRI) ventilation defect percent (VDP) were recently shown to independently predict response to benralizumab measured using the asthma-control-questionnaire (ACQ-6) score, 28-days after a single dose.[1] These findings were not inconsistent with long-standing investigations[2,3] and more recent x-ray computed tomography (CT) findings of airway luminal occlusions or mucus-plugs[4,5] in patients with severe asthma. In the context of eosinophilic asthma, airway mucus-plugs were recently shown to persist over three years, despite treatment with high-dose inhaled and oral corticosteroids.[5] Mucus-plug formation in asthma may be driven in whole or in part by eosinophilic oxidation,[4] which is supported by work showing that two-thirds of patients with severe asthma and normal sputum eosinophils did not have CT evidence of central airway mucus.[6] Normalization of eosinophilic bronchitis may help disrupt airway mucus and hence, mucus-occlusions may be considered an asthma treatment target.[7]

Whilst anti-interleukin-5 (IL-5) biologic therapies aim to reduce airway inflammation by eliminating eosinophils,[8-12] previous investigations did not evaluate mucus response to such therapy. While some clues were provided by a single case study in two allergic bronchopulmonary aspergillosis cases treated with benralizumab,[13] the question remains: does eosinophilic depletion result in the clearance of mucus plugs in eosinophilic asthma?

In asthma, distal and central airway dysfunction may be quantified using hyperpolarized noble gas MRI ventilation defects.[14,15] Such defects have been shown to be spatially related to remodeled airways,[16] luminal occlusions[6,17] and air-trapping,[18] and to persist in the same spatial location over seven years of standard of care therapy in patients with asthma.[19] MRI ventilation defects are also related to sputum eosinophilia and airway inflammation,[20] and quality-of-life and asthma control.[21] MRI ventilation defects have been investigated as potential targets to guide and quantify treatment, such as bronchial thermoplasty and biologic therapy.[22-25] Together, thoracic CT and MRI provide reproducible and high spatial resolution structure-function measurements that directly evaluate the lung pathologies responsible for asthma symptoms, control and quality-of-life.

Hence, based on the fact that mucus occlusions and MRI ventilation defects predicted early response to benralizumab[1] in patients with poorly controlled eosinophilic asthma, here our objective was to use CT and MRI to longitudinally investigate the effect of continuous benralizumab treatment over 1- and 2.5-years on mucus-plugs and ventilation defects.

4.2 Materials and Methods

4.2.1 Study Participants and Design

Participants 18-80 years of age with poorly controlled, eosinophilic asthma according to the Global Initiative for Asthma[26] and no exacerbations within four weeks of enrollment provided

written-informed consent to an ethics board (HSREB #113224) and Health Canada-approved protocol (www.clinicaltrials.gov NCT03733535). Inclusion and exclusion criteria were previously described.[1]

Figure 4-1 provides the study design, which included eight visits over 2.5 years. Visits 1 through 4 were previously reported.[1] Here we report longitudinal follow-up measurements for Visit 7 (1-year) and Visit 8 (2.5-years) which both included imaging measurements. On Day-56 (Visit 5) and Day-112 (Visit 6), pre- and post-bronchodilator (BD) spirometry and oscillometry were completed in addition to the fraction of exhaled nitric oxide (FeNO) measurement and Asthma Control (ACQ),[27] Asthma Quality-of-Life (AQLQ)[28] and St. George's Respiratory (SGRQ)[29] questionnaires. Participants who continued on benralizumab therapy following Day-112 were invited back to the laboratory for optional 1-year (Visit 7) and 2.5-year (Visit 8) (HSREB #103516; www.clinicaltrials.gov NCT02351141) visits. At both visits, post-BD spirometry, oscillometry and ^{129}Xe MRI, as well as FeNO, ACQ-6, AQLQ and SGRQ were performed and chest CT was acquired at the 2.5-year visit. **Section 4.6** details methods for measuring spirometry, oscillometry, FeNO and quality-of-life.

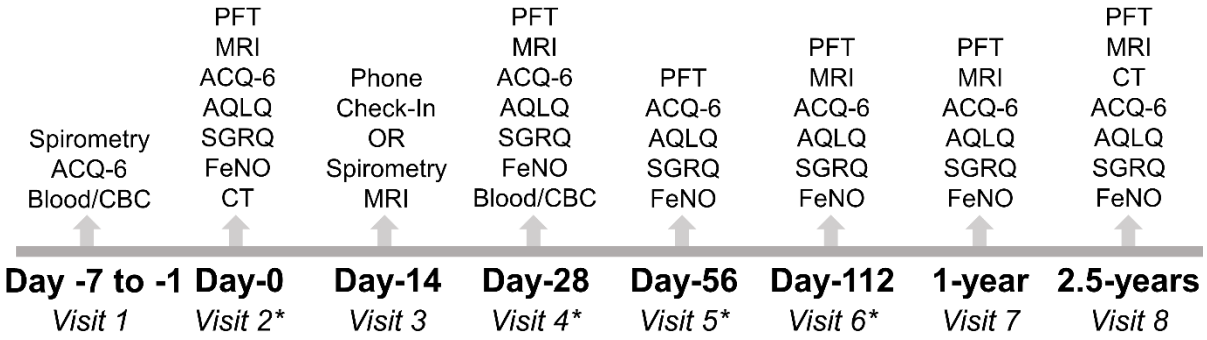

Figure 4-1. Study Design
Study design with Visit-1 as screening visit, Visit-2 on Day-0, Visit-3 on Day-14, Visit-4 on Day-28, Visit-5 on Day-56, Visit-6 on Day-112, Visit-7 after 1-year and Visit 8 after 2.5-years. **=received 30 mg subcutaneous benralizumab injection;*

ACQ=Asthma Control Questionnaire; CBC=complete blood count; PFT=Pulmonary Function Test; MRI=Magnetic Resonance Imaging; AQLQ=Asthma Quality-of-Life Questionnaire; SGRQ=St. George's Respiratory Questionnaire; FeNO=Fraction of exhaled nitric oxide; CT=computed tomography.

4.2.2 Thoracic Imaging and Analysis

Anatomic ^{1}H and ^{129}Xe static ventilation MRI were acquired at 3.0 Tesla (Discovery MR750; GE Healthcare), as previously described.[30] Supine participants were coached to inhale a gas mixture from a 1.0L bag (Tedlar; Jensen Inert Products, Coral Springs, FL, USA) from functional residual capacity with acquisition under breath-hold conditions. ^{129}Xe gas was polarized to 30-40% (Polarean; Xenispin 9820, Durham, NC, USA).[31] Quantitative MRI analysis was performed, as previously described,[32] using MATLAB 2019a (Mathworks, Natick, MA, USA).[33]

Within 30 minutes of MRI, CT was acquired post-BD after inhalation of 1.0L N_2 from functional residual capacity for volume-matching to MRI using a 64-slice LightSpeed VCT system (GE Healthcare, Milwaukee, WI, USA) on the Day-0 and 2.5-year visits using the same field-of-view and reconstruction method, as previously described.[34] CT airways were analyzed using the same version of VIDAvision software (VIDA Diagnostics Inc., Coralville, IA, USA) at both Day-0 and 2.5-years to generate total airway count (TAC).[35] Anatomically equivalent segmental, subsegmental and sub-subsegmental airways for all airway paths (third to fifth generation)[36] were also used to measure wall thickness (WT) and lumen area (LA). We previously reported a method,[1] which summed the total number of CT visible mucus occlusions to yield a whole lung mucus plug count for each participant, which will be referred to here as mucus-count. We also report mucus-score, previously described by Dunican et al.,[4,6] which is the number of occluded airway segments and results in a value ranging from zero to 20. **Section 1.1** contains additional image acquisition details.

4.2.3 Statistical Analysis

SPSS (SPSS Statistics 25.0; IBM, Armonk, NJ, USA) was used for all statistical analyses. Data were tested for normality using Shapiro-Wilk tests and nonparametric tests were performed when data were not normally distributed. Differences between participants with or without 1-year and/or 2.5-year visits were evaluated using independent samples tests and between time points using repeated measures analysis of variance. Spearman correlation p-values$\leq$0.20[37] were used to generate multivariable models to predict the change in ACQ-6 at 2.5-years. Variables were tested for collinearity and models were rejected when the variance inflation factor$\geq$5.[38] The Holm-Bonferroni correction was used for multiple comparisons. Results were considered statistically significant when the probability of making a type I error was less than 5% ($p<0.05$).

4.3 Results

4.3.1 Participant Demographics

Figure 4-2 provides a CONSORT diagram. Participation for Visits 1 through 4 was previously described.[1] A detailed description of participant disposition is provided in **Table 4-4** (**Section 1.1**). Twenty-nine participants were evaluated on Day-0 and Day-28, as previously reported.[1] Sixteen participants were evaluated at 1-year (13 female, 3 male; baseline age 60±13 years) and 13 participants were evaluated at 2.5-years (11 female, 2 male; baseline age 60±16 years). As shown in **Figure 4-2** and **Table 4-4**, for the 1-year follow-up, three participants were lost-to-follow-up, four participants were discontinued on benralizumab by their referring respirologist because of lack of response, two patients discontinued because of lack of affordable access to study treatment, three declined the study visit because of COVID concerns and a single participant withdrew because of a newly implanted MRI incompatible device. At

the 2.5-year visit, there were an additional four participants lost-to-follow-up (one of whom had previously declined because of COVID concerns), another patient discontinued because of lack of access and another withdrew for no stated reason.

Table 4-1 provides a summary of baseline demographic characteristics for participants in the Day-28, 1-year and 2.5-year visits whilst **Table 4-5** (**Section 1.1**), summarizes all baseline measurements by participation at the 1-year and 2.5-year visits. Except for baseline CT airway wall thickness percent (p=.02), these subgroups were not significantly different at baseline.

A by-participant listing of medications pre-treatment (Day-0) and at the 1-year and 2.5-year visits is shown in **Table 4-6**. At 1-year, 15/16 (94%) participants were prescribed inhaled corticosteroids, 14/16 (88%) participants were prescribed long-acting β-agonists and 1/16 (6%) participants were prescribed leukotriene receptor antagonists, as compared to 12/13 (92%), 11/13 (85%) and 1/13 (8%) participants, respectively, at 2.5-years. No participants at the 1- or 2.5-year visit were prescribed long-acting muscarinic antagonists (3% on Day-0) or oral corticosteroids (17% on Day-0).

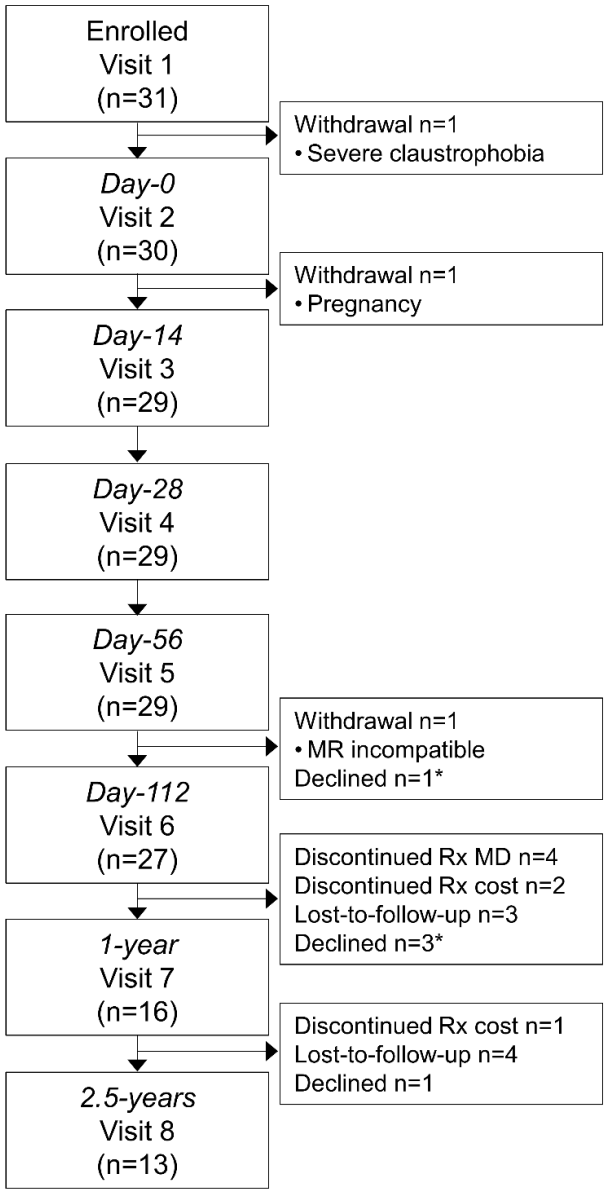

Figure 4-2. CONSORT Diagram
Twenty-nine participants completed Day-28 and Day-56 visits. One participant was excluded from the Day-112 visit due to a newly implanted medical device and one participant did not attend because of COVID-19 safety concerns.
For the 1-year visit, six participants discontinued benralizumab, three were lost-to-follow-up, three declined to participate and one participant who declined the Day-112 visit agreed to participate in the 1-year visit for a total of 16 participants. Two participants who declined to participate in the 1-year visit, agreed to attend the 2.5-year visit, an additional four were lost-to-follow-up, 1 declined due to COVID symptoms, one declined for no specific reason and another withdrew because they discontinued benralizumab because of a lack of funded access.
**some of these participants declined a single visit (COVID concerns) but then participated in a subsequent visit*

Table 4-1. Demographic characteristics prior to therapy

Parameter	Day-28 (n=29)	1-year (n=16)	2.5-years (n=13)
Age years	59 ± 12	60 ± 13	60 ± 16
Female n (%)	16 (69)	13 (81)	11 (85)
BMI kg/m^2	29 ± 5	28 ± 4	28 ± 4
Pack-years	7 ± 12	3 ± 8	5 ± 9
Median (IQR)	0 (0-45)	0 (0-30)	0 (0-30)
Duration of Asthma years	25 ± 22	20 ± 18	20 ± 17
Median (IQR)	25 (1-64)	11 (1-52)	12 (2-52)
Follow-up time years	-	1.2 ± 0.2	2.6 ± 0.3
Median (IQR)	-	1.2 (0.8-1.4)	2.7 (2.1-3.0)

Demographic data at enrollment for participants completing 28-days, 1 year and 2.5-year follow-up. Data are reported as mean ± standard deviation, unless indicated otherwise.

BMI=body mass index; IQR=interquartile range; Follow-up time=number of years between Day-0 and the visit.

4.3.2 Pulmonary Function, Asthma Control, Ventilation and Airway Changes

Figure 4-3 shows ^{129}Xe MRI ventilation co-registered with anatomical ^{1}H MRI on Day-0, Day-28, 1-year and 2.5-year visits, and three-dimensional airway trees and CT mucus plugs on Day-0 and 2.5-years, for two representative participants. In participant P08, the change in VDP at Day-28 was not visibly obvious and less than the minimal-clinically-important-difference (MCID) of 2%[39] (ΔVDP=+1.8%). However, there was a marked VDP improvement at 1-year (ΔVDP=-21.5%) and 2.5-years (ΔVDP=-24.9%) compared to baseline. In addition, there were a greater number of CT-visible segmented airways (Day-0/2.5-years TAC=77/141) and fewer mucus-plugs (Day-0/2.5-years mucus-score=5/0, mucus-count=5/0) at 2.5-years as compared to Day-0. In participant P29, there were marked VDP changes on Day-28 (ΔVDP=-9.6%), at 1-year (Δ=-16.5%) and at 2.5-years (Δ=-15.5%) as compared to Day-0 but not from 1-year to 2.5-years (Δ=+0.9%). There were a greater number of CT-visible airways (Day-0/2.5-years TAC=134/293) and fewer mucus plugs (Day-0/2.5-years mucus-score=14/0, mucus-count=39/0) at 2.5-years.

Table 4-2 shows measurements made on the Day-0, Day-28, 1-year and 2.5-year visits. Some of these measurements are also shown in box and whisker plots in **Figure 4-4**. CT mucus-score ($p=.03$), TAC ($p=.002$), LA ($p=.002$) and WT ($p<.001$) were significantly different at 2.5-years as compared to Day-0 when the baseline CT was acquired. Significant differences were also observed as compared to Day-0 for central airway resistance measured using oscillometry (R_{19}) at 1-year ($p=.007$) and 2.5-years ($p=.02$), ACQ-6 at 1-year ($p=.01$) and 2.5-years ($p=.003$), AQLQ at 1-year ($p<.001$) and 2.5-years ($p=.001$), SGRQ at 1-year ($p<.001$) and 2.5-years ($p<.001$), and forced expiratory volume in 1 second (FEV_1) at 2.5-years ($p=.04$). FeNO was significantly different at 2.5-years ($p=.03$) as compared to Day-28. ^{129}Xe MRI VDP was significantly different at 1-year ($p=.01$) and 2.5-years ($p=.003$) as compared to Day-0. Distal

airway resistance measured using oscillometry (R_{5-19}) was not significantly different at 1-year (p=.1) or 2.5-years (p=.4), as compared to Day-0. In addition, the total lung volume measured using CT was not significantly different at 2.5-years as compared to Day-0 (p=.4). The mean change in VDP at 2.5-years as compared to Day-28 (-4±3%) was greater than the MCID.[39] Other changes greater than the MCID are described in the online supplement.

4.3.3 Mucus Occlusions

Eight of the 12 (67%) participants who consented to CT at 2.5-years had mucus-plugs on Day-0; 18 of 27 (67%) participants enrolled also had mucus-plugs visible on CT at Day-0. Five participants had no CT evidence of mucus-plugs at 2.5-years (Day-0 mucus-count=11±16), a single participant had two fewer mucus-plugs (Day-0/2.5-years mucus-count=4/2), one participant had the same number of mucus-plugs (Day-0/2.5-years mucus-count=1/1) and four participants with no mucus-plugs on Day-0 also had no mucus-plugs at 2.5-years. A single participant had four more plugs at 2.5-years (Day-0/2.5-years mucus-count=9/13). As shown in detail in **Figure 4-5**, this participant (P27) had an increased mucus-count, despite a decreased mucus-score (Day-0/2.5-years mucus-score=9/5), because of the partial clearance of a large volume of mucus, which had previously completely occluded this airway on Day-0, resulting in multiple discontinuous plugs at 2.5-years, with corresponding improvements in ^{129}Xe MRI ventilation in spatially contiguous regions of the left lung.

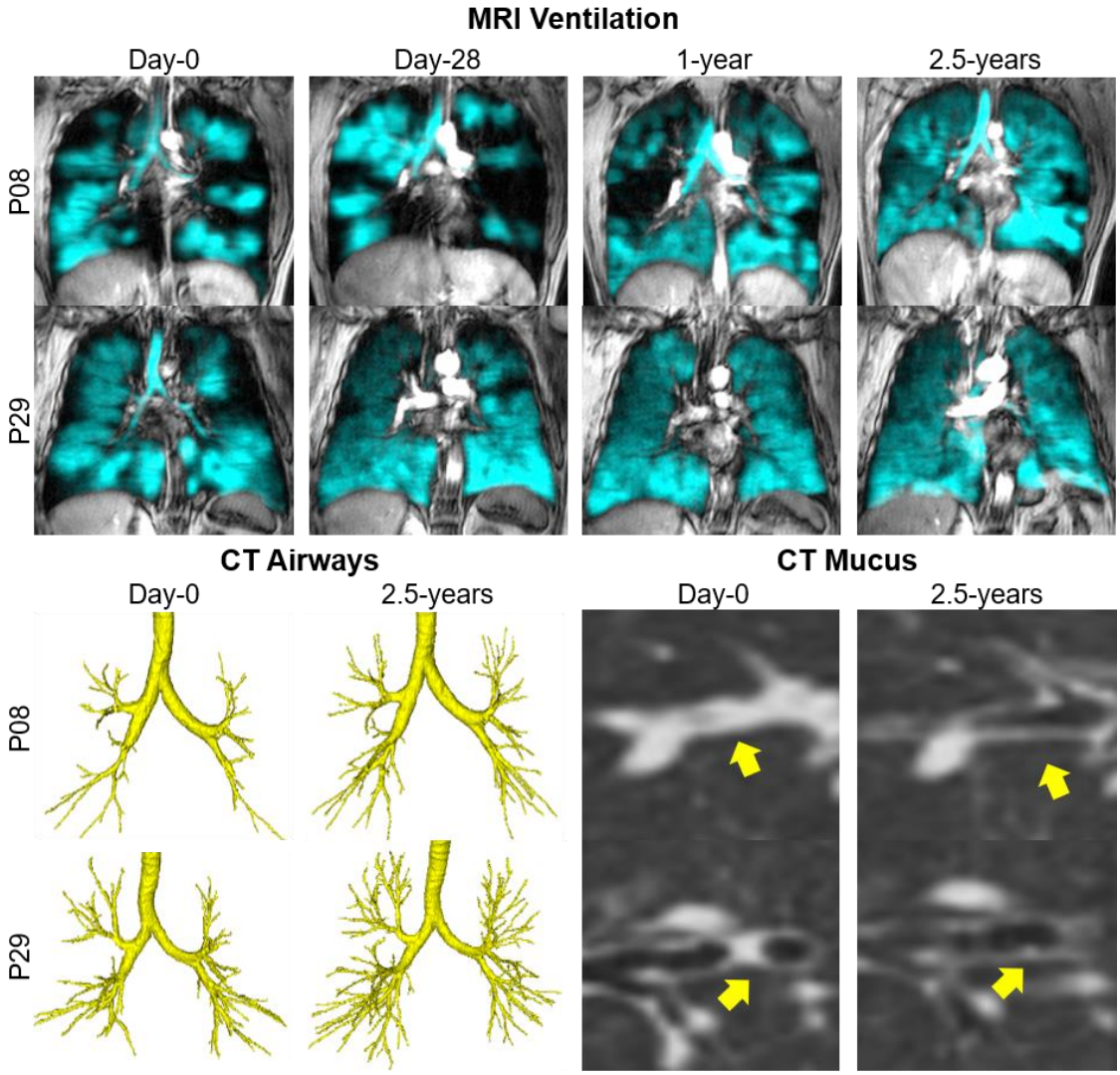

Figure 4-3. Qualitative imaging response
Centre coronal ^{1}H MRI slice (greyscale) co-registered with ^{129}Xe MRI slice (cyan) at Day-0, Day-28, 1- and 2.5-year follow-up, and three-dimensional representation of pulmonary airways and CT mucus plugs at Day-0 and 2.5-year follow-up. Yellow arrows point to mucus plugs that are cleared at 2.5-years.

P08 was a 20-year-old female at enrolment with eosinophil count=600 cells/μL.
Day-0: FEV_1=57%$_{pred}$, ACQ-6=3.3, VDP=34%; mucus-score=14; mucus count=39; TAC=134; **Day-28:** Eosinophil count=200 cells/μL, FEV_1=46%$_{pred}$, ACQ-6=2.2, VDP=36%; **1-year:** FEV_1=89%$_{pred}$, ACQ-6=1.5, VDP=12%; **2.5-years:** FEV_1=98%$_{pred}$, ACQ-6=0.5, VDP=9%; mucus-score=0, mucus count=0, TAC=141.

P29 was a 56-year-old female at enrolment with blood eosinophils=1700 cells/μL
Day-0: FEV_1=50%$_{pred}$, ACQ-6=3.33, VDP=18%; Mucus-score=5; mucus count=6; TAC=103; **Day-28:** Eosinophil count=0 cells/μL, FEV_1=87%$_{pred}$, ACQ-6=0, VDP=8%; **1-year:** FEV_1=108%$_{pred}$, ACQ-6=0, VDP=1%; **2.5-years:** FEV_1=110%$_{pred}$, ACQ-6=0, VDP=2%; mucus-score=0; mucus count=0; TAC=298.

Table 4-2. Pulmonary function, imaging and questionnaire data on Day-0 and post-benralizumab Day-28, 1-year and 2.5-years

Parameter	Day-0 (n=29)	Day-28 (n=29)	1-year (n=16)	p	2.5-years (n=13)	p*
Pulmonary function						
FEV_1 $\%_{pred}$	74±17 [74±3; 68-81]	80±19 [80±3; 73-87]	80±17 [80±4; 70-91]†	.9	90±18 [90±5; 79-101]	.2
FVC $\%_{pred}$	85±16 [85±3; 84-95]‡	89±14 [90±3; 84-95]	88±14 [88±4; 80-96]†	.8	97±14 [97±4; 89-106]	.2
FEV_1/FVC	68±12 [68±2; 63-72]‡	69±12 [69±2; 64-74]	66±21 [66±6; 54-78]†	.5	72±9 [72±3; 67-78]	.4
R_{19} cmH_2O•s/L	3.6±1.5 [3.3±0.2; 3.0-3.6]‡	3.5±1.0 [3.4±0.2; 3.0-3.8]§	3.2±1.2 [3.2±0.3; 2.6-3.8]	**.005**	3.0±0.7 [3.0±0.2; 2.6-3.4]	**.01**
R_{5-19} cmH_2O•s/L	1.4±1.0 [1.3±0.2; 1.0-1.7]‡	1.1±1.0 [1.0±0.2; 0.6-1.4]§	1.0±0.7 [1.0±0.2; 0.6-1.4]	1.0	0.8±0.9 [0.8±0.3; 0.3-1.4]	.9
Inflammatory markers						
FeNO ppb	48±35 [48±7; 35-62]§	57±53 [57±10; 36-79]‡	103±105 [103±53; -64-270]·	.3	54±55 [54±15; 21-88]	**.03**
Asthma QOL and control						
ACQ-6	2.3±1.5 [2.3±0.3; 1.7-2.9]	1.4±1.0 [1.4±0.2; 1.0-1.8]	0.5±0.6 [0.5±0.2; 0.1-1.1]	**.02**	0.5±0.5 [0.5±0.1; 0.1-1.1]	**.03**
AQLQ	4.3±1.4 [4.3±0.3; 3.8-4.9]	5.2±1.3 [5.2±0.2; 4.7-5.7]	6.1±1.0 [6.1±0.2; 5.6-6.6]	**.04**	6.4±0.6 [6.4±0.2; 6.0-6.7]	**.02**
SGRQ	50±21 [50±4; 42-58]	37±19 [37±4; 30-45]	16±15 [16±4; 8-24]	**<.001**	16±10 [16±3; 10-22]	**.003**
MRI						
VDP %	12±10 [12±2; 8-16]	9±9 [9±2; 5-12]	6±5 [6±1; 3-9]	.4	4±2 [4±1; 2-5]	.07
*CT***						
TAC n	140±50 [140±10; 120-160]§	-	-	-	197±59 [197±17; 160-234]:	**.002**
LA mm^2	8.0±2.6 [8.0±0.5; 7.0-9.0]§	-	-	-	11.7±2.5 [11.6±0.7; 10.0-13.3]:	**.002**
WT mm	1.2±0.1 [1.2±0.03; 1.1-1.2]§	-	-	-	1.4±0.1 [1.4±0.02; 1.3-1.4]:	**<.001**

WT%	19±1 [19±0.2; 18-19][§]	-	-	-	18±1 [18±0.3; 18-19]⁞	.8
Mucus Score	3±4 [4±1; 1-6][§]	-	-	-	1±1 [1±1; 0-6]⁞	**.03**
Mucus Count	5±9 [5±2; 2-9][§]	-	-	-	1±4 [1±1; -1-4]⁞	.2
TLV L	4.9±1.0 [4.9±0.2; 4.5-5.3]	-	-	-	4.7±0.8 [4.7±0.2; 4.2-5.2]	.4

Data acquired post-bronchodilator and are reported as mean ± standard deviation.
Abbreviations: FEV_1=forced expiratory volume in 1 second; $\%_{pred}$=percent of predicted value; FVC=forced vital capacity; FeNO=fraction of exhaled nitric oxide; ppb=parts per billion; QOL=quality-of-life; ACQ=Asthma Control Questionnaire; AQLQ=Asthma Quality-of-Life Questionnaire; SGRQ=St. George's Respiratory Questionnaire; MRI=magnetic resonance imaging; VDP=ventilation defect percent; TAC=total airway count; LA=lumen area; WT=wall thickness; TLV=CT total lung volume; p=significance value between Day-28 and 1-year; p*=significance value between Day-28 and 2.5-years; **=p indicates significance value between Day-0 and 2.5-years for CT measurements taken at that time; [†]n=15; [‡]n=28; [§]n=27; ⁞n=4; ⁞n=12.

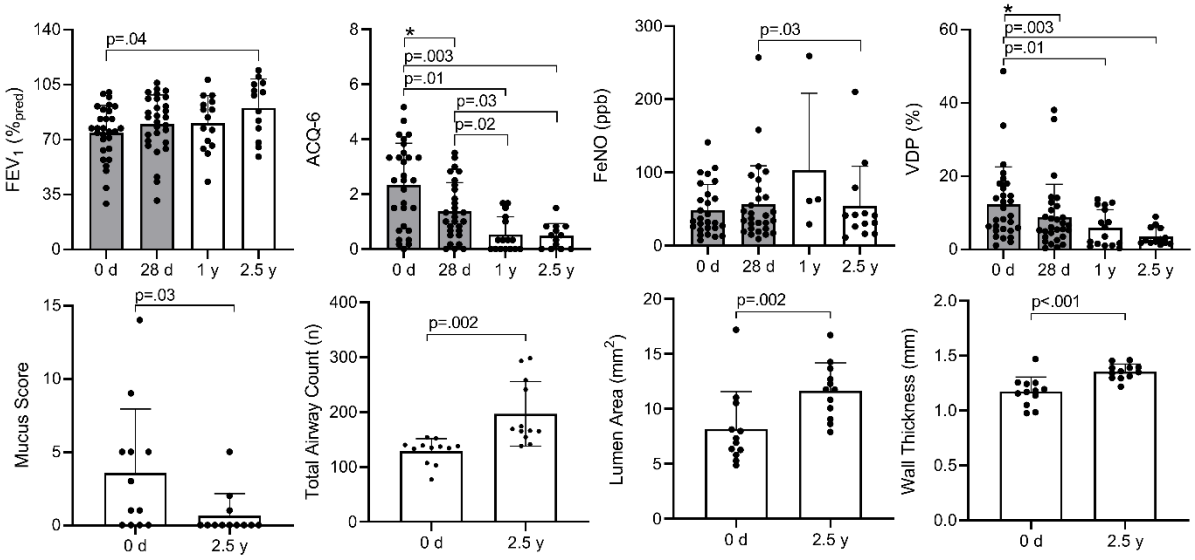

Figure 4-4. Pulmonary function, asthma control and ^{129}Xe MRI and CT after benralizumab FEV_1 significantly different between Day-0 and 2.5-years (p=.04). ACQ significantly different between Day-0 and 1-year (p=.01) and 2.5-years (p=.003), and between Day-28 and 1-year (p=.02) and 2.5-years (p=.03). FeNO significantly different between Day-28 and 2.5-years (p=.03). VDP significantly different between Day-0 and 1-year (p=.01) and 2.5-years (p=.003). CT mucus score (p=.03), total airway count (p=.002), airway lumen area (p=.002) and wall thickness (p<.001) significantly different between Day-0 and 2.5-years.

Note: FeNO was acquired in only four participants at 1-year due to COVID-19 safety concerns.

*FEV_1=forced expiratory volume in one second; $\%_{pred}$=percent of predicted value; ACQ-6=asthma control questionnaire; FeNO=fraction of exhaled nitric oxide; VDP=ventilation defect percent d=days; y=years; p=uncorrected significance value; grey bars=previously reported data, *=statistically significant difference previously reported.*

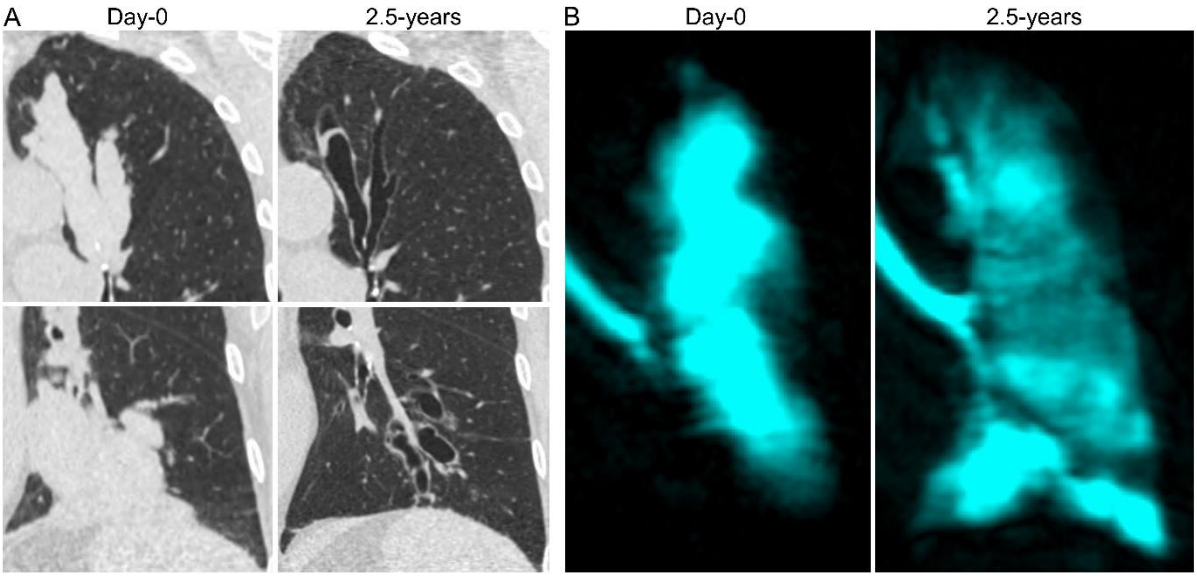

Figure 4-5. CT mucus-occlusion and MRI ventilation improvement at 2.5-years
Participant is a 77-year-old female with visually obvious improvements in airway occlusion with mucus on CT and ventilation on MRI at 2.5-years.

A. Completely continuous airway occlusion in the left upper (top) and left lower lobe (bottom) at Day-0 partially resolved to a discontinuous airway occlusion at 2.5 year visit.

B. Ventilation defects in the left lung corresponding to mucus occlusions on Day-0 also partially resolved at 2.5-years (VDP: Day-0=15%, Day-28=13%, Day-112=7%, 2.5-years=6%).

4.3.4 Relationships and Multivariable Models

As shown in **Section 1.1** in **Figure 4-6**, significant relationships were observed for the change in mucus-score with Day-0 R_{19} (ρ=-.71, p=.01) and VDP (ρ=-.73, p=.008). The change in ACQ-6 was also significantly related to Day-0 R_{19} (ρ=-.64, p=.02), VDP (ρ=-.63, p=.02), mucus-score (ρ=-.73, p=.005) and mucus-count (ρ=-.75, p=.003).

Multivariable models were generated to explain ΔACQ-6 at 2.5-years and these are shown in **Table 4-3**. Models 1 to 3 were generated using the enter method and were significant, whereby mucus-score and VDP were significant variables for ΔACQ-6 at 2.5-years, similar to previous model results for Day-28 ACQ-6 results.[1] We also generated a significant multivariable model, Model 4, using the stepwise approach to explain ΔACQ-6 at 2.5-years. Day-0 mucus-score was the only significant variable, whilst baseline FeNO, FEV_1, R_{19}, R_{5-19}, blood eosinophil count, VDP, mucus-count, LA and WT were not.

Table 4-3. Multivariable Linear Regression Models

Parameter	R^2	ANOVA p	Unstandardized B	Standardized β	Coefficients *p*
ΔACQ-6					
*Model 1**	0.443	.009			
Mucus Count			-0.122 ± 0.040	-0.666	**.009**
*Model 2**	0.675	<.001			
VDP			-0.122 ± 0.024	-0.822	**<.001**
*Model 3**	0.729	<.001			
Mucus Count			-0.052 ± 0.035	-0.284	0.169
VDP			-0.097 ± 0.029	-0.656	**0.06**
Model 4	0.700	<.001			
Mucus Score			-0.333 ± 0.063	-0.837	<**.001**

R^2=goodness-of-fit; ANOVA=analysis of variance; B=unstandardized regression coefficient ± standard error; β=standardized regression coefficient; Δ=change at 2.5-years; ACQ=asthma control questionnaire; VDP=ventilation defect percent; *analysis completed using enter method.

4.4 Discussion

In this longitudinal evaluation of eosinophilic asthma treated with benralizumab,[1] we observed: 1) significantly improved mean CT mucus-score and mucus-plug dissolution or decrease in 6 of 8 patients with pre-treatment mucus-plugs, 2) significantly improved asthma-control, central airway resistance, quality-of-life, FEV_1, airway lumen area, wall thickness and total airway count, at 2.5-years, 3) persistent MRI ventilation defect improvements after 2.5-years of continuous anti-IL-5Rα therapy, and, 4) MRI VDP and CT mucus-score measured just prior to therapy initiation independently predicted ACQ-6 response after 2.5-years of continuous therapy.

Previous work investigating mucus-plugs over three years revealed that these were spatially and quantitatively persistent, and that in ~4/5 asthma participants, mucus-plugs remained patent over the course of three years.[5] Here, 5/8 (63%) participants with CT evidence of airway mucus at treatment initiation had no evidence of mucus-occlusions after 2.5-years of benralizumab, which suggests that mucus-plug clearance resulted from treatment. Of the remaining participants with mucus-occlusions present at 2.5-years, one participant had fewer plugs and another had the same number of plugs but in a different lung location. We were also surprised to observe that in a single patient, a previously continuous and large airway mucus-occlusion appeared to be disrupted or dissolved into multiple, smaller, non-contiguous occlusions at the 2.5-year visit. While some of the treatment effects demonstrated here may be due to better adherence to baseline asthma therapies, recent work from the Severe Asthma Research Program[5] revealed that mucus plugs were persistent over three years in asthma patients treated with high-dose inhaled and oral corticosteroids. Taken together, these findings suggest that standard-of-care oral and inhaled asthma treatment alone may not substantially alter mucus plugs in moderate-to-severe asthma.

The observation here that mean VDP improvement on Day-28, after a single dose, persisted and surpassed the MCID at the 2.5-year visit, was in agreement with previous work that showed pulmonary function, asthma-control and quality-of-life improvements were maintained after two years of benralizumab therapy.[11,12] Our findings at 2.5-years are also consistent with a previous result in eosinophilic asthma, which showed that mucus-occlusions and ventilation defects independently explain improved asthma-control after a single benralizumab dose.[1] Improved asthma control in response to benralizumab may be mechanistically linked to mucus-occlusions and airway function, both of which appear to be modifiable outcomes. This adds to the growing body of evidence that CT and MRI may directly evaluate/measure the lung pathologies responsible for asthma control.

Following 2.5-years of benralizumab treatment, we were surprised to observe a greater number of CT-visible airways and decreased airway luminal narrowing. This result, of course, only reflects the CT-visible airways, which requires patent airway lumen and wall structures with sufficient girth to be captured within the spatial resolution of the CT acquisition protocol (0.625mm in the x, y, z planes). Previous work showed an apparent decrease in CT TAC and narrowed airway lumen with increasing asthma severity.[16] In this previous work, it was not clear whether this was the result of airway obliteration or obstruction, and whether this was a modifiable outcome. Here, we provide evidence of the latter – as the central (CT-visible) airways became less narrow and less obstructed by luminal plugs, they appear more numerous on CT following treatment. The resolution of air-trapping, possibly driven by diminished mucus in the distal airways, may also be responsible for the increased CT TAC observed here. Unfortunately, we cannot evaluate air-trapping changes here because plethysmography was not used at 2.5-years due to institutional COVID-19 constraints. Moreover, we did not undertake inspiratory/expiratory CT in this study, which also could have been used to evaluate

air-trapping over time. As of yet, the minimal-clinically-important-differences for CT airway measurements have not been reported, although TAC at 2.5-years in these participants was similar to previously reported measurements in mild-moderate asthma,[16] which is reassuring. Nevertheless, our findings suggest that in asthma, an abnormally low TAC may not be indicative of permanent pruning and may be reversible, as observed here.

This study was limited by a number of shortcomings including the small sample size at follow-up. Only those participants who reported a clinical response to benralizumab and continued treatment attended the 1-year and 2.5-year visits, which biases our results to responders only. Previous studies[9-12] reported retention rates of 88% and 72% at one- and two-years, respectively, compared to 55% and 45% at 1-year and 2.5-years, respectively, here. The retention rate at the conclusion of the original interventional study (Day-112 prior to the pandemic), was excellent with nearly 100% of participants returning. COVID concerns (1-year visit, n=3) and lack of funded access to benralizumab (1- and 2.5-year visit, n=4) certainly contributed to the relatively weak retention rate at 1- and 2.5-years in this study. Just the same, except for airway WT%, the 1-year and 2.5-year study subgroups were not different from the original group studied at 28-days post-benralizumab. We also acknowledge that at 1- and 2.5-year follow-up there were more females with a shorter asthma history overall, which is important to consider and may impact the generalizability of these findings. We can certainly learn more about mechanisms by evaluating imaging in non-responders as compared to responders, which will be the focus of future work. We must also acknowledge that follow-up CT was only acquired after 2.5-years of therapy and therefore, earlier mucus-plug measurements could not be made, and this stymies our ability to get more information about the dynamics of mucus-plug formation and dissolution. Previous work[6] suggested that elevated FeNO was indicative of airway mucus and could be used, in combination with CT evidence of

luminal plugging, to identify patients who may respond to anti-IL-4/IL-13 therapy. While one might expect that FeNO would normalize once airway mucus cleared, this was not observed here, in agreement with previous investigations,[9,10] perhaps due to measurement variability. Whether anti-IL-4/IL-13 treatment may also clear airway mucus while reducing FeNO levels, remains to be determined.

4.5 Interpretation

In summary, in a small group of participants with poorly controlled eosinophilic asthma, we observed significantly improved CT mucus-score, total airway count, airway lumen area and wall-thickness, as well as ACQ-6 score, central airways resistance (R_{19}) and FEV_1, after 2.5-years of continuous treatment with benralizumab. Improved mean VDP measured 28-days after the first dose, persisted 2.5-years later. MRI VDP and CT mucus-score measured just prior to therapy initiation independently predicted ACQ-6 response after 2.5-years of continuous therapy. These novel pulmonary imaging findings suggest that long-term benralizumab-driven eosinophil depletion also disrupts airway luminal occlusions and improves airway structure and function, which has implications for the management of eosinophilic asthma.

4.6 References

1. McIntosh, M.J., *et al.* Asthma Control, Airway Mucus, and (129)Xe MRI Ventilation After a Single Benralizumab Dose. *Chest* (2022).

2. Carroll, N., Elliot, J., Morton, A. & James, A. The structure of large and small airways in nonfatal and fatal asthma. *Am Rev Respir Dis* **147**, 405-410 (1993).

3. Hays, S.R. & Fahy, J.V. The role of mucus in fatal asthma. *Am J Med* **115**, 68-69 (2003).

4. Dunican, E.M., *et al.* Mucus plugs in patients with asthma linked to eosinophilia and airflow obstruction. *J Clin Invest* **128**, 997-1009 (2018).

5. Tang, M., *et al.* Mucus Plugs Persist in Asthma, and Changes in Mucus Plugs Associate with Changes in Airflow over Time. *Am J Respir Crit Care Med* **205**, 1036-1045 (2022).

6. Svenningsen, S., *et al.* CT and Functional MRI to Evaluate Airway Mucus in Severe Asthma. *Chest* **155**, 1178-1189 (2019).

7. Svenningsen, S. & Nair, P. Persistent Airway Plugs: A Call for Clinical Recognition and Novel Therapies. *Am J Respir Crit Care Med* **205**, 977-978 (2022).

8. Kolbeck, R., *et al.* MEDI-563, a humanized anti-IL-5 receptor alpha mAb with enhanced antibody-dependent cell-mediated cytotoxicity function. *J Allergy Clin Immunol* **125**, 1344-1353 e1342 (2010).

9. Bleecker, E.R., *et al.* Efficacy and safety of benralizumab for patients with severe asthma uncontrolled with high-dosage inhaled corticosteroids and long-acting beta2-agonists (SIROCCO): a randomised, multicentre, placebo-controlled phase 3 trial. *Lancet* **388**, 2115-2127 (2016).

10. FitzGerald, J.M., *et al.* Benralizumab, an anti-interleukin-5 receptor alpha monoclonal antibody, as add-on treatment for patients with severe, uncontrolled, eosinophilic asthma (CALIMA): a randomised, double-blind, placebo-controlled phase 3 trial. *Lancet* **388**, 2128-2141 (2016).

11. Busse, W.W., *et al.* Long-term safety and efficacy of benralizumab in patients with severe, uncontrolled asthma: 1-year results from the BORA phase 3 extension trial. *Lancet Respir Med* **7**, 46-59 (2019).

12. FitzGerald, J.M., *et al.* Two-Year Integrated Efficacy And Safety Analysis Of Benralizumab In Severe Asthma. *J Asthma Allergy* **12**, 401-413 (2019).

13. Tomomatsu, K., *et al.* Rapid clearance of mepolizumab-resistant bronchial mucus plugs in allergic bronchopulmonary aspergillosis with benralizumab treatment. *Allergol Int* **69**, 636-638 (2020).

14. Altes, T.A., *et al.* Hyperpolarized 3He MR lung ventilation imaging in asthmatics: preliminary findings. *J Magn Reson Imaging* **13**, 378-384 (2001).

15. Svenningsen, S., *et al.* What are ventilation defects in asthma? *Thorax* **69**, 63-71 (2014).

16. Eddy, R.L., *et al.* Is Computed Tomography Airway Count Related to Asthma Severity and Airway Structure and Function? *Am J Respir Crit Care Med* **201**, 923-933 (2020).

17. Mummy, D.G., *et al.* Mucus Plugs in Asthma at CT Associated with Regional Ventilation Defects at Helium 3 MRI. *Radiology*, 204616 (2021).

18. Fain, S.B., *et al.* Evaluation of structure-function relationships in asthma using multidetector CT and hyperpolarized He-3 MRI. *Acad Radiol* **15**, 753-762 (2008).

19. Eddy, R.L., Svenningsen, S., Licskai, C., McCormack, D.G. & Parraga, G. Hyperpolarized Helium 3 MRI in Mild-to-Moderate Asthma: Prediction of Postbronchodilator Reversibility. *Radiology* **293**, 212-220 (2019).

20. Svenningsen, S., *et al.* Sputum Eosinophilia and Magnetic Resonance Imaging Ventilation Heterogeneity in Severe Asthma. *Am J Respir Crit Care Med* **197**, 876-884 (2018).

21. Svenningsen, S., Nair, P., Guo, F., McCormack, D.G. & Parraga, G. Is ventilation heterogeneity related to asthma control? *Eur Respir J* **48**, 370-379 (2016).

22. Hall, C.S., *et al.* Single-Session Bronchial Thermoplasty Guided by (129)Xe Magnetic Resonance Imaging. A Pilot Randomized Controlled Clinical Trial. *Am J Respir Crit Care Med* **202**, 524-534 (2020).

23. Svenningsen, S., *et al.* Bronchial thermoplasty guided by hyperpolarised gas magnetic resonance imaging in adults with severe asthma: a 1-year pilot randomised trial. *ERJ Open Res* **7**(2021).

24. Thomen, R.P., *et al.* Regional ventilation changes in severe asthma after bronchial thermoplasty with (3)He MR imaging and CT. *Radiology* **274**, 250-259 (2015).

25. Svenningsen, S., Eddy, R.L., Kjarsgaard, M., Parraga, G. & Nair, P. Effects of Anti-T2 Biologic Treatment on Lung Ventilation Evaluated by MRI in Adults With Prednisone-Dependent Asthma. *Chest* **158**, 1350-1360 (2020).

26. Global Initiative for Asthma (GINA). Global Strategy for Asthma Management and Prevention. (2022).

27. Juniper, E.F., O'Byrne, P.M., Guyatt, G.H., Ferrie, P.J. & King, D.R. Development and validation of a questionnaire to measure asthma control. *Eur Respir J* **14**, 902-907 (1999).

28. Juniper, E.F., Buist, A.S., Cox, F.M., Ferrie, P.J. & King, D.R. Validation of a standardized version of the Asthma Quality of Life Questionnaire. *Chest* **115**, 1265-1270 (1999).

29. Jones, P.W., Quirk, F.H., Baveystock, C.M. & Littlejohns, P. A self-complete measure of health status for chronic airflow limitation. The St. George's Respiratory Questionnaire. *Am Rev Respir Dis* **145**, 1321-1327 (1992).

30. Svenningsen, S., *et al.* Hyperpolarized (3) He and (129) Xe MRI: differences in asthma before bronchodilation. *J Magn Reson Imaging* **38**, 1521-1530 (2013).

31. Walker, T.G. & Happer, W. Spin-exchange optical pumping of noble-gas nuclei. *Rev Mod Phys* **69**, 629-642 (1997).

32. Kirby, M., Wheatley, A., McCormack, D.G. & Parraga, G. Development and application of methods to quantify spatial and temporal hyperpolarized He-3 MRI ventilation dynamics: Preliminary results in chronic obstructive pulmonary disease. *Proc Spie* **7626**, 762605 (2010).

33. Kirby, M., *et al.* Hyperpolarized 3He magnetic resonance functional imaging semiautomated segmentation. *Acad Radiol* **19**, 141-152 (2012).

34. Kirby, M., *et al.* Longitudinal Computed Tomography and Magnetic Resonance Imaging of COPD: Thoracic Imaging Network of Canada (TINCan) Study Objectives. *Chronic Obstr Pulm Dis* **1**, 200-211 (2014).

35. Kirby, M., *et al.* Total Airway Count on Computed Tomography and the Risk of Chronic Obstructive Pulmonary Disease Progression. Findings from a Population-based Study. *Am J Respir Crit Care Med* **197**, 56-65 (2018).

36. Smith, B.M., *et al.* Comparison of spatially matched airways reveals thinner airway walls in COPD. The Multi-Ethnic Study of Atherosclerosis (MESA) COPD Study and the Subpopulations and Intermediate Outcomes in COPD Study (SPIROMICS). *Thorax* **69**, 987-996 (2014).

37. Sun, G.W., Shook, T.L. & Kay, G.L. Inappropriate use of bivariable analysis to screen risk factors for use in multivariable analysis. *J Clin Epidemiol* **49**, 907-916 (1996).

38. Vatcheva, K.P., Lee, M., McCormick, J.B. & Rahbar, M.H. Multicollinearity in Regression Analyses Conducted in Epidemiologic Studies. *Epidemiology (Sunnyvale)* **6**(2016).

39. Eddy, R.L., Svenningsen, S., McCormack, D.G. & Parraga, G. What is the minimal clinically important difference for helium-3 magnetic resonance imaging ventilation defects? *Eur Respir J* **51**(2018).

4.7 Supplement

4.7.1 Methods:

Pulmonary Function Tests and Questionnaires

Participants performed spirometry[1] and plethysmography[2] according to American Thoracic Society guidelines using a whole-body plethysmograph (MedGraphics Corporation, Saint Paul, MN, USA). Fraction of exhaled nitric oxide[3] was measured according to guidelines using the NIOX VERO® system (Circassia Pharmaceuticals Inc, Morrisville, NC, USA). Oscillometry[4] was performed according to European Respiratory Society guidelines using a tremoFlo C-100 Airwave Oscillometry System (Thorasys, Montreal, QC, Canada) to measure resistance (R) and reactance between 5 and 37 Hz. Post-bronchodilator (BD) measurements were performed 15 minutes after inhalation of 4×100 µg Novo-Salbutamol Hydrofluoroalkane (Teva Novopharm, Toronto, ON, Canada) using an AeroChamber (Trudell Medical International, London, ON, Canada). Participants withheld asthma medications before each face-to-face study visit according to American Thoracic Society guidelines.[1] Asthma control,[5] Asthma Quality-of-Life[6] and St. George's Respiratory questionnaires[7] were self-administered under supervision.

Thoracic Imaging and Analysis

Anatomic ^{1}H and ^{129}Xe static ventilation MRI were acquired at 3.0 Tesla (Discovery MR750; GE Healthcare), as described,[8] using a fast-spoiled gradient-recalled-echo sequence and a three-dimensional fast-spoiled gradient-recalled echo sequence, respectively. Supine participants were coached to inhale a 1.0L (400mL ^{129}Xe + 600mL ^{4}He for ^{129}Xe MRI and 1.0L N_2 for ^{1}H MRI) bag (Tedlar; Jensen Inert Products) from functional residual capacity with acquisition under breath-hold conditions. ^{129}Xe gas was polarized to 30-40% (Polarean; Xenispin 9820).[9]

Within 30 minutes of MRI, CT was acquired post-BD after inhalation of 1.0L N_2 from functional residual capacity using a 64-slice LightSpeed VCT system (General Electric Healthcare; parameters: 64×0.625 collimation, 120 peak kilovoltage, 100 mA, tube rotation time=500ms, pitch=1.25, standard reconstruction kernel, slice thickness=1.25mm, field-of-view=40cm^2), as previously described.[10]

4.7.2 Results:

Participant Demographics

Twenty-nine participants completed Day-56, with one participant not completing an in-person visit due to the onset of the COVID-19 pandemic. Twenty-seven completed Day-112 (one participant was excluded due to a newly implanted medical device that was MR incompatible and one declined to participate), of which 26 participants completed an in-person visit and one did not due to the pandemic; two participants completed this visit more than 112±7 days after Day-0 (172 and 217 days) as a result of restrictions during the pandemic.

Table 4-4 shows a by-participant list of those that did not complete Visit 7 and/or Visit 8. Four participants declined to participate in the optional 1-year visit, five had discontinued benralizumab treatment (n=3 MD decision, n=1 side effects, n=1 cost) and were not eligible and three were lost-to-follow-up. One participant declined to participate in the optional 2.5-year visit, one additional participant had discontinued benralizumab treatment (n=1 cost) and was not eligible, three participants were lost-to-follow-up, one participant had moved away and one participant had COVID and could not participate; two participants that did not participate in the 1-year visit completed the 2.5-year visit. CT was not acquired at 2.5-years in one participant.

Pulmonary Function, Asthma Control, Ventilation and Airway Changes

Changes in the ACQ-6 score greater than the MCID[11] were observed in 20/29 (67%) participants at Day-28, 12/16 (75%) participants at 1-year and 10/13 (77%) participants at 2.5-years. For FEV_1,[12] 8/29 (28%) participants reported an improvement greater than the MCID on Day-28, whilst 3/16 (19%) reported this at 1-year and 7/13 (54%) at 2.5-years. In a similar manner, changes in MRI VDP greater than the MCID[13] were observed in 15/29 (52%) participants on Day-28, 10/16 (63%) participants at 1-year and 10/13 (77%) participants at 2.5-years.

Table 4-4. Participation and Reasons for Withdrawal

Participant	1-year	Rx Access	2.5-years	Rx Access
P01	*Participated*	✓	Lost-to-follow-up	✓
P02	*Participated*	✓	*Participated*	✓
P03	Lost-to-follow-up	✓	Lost-to-follow-up	✓
P04	*Participated*	✓	*Participated*	✓
P05	*Participated*	✓	Discontinued Rx – cost	✗
P06	Discontinued Rx MD	✓	Discontinued Rx MD	✓
P07	*Participated*	✓	*Participated*	✓
P08	*Participated*	✓	*Participated*	✓
P09	*Participated*	✓	Declined	✓
P10	*Participated*	✓	*Participated*	✓
P11	Discontinued Rx MD	✓	Discontinued Rx MD	✓
P12	*Participated*	✓	*Participated*	✓
P13	*Participated*	✓	*Participated*	✓
P14	Discontinued Rx MD	✓	Discontinued Rx MD	✓
P15	*Participated*	✓	Lost-to-follow-up	✓
P16	*Participated*	✓	Lost-to-follow-up	✓
P17	Lost-to-follow-up	✓	Lost-to-follow-up	✓
P18	Discontinued Rx MD	✓	Discontinued Rx MD	✓
P19	*Participated*	✓	*Participated*	✓
P20	*Participated*	✓	*Participated*	✓
P21	Lost-to-follow-up	✓	Lost-to-follow-up	✓
P22	MR-contraindication	✓	MR-contraindication	✓
P23	*Participated*	✓	*Participated*	✓
P24	Discontinued Rx – cost	✗	Discontinued Rx – cost	✗
P25	Discontinued Rx – cost	✗	Discontinued Rx – cost	✗
P26	Declined – COVID	✓	*Participated*	✓
P27	Declined – COVID	✓	*Participated*	✓
P28	Declined – COVID	✓	Lost-to-follow-up	✓
P29	*Participated*	✓	*Participated*	✓

Grand Totals		
Participated	16	13
Lost-to-FU	3	7
Discont Rx. MD	4	4
Discont Rx. cost	2	3
COVID concerns	3	0
Declined no reason given	0	1
MRI incompatible	1	1

Table 4-5. Demographic, pulmonary function, imaging and questionnaire differences prior to therapy between those with and those without 1-year and 2.5-year visits

Parameter	1-year			2.5-years		
	With FU (n=16)	Without FU (n=13)	p	With FU (n=13)	Without FU (n=16)	p
Age years	60 ± 13	59 ± 12	.9	60 ± 16	59 ± 9	.7
Female n/%	13 (81)	3 (23)	-	11 (85)	5 (31)	-
BMI kg/m^2	28 ± 4	31 ± 7	.09	28 ± 4	30 ± 6	.4
Pack-years	3 ± 8	11 ± 16	.1	5 ± 9	8 ± 15	.4
Median (IQR)	0 (0-30)	0 (0-45)	-	0 (0-30)	0 (0-45)	-
Duration of Asthma years	20 ± 18	31 ± 24	.1	20 ± 17	30 ± 24	.2
Median (IQR)	11 (1-52)	32 (1-64)	-	12 (2-52)	31 (1-64)	-
Pulmonary function						
Pre-BD FEV_1 $\%_{pred}$	61 ± 19	62 ± 18	.9	66 ± 17	59 ± 20	.3
Post-BD FEV_1 $\%_{pred}$	73 ± 18	75 ± 18	.7	76 ± 15	73 ± 19	.6
Pre-BD FVC $\%_{pred}$	74 ± 15	80 ± 16	.4	77 ± 12	76 ± 19	.9
Post-BD FVC $\%_{pred}$	83 ± 15	87 ± 18	.5	86 ± 10	84 ± 20	.8
Post-BD FEV_1/FVC	68 ± 11	67 ± 11	.7	69 ± 11	67 ± 12	.7
Pre-BD RV/TLC	49 ± 11	51 ± 7	.8	49 ± 11	51 ± 8	.5
Post-BD RV/TLC	46 ± 10	47 ± 8	.8	46 ± 10	47 ± 9	.8
Inflammatory markers						
Eos cells/μL	670 ± 440	580 ± 300	.6	630 ± 380	630 ± 390	1.0
FeNO ppb	53 ± 39	43 ± 31	.5	45 ± 31	51 ± 39	.7
Asthma quality-of-life and control						
ACQ-6	1.9 ± 1.4	2.9 ± 1.5	.1	2.0 ± 1.4	2.6 ± 1.6	.3
AQLQ	4.6 ± 1.5	4.1 ± 1.4	.4	4.8 ± 1.2	4.0 ± 1.5	.1
SGRQ	48 ± 23	54 ± 18	.4	45 ± 22	55 ± 20	.2
CT imaging						
TAC	137 ± 30	144 ± 72	.7	128 ± 22	151 ± 66	.2
Mucus Score	4 ± 4	3 ± 4	.4	3 ± 4	3 ± 4	1.0
Mucus Count	6 ± 10	4 ± 7	.7	5 ± 11	5 ± 7	.9
Airway LA mm^2	8.1 ± 3.1	7.9 ± 1.8	.8	8.1 ± 3.3	7.9 ± 1.8	.8
Airway WT mm	1.2 ± 0.2	1.2 ± 0.1	.1	1.2 ± 0.1	1.2 ± 0.1	.5
Airway WT%	18.1 ± 0.8	19.2 ± 1.3	**.02**	18.3 ± 0.7	18.8 ± 1.4	.3
MRI						
Pre-BD VDP	16 ± 11	18 ± 9	.7	16 ± 13	18 ± 8	.7
Post-BD VDP	11 ± 8	14 ± 12	.5	11 ± 9	13 ± 11	.6

Data are reported as mean ± standard deviation, unless indicated otherwise. Bolded values indicate significant differences between groups.

Abbreviations: FU=follow-up; BMI=body mass index; IQR=interquartile range; BD=bronchodilator; FEV_1=forced expiratory volume in 1 second; $\%_{pred}$=percent of predicted value; FVC=forced vital capacity; RV=residual volume; TLC=total lung capacity; Eos=blood eosinophil count; FeNO=fraction of exhaled nitric oxide; ppb=parts per billion; ACQ=Asthma Control Questionnaire; AQLQ=Asthma Quality-of-Life Questionnaire; SGRQ=St. George's Respiratory Questionnaire; CT=computed tomography; TAC=total airway count; LA=lumen area; WT=wall thickness; TBV=total blood volume; BV_5=blood volume of vessels with cross sectional area less than 5 mm^2; $BV_{5\text{-}10}$=blood volume of vessels with cross sectional area between 5 and 10 mm^2; BV_{10}=blood volume of vessels with cross sectional area greater than 10 mm^2; MRI=magnetic resonance imaging; VDP=ventilation defect percent.

Table 4-6. Asthma Medications in addition to benralizumab

Participant	Day-0	1-year	2.5-years
P01	Zenhale: 2 puffs TID 200/5 Spiriva: 2 puffs QD	Zenhale: 2 puffs TID 200/5 Spiriva: 2 puffs QD	N/A
P02	Breo Ellipta: 1 puff QD 200/25 Montelukast: 20 mg QD	Breo Ellipta: 1 puff QD 200/25 Arnuity Ellipta: PRN	Breo Ellipta: 1 puff QD 200/25
P04	Symbicort: 1 puff BID		
P05	Symbicort: 2 puffs BID Pulmicort: 2 puffs BID 400 Prednisone: 5 mg TID Singulair: 10 mg QD	Symbicort: 2 puffs QD	N/A
P07	Symbicort: 2 puffs BID 200/6 Prednisone: 5 mg QD Umeclidinium: 1 puff QD	Symbicort: 2 puffs BID 200/6	Symbicort: 2 puffs BID 200/6
P08	Advair: 2 puffs BID 250/25 Spiriva: 2 puffs QAM	Symbicort: 2 puffs BID	Symbicort: 2 puffs BID
P09	Symbicort: 2 puffs BID 200/6 Spiriva: 1 puff QD	Symbicort: 2 puffs BID 200/6	N/A
P10	Symbicort: 2 puffs BID 200/6 Pulmicort: 2 puffs BID 400 Methylprednisolone: 80mg/mL Q10days	Symbicort: 2 puffs PRN 200/6	Symbicort: 2 puffs PRN 200/6
P12	Symbicort: 2 puffs TID 200/6	Symbicort: 1 puff BID 200/6	Breo Ellipta: 1 puff QAM 100/25
P13	Zenhale: 2 puffs TID 200/5 Breo Ellipta: 1 puff QD 200/25	Zenhale: 2 puffs BID 200/5	Zenhale: 2 puffs BID 200/5
P15	Symbicort: 2 puffs BID 200/6 Arnuity Ellipta: 200 µg QD	Symbicort: 2 puffs BID 200/6 Arnuity Ellipta: 200 µg QD	N/A
P16	Symbicort: 2 puffs QID 200/6 Spiriva: 2 puffs QD Prednisone: 10 mg QD Singulair: 10 mg QD	Symbicort: 2 puffs BID 200/6 Pulmicort: 2 puffs BID Spiriva: 2 puffs QD Alvesco: 2 puffs BID at 200µg	N/A
P19	Symbicort: 2 puffs BID 200/6 Singulair: 30 mg QD	Symbicort: 2 puffs BID 200/6 Singulair: 10 mg QD	Symbicort: 2 puffs BID 200/6
P20	Alvesco: 2 puffs BID at 200 µg *Xolair: 300 mg BIW	Alvesco: 2 puffs QD at 200 µg	Alvesco: 2 puffs QD at 200µg Enerzair Breezhaler: QD at 150/50/160 µg

P23	Symbicort: 2 puffs BID 200/6	Symbicort: 2 puffs BID 200/6	Symbicort: 2 puffs BID 200/6
P26	Symbicort: 2 puffs BID 200/6 Spiriva: 2 puffs QID Singulair: 10 mg QD	N/A	Symbicort: 2 puffs BID 200/6 Spiriva: 2 puffs QD Singulair: 10 mg QD Avamys: 1 spray QD
P27	Symbicort: 2 puffs BID 200/6 Spiriva: 2 puffs QID	N/A	Symbicort: 2 puffs BID 200/6 Spiriva: 2 puffs QD
P29	Symbicort: 2 puffs BID 200/6 Prednisone: 15 mg QD	Symbicort: 2 puffs BID 200/6	Symbicort: 2 puffs BID 200/6

TID=three times a day; QD=once a day; N/A=visit not completed; BID=twice a day; PRN=as needed; QAM=every morning; Q=every; QID=four times a day; BIW=twice a week; *Xolair washout ≥8 weeks

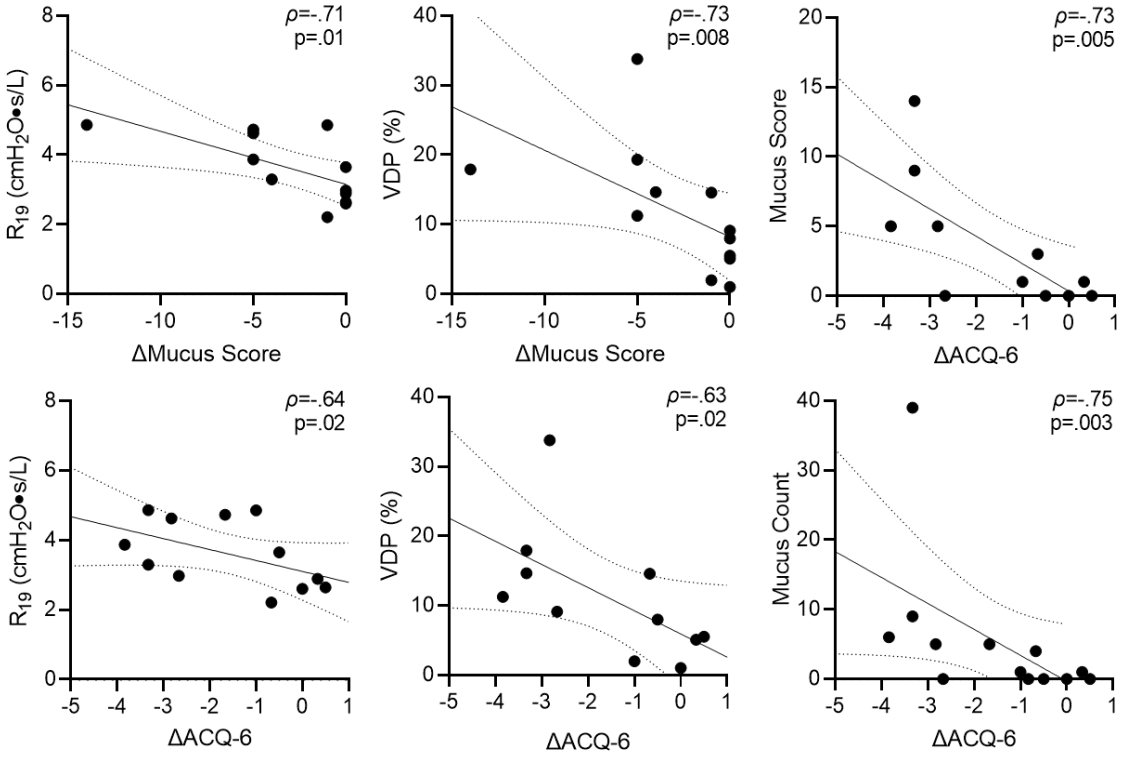

Figure 4-6. Relationships for mucus score and ACQ-6 changes with clinical and imaging measurements
Top left: Linear correlation for the change in mucus score with Day-0 R_{19} (ρ=-.71, p=.01).
Top middle: Linear correlation for the change in mucus score with Day-0 VDP (ρ=-.73, p=.008).
Top right: Linear correlation for the change in ACQ-6 with Day-0 mucus score (ρ=-.73, p=.005).
Bottom left: Linear correlation for the change in ACQ-6 with Day-0 R_{19} (ρ=-.64, p=.02).
Bottom middle: Linear correlation for the change in ACQ-6 with Day-0 VDP (ρ=-.63, p=.02).
Bottom right: Linear correlation for the change in mucus score with Day-0 mucus count (ρ=-.75, p=.003).

R=resistance; VDP=ventilation defect percent; ACQ-6=asthma control questionnaire score.

4.7.3 References:

1. Miller, M.R., *et al.* Standardisation of spirometry. *Eur Respir J* **26**, 319-338 (2005).

2. Wanger, J., *et al.* Standardisation of the measurement of lung volumes. *Eur Respir J* **26**, 511-522 (2005).

3. American Thoracic Society & European Respiratory Society. ATS/ERS recommendations for standardized procedures for the online and offline measurement of exhaled lower respiratory nitric oxide and nasal nitric oxide, 2005. *Am J Respir Crit Care Med* **171**, 912-930 (2005).

4. King, G.G., *et al.* Technical standards for respiratory oscillometry. *Eur Respir J* **55**(2020).

5. Juniper, E.F., O'Byrne, P.M., Guyatt, G.H., Ferrie, P.J. & King, D.R. Development and validation of a questionnaire to measure asthma control. *Eur Respir J* **14**, 902-907 (1999).

6. Juniper, E.F., Buist, A.S., Cox, F.M., Ferrie, P.J. & King, D.R. Validation of a standardized version of the Asthma Quality of Life Questionnaire. *Chest* **115**, 1265-1270 (1999).

7. Jones, P.W., Quirk, F.H., Baveystock, C.M. & Littlejohns, P. A self-complete measure of health status for chronic airflow limitation. The St. George's Respiratory Questionnaire. *Am Rev Respir Dis* **145**, 1321-1327 (1992).

8. Svenningsen, S., *et al.* Hyperpolarized (3) He and (129) Xe MRI: differences in asthma before bronchodilation. *J Magn Reson Imaging* **38**, 1521-1530 (2013).

9. Walker, T.G. & Happer, W. Spin-exchange optical pumping of noble-gas nuclei. *Rev Mod Phys* **69**, 629-642 (1997).

10. Kirby, M., *et al.* Longitudinal Computed Tomography and Magnetic Resonance Imaging of COPD: Thoracic Imaging Network of Canada (TINCan) Study Objectives. *Chronic Obstr Pulm Dis* **1**, 200-211 (2014).

11. Juniper, E.F., Svensson, K., Mork, A.C. & Stahl, E. Measurement properties and interpretation of three shortened versions of the asthma control questionnaire. *Respir Med* **99**, 553-558 (2005).

12. Santanello, N.C., Zhang, J., Seidenberg, B., Reiss, T.F. & Barber, B.L. What are minimal important changes for asthma measures in a clinical trial? *Eur Respir J* **14**, 23-27 (1999).

13. Eddy, R.L., Svenningsen, S., McCormack, D.G. & Parraga, G. What is the minimal clinically important difference for helium-3 magnetic resonance imaging ventilation defects? *Eur Respir J* **51**(2018).

Chapter 5

5 PULMONARY VASCULAR DIFFERENCES IN EOSINOPHILIC ASTHMA AFTER 2.5-YEARS ANTI-IL-5RA TREATMENT

To better understand the effect of long-term anti-IL-5Rα therapy on the pulmonary vasculature, we evaluated a subset of the patients described in Chapters 3-4. We quantified the change in small vessel and large vessel volumes after therapy and related these changes to baseline imaging and pulmonary function data to gain mechanistic insight about these changes.

The contents of this chapter were submitted to the American Journal of Respiratory and Critical Care Medicine: MJ McIntosh, AM Matheson, HK Kooner, RL Eddy, H Serajeddini, C Yamashita and G Parraga. Pulmonary Vascular Differences in Eosinophilic Asthma after 2.5-years anti-IL-5Rα Treatment. Submitted to American Journal of Respiratory and Critical Care Medicine (Manuscript ID Blue-202305-0804OC).

5.1 Introduction

Chest computed tomography (CT) imaging measurements from the Severe Asthma Research Program revealed significant pulmonary vascular abnormalities in severe asthma,[1] which were consistent with previous histological evidence.[2,3] These vascular abnormalities were associated with acute exacerbations, asthma severity and poor disease control, as well as increased peripheral and airway eosinophilia.[1] Anti-interleukin-5 (IL-5) biologic therapies have recently been introduced to eliminate systemic and airway eosinophils [4] and are highly effective in improving lung function and disease control, as well as reducing exacerbations in patients with asthma.[5,6] However, potential pulmonary vascular changes following such treatments have not yet been explored or determined.

Evidence to support pulmonary vascular therapy response is limited. Previous investigations showed that, two-years after smoking cessation, CT small-vessel volume increased in patients with chronic obstructive pulmonary disease (COPD).[7] In contrast, CT small-vessel volume significantly decreased in asthma-COPD overlap syndrome following three-months of inhaled corticosteroid (ICS) treatment,[8] which was postulated to be a consequence of downregulated

angiogenic remodeling.[9] Still, the long-term, downstream effects of biologic or inhaled therapy on the pulmonary vasculature in severe asthma are not well understood.

Previous work has proposed several mechanisms to explain the vascular abnormalities observed in asthma, including the compression of vessels via hyperinflation or air-trapping[10,11] or regional hypoxic vasoconstriction caused by airflow obstructions from various causes.[1,11,12] Eosinophilic infiltration of the airways can drive inflammation[13] and luminal obstruction or narrowing[14] as well as mucus plug formation,[14] and these pathophysiological features, along with CT air-trapping, have been shown to be related to hyperpolarized ^{129}Xe and ^{3}He MRI ventilation abnormalities.[15-18] Anti-IL-5 biologic treatments have recently been shown to resolve MRI ventilation defects as well as CT mucus plugs over the short-[19,20] and long-term.[21] Taken together, these findings are suggestive that in some lung regions, poor to nonexistent ventilation over long periods of time may result in regional hypoxic remodeling of the small pulmonary vessels.

Based on these previous results, and the relationships between vascular abnormalities, air-trapping and airflow obstruction,[1] we hypothesized that long-term anti-IL-5Rα biologic therapy would directly influence the finding of pulmonary vessel changes in severe asthma. Hence, here our objective was to quantify pulmonary vascular volume in the small and large pulmonary vessels in patients with poorly-controlled, eosinophilic asthma prior to anti-IL-5Rα treatment initiation and following 2.5-years of therapy.

5.2 Materials and Methods

5.2.1 Study Participants and Design

Participants 18 to 80 years of age with poorly-controlled eosinophilic asthma according to the Global Initiative for Asthma[22] provided written-informed consent to approved protocols

(www.clinicaltrials.gov NCT03733535 and NCT02351141). Inclusion and exclusion criteria as well as the study design have previously been described.[19] Briefly, participants with asthma control questionnaire score (ACQ-6) ≥1.5[23] and blood eosinophil count >300 cells/μL were enrolled. Post-bronchodilator spirometry, thoracic CT, ^{129}Xe MRI and the fraction of exhaled nitric oxide (FeNO) measurement in addition to ACQ-6,[24] Asthma Quality-of-Life (AQLQ)[25] and St. George's Respiratory (SGRQ)[26] questionnaires were completed at Day-0 and again following 2.5-years of continuous anti-IL-5Rα treatment; plethysmography was acquired at Day-0 only. The effect of 2.5-years anti-IL-5Rα therapy on quantitative CT airway measurements, mucus plugs and MRI ventilation defects in some of these participants was previously reported.[21] A convenience sample of healthy, elderly never-smokers, who completed spirometry, plethysmography, and CT, was retrospectively evaluated (www.clinicaltrials.gov NCT02483403).

5.2.2 Pulmonary Function Tests and Questionnaires

Participants performed spirometry[27] and plethysmography[28] according to American Thoracic Society (ATS) guidelines using a whole-body plethysmograph (MedGraphics Corporation, Saint Paul, MN, USA). FeNO[29] was measured according to ATS/ERS guidelines using the NIOX VERO® system (Circassia Pharmaceuticals Inc, Morrisville, NC, USA). Post-bronchodilator measurements were performed 15 minutes after inhalation of 4x100 μg Novo-Salbutamol Hydrofluoroalkane (Teva Novopharm, Toronto, ON, Canada) using an AeroChamber (Trudell Medical International, London, ON, Canada). Participants withheld any prescribed airways disease medications before each study visit according to ATS guidelines[27] (eg. short-acting β-agonists ≥6 hours, long-acting β-agonists ≥12 hours, long-acting muscarinic antagonists ≥24 hours). ACQ-6,[24] AQLQ[25] and SGRQ[26] were self-administered under the supervision of study personnel.

5.2.3 Computed Tomography and Analysis

CT was acquired after inhalation of a 1.0L bag (Tedlar; Jensen Inert Products, Coral Springs, FL, USA) of N_2 from the bottom of a tidal breath (functional residual capacity) for volume-matching with MRI using a 64-slice LightSpeed VCT system (General Electric Healthcare, Milwaukee, WI, USA; parameters: 64x0.625 collimation, 120 peak kilovoltage, 100 mA, tube rotation time=500ms, pitch=1.25, standard reconstruction kernel, slice thickness=0.625mm, field-of-view=40cm^2) as previously described.[30] The effective dose of 1.8 mSv was calculated using the ImPACT patient dosimetry calculator (UK Health Protection Agency NRPB-SR250 software).

CT pulmonary vasculature was analyzed using Chest Imaging Platform (Brigham and Women's Hospital, Boston, MA, USA)[31] to automatically generate pulmonary vascular measurements, including total blood volume (TBV) and the volume of blood vessels with cross sectional area less than 5 mm^2 (BV_5; representative of small vessels), between 5 and 10 mm^2 ($BV_{5\text{-}10}$; representative of mid-size vessels) and greater than 10 mm^2 (BV_{10}; representative of large vessels). CT airways were analyzed using VIDAvision software (VIDA Diagnostics Inc., Coralville, IA, USA) to generate total airway count, wall area percent, wall thickness and lumen area.[32,33] As previously described,[14] mucus plugs were identified as airway regions with complete occlusion that were more radio-dense than the lumen. Mucus-score was quantified as the sum of occluded airway segments[14,17] and mucus-count was quantified as the total number of CT visible mucus occlusions.[19]

5.2.4 Magnetic Resonance Imaging and Analysis

Anatomic proton (^{1}H) and ^{129}Xe static ventilation MRI were acquired prior to CT (within 30 minutes) using a 3.0 Tesla scanner (Discovery MR750; GE Healthcare, Milwaukee WI, USA) with broadband capability as previously described.[34] Supine participants were coached to

inhale a 1.0L bag (400mL ^{129}Xe + 600mL ^{4}He for ^{129}Xe MRI and 1.0L N_2 for ^{1}H MRI) from functional residual capacity with acquisition under breath-hold conditions. ^{129}Xe gas was polarized to 30-40% (Polarean; Xenispin 9820, Durham, NC, USA).[35] Quantitative MRI analysis was performed using a semi-automated segmentation algorithm, as previously described[36] using Matlab 2019a (Mathworks, Natick, MA, USA), which classifies voxels into five signal intensity clusters (signal void or ventilation defect volume and four signal intensity clusters ranging from low to high). VDP was generated by normalizing ventilation defect volume to the ^{1}H MRI thoracic cavity volume.

5.2.5 Statistical Analysis

SPSS (SPSS Statistics 25.0; IBM, Armonk, NJ, USA) was used for all statistical analyses. Data were tested for normality using Shapiro-Wilk tests and nonparametric tests were performed when data were not normally distributed. Differences between healthy controls and eosinophilic asthma participants were evaluated using independent samples t-tests. Differences in pulmonary vascular measurements at 2.5-years as compared to Day-0 were evaluated using paired samples t-tests. Univariate relationships were evaluated using Pearson (r) or Spearman (ρ) correlation coefficients. Pearson or Spearman correlations with p values ≤ 0.20[37] were used in multivariable models, generated using the backward approach, to predict the change in BV_5/TBV and ACQ-6 at 2.5-years. Regression coefficients for the variables in the multivariable models were expressed as the standardized β. The Holm-Bonferroni correction was performed to correct for multiple comparisons. Results were considered statistically significant when the probability of making a type I error was less than 5% ($p<0.05$).

5.3 Results

5.3.1 Participant Demographics

A CONSORT diagram is provided in **Figure 5-1**. Thirty-one participants were enrolled, one withdrew due to severe claustrophobia and two declined CT at the Day-0 visit and were excluded from the analysis. Twenty-eight participants consented to CT at Day-0 (19 female, 9 male; mean age 59±13yr). At 2.5-years, two participants withdrew (pregnancy n=1, MR contraindications n=1), seven discontinued anti-IL-5Rα treatment, five were lost-to-follow-up, one declined the visit and one declined CT. Thus, 12 participants were evaluated at 2.5-years (10 female, 2 male; mean age 61±16yr).

Table 5-1 provides a summary of baseline characteristics for all participants, while **Table 5-5** shows there were no significant differences among baseline characteristics for participants who completed a 2.5-year visit and those who did not. ICS was prescribed in all participants at Day-0 and to 11 of 12 participants (92%) at 2.5-years. In addition, shown in **Table 5-6**, the healthy, never-smoker control subgroup (n=42; 22 females) was significantly different for age (73±6yr) and body mass index (26±4 kg/m^2) as compared to eosinophilic asthma participants on Day-0 (age=59±13yr, $p<.001$; body mass index=29±5 kg/m^2, $p=.04$). There were no demographic characteristic differences between the groups at 2.5-years. The proportion of females in the control and eosinophilic asthma groups at both Day-0 and 2.5-years were not significantly different.

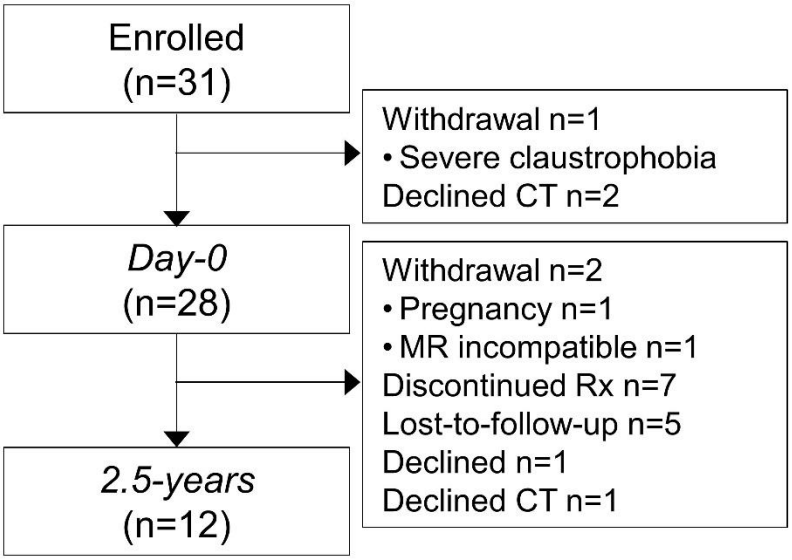

Figure 5-1. CONSORT Diagram
Twenty-eight participants completed Day-0 with CT. Of these, for the 2.5-year visit, seven participants discontinued anti-IL-5Rα, five were lost-to-follow-up, one declined to participate, two withdrew and one declined CT. Thus, 12 participants completed a visit with CT 2.5-years post-anti-IL-5Rα.

Table 5-1. Demographic characteristics prior to therapy

Parameter	All participants (n=28)	With 2.5-year visit (n=12)
Age years	59 ± 13	61 ± 16
Female n (%)	19 (68)	10 (83)
BMI kg/m^2	29 ± 5	28 ± 4
Pack-years	7 ± 13	4 ± 9
Median (min-max)	0 (0-45)	0 (0-30)
Duration of Asthma years	23 ± 21	21 ± 17
Median (min-max)	19 (1-63)	19 (2-52)
Follow-up time years	-	2.6 ± 0.3
Median (min-max)	-	2.6 (2.1-3.0)

Demographic data at enrollment for participants completing Day-0 and 2.5-year follow-up. Data are reported as mean ± standard deviation, unless indicated otherwise.

BMI=body mass index; Follow-up time=number of years between Day-0 and the 2.5-year visit; ICS=inhaled corticosteroids.

5.3.2 Pulmonary Blood Vessel Changes at 2.5-years

Figure 5-2 shows three-dimensional vascular trees on Day-0 and 2.5-year visits for two representative participants. In participant P02, there were more CT-visible small vessels shown in red (Day-0 BV_5/TBV=0.57; 2.5-years BV_5/TBV=0.63) at 2.5-years compared to Day-0. For this participant, changes in ACQ-6 score (Δ=-0.7) and VDP (Δ=-9%) were clinically relevant.[38,39] Participant P08 also had more CT-visible small vessels (Day-0 BV_5/TBV=0.47; 2.5-years BV_5/TBV=0.59) at 2.5-years and a visually obvious reduction in the volume of larger vessels (Day-0 BV_{10}/TBV=0.40; 2.5-years BV_{10}/TBV=0.28), as well as clinically relevant changes in ACQ-6 score (Δ=-2.8) and VDP (Δ=-25%).

As shown in **Table 5-2** and **Figure 5-3**, significant changes from Day-0 to 2.5-years were observed in BV_5/TBV (p=.02) and BV_{10}/TBV (p=.03), while TBV (p=.09) and $BV_{5\text{-}10}$/TBV (p=.3) were not significantly different. **Table 5-2** also shows that forced expiratory volume in 1-second (FEV_1) (p=.04), forced vital capacity (p=.03), ACQ-6 (p=.005), AQLQ (p=.001), SGRQ (p<.001), mucus-score (p=.03) and VDP (p=.004) were significantly different at 2.5-years as compared to Day-0, as previously reported.[21]

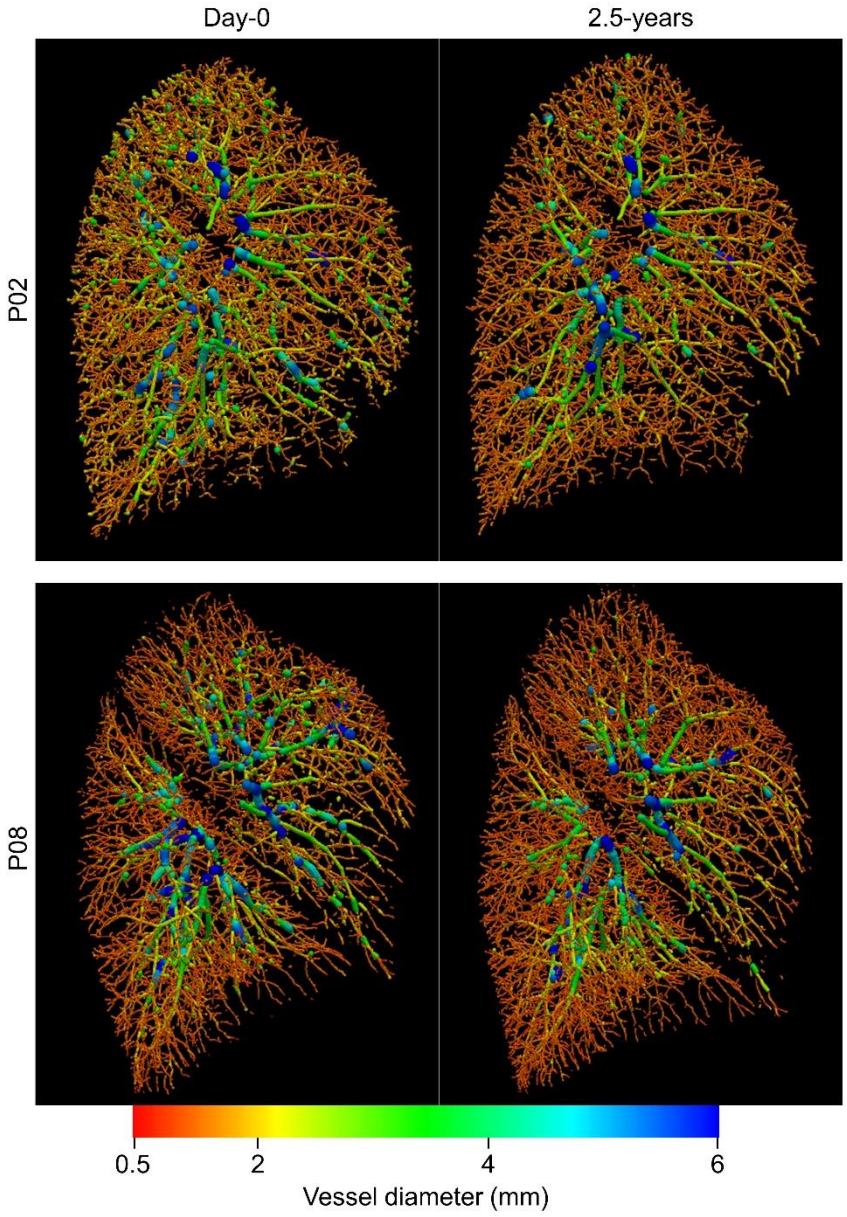

Figure 5-2. Qualitative imaging response
Sagittal view of the three-dimensional representation of pulmonary vessels in the left lung at Day-0 and 2.5-year follow-up, where red represents smaller vessels.

P02 was a 72-year-old female at enrolment with blood eosinophils=1000 cells/μL
Day-0: FEV_1=63%$_{pred}$, ACQ-6=0.7, VDP=15%, mucus-score=3, BV_5/TBV=0.57
2.5-years: FEV_1=77%$_{pred}$, ACQ-6=0, VDP=6%, mucus-score=2, BV_5/TBV=0.63

P08 was a 20-year-old female at enrolment with eosinophil count=600 cells/μL.
Day-0: FEV_1=57%$_{pred}$, ACQ-6=3.3, VDP=34%, mucus-score=5, BV_5/TBV=0.47
2.5-years: FEV_1=98%$_{pred}$, ACQ-6=0.5, VDP=9%, mucus-score=0, BV_5/TBV=0.59

Table 5-2. Pulmonary function, imaging and questionnaire data on Day-0 and 2.5-years post-anti-IL-5Rα

	Day-0		2.5-years	
Parameter	All participants (n=28)	With 2.5-year visit (n=12)	With 2.5-year visit (n=12)	Sig. p
Pulmonary function				
FEV_1 $\%_{pred}$	75 ± 19	74 ± 14	89 ± 19	**.04**
FVC $\%_{pred}$	85 ± 16	85 ± 11	97 ± 15	**.03**
FEV_1/FVC	68 ± 12	67 ± 10	72 ± 9	.2
RV/TLC	45 ± 9	47 ± 10	-	-
Inflammatory markers				
Eos cells/μL	660 ± 370	630 ± 400	-	-
FeNO ppb	49 ± 35	47 ± 32	56 ± 56	.4
Asthma QoL and control				
ACQ-6	2.3 ± 1.6	2.0 ± 1.5	0.5 ± 0.5	**.005**
AQLQ	4.4 ± 1.4	4.8 ± 1.2	6.4 ± 0.6	**.001**
SGRQ	50 ± 20	46 ± 22	15 ± 10	**<.001**
CT				
TBV mL	290 ± 85	273 ± 64	245 ± 33	.09
BV_5/TBV	0.52 ± 0.09	0.52 ± 0.08	0.57 ± 0.03	**.02**
$BV_{5\text{-}10}$/TBV	0.16 ± 0.03	0.16 ± 0.03	0.15 ± 0.02	.3
BV_{10}/TBV	0.32 ± 0.07	0.33 ± 0.06	0.28 ± 0.03	**.03**
Mucus-score	3 ± 4	4 ± 4	1 ± 1	**.03**
Mucus-count	5 ± 8	6 ± 11	1 ± 4	.2
MRI				
VDP %	12 ± 11	12 ± 9	4 ± 2	**.004**

Data acquired post-bronchodilator and are reported as mean ± standard deviation. Day-0: n=28 for all analyses except for FVC and FEV_1/FVC (n=27), RV/TLC and FeNO (n=26). 2.5-years: n=12 for all analyses.

Abbreviations: FEV_1=forced expiratory volume in 1 second; $\%_{pred}$=percent of predicted value; FVC=forced vital capacity; RV=residual volume; TLC=total lung capacity; Eos=blood eosinophil count; FeNO=fraction of exhaled nitric oxide; QoL=quality-of-life; ACQ=Asthma Control Questionnaire; AQLQ=Asthma Quality-of-Life Questionnaire; SGRQ=St. George's Respiratory Questionnaire; CT=computed tomography; TBV=total blood volume; BV_5=blood volume of vessels with cross sectional area less than 5 mm^2; $BV_{5\text{-}10}$=blood volume of vessels with cross sectional area between 5 and 10 mm^2; BV_{10}=blood volume of vessels with cross sectional area greater than 10 mm^2; MRI=magnetic resonance imaging; VDP=ventilation defect percent; p=paired samples t-test significance value between Day-0 and 2.5-years for n=12.

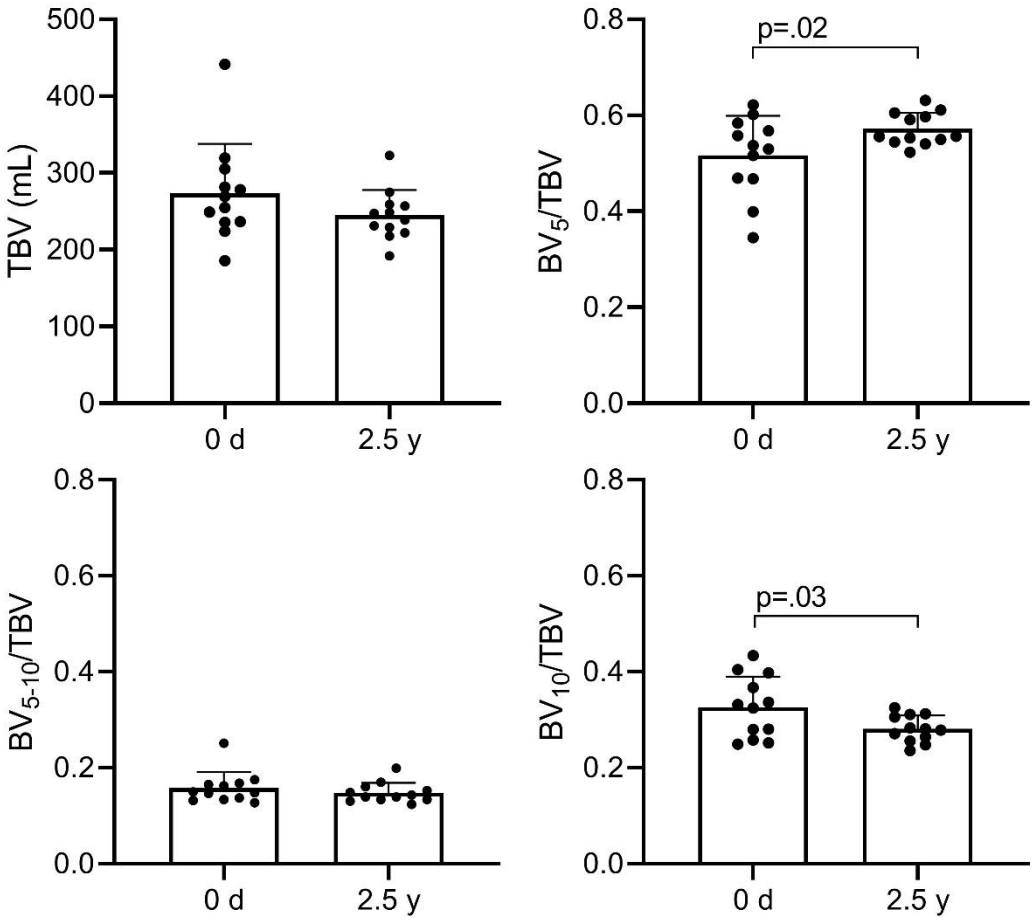

Figure 5-3. Vascular changes after anti-IL-5Rα
BV_5/TBV significantly different between Day-0 and 2.5-years (p=.02). BV_{10}/TBV significantly different between Day-0 and 2.5-years (p=.03). TBV and $BV_{5\text{-}10}$/TBV not significantly different between Day-0 and 2.5-years.

TBV=total blood volume; BV_5=blood volume of vessels with cross sectional area less than 5 mm^2; $BV_{5\text{-}10}$=blood volume of vessels with cross sectional area between 5 and 10 mm^2; BV_{10}=blood volume of vessels with cross sectional area greater than 10 mm^2; d=days; y=years; p=significance value for differences between Day-0 and 2.5-years.

CT vessel measurements at Day-0 and 2.5-years in eosinophilic asthma were compared to the healthy control subgroup, as shown in **Table 5-3**. At Day-0, eosinophilic asthma participants had significantly greater TBV (p=.04), BV_{5-10} (p=.007), BV_{5-10}/TBV (p=.008), BV_{10} (p=.01) and BV_{10}/TBV (p=.002) compared to the control subgroup, while BV_5/TBV (p<.001) was significantly less. However, at 2.5-years, there were no significant differences between eosinophilic asthma participants and the healthy control subgroup for any CT vessel measurements. **Table 5-6** shows that, for healthy control participants as compared to participants with eosinophilic asthma, FEV_1 (healthy control subgroup, 107±18%$_{pred}$; eosinophilic asthma subgroup, 75±19%$_{pred}$; p<.001), forced vital capacity (healthy control subgroup, 103±15%$_{pred}$; eosinophilic asthma subgroup, 85±16%$_{pred}$; p<.001), FEV_1 to forced vital capacity ratio (healthy control subgroup, 77±6; eosinophilic asthma, 68±11; p=.001) and residual volume normalized to total lung capacity (RV/TLC) (healthy control subgroup, 39±7; eosinophilic asthma, 45±9; p=.004) were significantly different at Day-0, while only FEV_1 (healthy control subgroup, 107±18%$_{pred}$; eosinophilic asthma, 89±19%$_{pred}$; p=.01) was significantly different at 2.5-years.

Table 5-3. CT vessel measurements in healthy control subgroup and eosinophilic asthma prior to and following 2.5-years anti-IL-5Rα

		Eosinophilic Asthma					
	Healthy	Day-0				2.5-years	
Parameter	Control Subgroup (n=42)	All participants (n=28)	With 2.5-year visit (n=12)	Sig. p	Sig. p*	With 2.5-year visit (n=12)	Sig. p*
TBV mL	251 ± 51	290 ± 85	273 ± 64	**.04**	.4	245 ± 33	1.0
BV_5 mL	149 ± 26	148 ± 36	139 ± 31	.97	.3	140 ± 23	1.0
BV_5/TBV	0.60 ± 0.06	0.52 ± 0.09	0.52 ± 0.08	**<.001**	**.002**	0.57 ± 0.03	.3
$BV_{5\text{-}10}$ mL	34 ± 9	46 ± 17	43 ± 13	**.007**	**.04**	36 ± 7	1.0
$BV_{5\text{-}10}$/TBV	0.13 ± 0.02	0.16 ± 0.03	0.16 ± 0.03	**.008**	**.01**	0.15 ± 0.02	.3
BV_{10} mL	68 ± 22	96 ± 54	91 ± 37	**.01**	**.03**	69 ± 9	.99
BV_{10}/TBV	0.27 ± 0.04	0.32 ± 0.07	0.33 ± 0.06	**.002**	**.004**	0.28 ± 0.03	1.0

Data reported as mean ± standard deviation.

Abbreviations: TBV=total blood volume; BV_5=blood volume of vessels with cross sectional area less than 5 mm^2; $BV_{5\text{-}10}$=blood volume of vessels with cross sectional area between 5 and 10 mm^2; BV_{10}=blood volume of vessels with cross sectional area greater than 10 mm^2; p=Holm-Bonferroni corrected significance value for differences at Day-0 between healthy control subgroup and all eosinophilic asthma participants; p*=Holm-Bonferroni corrected significance value for differences at Day-0 and 2.5-years between healthy control subgroup and eosinophilic asthma participants who completed 2.5-year visit.

5.3.3 Relationships and Multivariable Models

Table 5-7 details associations between Day-0 CT vessel measurements with Day-0 clinical, quality-of-life and imaging measurements. We observed significant relationships between BV_5/TBV with RV/TLC (ρ=-.42, p=.03), VDP (ρ=-.45, p=.02) and mucus-score (ρ=-.39, p=.04), but not with blood eosinophils (ρ=-.34, p=.07). There were also significant relationships between BV_{10}/TBV with VDP (ρ=.44, p=.02), mucus-score (ρ=.51, p=.01) and mucus-count (ρ=.49, p=.01). $BV_{5\text{-}10}$/TBV was related to airway lumen area (ρ=.39, p=.04) and wall thickness (ρ=.43, p=.02). CT vessel measurements were not significantly related to age in either subgroup (**Figure 5-5**). **Figure 5-6** shows the significant relationships for the change in BV_5/TBV at 2.5 years with Day-0 blood eosinophils (ρ=.78, p=.004), FEV_1 (ρ=-.64, p=.03), VDP (ρ=.83, p=.001) and mucus-score (ρ=.91, p<.001).

Multivariable models were generated to explain the change in BV_5/TBV at 2.5-years and these are shown in **Table 5-4**. The significant model (R^2=0.745, p=.002) employed Day-0 mucus-score (p=.046) and VDP (p=.035) as independent predictors of ΔBV_5/TBV at 2.5-years. Two additional models were generated using the backward approach to explain the change in ACQ-6 at 2.5-years, and these are shown in **Table 5-8**. In the first model, which included both MRI and CT measurements, Day-0 VDP (p=.006) and mucus-count significantly predicted the change in ACQ-6 (R^2=0.729, p<.001) while BV_5/TBV, $BV_{5\text{-}10}$/TBV and BV_{10}/TBV did not, similar to previous results.[21] The second model was generated using only CT vessel measurements as predictors, whereby BV_{10}/TBV (p=.001) significantly predicted the change in ACQ-6 (R^2=0.592, p=.001).

Table 5-4. Multivariable Linear Regression Models

Parameter	Unstandardized B	Standardized β	Coefficients *p*
$\Delta BV_5/TBV$			
Constant	-0.021 ± 0.020		.3
VDP	0.004 ± 0.002	0.506	**.04**
Mucus-score	0.008 ± 0.003	0.470	**.046**
Excluded			
Eosinophils	-	-0.161	.6
FEV_1	-	-0.192	.3

Model: R^2=0.745, p=.002

B=unstandardized regression coefficient ± standard error; β=standardized regression coefficient; Δ=change at 2.5-years; VDP=ventilation defect percent; FEV_1=forced expiratory volume in 1 second

Figure 5-4A shows ^{129}Xe MRI static ventilation co-registered with ^{1}H MRI on Day-0 and 2.5-years for a 43-year-old female participant. Ventilation defects on Day-0 were visually resolved at 2.5-years, and the reduction in VDP at 2.5-years from Day-0 was 9% (Day-0 VDP=11%, 2.5-year VDP=2%), which was greater than the minimal clinically important difference.[39] For the same participant, **Figure 5-4B** shows a three-dimensional model of the vascular tree co-registered with ^{129}Xe MRI ventilation at Day-0 and 2.5-years. In Day-0 ventilation defect regions that resolved at 2.5-years, there were more CT-visible small vessels and there was a reduction in the diameter of larger vessels at 2.5-years as compared to Day-0. Quantitatively, whole-lung BV_5/TBV increased (Day-0=0.47, 2.5-years=0.56, Δ=+0.09) while whole-lung BV_{10}/TBV decreased (Day-0=0.37, 2.5-years=0.28, Δ=-0.09) in this participant.

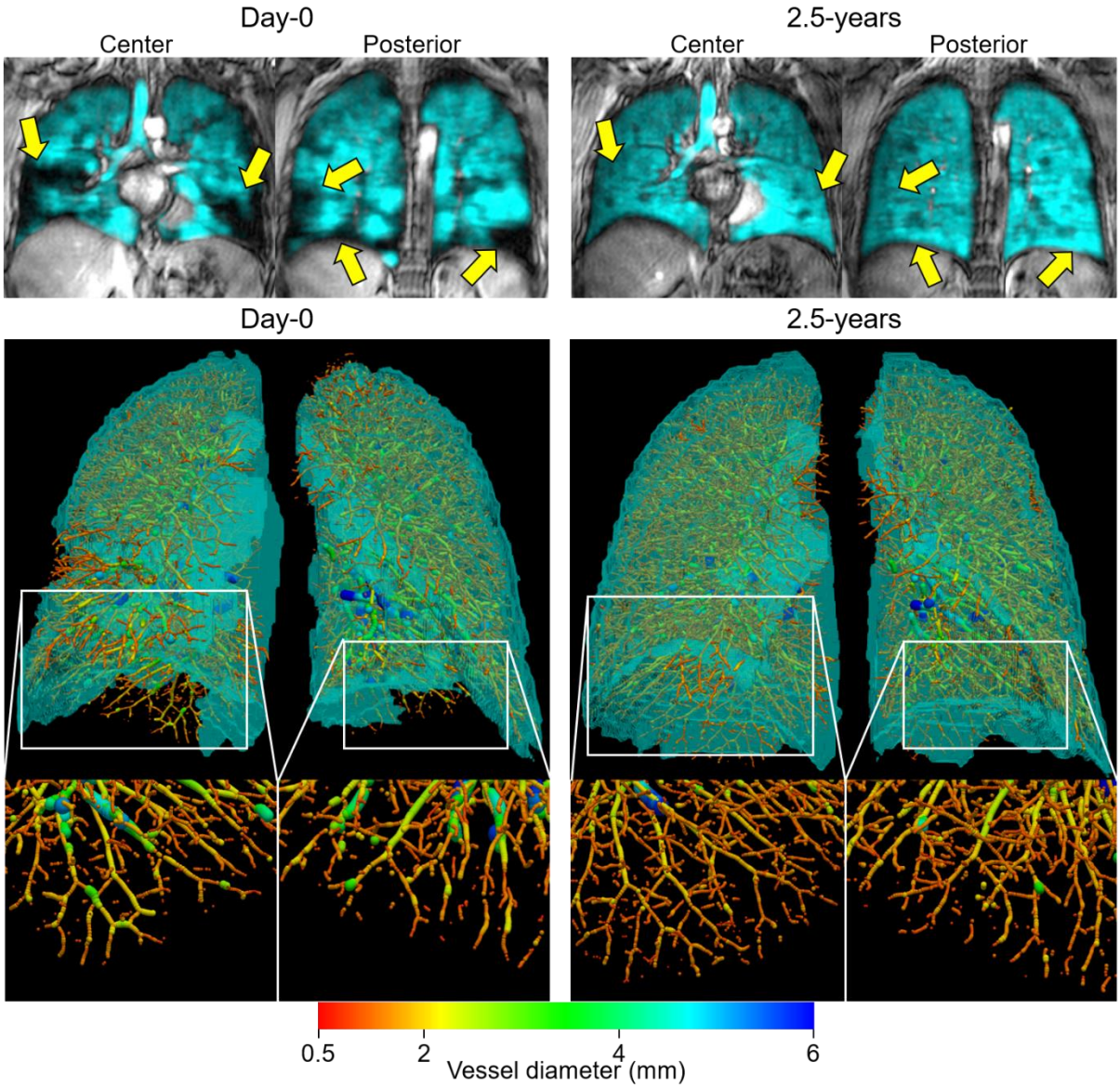

Figure 5-4. Vascular and MRI ventilation improvement at 2.5-years

Participant is a 43-year-old female with visually obvious improvement in MRI ventilation (cyan) at 2.5-years (yellow arrows), and in CT small vessels (red/orange) within Day-0 MRI ventilation defect regions.

A. ^{129}Xe MRI ventilation (cyan) co-registered with anatomic ^{1}H at Day-0 (left) and 2.5-years post-treatment initiation (right). Day-0 VDP=11%, 2.5-years VDP=2%.

B. Three-dimensional representation of Day-0 ^{129}Xe MRI ventilation (cyan) co-registered with CT pulmonary vessel tree at Day-0 (left) and 2.5-years post-treatment initiation (right). Day-0 BV_5/TBV=0.47, 2.5-years BV_5/TBV=0.56.

5.4 Discussion

In a small group of patients with eosinophilic asthma, who were treated for 2.5-years with anti-IL-5Rα and continued to respond to therapy, we observed: 1) increased BV_5/TBV alongside decreased BV_{10}/TBV following treatment, 2) significantly different BV_5/TBV and BV_{10}/TBV compared to healthy, elderly never-smokers at Day-0, but not 2.5-years, 3) significant relationships between BV_5/TBV and plethysmography-measured air-trapping, VDP and CT mucus-score, and, 4) VDP and mucus-score measured prior to anti-IL-5Rα therapy predicted the change in BV_5/TBV after 2.5-years.

Here we show, for the first time, that BV_5/TBV and BV_{10}/TBV change after 2.5-years of anti-IL-5Rα therapy, and that these changes were concomitant with improved airway dysfunction (ventilation defects) and obstruction (mucus-plugs and FEV_1), as well as asthma quality-of-life and disease control. The increase in BV_5/TBV was of similar magnitude to the decrease in BV_{10}/TBV in seven of 12 (58%) participants after 2.5-years of therapy. These findings, alongside stable total blood volume and BV_{5-10}/TBV post-treatment, suggest a redistribution of blood from the larger vessels to the smaller vessels following long-term therapy. In clinical trials, the reduction in exacerbation rates and eosinophil levels observed after 1- and 2-years of anti-IL-5Rα treatment[5,6,40,41] were maintained over 5-years.[42] Because of the relationships between vascular abnormalities, acute exacerbations and eosinophilia,[1] it is possible that the changes in vessel measurements observed here may be maintained over longer treatment periods.

To better understand these vessel changes in relation to normal values, we compared participants with eosinophilic asthma to healthy never-smokers with no previous or current diagnosis of COPD, asthma or unstable cardiovascular disease. In the participants with eosinophilic asthma prior to anti-IL-5Rα therapy initiation, BV_5/TBV was greater, while

BV_{10}/TBV was less compared to the same measurements in the control subgroup. More importantly, these measurements, made 2.5-years later, were not significantly different from the control subgroup. Moreover, BV_5/TBV prior to therapy (0.52±0.09) was less than previously reported values in severe (0.58±0.05) and poorly-controlled (0.58±0.07) asthma.[1] While the lower limit of normal and clinically relevant changes for such CT measurements have not yet been reported, these findings suggest that, following anti-IL-5Rα treatment, CT vessel measurements are migrating towards more normal values.

The associations between pre-treatment BV_5/TBV and clinical and imaging measurements may explain some of the mechanisms driving abnormal BV_5/TBV in eosinophilic asthma. Compression of pulmonary vasculature by hyperinflation or air-trapping may play a role in decreased CT vessel measurements.[10,11] Here we observed a relationship between Day-0 RV/TLC and BV_5/TBV, which, to our knowledge, has not been previously reported in severe asthma.[1] Unfortunately, plethysmography data were not acquired at 2.5-years because of pandemic limitations and we did not perform full inspiratory/expiratory CT. Thus, changes in either plethysmography or CT air-trapping in relation to CT vessel changes could not be evaluated here.

BV_5/TBV was also related to both luminal occlusions and ventilation abnormalities, and in multivariable models, VDP and mucus-score measured prior to therapy independently predicted the change in BV_5/TBV after 2.5-years of anti-IL-5Rα. Decreases in airway luminal occlusions and improved MRI ventilation may be responsible for matched increase in blood volume to regions that were previously unventilated. Together, these results support the previous notion that hypoxic vasoconstriction may mediate the pulmonary vessel changes observed here.[1,11,12] It remains to be determined whether regions of improved ventilation and/or air-trapping spatially correspond with regions of improved BV_5/TBV and/or BV_{10}/TBV.

In asthma, short-term ICS therapy was shown to decrease BV_5/TBV,[8] perhaps by inhibiting angiogenic remodeling.[9] At baseline, all asthma participants in this study were prescribed ICS therapy, and nearly all participants evaluated here (11/12) were still prescribed ICS at 2.5-years. Unfortunately, we did not measure patient-reported ICS use at 2.5-years. However, previous work reported that anti-IL-5Rα treatment resulted in decreased ICS use,[43] so it is possible that the patients studied here were also using less ICS at 2.5-years as compared to Day-0. This potential decrease in ICS use may have influenced the increases in BV_5/TBV observed here, but the effect of lower ICS use on BV_5/TBV values has not been reported in the literature. It remains difficult to ascertain the relationship between ICS use and pulmonary vascular measurements in these patients.

Despite previous work demonstrating an association between asthma control and CT vessel abnormalities,[1] the change in asthma control after 2.5-years in these asthma patients was primarily explained by Day-0 VDP and mucus-score, as previously described.[21] However, when considering only CT vessel measurements, BV_{10}/TBV was independently predictive of the change in ACQ and outperformed BV_5/TBV and BV_{5-10}/TBV. Moreover, at baseline, greater VDP and mucus-score were both associated with greater BV_{10}/TBV. These findings and previous work[1,19,21,44] suggest a complex relationship between ventilation defects, luminal obstruction and vascular abnormalities, all of which may drive poor asthma control. The resolution of both ventilation defects and mucus plugs may have downstream effects on pulmonary vasculature and thus, changes in such measurements may point to possible mechanisms of improved asthma control.

We acknowledge numerous study limitations, including the very small sample size and high drop-out at 2.5-years. Reasons for drop out included pregnancy, new MR contraindication, discontinuation of anti-IL-5Rα treatment, either by lack of clinical response as determined by

their referring respirologist or lack of funded access, and radiation concerns related to CT imaging. The eosinophilic asthma subgroup comprised a greater proportion of females at both time-points (Day-0=68%, 2.5-years=83%) than the healthy control subgroup (52%), although these differences were not significant. While there have been no published reports of sex differences in CT pulmonary vessel measurements, females typically have smaller lung volumes compared to males,[45] which may result in physiologic variability. We also note that at Day-0, the eosinophilic asthma subgroup was significantly younger than the healthy control subgroup; the specific contribution of aging to CT vessel changes should be considered. A previous report in healthy males in China (n=720) suggested that pulmonary vessel volume decreased with increasing age.[46] However, we did not observe significant relationships for age with any CT vessel measurements in either the eosinophilic asthma or the healthy control subgroup (**Section 5.6**).

In summary, in a pilot study of a small group of patients with poorly-controlled eosinophilic asthma, CT small-vessel volume (BV_5/TBV) significantly increased and CT large-vessel volume (BV_{10}/TBV) significantly decreased following 2.5-years anti-IL-5Rα therapy. To our knowledge, this is the first observation of pulmonary vascular changes after long-term biologic therapy in eosinophilic asthma. These novel findings are consistent with blood volume redistribution or normalization from the larger to smaller vessels. Long-term biologic therapy may improve pulmonary vascular abnormalities in poorly-controlled eosinophilic asthma.

5.5 References

1. Ash, S.Y., *et al.* Pruning of the Pulmonary Vasculature in Asthma. The Severe Asthma Research Program (SARP) Cohort. *Am J Respir Crit Care Med* **198**, 39-50 (2018).

2. Mostaco-Guidolin, L.B., Yang, C.X. & Hackett, T.L. Pulmonary Vascular Remodeling Is an Early Feature of Fatal and Nonfatal Asthma. *Am J Respir Cell Mol Biol* **65**, 114-118 (2021).

3. Saetta, M., Di Stefano, A., Rosina, C., Thiene, G. & Fabbri, L.M. Quantitative structural analysis of peripheral airways and arteries in sudden fatal asthma. *Am Rev Respir Dis* **143**, 138-143 (1991).

4. Kolbeck, R., *et al.* MEDI-563, a humanized anti-IL-5 receptor alpha mAb with enhanced antibody-dependent cell-mediated cytotoxicity function. *J Allergy Clin Immunol* **125**, 1344-1353 e1342 (2010).

5. Bleecker, E.R., *et al.* Efficacy and safety of benralizumab for patients with severe asthma uncontrolled with high-dosage inhaled corticosteroids and long-acting beta2-agonists (SIROCCO): a randomised, multicentre, placebo-controlled phase 3 trial. *Lancet* **388**, 2115-2127 (2016).

6. FitzGerald, J.M., *et al.* Benralizumab, an anti-interleukin-5 receptor alpha monoclonal antibody, as add-on treatment for patients with severe, uncontrolled, eosinophilic asthma (CALIMA): a randomised, double-blind, placebo-controlled phase 3 trial. *Lancet* **388**, 2128-2141 (2016).

7. Takayanagi, S., *et al.* Longitudinal changes in structural abnormalities using MDCT in COPD: do the CT measurements of airway wall thickness and small pulmonary vessels change in parallel with emphysematous progression? *Int J Chron Obstruct Pulmon Dis* **12**, 551-560 (2017).

8. Suzuki, T., *et al.* Clinical, physiological, and radiological features of asthma-chronic obstructive pulmonary disease overlap syndrome. *Int J Chron Obstruct Pulmon Dis* **10**, 947-954 (2015).

9. Feltis, B.N., *et al.* Effects of inhaled fluticasone on angiogenesis and vascular endothelial growth factor in asthma. *Thorax* **62**, 314-319 (2007).

10. Harris, R.S., *et al.* Regional pulmonary perfusion, inflation, and ventilation defects in bronchoconstricted patients with asthma. *Am J Respir Crit Care Med* **174**, 245-253 (2006).

11. Kelly, V.J., *et al.* Hypoxic Pulmonary Vasoconstriction Does Not Explain All Regional Perfusion Redistribution in Asthma. *Am J Respir Crit Care Med* **196**, 834-844 (2017).

12. Sverzellati, N. & Silva, M. The Matter of the Lung: Quantification of Vascular Substance in Asthma. *Am J Respir Crit Care Med* **198**, 1-2 (2018).

13. Bousquet, J., *et al.* Eosinophilic inflammation in asthma. *N Engl J Med* **323**, 1033-1039 (1990).

14. Dunican, E.M., *et al.* Mucus plugs in patients with asthma linked to eosinophilia and airflow obstruction. *J Clin Invest* **128**, 997-1009 (2018).

15. Svenningsen, S., *et al.* Sputum Eosinophilia and Magnetic Resonance Imaging Ventilation Heterogeneity in Severe Asthma. *Am J Respir Crit Care Med* **197**, 876-884 (2018).

16. Svenningsen, S., *et al.* What are ventilation defects in asthma? *Thorax* **69**, 63-71 (2014).

17. Svenningsen, S., *et al.* CT and Functional MRI to Evaluate Airway Mucus in Severe Asthma. *Chest* **155**, 1178-1189 (2019).

18. Fain, S.B., *et al.* Evaluation of structure-function relationships in asthma using multidetector CT and hyperpolarized He-3 MRI. *Acad Radiol* **15**, 753-762 (2008).

19. McIntosh, M.J., *et al.* Asthma Control, Airway Mucus, and (129)Xe MRI Ventilation After a Single Benralizumab Dose. *Chest* **162**, 520-533 (2022).

20. Svenningsen, S., Eddy, R.L., Kjarsgaard, M., Parraga, G. & Nair, P. Effects of Anti-T2 Biologic Treatment on Lung Ventilation Evaluated by MRI in Adults With Prednisone-Dependent Asthma. *Chest* **158**, 1350-1360 (2020).

21. McIntosh, M.J., *et al.* CT Mucus Score and (129)Xe MRI Ventilation Defects After 2.5 Years' Anti-IL-5Ralpha in Eosinophilic Asthma. *Chest* (2023).

22. Global Initiative for Asthma (GINA). Global Strategy for Asthma Management and Prevention. (2022).

23. Juniper, E.F., Bousquet, J., Abetz, L., Bateman, E.D. & GOAL Committee. Identifying 'well-controlled' and 'not well-controlled' asthma using the Asthma Control Questionnaire. *Respir Med* **100**, 616-621 (2006).

24. Juniper, E.F., O'Byrne, P.M., Guyatt, G.H., Ferrie, P.J. & King, D.R. Development and validation of a questionnaire to measure asthma control. *Eur Respir J* **14**, 902-907 (1999).

25. Juniper, E.F., Buist, A.S., Cox, F.M., Ferrie, P.J. & King, D.R. Validation of a standardized version of the Asthma Quality of Life Questionnaire. *Chest* **115**, 1265-1270 (1999).

26. Jones, P.W., Quirk, F.H., Baveystock, C.M. & Littlejohns, P. A self-complete measure of health status for chronic airflow limitation. The St. George's Respiratory Questionnaire. *Am Rev Respir Dis* **145**, 1321-1327 (1992).

27. Miller, M.R., *et al.* Standardisation of spirometry. *Eur Respir J* **26**, 319-338 (2005).

28. Wanger, J., *et al.* Standardisation of the measurement of lung volumes. *Eur Respir J* **26**, 511-522 (2005).

29. American Thoracic Society & European Respiratory Society. ATS/ERS recommendations for standardized procedures for the online and offline measurement of exhaled lower respiratory nitric oxide and nasal nitric oxide, 2005. *Am J Respir Crit Care Med* **171**, 912-930 (2005).

30. Kirby, M., *et al.* Longitudinal Computed Tomography and Magnetic Resonance Imaging of COPD: Thoracic Imaging Network of Canada (TINCan) Study Objectives. *Chronic Obstr Pulm Dis* **1**, 200-211 (2014).

31. Estepar, R.S., *et al.* Computational Vascular Morphometry for the Assessment of Pulmonary Vascular Disease Based on Scale-Space Particles. *Proc IEEE Int Symp Biomed Imaging*, 1479-1482 (2012).

32. Kirby, M., *et al.* Total Airway Count on Computed Tomography and the Risk of Chronic Obstructive Pulmonary Disease Progression. Findings from a Population-based Study. *Am J Respir Crit Care Med* **197**, 56-65 (2018).

33. Smith, B.M., *et al.* Comparison of spatially matched airways reveals thinner airway walls in COPD. The Multi-Ethnic Study of Atherosclerosis (MESA) COPD Study and the Subpopulations and Intermediate Outcomes in COPD Study (SPIROMICS). *Thorax* **69**, 987-996 (2014).

34. Svenningsen, S., *et al.* Hyperpolarized (3) He and (129) Xe MRI: differences in asthma before bronchodilation. *J Magn Reson Imaging* **38**, 1521-1530 (2013).

35. Walker, T.G. & Happer, W. Spin-exchange optical pumping of noble-gas nuclei. *Rev Mod Phys* **69**, 629-642 (1997).

36. Kirby, M., *et al.* Hyperpolarized 3He magnetic resonance functional imaging semiautomated segmentation. *Acad Radiol* **19**, 141-152 (2012).

37. Sun, G.W., Shook, T.L. & Kay, G.L. Inappropriate use of bivariable analysis to screen risk factors for use in multivariable analysis. *J Clin Epidemiol* **49**, 907-916 (1996).

38. Juniper, E.F., Svensson, K., Mork, A.C. & Stahl, E. Measurement properties and interpretation of three shortened versions of the asthma control questionnaire. *Respir Med* **99**, 553-558 (2005).

39. McIntosh, M.J., *et al.* (129)Xe MRI Ventilation Defects in Asthma: What is the Upper Limit of Normal and Minimal Clinically Important Difference? *Acad Radiol* (2023).

40. Busse, W.W., *et al.* Long-term safety and efficacy of benralizumab in patients with severe, uncontrolled asthma: 1-year results from the BORA phase 3 extension trial. *Lancet Respir Med* **7**, 46-59 (2019).

41. FitzGerald, J.M., *et al.* Two-Year Integrated Efficacy And Safety Analysis Of Benralizumab In Severe Asthma. *J Asthma Allergy* **12**, 401-413 (2019).

42. Korn, S., *et al.* Integrated Safety and Efficacy Among Patients Receiving Benralizumab for Up to 5 Years. *J Allergy Clin Immunol Pract* **9**, 4381-4392 e4384 (2021).

43. Padilla-Galo, A., *et al.* Real-life experience with benralizumab during 6 months. *BMC Pulm Med* **20**, 184 (2020).

44. Svenningsen, S., Nair, P., Guo, F., McCormack, D.G. & Parraga, G. Is ventilation heterogeneity related to asthma control? *Eur Respir J* **48**, 370-379 (2016).

45. Bellemare, F., Jeanneret, A. & Couture, J. Sex differences in thoracic dimensions and configuration. *Am J Respir Crit Care Med* **168**, 305-312 (2003).

46. Sun, X., *et al.* Quantification of pulmonary vessel volumes on low-dose computed tomography in a healthy male Chinese population: the effects of aging and smoking. *Quant Imaging Med Surg* **12**, 406-416 (2022).

5.6 Supplement

Table 5-5. Day-0 demographic, pulmonary function, imaging and questionnaire differences prior to therapy between those with and those without 2.5-year visit

Parameter	With 2.5-year visit (n=12)	Without 2.5-year visit (n=16)	p
Age years	61 ± 16	57 ± 10	1.0
Female n (%)	10 (83)	9 (57)	.6
BMI kg/m^2	28 ± 4	29 ± 6	.6
Pack-years	4 ± 9	9 ± 15	1.0
Median (min-max)	0 (0-30)	0 (0-45)	-
Duration of Asthma years	21 ± 17	25 ± 24	1.0
Median (min-max)	19 (2-52)	20 (1-63)	-
Pulmonary function			
FEV_1 $\%_{pred}$	74 ± 14	76 ± 22	1.0
FVC $\%_{pred}$	85 ± 11	86 ± 19	.9
FEV_1/FVC	67 ± 10	68 ± 12	1.0
RV/TLC	47 ± 10	45 ± 9	1.0
Inflammatory markers			
Eos cells/μL	630 ± 400	670 ± 370	.8
FeNO ppb	47 ± 32	52 ± 39	1.0
Asthma quality-of-life and control			
ACQ-6	2.0 ± 1.5	2.6 ± 1.7	1.0
AQLQ	4.8 ± 1.2	4.1 ± 1.5	1.0
SGRQ	46 ± 22	52 ± 19	1.0
CT imaging			1.0
TBV mL	273 ± 64	303 ± 98	1.0
BV_5 mL	139 ± 31	155 ± 39	1.0
BV_5/TBV	0.52 ± 0.08	0.53 ± 0.09	1.0
BV_{5-10} mL	43 ± 13	48 ± 19	1.0
BV_{5-10}/TBV	0.16 ± 0.03	0.16 ± 0.03	1.0
BV_{10} mL	91 ± 37	100 ± 64	1.0
BV_{10}/TBV	0.33 ± 0.06	0.32 ± 0.08	1.0
TAC	129 ± 22	149 ± 62	1.0
WA%	70 ± 2	70 ± 2	.9
LA	8.2 ± 3.4	8.1 ± 1.8	1.0
WT	1.2 ± 0.1	1.2 ± 0.1	1.0
WT%	18 ± 1	19 ± 1	1.0
Mucus-score	4 ± 4	3 ± 4	1.0
Mucus-count	6 ± 11	4 ± 6	1.0
MRI			
VDP	12 ± 9	12 ± 12	.9

Data are reported as mean ± standard deviation, unless indicated otherwise. Bolded values indicate significant differences between groups.

Abbreviations: BMI=body mass index; FEV_1=forced expiratory volume in 1 second; $\%_{pred}$=percent of predicted value; FVC=forced vital capacity; RV=residual volume; TLC=total lung capacity; Eos=blood eosinophil count; FeNO=fraction of exhaled nitric oxide; ppb=parts

per billion; ACQ=Asthma Control Questionnaire; AQLQ=Asthma Quality-of-Life Questionnaire; SGRQ=St. George's Respiratory Questionnaire; CT=computed tomography; TBV=total blood volume; BV_5=blood volume of vessels with cross sectional area less than 5 mm^2; BV_{5-10}=blood volume of vessels with cross sectional area between 5 and 10 mm^2; BV_{10}=blood volume of vessels with cross sectional area greater than 10 mm^2; TAC=total airway count; WA=wall area; LA=lumen area; WT=wall thickness; MRI=magnetic resonance imaging; VDP=ventilation defect percent; p=Holm-Bonferroni corrected significance value between groups.

Table 5-6. Demographic and pulmonary function differences between healthy control subgroup and eosinophilic asthma participants at Day-0 and 2.5-years

Parameter	Healthy Control Subgroup (n=42)	Day-0 Eos Asthma (n=28)	Sig. p	2.5-years Eos Asthma (n=12)	Sig. p*
Age years	73 ± 6	59 ± 13	**<.001**	64 ± 16	.08
Female n (%)	22 (52)	19 (68)	.2	10 (83)	.1
BMI kg/m^2	26 ± 4	29 ± 5	**.04**	28 ± 4	.1
Pulmonary function					
FEV_1 $\%_{pred}$	107 ± 18	75 ± 19	**<.001**	89 ± 19	**.01**
FVC $\%_{pred}$	103 ± 15	85 ± 16	**<.001**	97 ± 15	.052
FEV_1/FVC	77 ± 6	68 ± 11	**.001**	72 ± 77	.3
RV/TLC	39 ± 7	45 ± 9	**.004**	ND	-

Data are reported as mean ± standard deviation, unless otherwise indicated. Bolded values indicate significant differences between groups.

Abbreviations: BMI=body mass index; FEV_1=forced expiratory volume in 1 second; $\%_{pred}$=percent of predicted value; FVC=forced vital capacity; RV=residual volume; TLC=total lung capacity; ND=not done; p=Holm-Bonferroni corrected significance value between healthy control subgroup and eosinophilic asthma at Day-0; p*= Holm-Bonferroni corrected significance value between healthy control subgroup and eosinophilic asthma at 2.5-years.

Table 5-7. Associations between Day-0 CT vessel measurements with clinical and imaging measurements

	BV_5/TBV		BV_{5-10}/TBV		BV_{10}/TBV	
Parameter	ρ	p	ρ	p	ρ	p
FEV_1	.29	.1	-.07	.7	-.32	.1
FVC	.22	.3	-.08	.7	-.22	.3
FEV_1/FVC	.20	.3	-.09	.7	-.20	.3
RV/TLC	**-.42**	**.03**	.24	.2	.39	.051
Eos	-.34	.07	.21	.3	.31	.1
FeNO	.08	.7	.08	.7	-.14	.5
ACQ-6	.004	.99	-.03	.9	.12	.5
AQLQ	-.02	.9	.03	.9	-.08	.7
SGRQ	.08	.7	-.06	.8	.04	.8
VDP	**-.45**	**.02**	.22	.2	**.44**	**.02**
TAC	.06	.8	.16	.4	-.10	.6
WA%	-.03	.9	-.05	.8	-.05	.8
LA	-.11	.6	**.39**	**.04**	.05	.8
WT	-.21	.3	**.43**	**.02**	.11	.6
WT%	-.1	.6	.13	.5	-.02	.9
Mucus-score	**-.39**	**.04**	.04	.8	**.51**	**.01**
Mucus-count	-.36	.06	.03	.9	**.49**	**.01**

n=28 for all analyses except for FVC and FEV_1/FVC (n=27), RV/TLC and FeNO (n=26).

Abbreviations: BV_5=blood volume of vessels with cross sectional area less than 5 mm^2; TBV=total blood volume; BV_{5-10}=blood volume of vessels with cross sectional area between 5 and 10 mm^2; BV_{10}=blood volume of vessels with cross sectional area greater than 10 mm^2; FEV_1=forced expiratory volume in 1 second; FVC=forced vital capacity; RV=residual volume; TLC=total lung capacity; Eos=blood eosinophil count; FeNO=fraction of exhaled nitric oxide; ACQ=Asthma Control Questionnaire; AQLQ=Asthma Quality-of-Life Questionnaire; SGRQ=St. George's Respiratory Questionnaire; VDP=ventilation defect percent; TAC=total airway count; WA=wall area; LA=lumen area; WT=wall thickness; ρ=Spearman correlation coefficient; p=correlation significance value.

Table 5-8. Multivariable Linear Regression Models to predict the change in ACQ-6

Parameter	Unstandardized B	Standardized β	Coefficients *p*
ΔACQ-6			
Model 1			
VDP	-0.097 ± 0.029	-0.656	**.006**
Mucus-score	-0.052 ± 0.035	-0.284	.169
Excluded			
BV_5/TBV	-	-0.187	.5
$BV_{5\text{-}10}$/TBV	-	-0.121	.7
BV_{10}/TBV		-0.191	.6
Model 2			
BV_{10}/TBV	-4.877 ± 1.168	-0.770	**.001**
Excluded			
BV_5/TBV	-	0.275	.5
$BV_{5\text{-}10}$/TBV	-	1.101	.2

Model 1: R^2=0.729, p<.001; Model 2: R^2=0.592, p=.001.

B=unstandardized regression coefficient ± standard error; β=standardized regression coefficient; Δ=change at 2.5-years; ACQ=Asthma Control Questionnaire; VDP=ventilation defect percent; BV_5=blood volume of vessels with cross sectional area less than 5 mm^2; TBV=total blood volume; $BV_{5\text{-}10}$=blood volume of vessels with cross sectional area between 5 and 10 mm^2; BV_{10}=blood volume of vessels with cross sectional area greater than 10 mm^2.

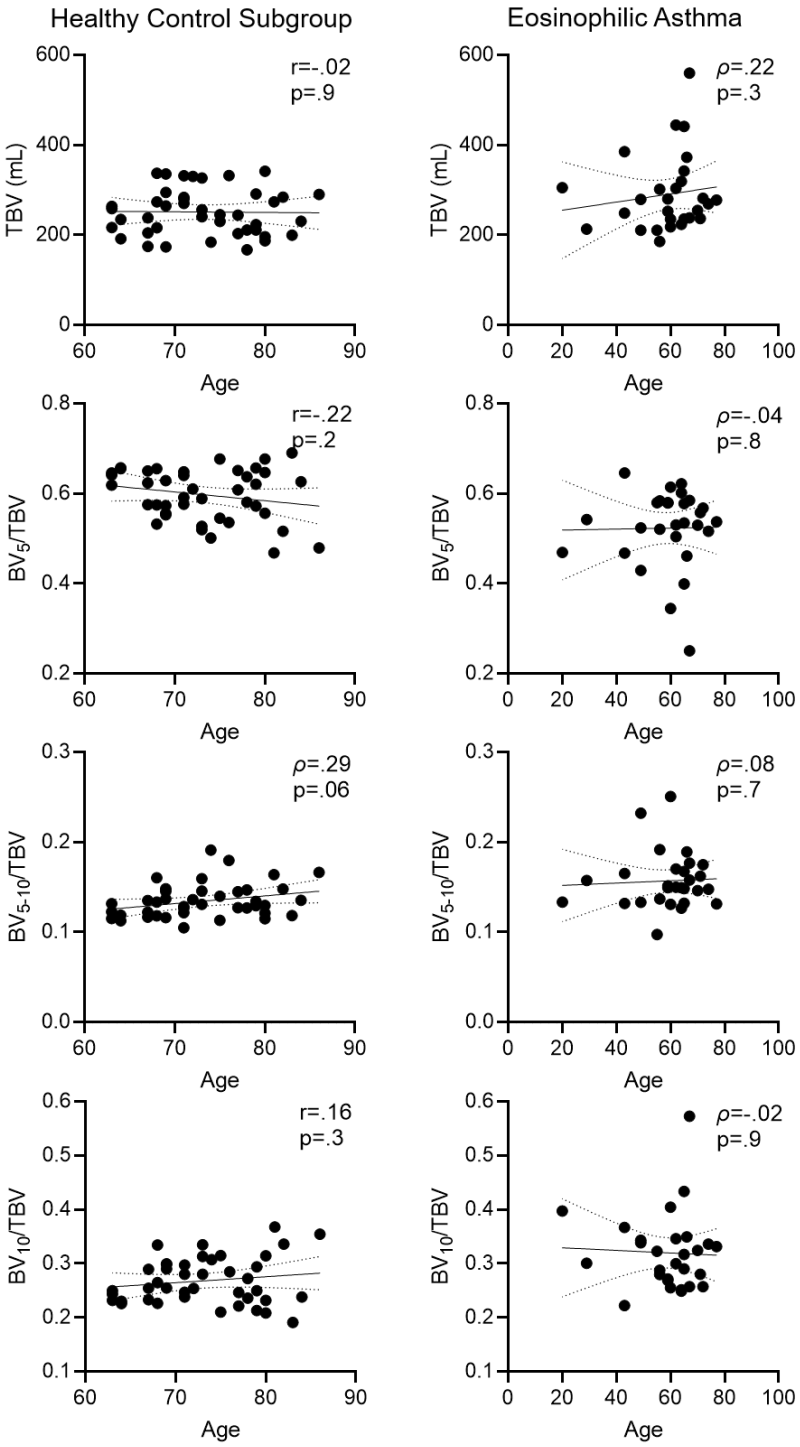

Figure 5-5. Relationships for CT vessel volumes with age
Age not significantly related with CT vessel measurements in healthy control subgroup (left column) or in eosinophilic asthma (right column).

*TBV=total blood volume; BV_5=blood volume of vessels with cross sectional area less than 5 mm^2**;** BV_{5-10}=blood volume of vessels with cross sectional area between 5 and 10 mm^2; BV_{10}=blood volume of vessels with cross sectional area greater than 10 mm*

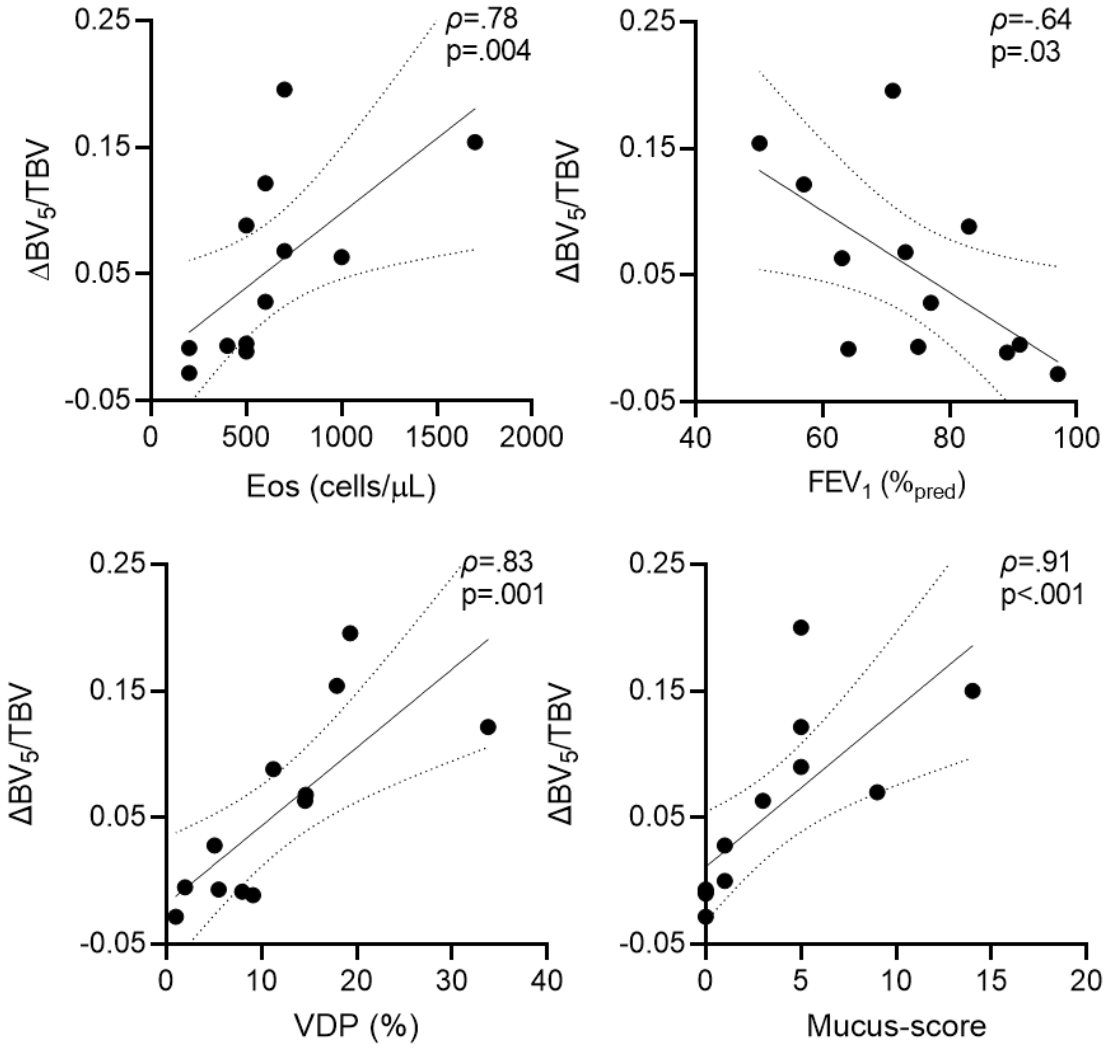

Figure 5-6. Relationships for small vessel volume changes with clinical and imaging measurements
Top left: Linear correlation for the change in BV_5/TBV at 2.5 years with Day-0 blood eosinophils (ρ=.78, p=.004).
Top right: Linear correlation for the change in BV_5/TBV with Day-0 FEV_1 (ρ=-.64, p=.03).
Bottom left: Linear correlation for the change in BV_5/TBV with Day-0 VDP (ρ=.83, p=.001).
Bottom right: Linear correlation for the change in BV_5/TBV with Day-0 mucus-score (ρ=.91, p<.001).

BV_5=blood volume of vessels with cross sectional area less than 5 mm^2; TBV=total blood volume; Eos=blood eosinophil count; FEV_1=forced expiratory volume in one second; $\%_{pred}$=percent of predicted value; VDP=ventilation defect percent.

Chapter 6

6 CONCLUSIONS AND FUTURE DIRECTIONS

The final chapter of this thesis summarizes the motivation and research questions related to this work, as well as the important results and conclusions of ***Chapters 2-5.*** *The specific and general study limitations are discussed. Finally, future work that stems from this thesis is outlined.*

6.1 Overview of Rationale and Research Questions

Despite the use of high-dose inhaled and oral corticosteroids, patients with severe eosinophilic asthma experience frequent exacerbations and poor quality of life alongside an increased risk of mortality,[1-3] which has prompted the development of novel biologic therapies targeting eosinophils.[4] Anti-IL-5Rα therapy results in the direct and rapid depletion of airway and systemic eosinophils,[5] improving airflow limitation and disease control.[6-8] However, the pathophysiological mechanisms acting on the eosinophilic airways as well as the pulmonary vasculature are not well understood, and thus, whether anti-IL-5Rα results in disease-modifying effects is not yet known.

Quantitative pulmonary imaging allows for the non-invasive evaluation of pulmonary structure and function measurements that are associated with characteristic features of asthma. Using hyperpolarized noble gas as an inhaled MRI contrast agent allows for the *in vivo* visualization of the ventilation distribution in asthma. Ventilation abnormalities in asthma are uniquely predictive of asthma control[9] and exacerbations, are related to airway inflammation,[10,11] sputum eosinophilia[10] and mucus plugging,[12,13] and have previously been shown to respond to asthma therapy.[14,15] In combination with computed tomography airway measurements, increasing asthma severity was associated with greater ventilation defect percent (VDP), thicker airway walls and fewer CT-visible airways.[16] Furthermore, CT measured mucus plugs and vascular remodelling[17] in asthma were associated with eosinophilia.[18]

The overarching objective of this thesis was to use hyperpolarized ^{129}Xe MRI and chest CT to evaluate pulmonary function and structure following continuous anti-IL-5Rα therapy and to compare with pre-treatment measurements to better our understanding of the mechanisms responsible for improved asthma control and airflow obstruction.

The overarching hypothesis was that airway function measured via ^{129}Xe MRI VDP and airway and vessel structure measured via chest CT would be significantly improved following anti-IL-5Rα treatment initiation, and that imaging biomarkers would significantly explain improved asthma control.

We showed that, after a single dose of anti-IL-5Rα, ^{129}Xe MRI VDP significantly improved and that these changes were clinically relevant. After 2.5-years of continuous therapy, mucus plugs resolved and significant changes in airway wall thickness, luminal diameter, the total number of CT-visible airways and pulmonary vascular blood volumes were observed. Furthermore, we showed that greater (worse) pre-treatment ^{129}Xe VDP, number of mucus plugs and large vessel blood volume significantly explained ACQ improvements. Together, these results suggest that anti-IL-5Rα does result in disease-modifying effects in patients with poorly-controlled eosinophilic asthma, which will be discussed in more detail in this chapter.

The specific research questions were: 1) What is the minimal clinically important difference and the upper limit of normal of ^{129}Xe MRI VDP measurements in patients with asthma? (**Chapter 2**); 2) Does ^{129}Xe MRI detect airway functional responses to eosinophil depletion after a single benralizumab dose and do airway mucus occlusions mediate this response? (**Chapter 3**); 3) Do early VDP responses to benralizumab measured at 28-days persist and does mucus-plug score improve during a 2.5-year treatment period? (**Chapter 4**); and 4) Do pulmonary vessel volumes measured using computed tomography change after 2.5-years of continuous treatment with anti-IL-5Rα? (**Chapter 5**).

6.2 Summary and Conclusions

In **Chapter 2**, we retrospectively evaluated 55 participants with asthma to calculate the minimal clinically important difference and in 27 healthy participants to determine the upper limit of normal for ^{129}Xe MRI VDP. The mean VDP was 1.6±1.2% for healthy and 13.7±12.9% for asthma participants. In asthma, ACQ-7 and VDP were significantly correlated (r=.37, p=.006; VDP=3.5·ACQ+4.9). Using ACQ-7 as an anchor, the MCID was 1.75% while the mean smallest detectable difference and distribution-based MCID was 2.25%. VDP was correlated with age for healthy participants (ρ=.56, p=.003; VDP=.04·Age-.01). The ULN for all healthy participants was 2.0%. By age tertiles, the ULN was 1.3% ages 18-39-years, 2.5% for 40-59-years and 3.8% for 60-79-years. These results estimate ^{129}Xe MRI VDP MCID, which was similar to the previously calculated ^{3}He MRI VDP MCID (2-4%); the ULN was estimated in healthy participants across a range of ages, both of which provide a way to interpret VDP measurements in clinical investigations.

In **Chapter 3**, we evaluated MRI VDP prior to and 28-days after a single dose of anti-IL-5Rα in 29 patients with eosinophilic asthma and investigated whether baseline mucus influenced ventilation changes. On Day-28 after a single benralizumab dose, there was significantly improved blood eosinophil count, VDP, ACQ-6, AQLQ (all p<.001) and $R_{5\text{-}19Hz}$ (p=.04) in all participants. On Day-28 there was also significantly improved VDP and ACQ-6 in the subgroup of nine participants with ≥5 mucus-plugs but not in the subgroup (n=18) with <5 mucus-plugs. Based on univariate relationships for ΔACQ-6, multivariable models were generated and showed that Day-0 VDP (p<.001) and Day-0 CT mucus score (p<.001) were significant variables for ΔACQ-6 on Day-28, post-benralizumab. These results show that ^{129}Xe ventilation significantly improved in participants with uncontrolled asthma, and suggests that

those patients with significant mucus plugging may have an enhanced ventilation response, after a single dose of benralizumab.

In **Chapter 4**, we investigated the longitudinal effect of 1- and 2.5-years of continuous anti-IL-5Rα therapy in a subset of the eosinophilic asthma patients described in **Chapter 3** using MRI and CT airway measurements. Of 29 participants evaluated at 28-days post-benralizumab, 16 participants returned for follow-up whilst on therapy at 1-year and 13 participants were evaluable whilst on therapy at 2.5-years, post-benralizumab initiation. As compared to 28-days post-benralizumab, ACQ-6 score (2.0±1.4) significantly improved after 1-year (0.5±0.6, p=.02; 95% confidence interval [CI], 0.1-1.1) and 2.5-years (0.5±0.5, p=.03; 95% CI, 0.1-1.1). The mean VDP change at 2.5-years (-4±3%) was greater than the minimal-clinically-important-difference, but not significantly different than VDP measured 28-days post-benralizumab. Mucus-score (3±4) was significantly improved at 2.5-years (1±1, p=.03; 95% CI, 0.3-5.5). In six of eight participants with previous occlusions, mucus-plugs vanished or substantially diminished 2.5-years later. VDP (p<.001) and mucus-score (p<.001) measured at baseline, but not FeNO or FEV_1, independently predicted ACQ-score after 2.5-years. Together, these results suggest that early MRI VDP responses at 28-days post-benralizumab persisted 2.5-years later, alongside significantly improved mucus-score and asthma-control.

In **Chapter 5**, we evaluated long-term, downstream effects of anti-IL-5Rα treatment on pulmonary vascular abnormalities measured using CT in a subgroup of participants described in **Chapters 3-4**. Twelve participants in which CT was acquired at Day-0 remained on anti-IL-5Rα 2.5-years later (10 females, 61±15y). After 2.5-years of therapy, BV_5/TBV (Δ=0.06±0.03, p=.02) and BV_{10}/TBV (Δ=-0.05±0.02, p=.03) were significantly different compared to Day-0. In seven of 12 (58%) participants, large-vessel volume decreases were concomitant with small-vessel volume increases. As compared to 42 control participants (22

females, 73±6y), BV_5/TBV (p<.001) and BV_{10}/TBV (p=.002) were significantly different than in participants with eosinophilic asthma on Day-0 but not after 2.5-years therapy. In multivariable models, Day-0 VDP (p=.04) and mucus-score (p=.046) explained ΔBV_5/TBV after 2.5-years therapy. This is the first observation of pulmonary vascular differences after 2.5-years anti-IL-5Rα therapy, findings consistent with blood volume redistribution from the larger to smaller vessels. Long-term biologic therapy may affect pulmonary vascular abnormalities in patients with eosinophilic asthma.

In summary, we have provided 1) a minimal clinically important difference and upper limit of normal for ^{129}Xe MRI VDP to allow for the clinical interpretation of VDP in asthma; 2) evidence of early airway functional improvements in eosinophilic asthma patients treated with anti-IL-5Rα that may be linked to mucus occlusions; 3) evidence to support the persistence of airway function improvements and the first observation of mucus plug resolution following long-term anti-IL-5Rα in eosinophilic asthma; and 4) evidence of a mechanistic link between the normalization of blood volumes following anti-IL-5Rα initiation and baseline ventilation abnormalities and luminal occlusions.

6.3 Limitations

6.3.1 Study Specific Limitations

Chapter 2: *^{129}Xe MRI Ventilation Defects in Asthma: What is the Upper Limit of Normal and Minimal Clinically Important Difference?*

In the study presented in **Chapter 2**, the ^{129}Xe MRI VDP MCID that we derived was limited by the use of participants with a single chronic airways disease. Moreover, the sample used to calculate MCID was dominated by patients with severe asthma. The ACQ questionnaire score, which specifically measures asthma control,[19] was used as an anchor to calculate the MCID in

these patients, limiting the generalizability of this threshold. We do note that both the anchor- and distribution-based approaches resulted in the same MCID. Nevertheless, it will be important to consider this limitation when evaluating chronic airways and parenchymal diseases other than asthma using ^{129}Xe MRI VDP. It will also be important to evaluate the MCID using other disease specific anchors, such as the SGRQ for COPD.

This study was also limited by the use of a single segmentation and registration algorithm to measure ventilation defects. The semi-automated method used relies on k-means clustering of the ^{129}Xe signal intensity,[20] although other methods include mean-anchored thresholding,[21] linear binning,[22] or fuzzy c-means.[23] In a head-to-head comparison, these quantification methods generated different VDP values per participant, which suggests that each method has may have different precisions. Certainly, automated methods[24] have the potential to further improve precision. We did not perform bias-field correction of the ^{129}Xe signal intensity because the field artefacts at our center are rather infrequent because of the use of rigid coils. This could have a greater impact on VDP measurement using other coils, and some software packages include such a correction.[22,25] Moreover, we used 1.0L inhaled doses for all participants rather than participant-specific volumes,[26] and this could further contribute to differences in measured VDP.[27] Recommendations for standardized ^{129}XeMRI methods[26] will likely focus next on standardizing VDP measurement algorithms and this may help determine generalizable MCID and ULN values.

Chapter 3: *Asthma Control, Airway Mucus and ^{129}Xe MRI Ventilation after a Single Benralizumab Dose*

In the study presented in **Chapter 3**, we were limited by the small sample size which was mainly older and female, particularly at the Day-14 timepoint and in the ≥5 mucus-plugs

subgroup. However, this study and others have demonstrated the high sensitivity of ^{129}Xe MRI and have shown that significant differences may be detected even in small sample sizes. It appears that mucus plug score and ACQ-6 response to benralizumab may be related, so it is worth pointing out that 18/27 (67%) of the participants evaluated showed CT evidence of airway mucous, which is similar to reports from the Severe Asthma Research program cohort (65/96 or 68%).[28]

We also recognize that the lack of follow-up CT and airway lumen sputum sampling also limits our ability to more deeply understand the role of airway mucus, eosinophils and ventilation defects in these patients.

Chapter 4: *CT Mucus Score and ^{129}Xe MRI Ventilation Defects after 2.5-years Anti-IL-5Rα in Eosinophilic Asthma*

In the study presented in **Chapter 4**, we were limited by the small sample size at follow-up. Only those participants who reported a clinical response to benralizumab and continued treatment attended the 1-year and 2.5-year visits, which biases our results to responders only. Previous studies[6-8,29] reported retention rates of 88% and 72% at one- and two-years, respectively, compared to 55% and 45% at 1-year and 2.5-years, respectively, here. The retention rate at the conclusion of the original interventional study (Day-112 prior to the pandemic), was excellent with nearly 100% of participants returning. COVID concerns (1-year visit, n=3) and lack of funded access to benralizumab (1- and 2.5-year visit, n=4) certainly contributed to the relatively weak retention rate at 1- and 2.5-years in this study. Just the same, except for airway WT%, the 1-year and 2.5-year study subgroups were not different from the original group studied at 28-days post-benralizumab. We also acknowledge that at 1- and 2.5-year follow-up there were more females with a shorter asthma history overall, which is

important to consider and may impact the generalizability of these findings. We can certainly learn more about mechanisms by evaluating imaging in non-responders as compared to responders, which will be the focus of future work. We must also acknowledge that follow-up CT was only acquired after 2.5-years of therapy and therefore, earlier mucus-plug measurements could not be made, and this stymies our ability to get more information about the dynamics of mucus-plug formation and dissolution. Previous work[13] suggested that elevated FeNO was indicative of airway mucus and could be used, in combination with CT evidence of luminal plugging, to identify patients who may respond to anti-IL-4/IL-13 therapy. While one might expect that FeNO would normalize once airway mucus cleared, this was not observed here, in agreement with previous investigations,[6,8] perhaps due to measurement variability. Whether anti-IL-4/IL-13 treatment may also clear airway mucus while reducing FeNO levels, remains to be determined.

Chapter 5: *Pulmonary Vascular Differences in Eosinophilic Asthma after 2.5-years Anti-IL-5Rα Treatment*

In the study presented in **Chapter 5** including the very small sample size and high drop-out at 2.5-years. Reasons for drop out included pregnancy, new MR contraindication, discontinuation of anti-IL-5Rα treatment, either by lack of clinical response as determined by their referring respirologist or lack of funded access, and radiation concerns related to CT imaging. The eosinophilic asthma subgroup comprised a greater proportion of females at both time-points (Day-0=68%, 2.5-years=83%) than the healthy control subgroup (52%), although these differences were not significant. While there have been no published reports of sex differences in CT pulmonary vessel measurements, females typically have smaller lung volumes compared to males,[30] which may result in physiologic variability. We also note that at Day-0, the

eosinophilic asthma subgroup was significantly younger than the healthy control subgroup; the specific contribution of aging to CT vessel changes should be considered. A previous report in healthy males in China (n=720) suggested that pulmonary vessel volume decreased with increasing age.[31] However, we did not observe significant relationships for age with any CT vessel measurements in either the eosinophilic asthma or the healthy control subgroup.

6.3.2 General Limitations

A general study limitation of **Chapters 2-5** is the lack of airway inflammatory cell counts, typically measured using induced sputum analysis. Here, we only acquired blood eosinophil counts, and while we assume that airway eosinophilia was also attenuated post-treatment, we cannot be sure without sputum analysis. Furthermore, the addition of sputum analysis may have allowed us to more deeply investigate the characteristics of anti-IL-5Rα responders and those with significant mucus plugging. The composition of luminal occlusions has long been thought to be mucus, however this remains to be proven. IL-4, IL-5 and IL-13 are important cytokines responsible for the manifestation, function and survival of eosinophils.[32,33] These cytokines, along with sputum and blood eosinophils, are associated with high mucus scores in asthma.[13,18] Thus, we cannot be certain that the CT luminal occlusions quantified here were actually composed of mucus.

We also note that CT was acquired at FRC+1L and that inspiratory and expiratory CT images were not acquired, thus we could not evaluate CT air-trapping. However, the mean functional residual capacity +1L volume is 0.8 of mean total lung capacity, which would have minimal impact on the visualization of airway mucus in this study.

Another limitation is that we used a semi-automated segmentation algorithm to quantify ventilation defects. This algorithm employs a k-means clustering approach to determine ventilation defects. This algorithm was optimized for ^{3}He segmentation and not for ^{129}Xe,

which was used in these studies. We know that the ventilation distribution is different in ^{3}He as compared to ^{129}Xe, which may be in part due to differences in the viscosity of these gases. Thus, the use of this algorithm may be over or underestimating the volume of ventilation defects in 129Xe MRI and future work should optimize this algorithm for 129Xe MRI and investigate the effects of this on ventilation defect analysis. In addition to this, VDP is a binary measurement and cannot evaluate the signal intensity differences in ventilation images. Texture analysis tools have been developed as a way to evaluate this signal intensity variation,[34] and have been shown to respond to bronchodilator in asthma.

We also recognize the lack of upper limit normal and minimal clinically important difference in quantitative airway and vessel measurements. Whilst the differences in these measurements following treatment presented in these studies are statistically significant, we are unable to comment on whether these changes are clinically relevant.

6.4 Future Directions

6.4.1 ^{129}Xe MRI Ventilation Texture to Predict Anti-IL-5Rα Response

The regional contributions of airway inflammation,[10] eosinophilia[10] and mucus-plugs,[12,13] which are important pathophysiologic features of poorly-controlled eosinophilic-asthma, to pulmonary ventilation abnormalities may be non-invasively evaluated using hyperpolarized noble gas MRI ventilation-defect-percent (VDP).[35] VDP assumes all ventilated regions contribute equally to global lung function. Signal intensity differences, or ventilation heterogeneity, in MR images may be quantified as texture features extracted from gray-level run-length (GLRLM), co-occurrence (GLCM), size-zone (GLSZM), and dependence (GLDM), and neighbourhood gray-tone difference (NGTDM) matrices.[36] We previously showed that hyperpolarized gas MRI-VDP and MRI GLRLM texture features could help

identify eosinophilic-asthma patients who would experience early, within 28-days of treatment initiation, responses to anti-IL-5Rα biologic therapy.[37] Whether these features, as well as GLCM, GLSZM, GLDM and NGTDM texture features, may allow for late (within 1-year of treatment initiation) response prediction remains unknown.

Here we hypothesized that hyperpolarized gas MRI texture features would significantly predict eosinophilic-asthma patients with early and late responses to anti-IL-5Rα biologic therapy, and that these features would outperform standard clinical measurements.

We retrospectively analyzed 29 participants with poorly-controlled eosinophilic-asthma just prior to anti-IL-5Rα treatment initiation (Day-0) and at Day-28 (n=29) and 1-year (n=16) following continuous anti-IL-5Rα therapy. Anatomic ^{1}H and ^{129}Xe static ventilation MRI were acquired using a 3T scanner as previously described.[38] Anatomic ^{1}H MRI was acquired using a fast-spoiled gradient-recalled-echo (FGRE) sequence (partial-echo acquisition; total acquisition time=8s; repetition-time msec/echo-time msec=4.7/1.2; flip-angle=30°; field-of-view=40×40cm^2; bandwidth=24.4kHz; 128×80 matrix, zero-padded to 128×128; partial-echo percent=62.5%; 15-17×15mm slices). ^{129}Xe MRI was acquired using a three-dimensional FGRE sequence (total acquisition time=14s; repetition-time msec/echo-time msec=6.7/1.5; variable flip-angle; field-of-view=40×40cm^2; bandwidth=15.63kHz; 128×128 matrix (zero-padded); 14×15mm slices). Supine participants were coached to inhale a 1.0L bag (400mL ^{129}Xe + 600mL ^{4}He for ^{129}Xe MRI; 1.0L N_2 for ^{1}H MRI) from the bottom of a tidal breath with acquisition under breath-hold conditions. Participants performed spirometry[39] and fractional exhaled nitric oxide[40] according to guidelines. The Asthma Control Questionnaire (ACQ-6)[41] was self-administered under the supervision of study personnel. Participants were dichotomized as responders if the reduction in ACQ-6 at Day-28 or 1-year compared to Day-0 was greater than the minimal-clinically-important-difference (0.5).[19]

Quantitative MRI analysis was performed on Day-0, post-bronchodilator MR images using a semi-automated segmentation algorithm, as previously described.[20] Texture features were extracted from the 3D-application of GLRLM, GLCM, GLSZM, GLDM and NGTDM using the PyRadiomics platform.[36] Shape-based and first-order (FO) features were also extracted. Feature selection was performed using area-under the receiver-operating-characteristic curve (AUC-ROC) to independently rank extracted texture features, including MRI-VDP, and clinical features. Separate logistic regression models were generated using the highest performing MRI texture features and clinical features. Model performance was evaluated using accuracy, sensitivity and specificity.

Table 1 provides demographic characteristics for all participants and by ACQ-6 response. Twenty participants had Day-28 response, of which nine were persistent, and three participants had 1-year response only. Figure 1 provides ^{129}Xe MRI ventilation images for representative participants with and without ACQ-6 response at Day-0, Day-28 and 1-year.

Using AUC, we identified five unique features for Day-28, three unique features for 1-year and one common feature that were used to identify anti-IL-5Rα response (Table 2, Figure 2). VDP was not identified as a significant feature for either time-point (rank: 10/107 and 13/107, respectively), but did outperform all clinical variables (Day-28: VDP AUC=0.756 versus blood eosinophils AUC=0.703; 1-year: VDP AUC=0.771 versus mucus count AUC=0.646). Table 3 shows logistic regression models for MRI texture features and clinical features for Day-28 and 1-year. The highest accuracy was achieved with MRI texture features for Day-28 (accuracy=76%, sensitivity=67%, specificity=80%) and 1-year response (accuracy=81%, sensitivity=50%, specificity=92%).

Table 6-1. Participant Characteristics

Parameter mean±SD	All participants (n=29)	Day-28 Responders (n=20)	Day-28 Non-Responders (n=9)	p	1-year Responders (n=12)	1-year Non-Responders (n=4)	p*
Age years	59 ± 12	58 ± 14	63 ± 8	.3	59 ± 13	61 ± 13	.9
Female n (%)		14 (70)	6 (67)	.9	10 (83)	3 (75)	.7
BMI kg/m^2	29 ± 5	29 ± 6	31 ± 4	.4	28 ± 4	27 ± 4	.7
Pre-BD FEV_1 $\%_{pred}$	62 ± 18	61 ± 19	65 ± 17	.6	58 ± 20	71 ± 17	.3
Post-BD FEV_1 $\%_{pred}$	74 ± 17	73 ± 19	77 ± 13	.6	70 ± 19	84 ± 11	.2
Post-BD FEV_1/FVC %	68 ± 11	67 ± 11	70 ± 12	.5	66 ± 11	75 ± 12	.2
FeNO ppb	48 ± 35	48 ± 36	49 ± 34	1.0	58 ± 44	38 ± 14	.2
Eos cells/µL	630 ± 380	695 ± 350	490 ± 430	.2	635 ± 440	775 ± 490	.6
VDP %	12 ± 10	14 ± 11	7 ± 6	.1	12 ± 9	6 ± 2	.2
Mucus count	5 ± 9	7 ± 10	2 ± 4	.2	7 ± 11	3 ± 6	.6

Abbreviations: BMI=body mass index; BD=bronchodilator; FEV_1=forced expiratory volume in 1 second; $\%_{pred}$=percent of predicted value; FVC=forced vital capacity; FeNO=fractional exhaled nitric oxide; Eos=blood eosinophils; VDP=ventilation defect percent; p=significance value for differences between Responders and non-responders at Day-28; p=significance value for differences between Responders and non-responders at 1-year.

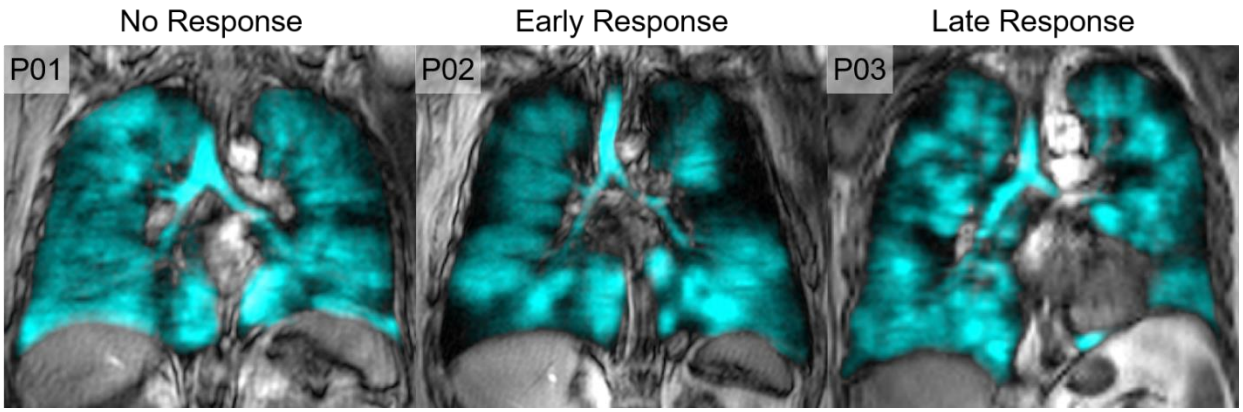

Figure 6-1. Qualitative results of no response, early response and late response
P01: 70 year old male, VDP=6%, GLSZM low gray-level zone emphasis=0.0003
P02: 65 year old female, VDP=18%, GLSZM low gray-level zone emphasis=0.0018
P03: 71 year old female, VDP=8%, GLSZM low gray-level zone emphasis=0.0008

Table 6-2. Top Ranked Features to Identify ACQ-6 Responders

Parameter	AUC
Day-28 Response	
MRI	
GLSZM Small area low gray level emphasis	0.778
GLSZM low gray level zone emphasis	0.772
GLDM small dependence low gray level emphasis	0.772
GLCM cluster shade	0.767
GLRLM Long run low gray level emphasis	0.767
GLRLM Short run low gray level emphasis	0.767
Clinical	
Blood eosinophils	0.703
Mucus count	0.688
Pre-BD FVC	0.596
Post-BD FVC	0.567
Pre-BD FEV_1	0.475
FeNO	0.454
1-year Response	
MRI	
GLCM Correlation	0.854
NGTDM Strength	0.833
FO Skewness	0.813
GLSZM Low gray level zone emphasis	0.813
GLSZM Small area low gray level emphasis	0.813
GLDM small dependence low gray level emphasis	0.813
Clinical	
Mucus count	0.646
FeNO	0.591
BMI	0.563
Pre-BD FVC	0.448
Post-BD FVC	0.438
Blood eosinophils	0.417

Bolded values indicate common features for Day-28 and 1-year responses. AUC=area under the receiver operater curve; GLSZM=gray level size zone matrix; GLDM=gray level dependence matrix; GLCM=gray level co-occurrence matrix; GLRLM=gray level run length matrix; BD=bronchodilator; FVC=forced vital capacity; FEV_1=forced expiratory volume in 1 second; FeNO=fractional exhaled nitric oxide; BMI=body mass index; NGTDM=neighbouring gray tone difference matrix; FO=first order.

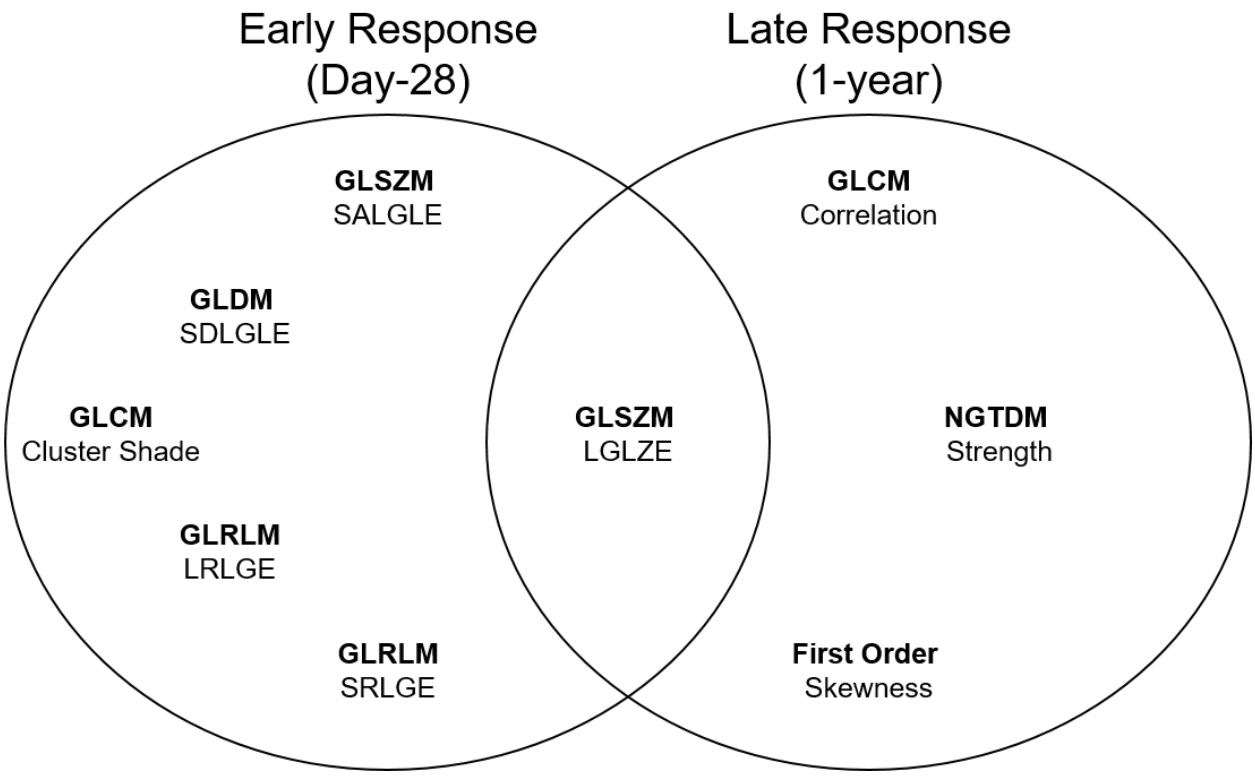

Figure 6-2. Top ranked predictors of early and late response to anti-IL-5Rα
GLSZM=gray level size zone matrix; GLDM=gray level dependence matrix; GLCM=gray level co-occurrence matrix; GLRLM=gray level run length matrix; NGTDM=neighbouring gray tone difference matrix; SALGLE=Small area low gray level emphasis; LGLZE=low gray level zone emphasis; SDLGLE=small dependence low gray level emphasis; LRLGE=Long run low gray level emphasis; SRLGE=Short run low gray level emphasis

Table 6-3. Logistic Regression Models

Parameter	Accuracy (%)	Sensitivity (%)	Specificity (%)
Day-28 Response			
MRI-based	75.9	66.7	80.0
Clinical-based	72.0	33.3	93.8
1-year Response			
MRI-based	81.3	50.0	91.7
Clinical*	73.3	0.0	100.0

Day-28 Models: MRI-based features= GLSZM Small area low gray level emphasis, GLSZM low gray level zone emphasis, GLDM small dependence low gray level emphasis, GLCM cluster shade, GLRLM Long run low gray level emphasis, GLRLM Short run low gray level emphasis; Clinical features= Blood eosinophils, mucus count, pre-BD FVC, pre-BD FEV_1, FeNO

1-year Models: MRI-based features= GLCM Correlation, NGTDM Strength, GLSZM low gray level zone emphasis, FO Skewness; Clinical features= Mucus count, FeNO, BMI, Pre-BD FVC

*=indicates classifier that predicted all participants as responders; GLSZM=gray level size zone matrix; GLDM=gray level dependence matrix; GLCM=gray level co-occurrence matrix; GLRLM=gray level run length matrix; FO=first order; BD=bronchodilator; FVC=forced vital capacity; FEV_1=forced expiratory volume in 1 second; FeNO=fractional exhaled nitric oxide; NGTDM=neighbouring gray tone difference matrix

There are currently six biologic therapies for the treatment of eosinophilic-asthma, however it is difficult to predict which patients may benefit prior to therapy initiation. Using preliminary data in a small group of 17 eosinophilic-asthma patients,[37] we previously showed that MRI texture features uniquely predicted patients who would experience early, within 28-days of treatment initiation, response to anti-IL-5Rα biologic therapy. Here, we developed highly accurate logistic regression models, using pre-treatment MRI texture features, to identify patients who experienced early and late responses to anti-IL-5Rα biologic therapy, and these models outperformed models developed with clinical features. High performing features included GLSZM small-area-low-gray-level-emphasis, GLSZM low-gray-level-zone-emphasis, GLDM small-dependence-low-gray-level-emphasis, GLCM cluster-shade, GLRLM short-run-low-gray-level-emphasis and FO skewness, which describe fine ventilation heterogeneity, more commonly referred to as "patchiness". In contrast, high performing features including GLCM correlation, NGTDM strength and GLRLM long-run-low-gray-level-emphasis describe large regions of similar signal intensities, with the latter specifically referring to regions with low signal intensity. Interestingly, GLSZM low gray-level zone emphasis predicted response irrespective of follow-up time. Twenty features for Day-28 response and 40 features for 1-year response outperformed all clinical features, further supporting the prognostic value of MRI texture features for predicting anti-IL-5Rα response.

Pre-treatment hyperpolarized ^{129}Xe MRI texture features identified eosinophilic-asthma patients who responded to anti-IL-5Rα biologic therapy within 28-days and 1-year of treatment initiation. Considering the high-cost (~$30,000 annually) of therapy, the increasing number of biologic therapy options and the inability to predict patients who will respond highlights the clinical relevance and importance of this work.

6.5 Significance and Impact

Despite the use of maximal guidelines based therapies, patients with severe eosinophilic asthma experience frequent exacerbations, poor quality of life and poor disease control alongside an increased risk of mortality.[1-3] This has prompted the development of monoclonal antibody therapies that specifically target eosinophilia.[179,181] Anti-IL-5Rα therapy rapidly depletes of airway and systemic eosinophils,[5] improving airflow limitation and disease control, and reduces exacerbations in patients with eosinophilic asthma.[6-8] Disease-modifying therapies[42] such as monoclonal antibodies[43,44] may help achieve a symptom-free state or asthma remission.[14,1545] However, it is difficult to determine whether anti-IL-5Rα results in disease-modifying effects due to the lack of sensitive pulmonary function measurements that inform on eosinophilic asthma pathology, including the eosinophilic airways and pulmonary vasculature.

In this thesis, I used ^{129}Xe MRI and chest CT to investigate whether eosinophil depletion via anti-IL-5Rα results in disease-modifying effects in patients with eosinophilic asthma. I have provided valuable insight about changes in airway structure, the resolution or abrogation of luminal occlusions and the subsequent improvements in airway function measured via ^{129}Xe MRI, as well as the redistribution and normalization of pulmonary blood volumes. I have demonstrated that ^{129}Xe MRI and CT provide valuable insight into short- and long-term treatment influence of eosinophilic depletion following anti-IL-5Rα therapy in patients with poorly controlled eosinophilic asthma. These important results suggest that anti-IL-5Rα results in disease-modifying in patients with eosinophilic asthma and that this therapy may help achieve asthma remission in some patients.

6.6 References

1. Chung, K.F., *et al.* International ERS/ATS guidelines on definition, evaluation and treatment of severe asthma. *Eur Respir J* **43**, 343-373 (2014).

2. Wenzel, S.E. Asthma: defining of the persistent adult phenotypes. *Lancet* **368**, 804-813 (2006).

3. Wenzel, S.E. Asthma phenotypes: the evolution from clinical to molecular approaches. *Nature medicine* **18**, 716-725 (2012).

4. Patel, S.S., Casale, T.B. & Cardet, J.C. Biological therapies for eosinophilic asthma. *Expert opinion on biological therapy* **18**, 747-754 (2018).

5. Kolbeck, R., *et al.* MEDI-563, a humanized anti-IL-5 receptor alpha mAb with enhanced antibody-dependent cell-mediated cytotoxicity function. *J Allergy Clin Immunol* **125**, 1344-1353 e1342 (2010).

6. Bleecker, E.R., *et al.* Efficacy and safety of benralizumab for patients with severe asthma uncontrolled with high-dosage inhaled corticosteroids and long-acting beta2-agonists (SIROCCO): a randomised, multicentre, placebo-controlled phase 3 trial. *Lancet* **388**, 2115-2127 (2016).

7. FitzGerald, J.M., *et al.* Two-Year Integrated Efficacy And Safety Analysis Of Benralizumab In Severe Asthma. *J Asthma Allergy* **12**, 401-413 (2019).

8. FitzGerald, J.M., *et al.* Benralizumab, an anti-interleukin-5 receptor alpha monoclonal antibody, as add-on treatment for patients with severe, uncontrolled, eosinophilic asthma (CALIMA): a randomised, double-blind, placebo-controlled phase 3 trial. *Lancet* **388**, 2128-2141 (2016).

9. Svenningsen, S., Nair, P., Guo, F., McCormack, D.G. & Parraga, G. Is ventilation heterogeneity related to asthma control? *Eur Respir J* **48**, 370-379 (2016).

10. Svenningsen, S., *et al.* Sputum Eosinophilia and Magnetic Resonance Imaging Ventilation Heterogeneity in Severe Asthma. *Am J Respir Crit Care Med* **197**, 876-884 (2018).

11. Svenningsen, S., *et al.* What are ventilation defects in asthma? *Thorax* **69**, 63-71 (2014).

12. Mummy, D.G., *et al.* Mucus Plugs in Asthma at CT Associated with Regional Ventilation Defects at Helium 3 MRI. *Radiology*, 204616 (2021).

13. Svenningsen, S., *et al.* CT and Functional MRI to Evaluate Airway Mucus in Severe Asthma. *Chest* **155**, 1178-1189 (2019).

14. Svenningsen, S., Eddy, R.L., Kjarsgaard, M., Parraga, G. & Nair, P. Effects of Anti-T2 Biologic Treatment on Lung Ventilation Evaluated by MRI in Adults With Prednisone-Dependent Asthma. *Chest* **158**, 1350-1360 (2020).

15. Thomen, R.P., *et al.* Regional ventilation changes in severe asthma after bronchial thermoplasty with (3)He MR imaging and CT. *Radiology* **274**, 250-259 (2015).

16. Eddy, R.L., *et al.* Is Computed Tomography Airway Count Related to Asthma Severity and Airway Structure and Function? *Am J Respir Crit Care Med* **201**, 923-933 (2020).

17. Ash, S.Y., *et al.* Pruning of the Pulmonary Vasculature in Asthma. The Severe Asthma Research Program (SARP) Cohort. *Am J Respir Crit Care Med* **198**, 39-50 (2018).

18. Dunican, E.M., *et al.* Mucus plugs in patients with asthma linked to eosinophilia and airflow obstruction. *J Clin Invest* **128**, 997-1009 (2018).

19. Juniper, E.F., Svensson, K., Mork, A.C. & Stahl, E. Measurement properties and interpretation of three shortened versions of the asthma control questionnaire. *Respir Med* **99**, 553-558 (2005).

20. Kirby, M., *et al.* Hyperpolarized 3He magnetic resonance functional imaging semiautomated segmentation. *Academic radiology* **19**, 141-152 (2012).

21. Thomen, R.P., *et al.* Hyperpolarized (129)Xe for investigation of mild cystic fibrosis lung disease in pediatric patients. *J Cyst Fibros* **16**, 275-282 (2017).

22. He, M., *et al.* Extending semiautomatic ventilation defect analysis for hyperpolarized (129)Xe ventilation MRI. *Acad Radiol* **21**, 1530-1541 (2014).

23. Hughes, P.J.C., *et al.* Spatial fuzzy c-means thresholding for semiautomated calculation of percentage lung ventilated volume from hyperpolarized gas and (1) H MRI. *J Magn Reson Imaging* **47**, 640-646 (2018).

24. Astley, J.R., *et al.* Large-scale investigation of deep learning approaches for ventilated lung segmentation using multi-nuclear hyperpolarized gas MRI. *Sci Rep* **12**, 10566 (2022).

25. Lu, J., *et al.* Bias field correction in hyperpolarized (129) Xe ventilation MRI using templates derived by RF-depolarization mapping. *Magn Reson Med* **88**, 802-816 (2022).

26. Niedbalski, P.J., *et al.* Protocols for multi-site trials using hyperpolarized (129) Xe MRI for imaging of ventilation, alveolar-airspace size, and gas exchange: A position paper from the (129) Xe MRI clinical trials consortium. *Magn Reson Med* **86**, 2966-2986 (2021).

27. Hughes, P.J.C., *et al.* Assessment of the influence of lung inflation state on the quantitative parameters derived from hyperpolarized gas lung ventilation MRI in healthy volunteers. *J Appl Physiol (1985)* **126**, 183-192 (2019).

28. Dunican, E.M., *et al.* Mucus plugs in patients with asthma linked to eosinophilia and airflow obstruction. *J Clin Invest* **128**, 997-1009 (2018).

29. Busse, W.W., *et al.* Long-term safety and efficacy of benralizumab in patients with severe, uncontrolled asthma: 1-year results from the BORA phase 3 extension trial. *Lancet Respir Med* **7**, 46-59 (2019).

30. Bellemare, F., Jeanneret, A. & Couture, J. Sex differences in thoracic dimensions and configuration. *Am J Respir Crit Care Med* **168**, 305-312 (2003).

31. Sun, X., *et al.* Quantification of pulmonary vessel volumes on low-dose computed tomography in a healthy male Chinese population: the effects of aging and smoking. *Quant Imaging Med Surg* **12**, 406-416 (2022).

32. Pope, S.M., *et al.* IL-13 induces eosinophil recruitment into the lung by an IL-5- and eotaxin-dependent mechanism. *J Allergy Clin Immunol* **108**, 594-601 (2001).

33. Rankin, S.M., Conroy, D.M. & Williams, T.J. Eotaxin and eosinophil recruitment: implications for human disease. *Mol Med Today* **6**, 20-27 (2000).

34. Zha, N., *et al.* Second-order Texture Measurements of (3)He Ventilation MRI: Proof-of-concept Evaluation of Asthma Bronchodilator Response. *Acad Radiol* **23**, 176-185 (2016).

35. Kirby, M., Wheatley, A., McCormack, D.G. & Parraga, G. Development and application of methods to quantify spatial and temporal hyperpolarized He-3 MRI ventilation dynamics: Preliminary results in chronic obstructive pulmonary disease. *Proc Spie* **7626**, 762605 (2010).

36. van Griethuysen, J.J.M., *et al.* Computational Radiomics System to Decode the Radiographic Phenotype. *Cancer Res* **77**, e104-e107 (2017).

37. McIntosh, M.J.E., R.L.; Knipping, D.; Lindenmaier, T.; McCormack, D.G.; Licskai, C.; Yamashita, C.; Parraga, G. Supervised shallow learning of 129Xe MRI texture features to predict response to Anti-IL-5 biologic therapy in severe asthma. *ISMRM* (2020).

38. Svenningsen, S., *et al.* Hyperpolarized (3) He and (129) Xe MRI: differences in asthma before bronchodilation. *J Magn Reson Imaging* **38**, 1521-1530 (2013).

39. Miller, M.R., *et al.* Standardisation of spirometry. *Eur Respir J* **26**, 319-338 (2005).

40. Dweik, R.A., *et al.* An official ATS clinical practice guideline: interpretation of exhaled nitric oxide levels (FENO) for clinical applications. *Am J Respir Crit Care Med* **184**, 602-615 (2011).

41. Juniper, E.F., O'Byrne, P.M., Guyatt, G.H., Ferrie, P.J. & King, D.R. Development and validation of a questionnaire to measure asthma control. *Eur Respir J* **14**, 902-907 (1999).

42. Busse, W.W., Melen, E. & Menzies-Gow, A.N. Holy Grail: the journey towards disease modification in asthma. *Eur Respir Rev* **31**(2022).

43. Arnold, S., *et al.* Discontinuation of biologic DMARDs in a real-world population of patients with rheumatoid arthritis in remission: outcome and risk factors. *Rheumatology (Oxford)* **61**, 131-138 (2021).

44. Schlager, L., Loiskandl, M., Aletaha, D. & Radner, H. Predictors of successful discontinuation of biologic and targeted synthetic DMARDs in patients with rheumatoid arthritis in remission or low disease activity: a systematic literature review. *Rheumatology (Oxford)* **59**, 324-334 (2020).

45. Menzies-Gow, A., *et al.* An expert consensus framework for asthma remission as a treatment goal. *J Allergy Clin Immunol* **145**, 757-765 (2020).

Appendix A – Permission for Reproduction of Scientific Articles

Chapters 2-4 were published under Creatives Commons license BY-NC-ND 4.0. As author of the original articles, I do not require permission to reproduce these beyond citing the original source.

Figure 1-5: Permission to reproduce

RE: Request to Reproduce Figure in Thesis

European Respiratory Society Permissions
Wed 6/14/2023 3:35 AM
To:Marrissa McIntosh

Dear Marissa,

Thank you for your permission enquiry.

Please be aware that the ERS does make provisions for authors to reuse their own content in certain ways, as outlined in https://www.ersjournals.com/reuse/permissions

European Respiratory Society hereby grants you permission to reproduce the material as requested for your dissertation/thesis (print and digital) and full acknowledgement must be given.

Citation:	Extracellular matrix components and regulators in the airway smooth muscle in asthma B. B. Araujo, M. Dolhnikoff, L. F. F. Silva, J. Elliot, J. H. N. Lindeman, D. S. Ferreira, A. Mulder, H. A. P. Gomes, S. M. Fernezlian, A. James, T. Mauad European Respiratory Journal Jul 2008, 32 (1) 61-69; **DOI:** 10.1183/09031936.00147807
Material:	Figure 2
Acknowledgement Wording:	Reproduced with permission of the © ERS 2023: European Respiratory Journal Jul 2008, 32 (1) 61-69; **DOI:** 10.1183/09031936.00147807

Copyright remains with © ERS 2023. These publications are copyrighted material and must not be copied, reproduced, transferred, distributed, leased, licensed, placed in a storage retrieval system or publicly performed or used in any way except as specifically permitted in writing by the publishers (European Respiratory Society), as allowed under the terms and conditions of which it was purchased or as strictly permitted by applicable copyright law. Reproduction of this is material is confined to the purpose and/or media for which permission is hereby given. Altering/Modifying Material: This is not permitted, however figures and illustrations maybe altered/adapted minimally to serve your work. Please be aware that the permission fee for the requested use of this material is waived in this instance but please be advised that your future requests for materials may attract a fee. This agreement is personal to you and may not be sublicense, assigned or transferred by you to any other person without our written permission. Any unauthorised distribution or use of this text may be a direct infringement of the publisher's rights and those responsible may be liable in law accordingly

"Green" open access and author archiving (where applicable)

Authors who do not wish to pay for their article to be published open access in the *ERJ* will still have their manuscripts made free to access via the *ERJ* online archive following the journal's 18-month embargo period. Authors also have licence to make their manuscripts available in an institutional (or similar) repository for public archiving, 12 months after final publication, provided the following requirements are met:

1) The final, peer-reviewed, author-submitted version that was accepted for publication is used (before copy-editing and publication).

2) A permanent link is provided to the version of the article published in the ERJ, through the dx.doi.org platform. For example, if your manuscript has the DOI 10.1183/13993003.06543-2018, then the link you provide must be https://doi.org/10.1183/13993003.06543-2018

3) The repository on which the manuscript is deposited is not used for systematic distribution or commercial sales purposes.

4) The following required archiving statement appears on the title page of the archived manuscript: "This is an author-submitted, peer-reviewed version of a manuscript that has been accepted for publication in the European Respiratory Journal, prior to copy-editing, formatting and typesetting. This version of the manuscript may not be duplicated or reproduced without prior permission from the copyright owner, the European Respiratory Society. The publisher is not responsible or liable for any errors or omissions in this version of the manuscript or in any version derived from it by any other parties. The final, copy-edited, published article, which is the version of record, is available without a subscription 18 months after the date of issue publication."

For manuscripts with Europe PMC funding (https://europepmc.org/Funders/), the author retains the right to provide a copy of the final, peer-reviewed author-supplied manuscript (before copy-editing and publication) for public archiving in compliance with the requirements of the funder, i.e. 6 months after final publication for authors with funding from Europe PubMed Central Funders Group members.

For articles with Coalition S funding (https://www.coalition-s.org/organisations/), the author retains the right to archive the peer-reviewed author-submitted manuscript (before copy-editing and publication) under a CC-BY licence without embargo.

If your research body or employer mandates an access or archiving model that is not addressed above, please contact

Kind regards,

Kay

ERS

ERS EUROPEAN RESPIRATORY SOCIETY INTERNATIONAL CONGRESS 2023 MILAN Italy, 9-13 September

RE: Request Permission to Reprint Figure for Thesis

ATS Permission Requests
Wed 6/14/2023 9:38 AM
To:Marrissa McIntosh

Dear Marrissa,

Thank you for your request. Because this is for thesis use, permission is granted at no charge. Please complete the below and use it beneath the material. Thank you.

Reprinted with permission of the American Thoracic Society.
Copyright © 2023 American Thoracic Society. All rights reserved.
Cite: Author(s)/Year/Title/Journal title/Volume/Pages.
The American Journal of Respiratory Cell and Molecular Biology is an official journal of the American Thoracic Society.

Best regards,

Libby Fellbaum
Production Coordinator, Journals

American Thoracic Society

From: Marrissa McIntosh
Sent: Tuesday, June 13, 2023 8:33 PM
To: ATS Permission Requests
Subject: Request Permission to Reprint Figure for Thesis

Good evening,

I am writing to request permission to reproduce Figure 1A-D from the following article in my PhD thesis:

Mostaco-Guidolin, L.B., Yang, C.X. & Hackett, T.L. Pulmonary Vascular Remodeling Is an Early Feature of Fatal and Nonfatal Asthma. Am J Respir Cell Mol Biol 65, 114-118 (2021).

This thesis, entitled Eosinophilic Asthma Response to Therapy: ^{129}Xe Magnetic Resonance Imaging and Computed Tomography, will be published electronically shortly after July 27 2023 at https://ir.lib.uwo.ca/etd/.

Kind regards,
Marrissa McIntosh

Figure 1-10: Permission to reproduce

JOHN WILEY AND SONS LICENSE
TERMS AND CONDITIONS

Jun 14, 2023

This Agreement between Marrissa McIntosh ("You") and John Wiley and Sons ("John Wiley and Sons") consists of your license details and the terms and conditions provided by John Wiley and Sons and Copyright Clearance Center.

License Number	5567880153339
License date	Jun 14, 2023
Licensed Content Publisher	John Wiley and Sons
Licensed Content Publication	Respirology
Licensed Content Title	Pulmonary functional MRI: Detecting the structure–function pathologies that drive asthma symptoms and quality of life
Licensed Content Author	Harkiran K. Kooner, Marrissa J. McIntosh, Vedanth Desaigoudar, et al
Licensed Content Date	Jan 10, 2022
Licensed Content Volume	27
Licensed Content Issue	2
Licensed Content Pages	20
Type of use	Dissertation/Thesis

Requestor type	Author of this Wiley article
Format	Electronic
Portion	Figure/table
Number of figures/tables	1
Will you be translating?	No
Title	Eosinophilic Asthma Response to Therapy: 129Xe Magnetic Resonance Imaging and Computed Tomography
Institution name	Western University
Expected presentation date	Jul 2023
Portions	Figure 6
	Marrissa McIntosh
Requestor Location	London, ON N5X0G9 Canada Attn: Western University
Publisher Tax ID	EU826007151
Total	0.00 USD
Terms and Conditions	

TERMS AND CONDITIONS

This copyrighted material is owned by or exclusively licensed to John Wiley & Sons, Inc. or one of its group companies (each a"Wiley Company") or handled on behalf of a society with which a Wiley Company has exclusive publishing rights in relation to a particular work

Appendix B – Health Science Research Ethics Board Approval Notices

Western Research

Date: 18 January 2019

To: Dr. Grace Parraga

Project ID: 113224

Study Title: A Mechanistic Pilot Open-label Study to Evaluate the Effect of Benralizumab on Airway Function and Inflammation in Patients with Severe, Poorly-controlled Eosinophilic Asthma Using Inhaled Hyperpolarized 129Xe MRI (AERFLO)

Application Type: HSREB Initial Application

Review Type: Full Board

Meeting Date: 15/Jan/2019

Date Approval Issued: 18/Jan/2019

REB Approval Expiry Date: 18/Jan/2020

Dear Dr. Grace Parraga

The Western University Health Science Research Ethics Board (HSREB) has reviewed and approved the above mentioned study as described in the WREM application form, as of the HSREB Initial Approval Date noted above. This research study is to be conducted by the investigator noted above. All other required institutional approvals must also be obtained prior to the conduct of the study.

Documents Approved:

Document Name	Document Type	Document Date	Document Version
ACQ - Asthma Control Questionnaire	Paper Survey		6
AQLQ - Asthma Quality of Life Questionnaire	Paper Survey		
CGIS	Paper Survey		
Febrile Respiratory Illness	Paper Survey	31/Aug/2018	1
Flyer V2 December 20 2018 with tabs	Recruitment Materials	20/Dec/2018	2
Flyer V2 December 20 2018 without tabs	Recruitment Materials	20/Dec/2018	2
MRI Screening Form	Paper Survey		
PGIC - Patient Global Impression of Change	Paper Survey		
ROB0042 AZ Letter of Information v3 Jan 17 2019	Written Consent/Assent	17/Jan/2019	3
Robarts Sponsored Protocol v14 Jan 4 2019	Protocol	04/Jan/2019	14
SGRQ - St. George's Respiratory Questionnaire	Paper Survey		
Telephone Script Nov 15 2018	Other Data Collection Instruments	15/Nov/2018	1

Documents Acknowledged:

Document Name	Document Type	Document Date	Document Version
ROB0042 Health Canada No Objection Letter	NOL/NOA	08/Jan/2019	Control No. 222942
ROB0042 Polarean Partners IB Nov 21 2018	Investigator Brochure	21/Nov/2018	1
Robarts IB 129Xe v7 Nov 2 2018	Investigator Brochure	02/Nov/2018	7

No deviations from, or changes to, the protocol or WREM application should be initiated without prior written approval of an appropriate amendment from Western HSREB , except when necessary to eliminate immediate hazard(s) to study participants or when the change(s) involves only administrative or logistical aspects of the trial.

REB members involved in the research project do not participate in the review, discussion or decision.

The Western University HSREB operates in compliance with, and is constituted in accordance with, the requirements of the TriCouncil Policy Statement: Ethical Conduct for Research Involving Humans (TCPS 2); the International Conference on Harmonisation Good Clinical Practice Consolidated Guideline (ICH GCP); Part C, Division 5 of the Food and Drug Regulations; Part 4 of the Natural Health Products Regulations; Part 3 of the Medical Devices Regulations and the provisions of the Ontario Personal Health Information Protection Act (PHIPA 2004) and its applicable regulations. The HSREB is registered with the U.S. Department of Health & Human Services under the IRB registration number IRB 00000940.

Please do not hesitate to contact us if you have any questions.

Sincerely,

Karen Gopaul, Ethics Officer on behalf of Dr. Philip Jones, HSREB Vice-Chair

Note: This correspondence includes an electronic signature (validation and approval via an online system that is compliant with all regulations).

Western Research

Date: 21 December 2022

To: Dr. Grace Parraga

Project ID: 113224

Review Reference: 2022-113224-73919

Study Title: A Mechanistic Pilot Open-label Study to Evaluate the Effect of Benralizumab on Airway Function and Inflammation in Patients with Severe, Poorly-controlled Eosinophilic Asthma Using Inhaled Hyperpolarized 129Xe MRI (AERFLO)

Application Type: Continuing Ethics Review (CER) Form

Review Type: Delegated

REB Meeting Date: 10/Jan/2023

Date Approval Issued: 21/Dec/2022 07:08

REB Approval Expiry Date: 18/Jan/2024

Dear Dr. Grace Parraga,

The Western University Research Ethics Board has reviewed the application. This study, including all currently approved documents, has been re-approved until the expiry date noted above.

REB members involved in the research project do not participate in the review, discussion or decision.

Western University REB operates in compliance with, and is constituted in accordance with, the requirements of the Tri-Council Policy Statement: Ethical Conduct for Research Involving Humans (TCPS 2); the International Conference on Harmonisation Good Clinical Practice Consolidated Guideline (ICH GCP); Part C, Division 5 of the Food and Drug Regulations; Part 4 of the Natural Health Products Regulations; Part 3 of the Medical Devices Regulations and the provisions of the Ontario Personal Health Information Protection Act (PHIPA 2004) and its applicable regulations. The REB is registered with the U.S. Department of Health & Human Services under the IRB registration number IRB 00000940.

Please do not hesitate to contact us if you have any questions.

Electronically signed by:

Karen Gopaul, Ethics Officer on behalf of Dr. P. Jones, HSREB Chair 21/Dec/2022 07:08

Reason: I am approving this document

Note: This correspondence includes an electronic signature (validation and approval via an online system that is compliant with all regulations).

Western Research

Use of Human Participants - Ethics Approval Notice

Principal Investigator: Dr. Grace Parraga
File Number:103516
Review Level: Full Board
Approved Local Adult Participants:200
Approved Local Minor Participants:0
Protocol Title: Structure and Function MRI of Asthma
Department & Institution: Schulich School of Medicine and Dentistry\Imaging,Robarts Research Institute
Sponsor:
Ethics Approval Date: April 08, 2013
Ethics Expiry Date: March 31, 2020

Documents Reviewed & Approved & Documents Received for Information:

Document Name	Comments	Version Date
Protocol	Robarts Protocol - Received for information only	2013/02/06
Instruments	Telephone Script	2013/03/14
Letter of Information & Consent	ROB0037 ICF March 13 2013	2013/03/13
Western University Protocol	(including study instruments & questionnaires)	

This is to notify you that the University of Western Ontario Health Sciences Research Ethics Board (HSREB) which is organized and operates according to the Tri-Council Policy Statement: Ethical Conduct of Research Involving Humans and the Health Canada/ICH Good Clinical Practice Practices: Consolidated Guidelines; and the applicable laws and regulations of Ontario has reviewed and granted approval to the above referenced study on the approval date noted above. The membership of this HSREB also complies with the membership requirements for REB's as defined in Division 5 of the Food and Drug Regulations.

The ethics approval for this study shall remain valid until the expiry date noted above assuming timely and acceptable responses to the HSREB's periodic requests for surveillance and monitoring information. If you require an updated approval notice prior to that time you must request it using the University of Western Ontario Updated Approval Request form.

Member of the HSREB that are named as investigators in research studies, or declare a conflict of interest, do not participate in discussions related to, nor vote on, such studies when they are presented to the HSREB.

The Chair of the HSREB is Dr. Joseph Gilbert. The HSREB is registered with the U.S. Department of Health & Human Services under the IRB registration number IRB 00000940.

Ethics Officer to Contact for Further Information

✓ Janice Sutherland	Grace Kelly	Shantel Walcott

This is an official document. Please retain the original in your files.

Western Research

Date: 31 January 2023

To: Dr. Grace Parraga

Project ID: 103516

Review Reference: 2023-103516-75680

Study Title: Structure and Function MRI of Asthma

Application Type: Continuing Ethics Review (CER) Form

Review Type: Delegated

REB Meeting Report Date: 21/Feb/2023

Date Approval Issued: 31/Jan/2023 12:44

REB Approval Expiry Date: 19/Feb/2024

Dear Dr. Grace Parraga,

The Western University Research Ethics Board has reviewed the application. This study, including all currently approved documents, has been re-approved until the expiry date noted above.

REB members involved in the research project do not participate in the review, discussion or decision.

Western University REB operates in compliance with, and is constituted in accordance with, the requirements of the Tri-Council Policy Statement: Ethical Conduct for Research Involving Humans (TCPS 2); the International Conference on Harmonisation Good Clinical Practice Consolidated Guideline (ICH GCP); Part C, Division 5 of the Food and Drug Regulations; Part 4 of the Natural Health Products Regulations; Part 3 of the Medical Devices Regulations and the provisions of the Ontario Personal Health Information Protection Act (PHIPA 2004) and its applicable regulations. The REB is registered with the U.S. Department of Health & Human Services under the IRB registration number IRB 00000940.

Please do not hesitate to contact us if you have any questions.

Electronically signed by:

Patricia Sargeant, Ethics Officer ( ) on behalf of Dr. P. Jones, HSREB Chair 31/Jan/2023 12:44

Reason: I am approving this document

Note: This correspondence includes an electronic signature (validation and approval via an online system that is compliant with all regulations).

Office of Research Ethics

The University of Western Ontario
Room 4180 Support Services Building, London, ON, Canada N6A 5C1
Telephone: (519) 661-3036 Fax: (519) 850-2466 Email: ethics@uwo.ca
Website: www.uwo.ca/research/ethics

Use of Human Subjects - Ethics Approval Notice

Principal Investigator: Dr. G. Parraga
Review Number: 17396 **Review Level:** Full Board
Review Date: September 14, 2010 **Approved Local # of Participants:** 180
Protocol Title: Longitudinal 3He Magnetic Resonance Imaging of Health Lung
Department and Institution: Imaging, Robarts Research Institute
Sponsor: CIHR-CANADIAN INSTITUTE OF HEALTH RESEARCH
Ethics Approval Date: November 09, 2010 **Expiry Date:** September 30, 2014
Documents Reviewed and Approved: UWO Protocol (including instruments noted in Section 8.1), Letter of Information and Consent Form dated Sept. 27, 2010 version 2, and Advertisement.
Documents Received for Information: Clinical Study Protocol Version #1 27 August 2010; IB NC100182-Inhalation (Hyperpolarised 3HE) 6th edition 09 Sep 05; NC1000182 IB April 7, 2009; Product Monograph Ventolin HFA

This is to notify you that The University of Western Ontario Research Ethics Board for Health Sciences Research Involving Human Subjects (HSREB) which is organized and operates according to the Tri-Council Policy Statement: Ethical Conduct of Research Involving Humans and the Health Canada/ICH Good Clinical Practice Practices: Consolidated Guidelines; and the applicable laws and regulations of Ontario has reviewed and granted approval to the above referenced study on the approval date noted above. The membership of this REB also complies with the membership requirements for REB's as defined in Division 5 of the Food and Drug Regulations.

e ethics approval for this study shall remain valid until the expiry date noted above assuming timely and acceptable responses to the HSREB's periodic requests for surveillance and monitoring information. If you require an updated approval notice prior to that time you must request it using the UWO Updated Approval Request Form.

During the course of the research, no deviations from, or changes to, the protocol or consent form may be initiated without prior written approval from the HSREB except when necessary to eliminate immediate hazards to the subject or when the change(s) involve only logistical or administrative aspects of the study (e.g. change of monitor, telephone number). Expedited review of minor change(s) in ongoing studies will be considered. Subjects must receive a copy of the signed information/consent documentation.

Investigators must promptly also report to the HSREB:

a) changes increasing the risk to the participant(s) and/or affecting significantly the conduct of the study;
b) all adverse and unexpected experiences or events that are both serious and unexpected;
c) new information that may adversely affect the safety of the subjects or the conduct of the study.

If these changes/adverse events require a change to the information/consent documentation, and/or recruitment advertisement, the newly revised information/consent documentation, and/or advertisement, must be submitted to this office for approval.

Members of the HSREB who are named as investigators in research studies, or declare a conflict of interest, do not participate in discussion related to, nor vote on, such studies when they are presented to the HSREB.

hair of HSREB: Dr. Joseph Gilbert
FDA Ref. #: IRB 00000940

Ethics Officer to Contact for Further Information			
☐ Janice Sutherland	☑ Elizabeth Wambolt	☐ Grace Kelly	

This is an official document. Please retain the original in your files.

cc: ORE File
LHRI

Western Research

Date: 11 October 2022

To: Grace Parraga

Project ID: 7320

Review Reference: 2022-7320-71856

Study Title: Longitudinal 3He Magnetic Resonance Imaging of Healthy Lung (REB #17396)

Application Type: Continuing Ethics Review (CER) Form

Review Type: Delegated

REB Meeting Date: 25/Oct/2022

Date Approval Issued: 11/Oct/2022 10:42

REB Approval Expiry Date: 09/Nov/2023

Dear Grace Parraga,

The Western University Research Ethics Board has reviewed the application. This study, including all currently approved documents, has been re-approved until the expiry date noted above.

REB members involved in the research project do not participate in the review, discussion or decision.

Western University REB operates in compliance with, and is constituted in accordance with, the requirements of the Tri-Council Policy Statement: Ethical Conduct for Research Involving Humans (TCPS 2); the International Conference on Harmonisation Good Clinical Practice Consolidated Guideline (ICH GCP); Part C, Division 5 of the Food and Drug Regulations; Part 4 of the Natural Health Products Regulations; Part 3 of the Medical Devices Regulations and the provisions of the Ontario Personal Health Information Protection Act (PHIPA 2004) and its applicable regulations. The REB is registered with the U.S. Department of Health & Human Services under the IRB registration number IRB 00000940.

Please do not hesitate to contact us if you have any questions.

Electronically signed by:

Ms. Nicola Geoghegan-Morphet, Ethics Officer on behalf of Dr. P. Jones, HSREB Chair 11/Oct/2022 10:42

Reason: I am approving this document

Note: This correspondence includes an electronic signature (validation and approval via an online system that is compliant with all regulations).

Western Research

Research Ethics

Use of Human Participants - Initial Ethics Approval Notice

Principal Investigator: Dr. Grace Parraga
File Number:104200
Review Level: Full Board
Protocol Title: Hyperpolarized Magnetic Resonance Imaging in Asthma Pre- and Post-Bronchial Thermoplasty
Department & Institution: Schulich School of Medicine and Dentistry\Imaging,Robarts Research Institute
Sponsor: Lawson Health Research Institute

Ethics Approval Date: January 03, 2014
Ethics Expiry Date: February 28, 2017

Documents Reviewed & Approved & Documents Received for Information:

Document Name	Comments	Version Date
Instruments	Asthma Quality of Life Questionnaire with Standardized Activities (AQLQ(S))	2013/08/15
Instruments	Asthma Control Questionnaire	2013/08/15
Instruments	Modified Borg Scale Questionnaire	2013/08/15
Instruments	mMRC Dyspnea Score Questionnaire	2013/08/15
Protocol	Robarts Protocol-Received for Information	2013/12/19
Letter of Information & Consent	version 2	2013/12/19
Western University Protocol	including Study Design diagram	

This is to notify you that the University of Western Ontario Health Sciences Research Ethics Board (HSREB) which is organized and operates according to the Tri-Council Policy Statement: Ethical Conduct of Research Involving Humans and the Health Canada/ICH Good Clinical Practice Practices: Consolidated Guidelines; and the applicable laws and regulations of Ontario has reviewed and granted approval to the above referenced study on the approval date noted above. The membership of this HSREB also complies with the membership requirements for REB's as defined in Division 5 of the Food and Drug Regulations.

The ethics approval for this study shall remain valid until the expiry date noted above assuming timely and acceptable responses to the HSREB's periodic requests for surveillance and monitoring information. If you require an updated approval notice prior to that time you must request it using the University of Western Ontario Updated Approval Request form.

Member of the HSREB that are named as investigators in research studies, or declare a conflict of interest, do not participate in discussions related to, nor vote on, such studies when they are presented to the HSREB.

The Chair of the HSREB is Dr. Joseph Gilbert. The HSREB is registered with the U.S. Department of Health & Human Services under the IRB registration number IRB 00000940.

Signature

Ethics Officer to Contact for Further Information

✓ Erika Basile	Grace Kelly	Mina Mikhail	Vikki Tran

This is an official document. Please retain the original in your files.

Western Research

Date: 4 August 2020

To: Grace Parraga

Project ID: 104200

Study Title: Hyperpolarized Magnetic Resonance Imaging in Asthma Pre- and Post-Bronchial Thermoplasty

Application Type: Study Closure Form

Review Type: Delegated

Date Acknowledgement Issued: 04/Aug/2020

Dear Grace Parraga,

The Western University Research Ethics Board has reviewed the application, and the closure of this study is acknowledged. The REB file on this study is now officially closed.

Thank you for using the Western Research Ethics Manager System (WREM).

Sincerely,

The Office of Human Research Ethics

Note: This correspondence includes an electronic signature (validation and approval via an online system that is compliant with all regulations).

Appendix C – Curriculum Vitae

Curriculum Vitae

Marrissa McIntosh BSc

CAMPEP PhD Candidate
Department of Medical Biophysics
Supervisor: Dr. Grace Parraga
Western University

EDUCATION

2019- Doctor of Philosophy in Medical Biophysics (*Candidate*)
Clinical Master of Science CAMPEP
Department of Medical Biophysics
Western University, London Canada
Supervisor: Dr. Grace Parraga
Project: Development and Application of ^{129}Xe MRI Quantification Tools

2015-2019 Bachelor of Science (Physics)
Mount Allison University, Sackville Canada
Independent Study in Radiation Therapy
Supervisor: Dr. David Fleming

ACADEMIC POSITIONS AND EMPLOYMENT

2020- **Western University**
Teaching Assistant
Department of Medical Biophysics

2019 **Robarts Research Institute**
Summer Student Researcher

2016-2018 **Mount Allison University**
Teaching Assistant
Department of Physics

2017 **Mount Allison University**
Summer Research Assistant
Department of Physics
Supervisors: Dr. Mohammed Ahmady and Dr. Ruben Sandapen

LEADERSHIP

2018-2019 **Because I Am A Girl Mount Allison University**
Chapter President

HONOURS, AWARDS AND RECOGNITIONS

A National and International

2023

Assembly on Respiratory Structure and Function Abstract Scholarship
Awarded to an ATS member who submitted an outstanding abstract to the ATS Annual Meeting
International
$380 USD

International Society for Magnetic Resonance in Medicine Educational Stipend
Awarded to an ISMRM member who submitted an outstanding abstract to the ISMRM Annual Meeting
International
$475 USD

CIHR Institute of Respiratory and Circulatory Health Travel Award
Awarded to a trainee to support the presentation of their research at national or international meetings, conferences or symposia
National
$1,500 CAD

International Workshop on Pulmonary Imaging Educational Stipend
Awarded to a junior speaker who submitted an outstanding abstract to the IWPI Bi-annual Meeting
International
$500 USD

CTS Research Poster Competition
The top 30 abstracts submitted by Canadian trainees to ATS annual meeting are selected to compete in a poster competition
National

2022

Canadian Respiratory Research Network PhD Studentship
Awarded to high-calibre PhD students engaged in research related to airways disease
National
$9,000 CAD

International Society for Magnetic Resonance in Medicine Educational Stipend
Awarded to an ISMRM member who submitted an outstanding abstract to the ISMRM Annual Meeting
International
$655 USD

Natural Sciences and Engineering Research Council – PGS-D Award
Awarded to high-calibre students engaged in an eligible doctoral program in the natural sciences or engineering
National
$63,000 CAD

2021

Assembly on Respiratory Structure and Function Abstract Scholarship
Awarded to an ATS member who submitted an outstanding abstract to the ATS Annual Meeting

International
$175 USD

2020 **Assembly on Respiratory Structure and Function Abstract Scholarship**
Awarded to an ATS member who submitted an outstanding abstract to the ATS Annual Meeting
International
$50 USD

CTS Research Poster Competition
The top 30 abstracts submitted by Canadian trainees to ATS annual meeting are selected to compete in a poster competition
National

B Institutional

2022 **Western Graduate Research Scholarship, Western University**
Awarded to a full time graduate student for stipend support who had maintained an average of 80% or more
Institutional
$5,000 CAD

Scientific Presentation Certificate of Merit
Peer-reviewed scientific award
Institutional

2021 **Western Graduate Research Scholarship, Western University**
Awarded to a full time graduate student for stipend support who had maintained an average of 80% or more
Institutional
$5,000 CAD

2020 **Western Graduate Research Scholarship, Western University**
Awarded to a full time graduate student for stipend support who had maintained an average of 80% or more
Institutional
$5,000 CAD

2019 **Western Graduate Research Scholarship, Western University**
Awarded to a full time graduate student for stipend support who had maintained an average of 80% or more
Institutional
$5,000 CAD

Marc E. Vallée Memorial Scholarship, Mount Allison University
Awarded to a senior student pursuing a post-graduate program in Medical Physics for academic excellence, involvement in the university and wider community, and strength of character
Institutional
$4,500 CAD

Teaching Assistant Certificate
Mount Allison University
Department of Physics

2018 **Joyce Foundation Purdy Crawford Bursary, Mount Allison University**

Institutional
$5,000 CAD

2017 **Sally Rodd Bursary**
Institutional
$2,314 CAD

2015 **Enhanced Entrance Scholarship, Mount Allison University**
Awarded to an incoming student with an average of 90% or more and significant involvement in their high school and wider community
Institutional
$4,000 CAD

COMMUNITY AND VOLUNTEER ACTIVITIES

2023 **Thames Valley Science and Engineering Fair**
Judge

2022 **St. John the Evangelist Anglican Church Dinner Service**
Volunteer

Ronald McDonald House Charity
Volunteer

Canada Wide Science Fair
Mentor
Bronze Medallist

Thames Valley Science and Engineering Fair
Judge

Medical Biophysics – Undergraduate Three Minute Thesis Competition
Judge

2021 **Thames Valley Science and Engineering Fair**
Judge

Medical Biophysics – Undergraduate Three Minute Thesis Competition
Judge

PUBLICATIONS AND PRESENTATIONS

A Peer-Reviewed Journal Manuscripts

Submitted (1)

1. **MJ McIntosh**, AM Matheson, HK Kooner, RL Eddy, H Serajeddini, C Yamashita and G Parraga. Pulmonary Vascular Differences in Eosinophilic Asthma after 2.5-years anti-IL-5Rα Treatment. *Submitted to American Journal of Respiratory and Critical Care Medicine (*Manuscript ID Blue-202305-0804OC).

Published (12)

1. HK Kooner, **MJ McIntosh**, AM Matheson, S Svenningsen and G Parraga. More Data about ^{129}Xe MRI Ventilation Defects in Long COVID-19. Radiology 2023. doi: 10.1148/radiol.230479.

2. **MJ McIntosh**, A Biancaniello, HK Kooner, A Bhalla, H Serajeddini, C Yamashita, G Parraga, and RL Eddy. ^{129}Xe MRI Ventilation Defects: What is the Upper Limit of Normal and Minimal Clinically Important Difference? Acad Radiol 2023. doi: 10.1016/j.acra.2023.03.010.

3. **MJ McIntosh*** & HK Kooner*, RL Eddy, H Serajeddini, A Bhalla, C Licskai, CA Mackenzie, C Yamashita and G Parraga. CT Mucus Score and ^{129}Xe MRI Ventilation following 2.5-years' Anti-IL-5Rα in Eosinophilic Asthma. CHEST 2023. doi: 10.1016/j.chest.2023.02.009.
   **co-primary authors*

4. HK Kooner, **MJ McIntosh**, AM Matheson, M Abdelrazek, MS Albert, I Dhaliwal, M Kirby, A Ouriadov, GE Santyr, C Venegas, N Radadia, S Svenningsen, JM Nicholson, and G Parraga. Post-Acute COVID-19 Syndrome: ^{129}Xe MRI Ventilation Defects and Respiratory Outcomes One Year Later. Radiology 2023; 222557. doi: 10.1148/radiol.222557.

5. AM Matheson, **MJ McIntosh**, HK Kooner, M Abdelrazek, M Albert, I Dhaliwal, JM Nicholson, A Ouriadov, S Svenningsen and G Parraga. Longitudinal follow-up of post-acute COVID-19 syndrome: Improved DL_{CO}, Quality-of-Life and MRI pulmonary gas-exchange abnormalities. Thorax 2023. doi:10.1136/thorax-2022-219378.

6. HK Kooner* & **MJ McIntosh***, AM Matheson, C Venegas, N Radadia, T Ho, E Haider, N Konyer, GE Santyr, MS Albert, A Ouriadov, M Abdelrazek, M Kirby, I Dhaliwal, JM Nicholson, P Nair, S Svenningsen and G Parraga. ^{129}Xe MRI ventilation defects in ever-hospitalised and never-hospitalised people with post-acute COVID-19 syndrome. BMJ Open Resp Res 2022; 9:e001235. doi:10.1136/bmjresp-2022-001235.
   **co-primary authors*

7. AM Matheson, **MJ McIntosh**, HK Kooner, J Lee, V Desaigoudar, E Bier, B Driehuys, S Svenningsen, G Santyr, M Kirby, MS Albert, Y Shepelytskyi, V Grynko, A Ouriadov, M Abdelrazek, I Dhaliwal, JM Nicholson, G Parraga. Persistent ^{129}Xe MRI Pulmonary and CT Vascular Abnormalities in Symptomatic Individuals with Post-acute COVID-19 Syndrome. Radiology 2022; 305:466-476. doi: 10.1148/radiol.220492.

8. RL Eddy, **MJ McIntosh**, AM Matheson, DG McCormack, C Licskai, G Parraga. Pulmonary Imaging Biomarkers and Cluster Analysis to Identify Novel Asthma Phenotypes: Proof-of-Concept Evaluation. JMRI 2022. doi:10.1002/jmri.28152.

9. **MJ McIntosh*** & HK Kooner*, RL Eddy, S Jeimy, C Licskai, CA MacKenzie, S Svenningsen, P Nair, C Yamashita, and G Parraga. Asthma control, Airway mucus and ^{129}Xe MRI ventilation after a single Benralizumab dose. CHEST 2022; 162(3): 520-533. doi:10.1016/j.chest.2022.03.003.
   **co-primary authors*

10. HK Kooner, **MJ McIntosh**, V Desaigoudar, JH Rayment, RL Eddy, B Driehuys and G Parraga. Pulmonary Functional MRI: Detecting the Structure-Function Pathologies that Drive Asthma Symptoms and Quality-of-Life. Respirology 2022; 27(2): 114-133. doi: 10.1111/resp.14197.

11. S Svenningsen, P Nair, RL Eddy, **MJ McIntosh**, M Kjarsgaard, H Lim, DG McCormack, G Cox, and G Parraga. Bronchial thermoplasty guided by hyperpolarized gas MRI in adults with severe asthma: A one-year pilot randomized trial. ERJ Open Res 2021; 7(3). doi: 10.1183/23120541.00268-2021.

12. S Svenningsen, **M McIntosh**, A Ouriadov, AM Matheson, NB Konyer, RL Eddy, DG McCormack, MD Noseworthy, P Nair, G Parraga. Reproducibility of Hyperpolarized ^{129}Xe MRI Ventilation Defect Percent in Severe Asthma to Evaluate Clinical Trial Feasibility. Acad Radiol 2021; 28(6):817-826. doi: 10.1016/j.acra.2020.04.025.

B Abstracts

Accepted (3)

1. **MJ McIntosh**, M Sharma, HK Kooner, H Serajeddini, A Bhalla, C Yamashita, and G Parraga. Hyperpolarized ^{129}Xe MRI ventilation textures predict short and long-term response to Anti-IL-5Rα Biologic Therapy in Eosinophilic Asthma. Annual International Society of Magnetic Resonance in Medicine Scientific Meeting 2023, Toronto, Canada. June 3-8, 2023.

2. AM Matheson, **MJ McIntosh**, N Paul, A Bhalla, C Yamashita, and G Parraga. ^{129}Xe MRS Gas-Exchange Abnormalities in Poorly-controlled Asthma. Annual International Society of Magnetic Resonance in Medicine Scientific Meeting 2023, Toronto, Canada. June 3-8, 2023.

3. HK Kooner, M Sharma, **MJ McIntosh**, I Dhaliwal, JM Nicholson, and G Parraga. ^{129}Xe MRI Ventilation Predicts Longitudinal Quality-of-Life Improvement in Post-Acute COVID-19 Syndrome. Annual International Society of Magnetic Resonance in Medicine Scientific Meeting 2023, Toronto, Canada. June 3-8, 2023.

Published (18)

1. **MJ McIntosh**, AM Matheson, HK Kooner, RL Eddy, C Yamashita and G Parraga. Pulmonary Vascular Redistribution following 2.5-years anti-IL5-Rα treatment in Eosinophilic Asthma. American Thoracic Society Annual Scientific Meeting. AJRCCM 2023; 207:A2529. doi: 10.1164/ajrccm-conference.2023.207.1_MeetingAbstracts.A2529

2. AM Matheson, **MJ McIntosh**, N Paul, A Bhalla, C Yamashita and G Parraga. ^{129}Xe Gas-Exchange MRI and CT Pulmonary Vascular Abnormalities in GINA 4-5 Asthma. AJRCCM 2023; 207:A1043. doi: 10.1164/ajrccm-conference.2023.207.1_MeetingAbstracts.A1043

3. M Sharma, PV Wyszkiewicz, **MJ McIntosh**, HK Kooner, AM Matheson, DG McCormack and G Parraga. MRI and CT Measurements Uniquely Explain All-cause Mortality in Ex-smokers with and without COPD. AJRCCM 2023; 207:A6590. doi: 10.1164/ajrccm-conference.2023.207.1_MeetingAbstracts.A6590

4. HK Kooner, M Faran, **MJ McIntosh**, AM Matheson, PV Wyszkiewicz, I Dhaliwal, M Abdelrazek, JM Nicholson, and G Parraga. Sex Differences in CT Airway Measurements and their Relationship to Post-Acute COVID-19 Syndrome. AJRCCM 2023; 207:A6791. doi: 10.1164/ajrccm-conference.2023.207.1_MeetingAbstracts.A6791

5. JM Nicholson, AM Matheson, HK Kooner, **MJ McIntosh**, S Svenningsen and G Parraga. Unique MRI Phenotypes help explain Post-Acute COVID-19 syndrome. AJRCCM 2023; 207:A6785. doi: 10.1164/ajrccm-conference.2023.207.1_MeetingAbstracts.A6785

6. A Biancaniello, **MJ McIntosh**, HK Kooner, A Bhalla, C Yamashita, G Parraga, RL Eddy, and H Serajeddini. Minimal Clinically Important Difference for ^{129}Xe MRI Ventilation Defect Percent in Patients with Asthma. AJRCCM 2023; 207:A2320. doi: 10.1164/ajrccm-conference.2023.207.1_MeetingAbstracts.A2320

7. M Sharma, **MJ McIntosh**, HK Kooner, DG McCormack and G Parraga. Machine-Learning and Texture Analysis of Hyperpolarized ^{3}He MRI Ventilation Predicts Quality-of-life Worsening in Ex-smokers with and without COPD. Med Phys 2022; 49(8):5632-5632-826. doi: 10.1002/mp.15896.

8. **MJ McIntosh**, AM Matheson, M Sharma, HK Kooner, RL Eddy, DG McCormack, C Yamashita and G Parraga. Pulmonary ^{1}H MRI Lobar Classification Using Convolutional Neural Networks. Med Phys 2021; 48(8):4700-4700. doi:10.1002/mp/15102

9. **MJ McIntosh**, HK Kooner, RL Eddy, C Licskai, C Yamashita, A Gendron and G Parraga. Response to Benralizumab in Severe Asthma: Oscillometry and MRI Ventilation Defect Improvements in Participants with Abnormal FeNO. AJRCCM 2021; 203:A1111. doi: 10.1164/ajrccm-conference.2021.203.1_MeetingAbstracts.A1111

10. M Sharma, **MJ McIntosh**, AM Matheson, HK Kooner, DG McCormack, DA Palma and G Parraga. 6MWD Worsening in COPD Predicted using CT and MRI Texture Features and Machine Learning. AJRCCM 2021; 203:A1051. doi: 10.1164/ajrccm-conference.2021.203.1_MeetingAbstracts.A1051

11. AM Matheson, **MJ McIntosh**, Y Rajapaksa, IS Dhaliwal, M Nicholson and G Parraga. This is What COVID-19 Survival Looks Like: ^{129}Xe MRI, Oscillometry and Pulmonary Function Measurements. AJRCCM 2021; 203:A4453. doi: 10.1164/ajrccm-conference.2021.203.1_MeetingAbstracts.A4453

12. HK Kooner, **MJ McIntosh**, RL Eddy, A Gendron, C Licskai, C Yamashita and G Parraga. CT Mucus Score Predicts Benralizumab Response in Severe Asthma. AJRCCM 2021; 203:A4531. doi: 10.1164/ajrccm-conference.2021.203.1_MeetingAbstracts.A4531

13. RL Eddy, **MJ McIntosh**, AM Matheson, C Licskai, DG McCormack, and G Parraga. Structure-function Imaging Phenotypes of Asthma Using CT and ^{129}Xe MRI.

AJRCCM 2021; 203:A1112. doi: 10.1164/ajrccm-conference.2021.203.1_MeetingAbstracts.A1112

14. S Svenningsen, P Nair, RL Eddy, **M McIntosh**, M Kjarsgaard, HF Lim, DG McCormack, G Cox and G Parraga. Bronchial thermoplasty guided by inhaled hyperpolarized gas magnetic resonance imaging in severe asthma: A one-year pilot randomized trial. AJRCCM 2021; 203:A1110. doi: 10.1164/ajrccm-conference.2021.203.1_MeetingAbstracts.A1110

15. FR Salerno, T Lindenmaier, A Matheson, RL Eddy, **M McIntosh**, J Dorie, G Parraga, and CW McIntyre. Noninvasive assessment of pulmonary hypertension using quantitative imaging in hemodialysis patients. Nephrology Dialysis Transplantation 2020:35(Supplement 3). doi: 10.1093/ndt/gfaa142.P1302

16. **MJ McIntosh**, RL Eddy, D Knipping, AL Barker, T Lindenmaier, C Yamashita, and G Parraga. Response to benralizumab in severe asthma: ^{129}Xe MRI, oscillometry and clinical measurements. AJRCCM 2020; 201:A6244. doi: 10.1164/ajrccm-conference.2020.201.1_MeetingAbstracts.A6244

17. RL Eddy, **MJ McIntosh**, AM Matheson, D Knipping, C Licskai, DG McCormack, G Parraga. ^{129}Xe MRI Ventilation Heterogeneity Phenotypes of Asthma. AJRCCM 2020; 201:A6243. doi: 10.1164/ajrccm-conference.2020.201.1_MeetingAbstracts.A6243

18. **MJ McIntosh**, RL Eddy, JL MacNeil, A Matheson and G Parraga. Automated quantification of spatially abnormal ^{129}Xe MRI ventilation and perfusion: implications for lung cancer, asthma, and COPD interventions. Med Phys 2020: 47(6):E301-E301. doi: 10.1002/mp.14316

C Proffered Oral Presentations (27) **presenter*

1. **MJ McIntosh**, M Sharma, HK Kooner, H Serajeddini, A Bhalla, C Yamashita, and G Parraga. Hyperpolarized ^{129}Xe MRI ventilation textures predict short and long-term response to Anti-IL-5Rα Biologic Therapy in Eosinophilic Asthma. Imaging Network of Ontario Annual Symposium. London, Canada, 2023.
2. AM Matheson, **MJ McIntosh**, N Paul, A Bhalla, C Yamashita and G Parraga. ^{129}Xe Gas-Exchange MRI and CT Pulmonary Vascular Abnormalities in GINA 4-5 Asthma. Imaging Network of Ontario Annual Symposium. London, Canada, 2023.
3. **MJ McIntosh**, AM Matheson, HK Kooner, RL Eddy, C Yamashita and G Parraga. Pulmonary Vasculature in Asthma: Redistribution following 2.5-years anti-IL5-Rα. The 2023 International Workshop on Pulmonary Imaging. Philadelphia, PA, 2023.
4. **MJ McIntosh***, G Parraga. Early and Late Imaging Biomarkers of Response to Benralizumab in Poorly Controlled Asthma. Canadian Respiratory Research Network Annual Meeting, The Westin, Ottawa, Canada, 2022.
5. HK Kooner*, **MJ McIntosh**, AM Matheson, M Abdelrazek, I Dhaliwal, JM Nicholson, and G Parraga. ^{129}Xe MRI Ventilation Improvements 15 Months Post-COVID Infection. International Workshop on Pulmonary Functional Imaging 2022, Hannover, Germany, 2022.
6. HK Kooner, **MJ McIntosh**, AM Matheson, M Sharma, PV Wyszkiewicz, I Dhaliwal, M Abdelrazek, M Nicholson, and G Parraga. ^{129}Xe MRI Ventilation Defects in People with Post-Acute COVID-19 Syndrome. Robarts Research Retreat. London ON, Canada, 2022.

7. **MJ McIntosh***, HK Kooner, RL Eddy, C Licskai, C Yamashita and G Parraga. ^{129}Xe MRI Ventilation Response to Benralizumab in Severe Asthma. London Imaging Discovery Day, London ON, Canada, 2022.
8. HK Kooner*, **MJ McIntosh**, AM Matheson, M Sharma, PV Wyszkiewicz, I Dhaliwal, M Nicholson, M Abdelrazek, and G Parraga. ^{129}Xe MRI Ventilation Defects in People with Post-Acute COVID-19 Syndrome. London Imaging Discovery Day, London ON, Canada, 2022.
9. M Sharma*, **MJ McIntosh**, HK Kooner, AM Matheson, PV Wyszkiewicz, DG McCormack, and G Parraga. Texture Analysis and Machine Learning of Hyperpolarized ^{3}He MRI Ventilation Predicts Quality-of-life Worsening in Ex-smokers with and without COPD. London Imaging Discovery Day, London ON, Canada, 2022.
10. AM Matheson*, **MJ McIntosh**, HK Kooner, J Lee, V Desaigoudar, A Ouriadov, M Abdelrazek, I Dhaliwal, JM Nicholson and G Parraga. ^{129}Xe Gas-Transfer MRI RBC-to-Barrier Ratio in Post-Acute COVID19 Syndrome: Clinically-relevant? London Imaging Discovery Day, London ON, Canada, 2022.
11. M Sharma*, **MJ McIntosh**, HK Kooner, DG McCormack and G Parraga. Machine-Learning and Texture Analysis of Hyperpolarized ^{3}He MRI Ventilation Predicts Quality-of-life Worsening in Ex-smokers with and without COPD. 68th annual Canadian Organization of Medical Physicists (COMP) scientific meeting, Quebec City, QC, Canada, 2022.
12. **MJ McIntosh***, AM Matheson, M Sharma, HK Kooner, RL Eddy, DG McCormack, C Yamashita and G Parraga. Pulmonary ^{1}H MRI Lobar Classification Using Convolutional Neural Networks. Canadian Organization of Medical Physicists Annual Scientific Meeting, Virtual, 2021.
13. **MJ McIntosh***, AM Matheson, M Sharma, HK Kooner, RL Eddy, DG McCormack, C Yamashita and G Parraga. Pulmonary ^{1}H MRI Lobar Classification Using Convolutional Neural Networks. Robarts Research Retreat, Virtual, 2021.
14. **MJ McIntosh***, HK Kooner, RL Eddy, C Licskai, C Yamashita, A Gendron and G Parraga. Response to Benralizumab in Severe Asthma: Oscillometry and MRI Ventilation Defect Improvements in Participants with Abnormal FeNO. American Thoracic Society Annual Scientific Meeting, Virtual, 2021.
15. M Sharma*, **MJ McIntosh**, AM Matheson, HK Kooner, DG McCormack, DA Palma and G Parraga. 6MWD Worsening in COPD Predicted using CT and MRI Texture Features and Machine Learning. American Thoracic Society Annual Scientific Meeting, Virtual, 2021.
16. RL Eddy*, **MJ McIntosh**, AM Matheson, C Licskai, DG McCormack, and G Parraga. Structure-function Imaging Phenotypes of Asthma Using CT and ^{129}Xe MRI. American Thoracic Society Annual Scientific Meeting, Virtual, 2021.
17. S Svenningsen*, P Nair, RL Eddy, **M McIntosh**, M Kjarsgaard, HF Lim, DG McCormack, G Cox and G Parraga. Bronchial thermoplasty guided by inhaled hyperpolarized gas magnetic resonance imaging in severe asthma: A one-year pilot randomized trial. American Thoracic Society Annual Scientific Meeting, Virtual, 2021.
18. **MJ McIntosh**, RL Eddy, D Knipping, AL Barker, T Lindenmaier, C Yamashita, and G Parraga. Response to benralizumab in severe asthma: ^{129}Xe MRI, oscillometry and clinical measurements. American Thoracic Society Annual Scientific Meeting, *CANCELLED*.
19. RL Eddy, **MJ McIntosh**, AM Matheson, D Knipping, C Licskai, DG McCormack, G Parraga. ^{129}Xe MRI Ventilation Heterogeneity Phenotypes of Asthma. American Thoracic Society Annual Scientific Meeting 2020, *CANCELLED*.
20. **MJ McIntosh***, RL Eddy, D Knipping, T Lindenmaier, D McCormack, C Licskai, C Yamashita, and G Parraga. Pulmonary MRI to Predict Therapy Response.

International Society of Magnetic Resonance in Medicine Annual Scientific Meeting, Virtual Conference, 2020.

21. A Matheson*, RL Eddy, J MacNeil, **MJ McIntosh**, and G Parraga. Fully Automated ^{1}H MRI Thoracic Cavity Segmentation for Hyperpolarized Gas Imaging using a Convolutional Neural Network. International Society of Magnetic Resonance in Medicine Annual Scientific Meeting, Virtual Conference, 2020.
22. **MJ McIntosh***, RL Eddy, JL MacNeil, A Matheson and G Parraga. Automated Quantification of ^{129}Xe Ventilation. AAPM-COMP Joint Conference, Virtual Conference, 2020.
23. **MJ McIntosh***, RL Eddy, D Knipping, T Lindemaier, DG McCormack, C Licskai, C Yamashita, G Parraga. Pulmonary MRI to Predict Anti-IL-5Rα Therapy Response. Imaging Network of Ontario Annual Meeting, Virtual Conference, 2020.
24. AM Matheson*, RL Eddy, J MacNeil, **MJ McIntosh** and G Parraga. Convolutional Neural Network ^{1}H MRI Lung Segmentation for Hyperpolarized Gas Imaging. Imaging Network Ontario 2020 Conference. Virtual Conference, 2020.
25. **MJ McIntosh***, G Parraga. ^{129}Xe MRI Response to Anti-IL-5Rα. Canadian Respiratory Research Network Annual Meeting, Chateau Laurier, Ottawa, Canada, 2020.
26. D Knipping*, **MJ McIntosh**. AERFLO Study: Interim results, successes and challenges. Departments of Respirology and Allergy and Immunology, St. Joseph's Hospital, London, Canada, 2019.
27. **MJ McIntosh***, D Fleming. Image-Guided Robotic Brachytherapy. Mount Allison University Physics Honours and Special Topics Presentations, Sackville, Canada, 2019.

D Invited Oral Presentations (3) **presenter*

1. **MJ McIntosh***, HK Kooner, G Parraga. Mucus Plugs in Eosinophilic Asthma: Clearance after Benralizumab. Department of Respirology Rounds, London Health Sciences Centre, Virtual, 2023.
2. **MJ McIntosh***. Medical Biophysics Program at Western University. Graduate School Information Session Panel, Department of Physics, Mount Allison University, Virtual, 2022.
3. CA Mackenzie*, **MJ McIntosh***, G Parraga. Irritant-induced asthma - How similar is it to allergic asthma? Department of Respirology Rounds, London Health Sciences Centre, Virtual, 2021.

E Proffered Poster Presentations (20) **presenter*

1. **MJ McIntosh***, AM Matheson, HK Kooner, RL Eddy, C Yamashita and G Parraga. Pulmonary Vascular Redistribution following 2.5-years anti-IL5-Rα treatment in Eosinophilic Asthma. Canadian Thoracic Society Poster Competition, Washington DC, USA, 2023.
2. M Sharma*, PV Wyszkiewicz, **MJ McIntosh**, HK Kooner, AM Matheson, DG McCormack and G Parraga. CT and MRI Measurements Uniquely Explain All-cause Mortality in Ex-smokers. Imaging Network of Ontario Annual Symposium. London, Canada, 2023.
3. HK Kooner*, M Faran, **MJ McIntosh**, AM Matheson, PV Wyszkiewicz, I Dhaliwal, M Abdelrazek, JM Nicholson, and G Parraga. Sex Differences in CT Airway Measurements and their Relationship to Post-Acute COVID-19 Syndrome. Imaging Network of Ontario Annual Symposium. London, Canada, 2023.
4. V Desaigoudar*, PV Wyszkiewicz, AM Matheson, M Sharma, **MJ McIntosh**, HK Kooner, DG McCormack and G Parraga. Pulmonary Small Vessel Worsening in Ex-

smokers with COPD. Imaging Network Ontario Annual Symposium. London, Canada, 2023.

5. A Biancaniello*, H Serajeddini, **MJ McIntosh**, HK Kooner, A Bhalla, C Yamashita, RL Eddy, and G Parraga. Minimal Clinically Important Difference for ^{129}Xe MRI Ventilation Defect Percent in Patients with Asthma. Imaging Network of Ontario Annual Symposium. London, Canada, 2023.
6. AM Matheson*, **MJ McIntosh**, N Paul, A Bhalla, C Yamashita and G Parraga. 129Xe MRS Gas-Exchange Variability in Asthma: Demographics, Blood and Lung-Function. The 2023 International Workshop on Pulmonary Imaging. Philadelphia, PA, 2023.
7. AM Matheson*, **MJ McIntosh**, HK Kooner, C Yamashita, N Paul and G Parraga. ^{129}Xe Magnetic Resonance Spectroscopy: Abnormal Cardiogenic Oscillations in Severe Asthma. International Workshop on Pulmonary Functional Imaging 2022. Hannover, Germany, 2022.
8. V Desaigoudar*, PV Wyszkiewicz, AM Matheson, M Sharma, **MJ McIntosh**, HK Kooner, DG McCormack and G Parraga. CT Pulmonary Vascular, Airway, Pulmonary Artery and Aorta Measurements in Ex-Smokers with and without COPD. Canadian Undergraduate Medical Physics Conference, Virtual, 2022.
9. **MJ McIntosh***, HK Kooner, RL Eddy, C Licskai, C Yamashita and G Parraga. 129Xe MRI Ventilation Response to Benralizumab in Severe Asthma. Robarts Research Retreat. London ON, Canada, 2022.
10. M Sharma*, **MJ McIntosh**, HK Kooner, AM Matheson, PV Wyszkiewicz, DG McCormack, and G Parraga. Texture Analysis and Machine Learning of Hyperpolarized 3He MRI Ventilation Predicts Quality-of-life Worsening in Ex-smokers with and without COPD. Robarts Research Retreat. London ON, Canada, 2022.
11. AM Matheson*, **MJ McIntosh**, HK Kooner, J Lee, V Desaigoudar, A Ouriadov, M Abdelrazek, I Dhaliwal, JM Nicholson and G Parraga. ^{129}Xe Gas-Transfer MRI RBC-to-Barrier Ratio in Post-Acute COVID19 Syndrome: Clinically-relevant? Robarts Research Retreat. London ON, Canada, 2022.
12. **MJ McIntosh***, M Sharma, AM Matheson, HK Kooner, RL Eddy, C Licksai, DG McCormack, M Nicholson, C Yamashita and G Parraga. Respiratory System Resistance Explained using Hyperpolarized ^{129}Xe MRI Texture Features and Machine Learning. Joint annual International Society of Magnetic Resonance in Medicine-European Society for Magnetic Resonance in Medicine and Biology (ISMRM-ESMRMB) Scientific Meeting 2022, London, England, UK, 2022.
13. HK Kooner*, **MJ McIntosh**, M Sharma, GV Singh, N Nasir, E Blake, I Dhaliwal, M Nicholson, M Kirby and G Parraga. Post-Acute COVID-19 Syndrome: Longitudinal 129Xe MRI Ventilation Heterogeneity Measurements. Joint annual International Society of Magnetic Resonance in Medicine-European Society for Magnetic Resonance in Medicine and Biology (ISMRM-ESMRMB) Scientific Meeting 2022, London, England, UK, 2022.
14. M Sharma*, HK Kooner, **MJ McIntosh**, DG McCormack and G Parraga. Quality-of-life Worsening Predicted Using Baseline Hyperpolarized ^{3}He MRI Ventilation Texture Features and Machine-Learning. Joint annual International Society of Magnetic Resonance in Medicine-European Society for Magnetic Resonance in Medicine and Biology (ISMRM-ESMRMB) Scientific Meeting 2022, London, England, UK, 2022.
15. AM Matheson*, **MJ McIntosh**, Y Rajapaksa, IS Dhaliwal, M Nicholson and G Parraga. This is What COVID-19 Survival Looks Like: ^{129}Xe MRI, Oscillometry and Pulmonary Function Measurements. American Thoracic Society Annual Scientific Meeting, Virtual, 2021.

16. HK Kooner*, **MJ McIntosh**, RL Eddy, A Gendron, C Licskai, C Yamashita and G Parraga. CT Mucus Score Predicts Benralizumab Response in Severe Asthma. American Thoracic Society Annual Scientific Meeting, Virtual, 2021.
17. AM Matheson*, RL Eddy, JL MacNeil, **MJ McIntosh** and G Parraga. Fully-automated Multi-spectral Pulmonary Registration for Hyperpolarized Noble Gas MRI Using Neural Networks. International Society of Magnetic Resonance in Medicine Annual Scientific Meeting, Virtual, 2021.
18. HK Kooner*, **MJ McIntosh**, M Sharma, AM Matheson, Y Rajapaksa, IS Dhaliwal, M Nicholson and G Parraga. Hyperpolarized ^{129}Xe MRI Ventilation Texture Features to Characterize Long-haul COVID-19 Survivors. International Society of Magnetic Resonance in Medicine Annual Scientific Meeting, Virtual 2021.
19. RL Eddy*, AM Matheson, **MJ McIntosh** and G Parraga. Evaluating the Fractal Nature of ^{129}Xe MRI Ventilation Heterogeneity. International Society of Magnetic Resonance in Medicine Annual Scientific Meeting, Virtual, 2021.
20. FR Salerno, T Lindenmaier, A Matheson, RL Eddy, **M McIntosh**, J Dorie, G Parraga, and CW McIntyre. Noninvasive assessment of pulmonary hypertension using quantitative imaging in hemodialysis patients. European Nephrology Conference, Virtual, 2020.

MEDIA CONTRIBUTIONS

1. ^{129}Xe MRI Offers Detailed View of Pulmonary Function and Huge Clinical Potential. Pulmonary Advisor. Lay Article. https://www.pulmonologyadvisor.com/home/general-pulmonology/129xe-mri-offers-detailed-view-of-pulmonary-function-and-huge-clinical-potential. 19 August 2022.

COMMITTEES AND PROFESSIONAL ACTIVITIES

2022
UWO School of Graduate Studies Finance Committee
COMMITTEE MEMBER (2022-Present)

2021
UWO Medical Biophysics Deep Learning Club
MEMBER (2020-Present)

2020
UWO Medical Biophysics CAMPEP Student Club
MEMBER (2020-Present)

2018
Mount Allison Physics Society
MEMBER: Vice President of Promotions (2018-2019)

2017
Because I Am A Girl Mount Allison
MEMBER: Vice President of External Affairs (2017-2018)

2015
Best Buddies Mount Allison
MEMBER: Peer Buddy (2015-2019)

Because I Am A Girl Mount Allison
MEMBER (2015-2017)

POST-GRADUATE EDUCATION DEVELOPMENT and EXPERIENCES

11/2022 **Panel Organizer**
Graduate School Information Session Panel
Department of Physics, Mount Allison University, Virtual, 2022

05/2021-09/2021 **Graduate Student Mentor**
Medical Student: Carolyn Tran BSc
Project: "Small Airway Changes Following Benralizumab Therapy in Severe Eosinophilic Asthma"

09/2020-05/2021 **Graduate Student Mentor**
Undergraduate Student: Yasal Rajapaksa BSc Candidate Physiology and Pharmacology
Project: "Hyperpolarized ^{129}Xe MRI to Evaluate Long Term Effects of COVID-19"

05/2020-09/2021 **Graduate Student Mentor**
Undergraduate Student: Vedanth Desaigoudor BSc Candidate
Project: "Pulmonary CT and MRI Treatable Traits: Where we are and where we need to go"

PROFESSIONAL SOCIETIES

2022- American Association of Physicists in Medicine Society (AAPM)
Student Member

2020- European Respiratory Society (ERS)
Student Member

2019- International Society of Magnetic Resonance in Medicine (ISMRM)
Student Member

2019- Canadian Organization of Medical Physicists (COMP)
Student Member

2019- Canadian Thoracic Society (CTS)
Student Member

2019- American Thoracic Society (ATS)
Trainee Member